Tris(trimethylsilyl)silyl Substituted Alkali- and Transition Metal Guaiazulenides

Dissertation

Submitted in Partial Fulfilment of the Requirements for the Degree of
Doctor of Natural Science
-Dr.rer.nat.-

In the Institute of Inorganic and Analytical Chemistry

Department of Chemistry and Pharmacy

at

Johannes Gutenberg - University of Mainz

by

Yun Xiong

from P. R. China

Mainz 2004

1 INTRODUCTION 1

1.1 ALKALI METAL HYPERSILANIDES 1
1.2 COORDINATION CHEMISTRY OF AZULENE SYSTEM 4

2 RESEARCH PROCESS 14

2.1 THEORETICAL ANALYSIS 14
2.2 MONO-HYP SUBSTITUTED ALKALIMETAL GUAIAZULENIDES 17
2.2.1 Addition 17
2.2.1.1 Addition of Lithium Hypersilanide to Guaiazulene 17
2.2.1.2 Addition of Potassium Hypersilanide to Guaiazulene 17
2.2.1.3 Addition of Cesium Hypersilanide to Guaiazulene 19
2.2.2 NMR Spectroscopy 21
2.2.2.1 ^{1}H NMR Spectroscopy 21
2.2.2.2 ^{13}C NMR Spectroscopy 26
2.2.2.3 ^{29}Si NMR Spectroscopy 27
2.2.2.4 ^{7}Li NMR Spectroscopy 28
2.2.3 Molecular Structures of Compounds 1 and 2a 29
2.2.3.1 Molecular Structure of $[Li(6\text{-}Hyp\text{-}Hgual)]_2$ (1) 29
2.2.3.2 Molecular Structure of $(thf)_4 \cdot K(6\text{-}Hyp\text{-}Hgual)$ (2a) 33
2.3 MONO-HYP SUBSTITUTED METALLOCENE DERIVATIVES 35
2.3.1 Reactions 35
2.3.1.1 Metathesis of M(6-Hyp-Hgual) (M=Li, K) with $MnBr_2$, $FeCl_2$ 35
2.3.1.2 Metathesis of K(8-Hyp-Hgual) with $FeCl_2$ 37
2.3.1.3 Reaction of K(6-Hyp-Hgual) with $NiCl_2$ or other Metal Halides 37
2.3.2 NMR Spectroscopy 39
2.3.2.1 NMR Spectra of $Fe(6\text{-}Hyp\text{-}Hgual)_2$ (6) and $Fe(8\text{-}Hyp\text{-}Hgual)_2$ (7) 39
2.3.2.1.1 ^{1}H NMR Spectroscopy 40
2.3.2.1.2 ^{13}C NMR Spectroscopy 42
2.3.2.1.3 ^{29}Si NMR Spectroscopy 43
2.3.2.2 NMR Spectroscopy of $(3\text{-}Hyp\text{-}6\text{-}Hgua)_2$ (9) 43
2.3.2.2.1 ^{1}H NMR Spectroscopy 43
2.3.2.2.2 ^{13}C NMR Spectroscopy 46
2.3.2.2.3 ^{29}Si NMR Spectroscopy 47
2.3.3 Molecular Structures of Compounds 5, 6, 7, 8, and 9 47
2.3.3.1 Molecular Structures of (RR)- and (SS)-$M(6\text{-}Hyp\text{-}Hgual)_2$ (M=Mn 5, Fe 6, and Ni 8) 47
2.3.3.2 Molecular Structure of $Fe(8\text{-}Hyp\text{-}Hgual)_2$ (7) 55
2.3.3.3 Conformation Analysis of (R,S)-$Fe(6\text{-}Hyp\text{-}Hgual)_2$ (6) and (R,S)-$Fe(8\text{-}Hyp\text{-}Hgual)_2$ (7) 59
2.3.3.4 Molecular Structure of $(3\text{-}Hyp\text{-}6\text{-}Hgual)_2$ (9) 60
2.4 MONO-HYP SUBSTITUTED METALLOCENE DICHLORIDE DERIVATIVES 62
2.4.1 Reactions 62
2.4.1.1 Reaction of $TiCl_3$ with K(6-Hyp-Hgual)(2) 62
2.4.1.2 Reactions of MCl_4 (M=Zr(IV), Hf(IV)) with K(6-Hyp-Hgual) (2) 63
2.4.1.3 Reaction of $ZrCp^*Cl_3$ with K(6-Hyp-Hgual) 64
2.4.2 NMR Spectroscopy 64
2.4.2.1 ^{1}H NMR Spectroscopy 64
2.4.2.2 ^{13}C NMR Spectroscopy 67
2.4.2.3 ^{29}Si NMR Spectroscopy 67
2.4.3 Molecular Structures of 10, 11 and 12 68
2.5 BIS-HYP SUBSTITUTED LITHIUM GUAIAZULENIDE 73
2.5.1 Bis-Hyp Substituted Guaiazulene 73
2.5.1.1 Reaction 73
2.5.1.2 NMR Spectroscopy 74
2.5.1.2.1 ^{1}H NMR Spectroscopy 74
2.5.1.2.2 ^{13}C NMR Spectroscopy 77
2.5.1.2.3 ^{29}Si NMR Spectroscopy 77
2.5.1.3 Molecular structure of 2,6-bis(Hyp)-H_2gua (14) 78
2.5.2 Bis-Hyp Substituted Lithium Guaiazulenide 79
2.5.2.1 Reaction 79
2.5.2.2 NMR Spectroscopy 81
2.5.2.2.1 ^{1}H NMR Spectroscopy 81
2.5.2.2.2 ^{13}C NMR Spectroscopy 81
2.5.2.2.3 ^{29}Si NMR Spectroscopy 82
2.4.2.2.4 ^{7}Li NMR Spectroscopy 83
2.5.2.3 Molecular Structure of $[Li(2,6\text{-}bis(Hyp)\text{-}Hgual)]_2$ (15) 83

3 EXPERIMENT SECTION 87

3.1 General Comments 87
3.2 Characterization 87
3.2.1 Element Analysis *87*
3.2.2 Melting Point *87*
3.2.3 NMR-Spectroscopy *87*
3.2.4 X-ray diffraction analysis *88*
3.3 Synthesis and Characterization 88
3.3.1 Syntheses of Reactants *88*
3.3.1.1 Synthesis of $Si(SiMe_3)_4$ 88
3.3.1.2 Synthesis of $KSi(SiMe_3)_3$ 89
3.3.1.3 Synthesis of $LiSi(SiMe_3)_3$ 90
3.3.1.4 Synthesis of $CsSi(SiMe_3)_3$ 91
3.3.2 Syntheses and Characterization of New Compounds *91*
3.3.2.1 $[Li(6\text{-}Hyp\text{-}Hgual)]_2$ (1) 91
3.3.2.2 K(6-Hyp-Hgual) (2) and K(8-Hyp-Hgual) (3) 93
3.3.2.3 Cs(6-Hyp-Hgual) (4) 95
3.3.2.4 $Mn(6\text{-}Hyp\text{-}Hgual)_2$ (5) 96
3.3.2.5 $Fe(6\text{-}Hyp\text{-}Hgual)_2$ (6) 97
3.3.2.6 $Fe(8\text{-}Hyp\text{-}Hgual)_2$ (7) 99
3.3.2.7 $Ni(6\text{-}Hyp\text{-}Hgual)_2$ (8) 100
3.3.2.8 $(3\text{-}Hyp\text{-}6\text{-}Hgua)_2$ (9) 100
3.3.2.9 $Ti(6\text{-}Hyp\text{-}Hgual)_2Cl_2$ (10) 102
3.3.2.10 $Zr(6\text{-}Hyp\text{-}Hgual)_2Cl_2$ (11) 103
3.3.2.11 $Hf(6\text{-}Hyp\text{-}Hgual)_2Cl_2$ (12) 104
3.3.2.12 $ZrCp^*(6\text{-}Hyp\text{-}Hgual)Cl_2 \cdot KCl$ (13) 105
3.3.2.13 2,6-bis(Hyp)-H_2gua (14) 106
3.3.2.14 $[Li(2,6\text{-}bis(Hyp)\text{-}Hgual)]_2$ (15) 107

4 SUMMARY 110

5 APPENDIX 125

5.1 Crystallographic data for Li(6-Hyp-Hgual) 125
5.2 Crystallographic data for $(THF)_4 \cdot [K(6\text{-}Hyp\text{-}Hgual)]$ 127
5.3 Crystallographic data for 2,6-bis(Hyp)-H_2gua 130
5.4 Crystallographic data for Li(2,6-bis(Hyp)-Hgual) 132
5.5 Crystallographic data for $Mn(6\text{-}Hyp\text{-}Hgual)_2$ 136
5.6 Crystallographic data for $Fe(6\text{-}Hyp\text{-}Hgual)_2$ 140
5.7 Crystallographic data for $Fe(8\text{-}Hyp\text{-}Hgual)_2$ 143
5.8 Crystallographic data for $Ni(6\text{-}HypHgual)_2$ 149
5.9 Crystallographic data for $(3\text{-}Hyp\text{-}6\text{-}H_2gua)_2$ 152
5.10 Crystallographic data for $Ti(6\text{-}Hyp\text{-}Hgual)_2Cl_2$ 154
5.11 Crystallographic data for $Zr(6\text{-}Hyp\text{-}Hgual)_2Cl_2$ 158
5.12 Crystallographic data for $Hf(6\text{-}Hyp\text{-}Hgual)_2Cl_2$ 162

6 LIST OF ABBREVIATIONS 166

7 NUMBERING LIST OF THE NEW COMPLEXES 167

8 LITERATURE 168

1 Introduction

1.1 Alkali Metal Hypersilanides

Bulky silyl groups, such as tris(tertiary-butyl)silyl, triphenylsilyl, and tris(trimethylsilyl)silyl, due to their good electron releasing properties and large steric demand, can be employed as protection groups in the synthesis of organic compounds to build regio- and stereo-selective collection of C-C bonds under mild reaction conditions[1, 2, 3]. They can also stabilize some reactive intermediated state and/or metal centre in unusual oxidation state, which established their important positions in the organometallic synthesis of low valent main group-[4, 5, 6] and transition metal[7] complexes.

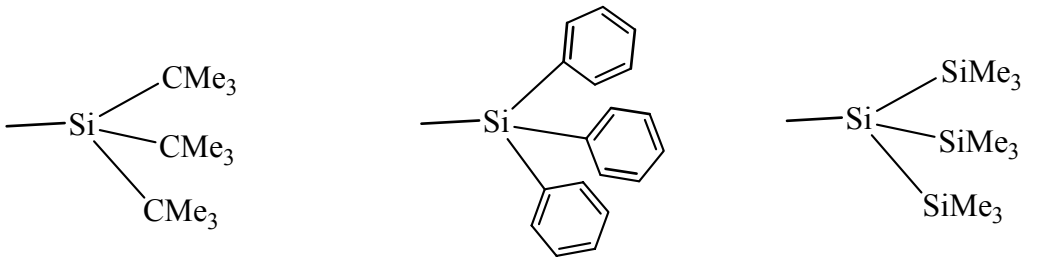

Tris(tertiary-butyl)silyl Triphenylsilyl Tris(trimethylsilyl)silyl

Fig. 1 Several bulky silyl groups

Tris(trimethylsilyl)silyl group, -Si($SiMe_3$)$_3$, which is named also as hypersilyl, and in the following will be abbreviated as "Hyp"[8], has some advantages as an overloaded reactive substituent. The possibility of cleavage of the Si-Si bonds leads abundant further reactions, e.g. for the synthesis of polysilane[9], silyene $(Me_3Si)_2Si=CR(OSiMe_3)$[10] etc.. Recently the development of the combination of metallocene units with the architectural diversity of dendrimers makes the hypersilyl chemistry have more fascinating prospect [11] . The introduction of hypersilyl group to metallocene units should offer possibility to furnish new materials with interesting physical and chemical properties[12].

Traditionally, lithiumsilanides are easy to synthesize, simply to purify and trouble free to manipulate when compare with their heavier alkali metal homologues. Therefore, lithiumsilanides are the most widely used reagents in the organometallic chemistry for synthesis of transition metal silyl compounds, for the generation of silenes, and for a number of other purposes[1, 13, 14]. The synthesis and crystal structure of lithium silanides have been extensively studied. Early in 1960´s Gilman and Smith have designed and synthesized some bulky silyl compounds[15, 16, 17]. From tetrakis(trimethylsilyl)silane they obtained firstly *in situ* lithium hypersilanide[18].

Eq. 1

$$Si(SiMe_3)_4 + MeLi \xrightarrow{<\ THF\ >} LiSi(SiMe_3)_3 + SiMe_4$$

Later it was isolated as DME[19] and THF[20, 21] solvated complexes.

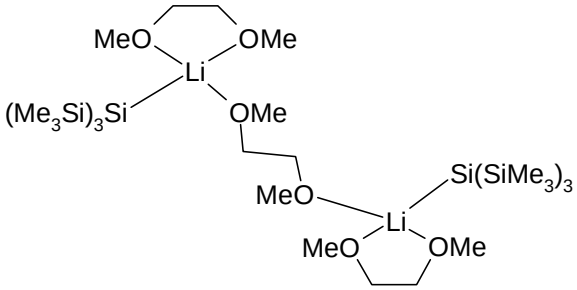

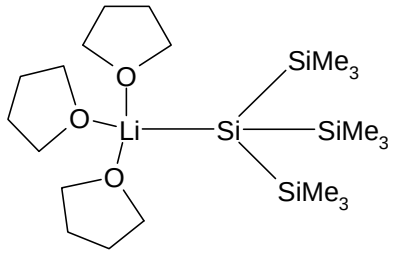

Fig. 2 Solvated $LiSi(SiMe_3)_3$

The first synthesis of base-free lithium hypersilanide was investigated by Klinkhammer with transmetallation between mercury-dihypersilanide and elemental lithium in n-pentane[22].

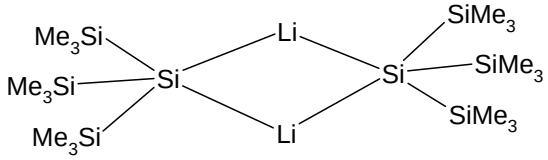

Fig. 3 Dimeric structure of base-free $LiSi(SiMe_3)_3$

The possibility to produce this reagent in high outputs through conversion of chlorohypersilane ClHyp with lithium powder in toluene was recognized by Weidlein[23].

Eq. 2

$$ClSi(SiMe_3)_3 + 2\ Li \xrightarrow{toluene} LiSi(SiMe_3)_3 + LiCl$$

Lithium hypersilanide, although so widely accepted, for about three decades has rarely been the subject of variation. In 1990´s K. W. Klinkhammer has systematically investigated the syntheses and structures of base-free alkali metal hypersilanides $MSi(SiMe_3)_3$ (M=Li, Na, K, Rb, Cs) [24]. Through transmetallation of the dihypersilyl derivatives of the zinc group with alkali metals he obtained firstly the heavy homologues of lithium hypersilanide. All of them possess dimeric structure as shown for LiHyp in Fig. 3.

Eq. 3

$$EHyp_2 + 2M \longrightarrow 2MHyp + E \qquad (E=Zn, Cd, Hg)$$

(M=Li, Na, K, Rb, Cs)

In 1998 Marschner reported a new pathway of synthesis of potassium hypersilanide from tetrakis(trimethylsilyl)silane [25]. Analogue to Gilman´s method for synthesis of lithium hypersilanide, Marschner used KO^tBu instead of MeLi in the metallation reaction.

Eq. 4

$$Si(SiMe_3)_4 + KO^tBu \xrightarrow{THF} KSi(SiMe_3)_3 + Me_3SiO^tBu$$

Potassium hypersilanide can be crystallized from the reaction mixture as THF solvate, but on prolonged heating in dynamic vacuum it can be even obtained in solvent-free form. Therefore, the Maschner-route gives a less hazardous access to solvent-free potassium hypersilanide than the mentioned trans-metallation route with the hypersilyl derivatives of the zinc group, where poisonous starting materials and side-products occur.

The Marschner-route is also suitable for syntheses of RbHyp and CsHyp, where the reagent KO^tBu in Eq. 4 is replaced with RbO^tBu and CsO^tBu, respectively. Perhaps owing to the hazards and costs of Rb and Cs, rubidium- and cesiumhypersilanides have not been extensively used in synthesis. Similar to LiHyp, NaHyp can not be obtained with Marschner-route. Owing to its relatively difficult synthesis the research and application of sodium-hypersilanide is also still deficient.

The heavier alkali metal hypersilanide showed in our research group some advantages. The application of potassium hypersilanide for the synthesis of CuHyp is a typical instance[26].

Nowadays, the reactivity of hypersilyl compounds of the group 1 elements, especially lithium hypersilanide, with compounds of the p, d and f block metals or metalloid halides[27, 28, 29, 30, 31, 32, 33, 34, 35, 36], with organometallic compounds [37, 38, 39], and with organic halides[40, 41, 42, 43] keep increasing research interest. However, the research of their reactivity with unsaturated system has been reported rarely. Only some much smaller silylmetallic reagents such as lithium-trimethylsilanide $LiSiMe_3$ [44]or lithiumdimethylphenylsilylanide $LiSiMe_2Ph$ [45] etc. are by far

the most investigated in the reactions with organic unsaturated systems. The research on the related α,β-unsaturated ketones showed that the smallest lithium silanide reagent $LiSiH_3$ in general attack via 1,2-addition[46,47, 48], whereas lithium trimethylsilanide $LiSiMe_3$ as well as silylcuprates and silylzincates attack via 1,4-addition[49, 50, 51, 52, 53, 54].

1.2 Coordination Chemistry of Azulene System

Azulene and its derivatives, such as guaiazulene (7-isopropyl-1,4-dimethyl-azulen), and chamazulene (7-ethyl-1,4-dimethyl-azulene) etc., are stable cyclic-π-conjugated hydrocarbons. With the conjugated π-electrons they undergo easy electrophilic and nucleophilic reactions.

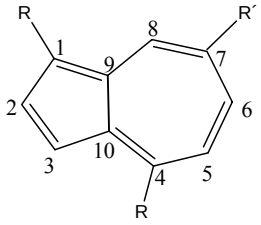

R, R´=H, azulen; R=Me, R´=iPr, guaiazulene, R=Me, R´=Et, chamazulene

Fig. 4 Azulene system

Theoretical calculation[55, 56, 57, 58, 59] of the electron density in azulene revealed that the carbon atoms C1/C3 possess the highest electron density, followed by C9/C10, C5/C7 and C2.

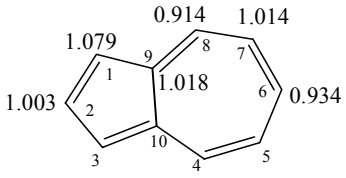

Fig. 5 Theoretically calculated electron density in azulene

Electrophiles therefore attack preferably at C1/C3, and most electrophilic substitutions take place in these two positions[60, 61, 62]. If C1/C3 are blocked by other substituents, the position C5/C7 will become the alternative places to be attacked. In some cases, owing to the steric demand of the introducing substituents, C2 is preferably attacked instead of C1/C3. In nucleophilic reactions, C4/C8 and C6 possessing smaller electron density will be attacked preferably.

Some of the known reactions, moreover, lead to derivatives of the stable ionic aromatic systems cyclopentadienide and tropylium, respectively. Already in azulene itself the seven-

membered ring has a tendency to give one of its π-electrons to the five-membered ring, so that each of the two rings has just 6 π-electrons and fulfil the Hueckel rule. Thus, in azulene a significant dipole moment exists between the five-membered ring and the seven-membered ring, and the five-membered ring is at the negative end of the dipole. The observed dipole moment in azulene is 0.95D[63], which is close to the calculated value of 1.23D[64].

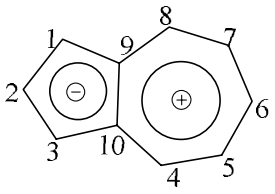

Fig. 6 Polarity properties in azulene

Like electron-rich aromatic compounds, azulene systems undergo electrophilic halogenation, nitration, sulfonation and acylation.

Both of the pseudo-Cp section in the five-membered ring and the pseudo-tropylium section in the seven-membered ring in azulene form easy π-complexes with metal ions. Azulene- or guaiazulene-metal π-complexes have been obtained via *ligand substitution*, *red-ox reaction* of azulene or guaiazulene with metal halides or activated metals, as well as *nucleophilic addition.*

Via ligand substitution Behrens[65] obtained (azulene)-(benzene)Mo (Eq. 5) and (azulene)-(benzene)Mo-$M(CO)_3$ (M=Cr, Mo and W) (Eq. 6).

Eq. 5

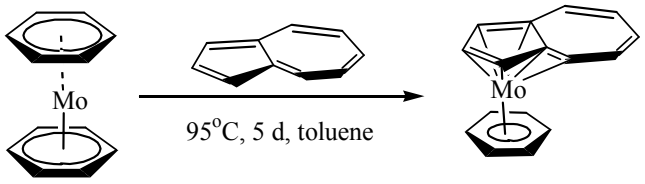

(azulen)-(benzene)-Mo

Eq. 6

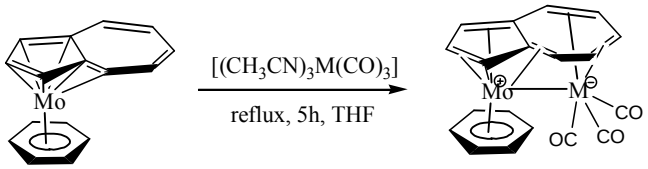

M=Cr, Mo, W

In the complexes the metal atoms (M=Cr, Mo and W) are coordinated by azulene via either η^6- or η^4-mode, respectively, leading to a valence electron count on each metal atom of just 18. Azulene as ligand did not change its π-electron distribution between two rings.

However, it is found that in most complexes the π-electrons in the ligands azulene or guaiazulene are polarized due to the coordination. Thus, the five-membered ring always tends to coordinate to metals as pseudo-Cp ligand in η^5-mode. For the seven-membered ring different bonding modes are observed, depending on the conditions (Fig. 7).

The partly substitution of carbonyl by azulene or guaiazulene enriched the coordination chemistry of azulene system. Through thermal reaction of azulene or guaiazulene with metal-carbonyl compounds a series of mixed multinuclear azulene- or guaiazulene-metal-carbonyls of iron, ruthenium, molybdenum, and manganese[66, 67, 68, 69] were reported since 1958. The crystal structures of $[C_{10}H_8Fe_2(CO)_5]$ (**I**) [70], $[C_{15}H_{18}Fe_2(CO)_5]$ (**II**) [71], $[C_{15}H_{18}Ru_2(CO)_5]$ (**III**) [71], $[C_{10}H_8Mo_2(CO)_6]$ (**IV**) [72, 73], $[C_{15}H_{18}Mo_2(CO)_6]$ (**V**) [74], $[C_{10}H_8Mn_2(CO)_6]$ (**VI**) [75, 76], and $[C_{15}H_{18}Mn_2(CO)_6$ [77] (**VII**) were determined by X-ray diffraction analyses.

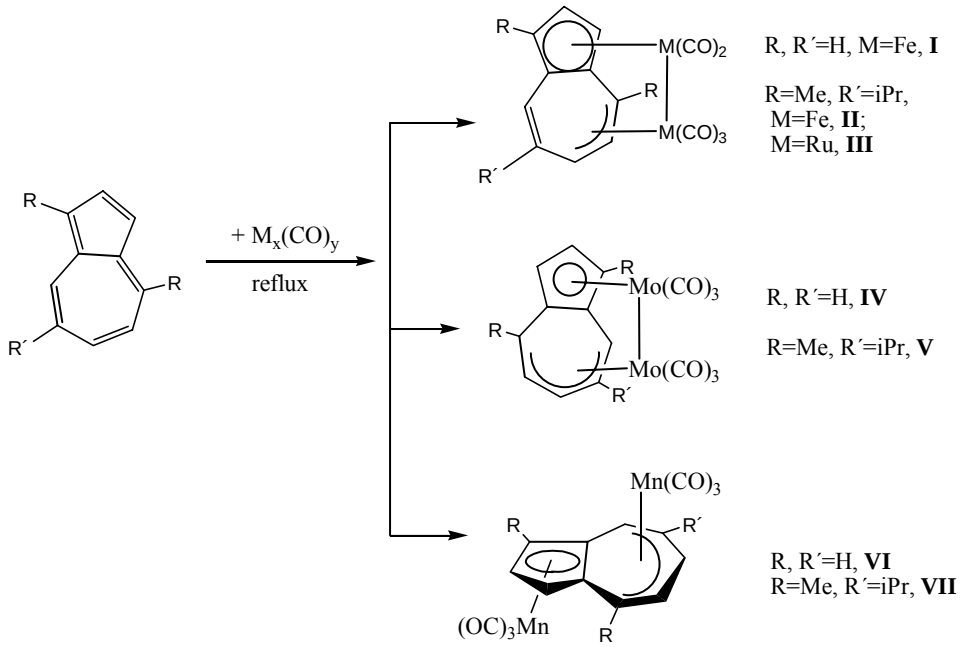

Fig. 7 Reactions of azulene or guaiazulene with metal-carbonyl

In all these compounds the five-membered ring coordinates to metals as a pentahapto ligand, whereas the seven-membered ring coordinated to metal atoms either as trihapto or pentahapto ligand. In each case, 18 valence electron complexes are obtained.

The coordination chemistry of azulene or guaiazulene with metal-carbonyl can be understood as following:

1. Due to the strong coordination power of the carbonyl ligand, not all CO molecules can be substituted by azulene or guaiazulene ligands in the reaction. Thus, preferably the formation of di-nuclear complexes instead of mono-nuclear sandwich metallocene complexes is observed.

2. The spin density of the initially formed radical is dominantly located in 4-, 6- or 8-position (Fig. 8).

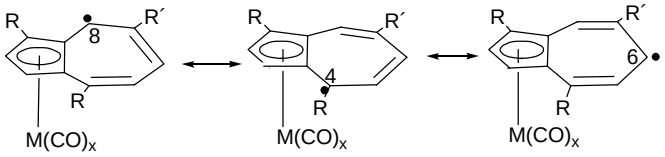

R, R´=H, azulene
R=Me, R´=iPr, guaiazulene

Fig. 8 Resonance structures of the intermediate

(1) If the metal cation, which is directly coordinated to the pseudo-Cp ligand, has only 17-valence electrons, two possibilities for the complementation of the unsaturated coordination of the metal and for the fate of the seven-membered ring radical exist:

(i) A metal-metal bond is formed. The linked second metal cation can coordinate further to the seven-membered ring of the same azulene moiety either via a η^3- (*i.e.* π-allyl) or η^5- (*i.e.* π-pentadienyl) linkage, in order to fulfil the 18-valence-electron rule. Complexes **I**, **II**, **III**, **IV** and **V** are examples of this type.

(ii) Dimerization is the second possibility[78, 79], e.g. the formation of **VIII**, where a simultaneous C-C and M-M bond formation is observed as shown in Eq. 7.

Eq. 7

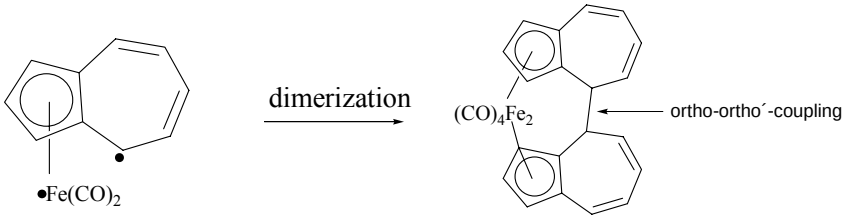

VIII

The coupling mode of the azulene ligand will depend on the relative energies for localization of an electron on the 4-, 6- and 8-positions. Qualitatively, coupling at the ortho-ortho´-positions in azulene would seem to be more probable than at the ortho-para´-positions, since the former conserves a conjugated butadiene system. However, in guaiazulene one must consider yet the steric hindrance of the methyl group in 4-

position, thus, the "ortho-ortho´"-coupling is often observed at the 8,8´- positions. Similarly, the coupling at the 6,8´-positions in guaiazulene has smaller probability.

(2) If the metal cation, which directly coordinated to the pseudo-π-Cp ligand, already attain an 18-valence electron configuration, the subsequent processes must affect only the seven-membered ring radical.

(i) A further metal-carbonyl residue may combine independently to the seven membered ring in η^3- or η^5-mode to form trans-product such as complexes **VI** and **VII**. Similar examples were reported by Klein in 1994[80].

Eq. 8

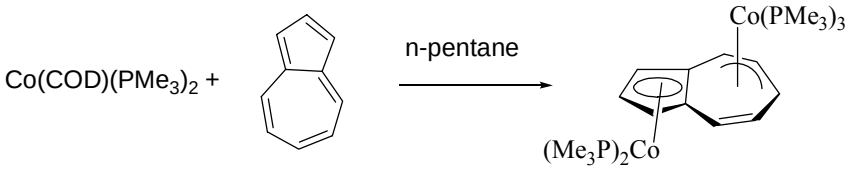

(ii) The second possibility is radical coupling. The radicals dimerize via a carbon-carbon bond. This kind of dimerization has been observed by Wilkinson and Churchill[68, 81].

Eq. 9

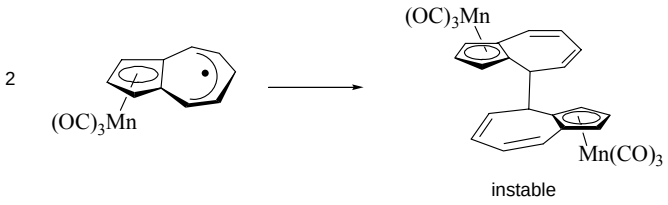

IX

Through red-ox reaction of azulene or guaiazulene with metal halides in the presence of Grignard reagents, or with simply activated metals, metallocene derivatives were obtained. Although the coordination chemistry of azulene- and guaiazulene-metal-carbonyl have developed since early 1960´s, subsequent investigations on the azulene- and guaiazulene-metal-complexes without the participation of CO-ligands are still a less developed subject to chemical research.

In 1964 Fischer and Müller reported firstly a kind of di-azulene iron complexe obtained via following reaction:

Eq. 10

$$FeCl_3 + 2\ C_{10}H_8 \xrightarrow[MgBrX]{\text{ether}} FeC_{20}H_{16}$$

(azulene)

The coordination chemistry of this compound was not clear at this time. They described: "für das Zentralmetall bei der Verbindungsbildung hier die Wahl besteht, entweder π-Elektronen des Sieben- oder des Fünfringes des kondensierten Systems in Anspruch zu nehmen"[82]. Based on the fact that one molecule $FeC_{20}H_{16}$ can absorb five molecules hydrogen, they assumed that the iron was coordinated in a μ-η^4:η^6-mode with four olefinic carbon atoms in the five-membered ring from one azulene molecule and with six olefinic carbon atoms in the seven-membered ring from another azulene molecule.

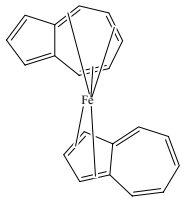

Fig. 9 Supposed structure of Di-azulene-iron(0)

The real structure of this di-azulene-iron complex was revealed four years later in 1968 by Churchill and Wormald by X-ray crystallography[83]. To their surprise, the structure is totally different from the anticipated one. The two azulene ligands have dimerized via ortho-para´ (4-endo, 6´-endo) coupling. Note, however, that similar dimerization reactions through ortho-ortho´(*i.e.* 4,4´) coupling had been reported before for $(C_{10}H_8)_2Fe_2(CO)_8$ [79] (Eq. 7). The azulene moiety again had acted as pseudo-Cp ligand, the iron atom adopts a μ-η^5:η^5-coordination. It is just a substituted ferrocene!

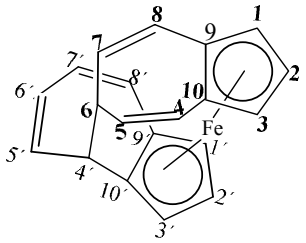

X

Fig. 10 Structure of di-azulene-iron

In 1989 Brintzinger and co-workers reported the structure of 8,8´-biguaiazulenide titanium dichloride[84], where the titanium atom is coordinated also in μ-η^5:η^5-mode with two five-membered rings, and the two seven-membered rings couple with each other in 8,8´-positions.

Eq. 11

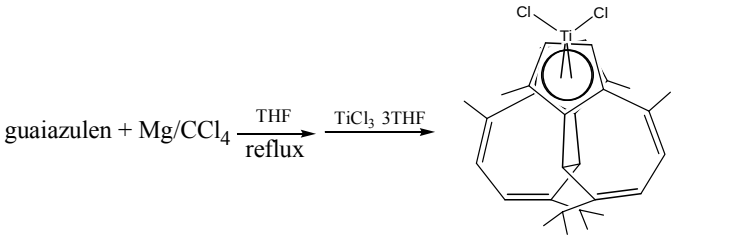

8,8´-biguaiazulenide titanium dichloride

XI

Recently, the research group of Shapiro reported similar calcium mediated fulvene coupling. The reductive coupling of guaiazulene with activated calcium resulted in firstly a mixture of 8,6'- (**XII**) and 8,8'-(diguaiazulenide)calcium (**XIII**) isomers; the former would convert to the latter through thermal rearrangement [85].

Eq. 12

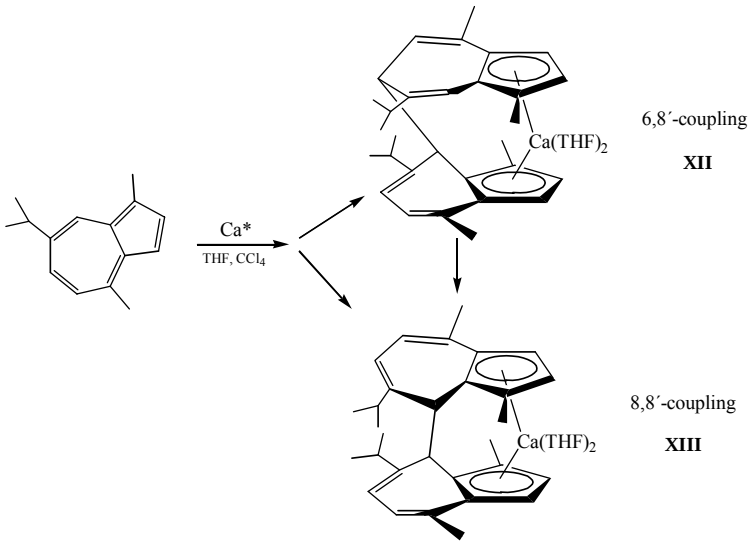

In all these metallocene complexes the coupling modes are similar to the dimerization modes occurred in the formation of metal-carbonyl-azulene-complexes. In azulenyl the seven-membered rings couple with each other either in ortho-ortho´ (4,4´-positions) or in ortho-para´ fashion (4,6´-positions as in compound **X**); in guaiazulenyl either in 8,8´- (**XI**, **XIII**) or in 6,8´-fashion (compound **XII**).

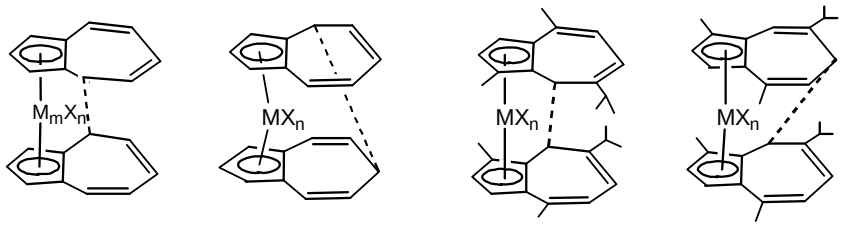

Coupling in: ortho-ortho´ ortho-para´ 8,8´- 6,8´-

Examples: M=Fe, m=2, X=CO, n=4, **VIII** **IX** is special example

M=Fe, n=0, **X**

M=Ti, n=2, **XI**
M=Ca, n=0, **XIII**

M=Ca, n=0, **XII**

Fig. 11 Coupling of the seven-membered rings

The unique coordination mode η^5:η^5-ML_2 in above metallocene derivatives indicate that in the absence of carbonyl the C_5-ring has the strongest coordination ability. Each metal atom attempts to coordinate with two azulene or guaiazulene ligands equally to form mono- rather than multinuclear complexes.

Through nucleophilic addition of organometallic compounds to azulene and subsequent metathesis ferrocene derivatives have been also obtained.

As mentioned above, in azulene the C4/C8 possess the smallest electron density, followed by C6. Thus the organometallic compound with the center of negative charge on the alkyl or aryl group would prefer to attack C4/C8, forming Meisenheimer-type complex, C6 is the alternative addition position.

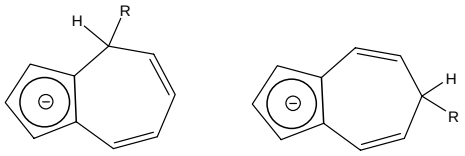

Fig. 12 Meisenheimer-Type Anions

Hafner and Weldes[86] have achieved in 1957 preliminary conclusion that the addition of alkyl-lithium to azulene afforded lithium 4-alkyl-azulenide. The reactions of azulene with several other lithium- and sodium complexes were investigated further by McDonald etc.[87]. It was found that if the bulky triphenylmethanide or dicyclohexylamide were utilized, exclusive addition in 6-position was observed. However, in the case of small groups such as -NMe_2, -CD_2SOCD_3 and methyl group, mixtures of 4-position and 6-position adducts were obtained, in which the former one was preferably formed.

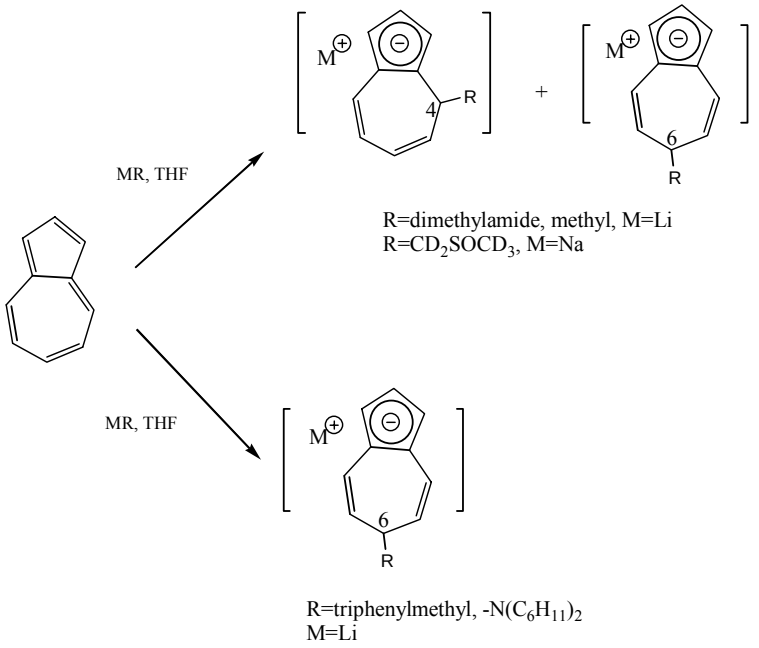

Scheme 1 Nucleophilic addition

Although above nucleophilic adducts have been used as intermediate for synthesis of substituted azulene derivatives in the synthetic organic chemistry, the utilization of them as precursors for synthesis of metallocene or metallocene dichloride complexes is deficient to our best knowledge. The following reaction is the rare example[88].

Eq. 13

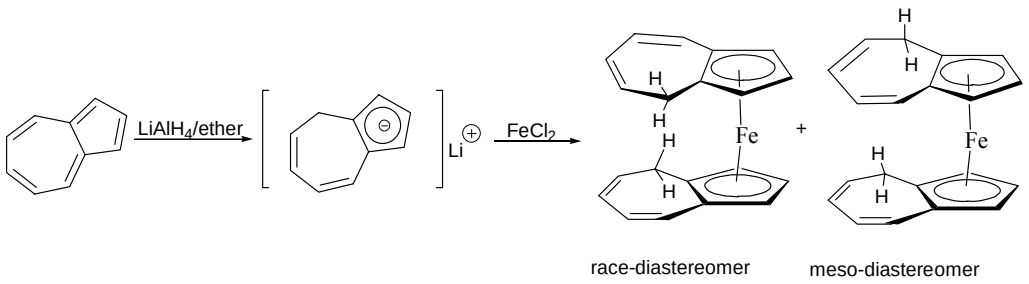

Through above metathesis between lithium 1,4-dihydro-azulene-1-id and iron dichloride two diastereomers of ferrocene derivatives were obtained and separated by chromatographic technique. The analog reaction of phenyl-lithium with azulene, followed with $FeCl_2$, produced a similar mixture [88]. Many problems on the research of this area remained.

Through above mentioned pathways, *i.e.* ligand substitution, red-ox reaction, and nucleophilic addition, a series of azulene or guaiazulene complexes were developed, showing the fascinating coordination chemistry of azulene system. With the increasing research interest in modification of metallocene compounds, especially in the research of Ziegler-Natta catalysts, the red-ox reaction and nucleophlic addition, which result in metallocene derivatives, have

important meaning. The annelleted ring system such as indenyl-, and fluorenyl groups as ligands have been intensive investigated in last several decades[89, 90, 91]. However, the investigation of azulene system as ligand is still deficient.

2 Research Process

2.1 Theoretical Analysis

As a natural product, guaiazulene, namely 7-isopropyl-1,4-dimethyl-azulene, is a relatively inexpensive and easy accessible source for pseudo-cyclopentadienide system.

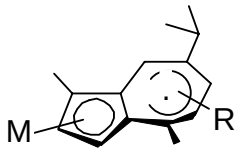

M=Li, Na, K, Rb, Cs

Fig. 13 Alkali metal π-pseudo-Cp guaiazulene complex

In guaiazulene, the *π-orbital density* on the carbon atoms of the seven-membered ring in the LUMO will influence the regio-selectivity of the nucleophilic addition. The consideration of the π-orbital characteristics of the LUMO of guaiazulene through semi-empirical calculations at the PM3 level confirmed that the bulk of the π-orbital density of the cycloheptatriene ring in the LUMO of guaiazulene are at carbon positions 8, 6, and 4 with absolute values of the orbital coefficients of 0.488, 0.457, and 0.289, respectively[85](Fig.14), which is consistent with the *electron density* calculated for azulene system (Fig. 5).

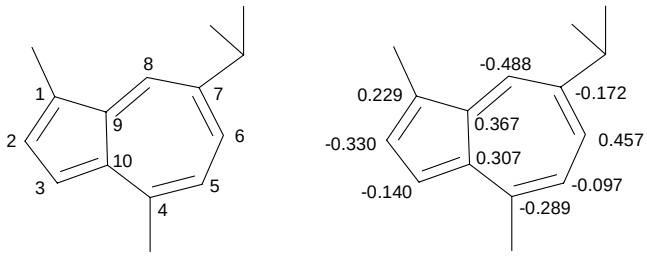

Fig. 14 Carbon atom numbering and carbon π–orbital coefficients of the LUMO from PM3 calculations

As by azulene, the nucleophilic addition of organometallic reagents MR (M=alkali metal, R=alkyl, amide etc.) to guaiazulene will result in constitutional- and stereo-isomers. Actually, due to the unsymmetrical substitution design of guaiazulene it forms more stereoisomers than by azulene.

Due to the steric interference from the methyl substituents at the ring position 4 as well as the much lower orbital coefficient at that position, the probability for carbon 4 to participate in the addition should be much smaller than that for carbon 8 and carbon 6. Thus, the ring 6 and 8 positions are the possibly targets for attack of the nucleophile.

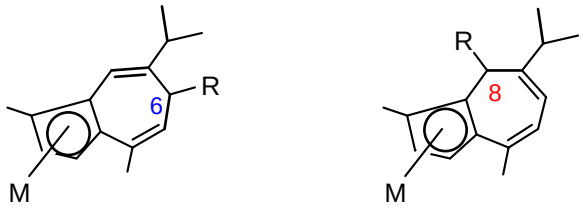

Fig. 15 Formation of constitutional isomer of 6- and 8-R adducts, M=Li, Na, K, Rb, Cs

In each case the R-bonded carbon atom (C6 or C8) becomes a chiral center, each of the constitutional-isomers in Fig. 15 results in two pairs of stereo-isomers, leading to four pairs of diastereomeric enantiomers.

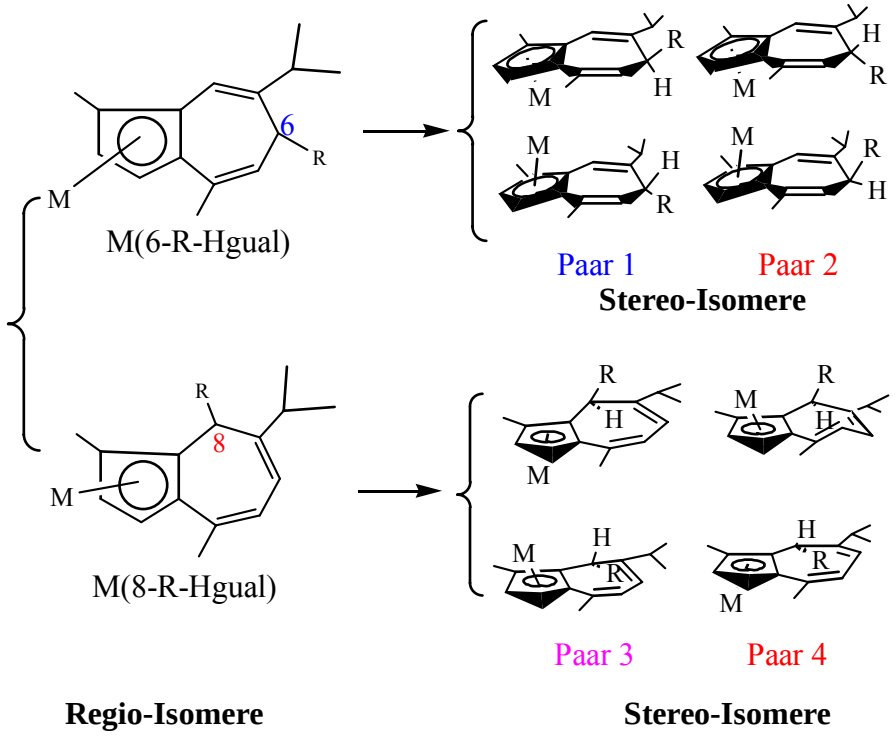

Fig. 16 Diastereomeric enantiomers, M=Li, Na, K, Rb, Cs

If the introduced nucleophile R is small, addition at the ring position 8 is preferable, at least two pairs of enantiomers resulted from the 8-position adduct will be observed; if R is in the middle size, a mixture of 8- and 6-position adducts will produce, and the former should be favourable since a conjugated butadiene system is conserved, however, the reaction system would comprise four pairs of enantiomers; if R is bulky, the addition at the ring position 6 will be preferable; in the extreme case, if R is bulky enough, the 6-position product will be the exclusive adduct, in this case the bulky nucleophile will block one side of the rings, therefore

resulting in only one pair of enantiomer. Hypersilyl group is such a potential bulky substituent, *i.e.* on the addition to guaiazulene the formation probability of ligands 6-Hyp-Hgual should be much larger than that of 8-Hyp-Hgual (Scheme 2),

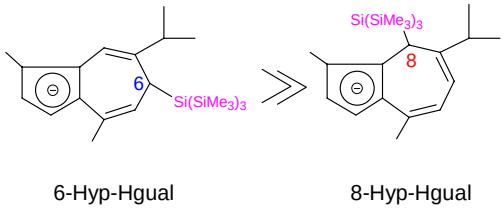

Scheme 2 Formation probability of two kinds of ligands

and from which one pair of stereo-isomer, in which the hypersilyl anion and alkali metal cation stay in two sides of the guaiazulene framework, will become the main stereo-isomer (Fig. 17).

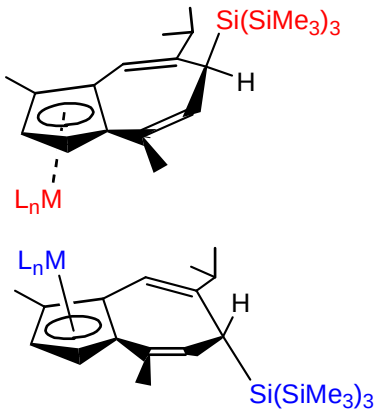

Fig. 17 The bulky nucleophile hypersilyl group may result in only one pair of enantiomer. L=solvent

Metal complexes with chiral ligand such as hypersilyl substituted guaiazulenide anion, where the formation of the ligand anion can be modified through selection or modification of the introduced nucleophile hypersilyl group, are promising candidate for catalysis of olefin polymerization and for some stereo specific or stereo selective syntheses. In this work we will investigate the reactivity of guaiazulene with alkali metal hypersilanides at first, the subsequent research will concentrate on the reactivity of these hypersilyl substituted alkali metal guaiazulenide towards suitable transition metal compounds.

2.2 Mono-Hyp Substituted Alkalimetal Guaiazulenides

2.2.1 Addition

2.2.1.1 Addition of Lithium Hypersilanide to Guaiazulene

When equimolar amounts of guaiazulene and lithium hypersilanide are brought together by adding the solution of the former *dropwise* to the solution of the latter at ambient temperature, either in n-pentane, toluene, or in tetrahydrofuran, the intense blue colour of the guaiazulene disappears immediately, signalling a fast and complete reaction. The nature of the products formed by the addition depends, however, strongly on the solvent used. In n-pentane a fine light yellow powder in 70% yield will precipitate from the solution. The ^{1}H NMR spectrum of the powder is interpreted as the exclusive product of $[Li(6\text{-Hyp-Hgual})]_2$ (**1**). Similarly, if the reaction is carried out in toluene, from the turbid solution exclusive product **1** is detected through ^{1}H NMR spectroscopy. The single crystals of **1** obtained from toluene solution possess dimeric structure.

Eq.14

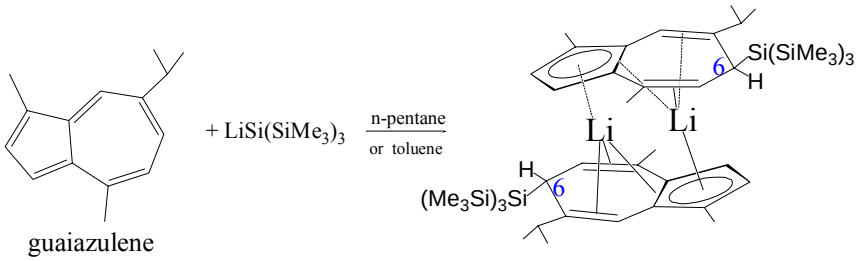

guaiazulene

$[Li(6\text{-Hyp-Hgual})]_2$ (**1**)

In tetrahydrofuran a clear reaction solution can be obtained, but in such a solution apart from the main 6-position adduct $(thf)_n$·Li(6-Hyp-Hgual) a small amount of its constitutional-isomer $(thf)_n$·Li(8-Hyp-Hgual) has been detected by NMR spectroscopy. This isomer has not yet been isolated from this reaction system, however. The ^{1}H NMR spectrum showed that in several weeks at room temperature the latter converted to the former.

2.2.1.2 Addition of Potassium Hypersilanide to Guaiazulene

The reaction of equimolar amounts of potassium hypersilanide and guaiazulene takes place quantitatively in n-pentane, toluene or tetrahydrofuran at room temperature (Scheme 3).

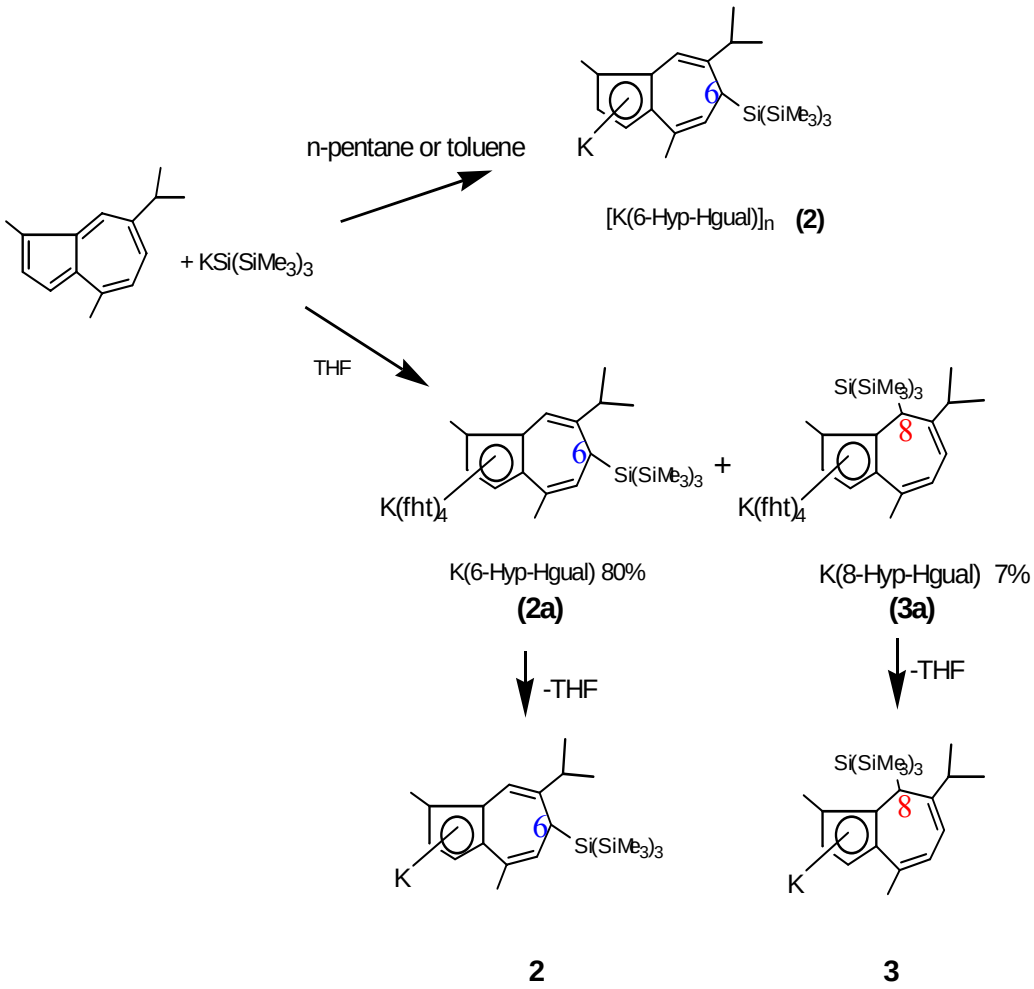

Scheme 3 **Addition of potassium hypersilanide to guaiazulene in different solvents**

Again in toluene or in n-pentane exclusive 6-position adduct is formed, whereas in tetrahydrofuran traces of 8-position adduct is detected, the main product is still the constitutional isomer 6-position adduct. In large-quantity synthesis the accumulated 8-position adduct formed in THF can be isolated by fractional crystallization from tetrahydrofuran.

Different from compound **1**, which can crystallize from toluene, the impure 6-position adduct of $[K(6\text{-hyp-Hgual})]_n$ (**2**) is difficult to purify from *toluene*, since in it compound **2** easy forms gel. Compound **3** has similar properties. Often their fresh prepared solutions in C_6D_6 in NMR tubes will turn to gel-like form in about half an hour, warming the gel it changes to clear solutions again which gives rise to same NMR spectrum as before. This character of solubility of compounds **2** and **3** implies that in toluene or in C_6D_6 they might form similar dimer as compound **1** or even oligomer. On the other hand, compounds **2** and **3** crystallize readily from tetrahydrofuran as solvated monomer. The separation and purification were achieved by virtue of their different solubility in THF. The major component 6-position adduct crystallized as solvate from tetrahydrofuran firstly as light yellow rod-shaped crystals in 80% yield; its structure was established as $(thf)_4$·K(6-Hyp-Hgual) (**2a**) by NMR spectroscopy and by single crystal X-ray diffraction analysis. The constitutional isomer 8-position adduct

crystallized from the concentrated residual solution as deep yellow rod-shaped tetrahydrofuran solvate in 7% yield. The identification of this isomer was accomplished by ^{1}H NMR spectroscopy. A preliminary X-ray crystal structure of the compound **3a** confirmed our assignment, *i.e.* the hypersilyl group is connected to C8 instead of to C6 as in **2a**, and also four tetrahydrofuran molecules coordinated to the potassium atom, resulting in the molecule with formula $(thf)_4$·K(8-Hyp-Hgual) (**3a**). Unfortunately, the quality of the crystallographic data for **3a** is not adequate for publication of the structure at this time. The solvent free potassium complexes $[K(6\text{-Hyp-Hgual})]_n$ (**2**) and $[K(8\text{-Hyp-Hgual})]_n$ (**3**) cab be obtained by warming the pure powder of **2a** and **3a** to 60ºC at reduced pressure (1.0×10^{-3} torr), respectively.

As expected, the isomer **3a** is unstable, in THF over a 1-week period at room temperature it will completely convert to its constitutional isomer **2a**.

2.2.1.3 Addition of Cesium Hypersilanide to Guaiazulene

The addition of cesium hypersilanide to guaiazulene is similar to those of its lighter homologue. In THF it takes place immediately at room temperature and furnishes a yellow-green solution. The NMR spectrum shows two sets of signals originated from $(thf)_n$·Cs(6-Hyp-Hgual) and $(thf)_n$·Cs(8-Hyp-Hgual), respectively. The little amount of latter $(thf)_n$·Cs(8-Hyp-Hgual) in the reaction mixture can convert to the former $(thf)_n$·Cs(6-Hyp-Hgual) by leaving the solution at room temperature for several weeks.

Eq.15

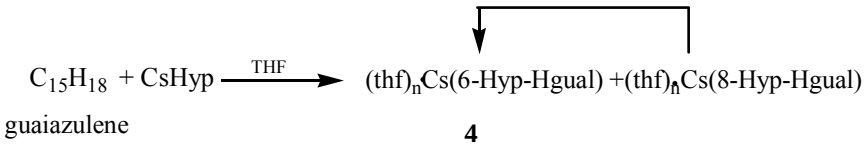

An interesting observation is that compound **4** behaves similar to compound **1** rather than to compound **2**, *i.e.* its solution in toluene does not change to gel even at low temperature, instead, it can crystallize either from toluene or from THF.

As mentioned, guaiazulene is prochiral compound, although through addition chiral carbon atom C6 and/or C8 produced, with the regio- and stereo- selectivity of the bulky hypersilyl group the produced adduct contains only one pair of 50:50 ratio rac-enantiomers. The synthetic approach employed in this study gave always the statistical 50:50 isomer ratio, as expected.

The utilization of chiral reagents, such as (1R)-(-)-fenchone or (-)-sparteine, to separate the two enantiomers, has been investigated. In the experiment the reagent (1R)-(-)-fenchone formed a complex with $[K(6\text{-Hyp-Hgual})]_n$ (**2**) in toluene and precipitated from the solution immediately. Attempts to get the NMR spectrum of the precipitate in d_8-THF or to isolate the two new diastereomers in this precipitate from THF resulted in ligand exchange, *i.e.* the

ligand (1R)-(-)-fenchone was replaced by THF and the two enantiomers **2a** were reproduced equally. Thus, little achievement using (1R)-(-)-fenchone for the separation of two enantiomers is reached.

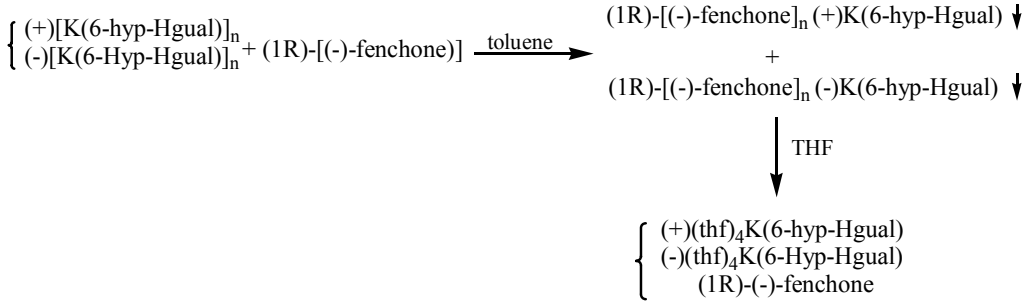

Scheme 4 Experiment of trying to isolate two enantiomers of 2 using (1R)-(-)-fenchone

On the other hand, the stronger base (-)-sparteine can form beautiful white needle-shaped crystals with $LiSi(SiMe_3)_3$, however, this white chiral complex does not show any selectivity in the following reaction with guaiazulene, 50:50 ratio diastereomeric isomers were always detected through NMR spectroscopy. The alternative route (Route 2 in Scheme 5), *i.e.* using (-)-sparteine to separate the enantiomer pair of (+)- and (-)-Li(6-Hyp-Hgual) directly, again did not success, since the two diastereomers dissolve in toluene and n-pentane very good, attempts to crystallize one of them or both of them failed.

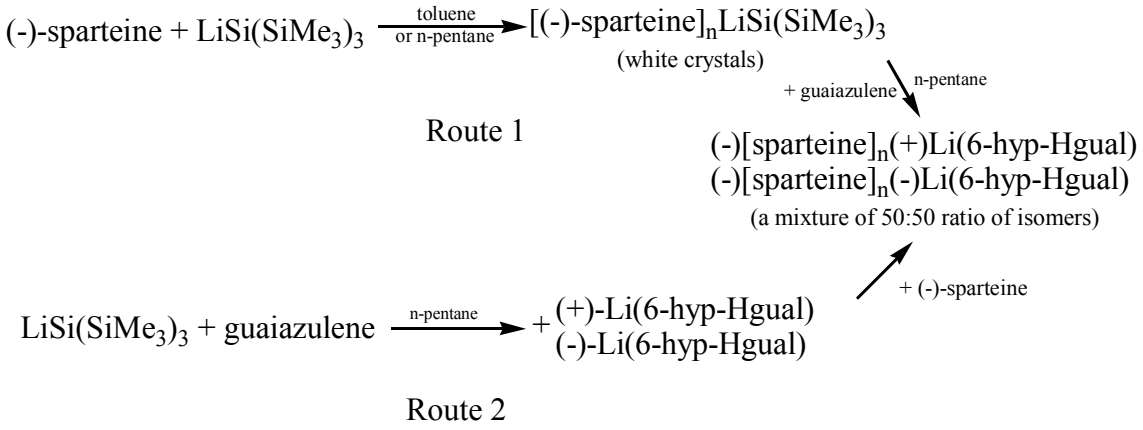

Scheme 5 Experiment of trying to isolate two enantiomers of 2 using (-)sparteine

2.2.2 NMR Spectroscopy

2.2.2.1 ^{1}H NMR Spectroscopy

The numbering of the hydrogen and carbon atoms in the ligands of compounds **1**, **2**, **2a**, **3**, **3a** and **4** are shown in Fig. 18.

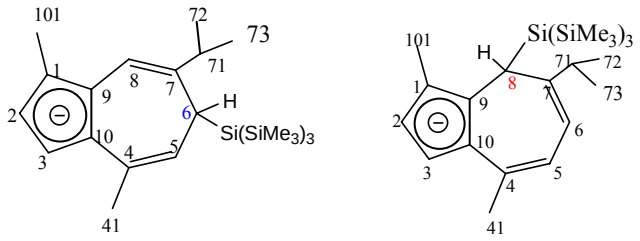

6-hyp-Hgual 8-hyp-Hgual

Fig. 18 Numbering of ligands 6-Hyp-Hgual and 8-Hyp-Hgual anions

In the ^{1}H NMR spectra each ligand of 6-Hyp-Hgual and 8-Hyp-Hgual can give at most 11 signals resulted from 11 different protons of H2, H3, H5, H8, H6, H71, H72, H73, H101, H41 and H_{Hyp}, respectively. Since all distal couplings ($^4J_{HH}$) between H2 and H101, H5 and H41 etc. in the one dimensional NMR spectrum are too weak to observe; only typical proximal coupling ($^3J_{HH}$) will be taken into account.

The most intensive singlet of proton H_{Hyp} (s, 27H) from the hypersilyl substituent – $Si(Si(CH_3)_3)_3$ appears always at the highest field due to low group electronegativity. At somewhat lower field the existens of two doublets of the protons in -$CH(CH_3)_2$ indicates that the free rotation of the two carbon atoms C72 and C73 is hindered (in guaiazulene these two methyl protons are identical, give only one doublet). The singlets of H101, H41 from the methyl protons of the guaiazulene ring, and one septet of the methine proton H71 from the isopropyl group follow successively as shown in Spe.1 for compound **4** and Spe.3 for compounds **2a** and **3a**.

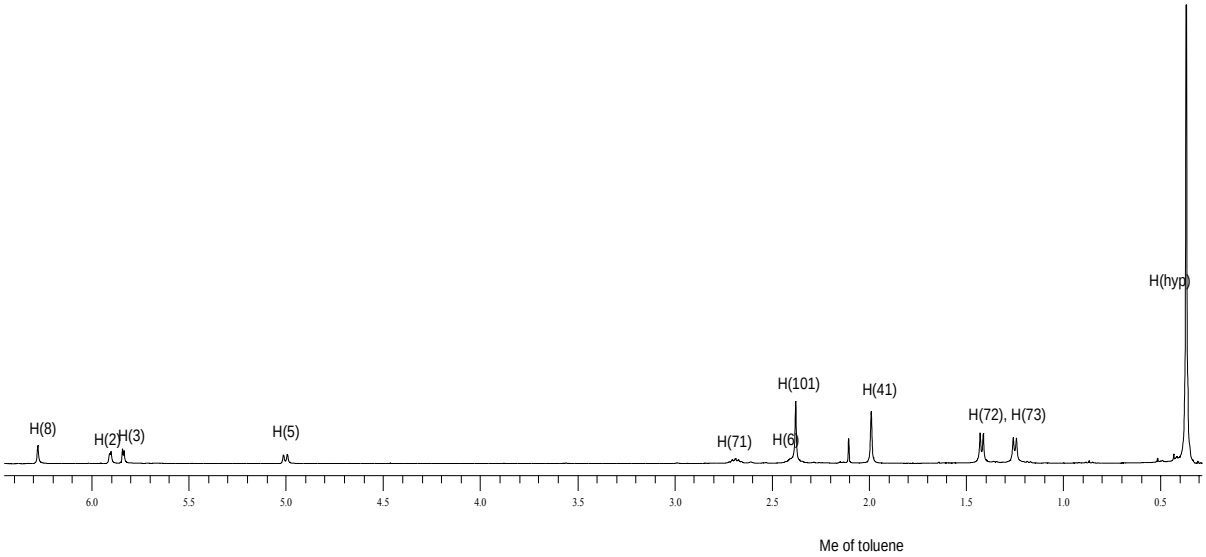

Spe. 1 ^{1}H NMR spectrum of Cs(6-Hyp-Hgual) (4), recorded in C_6D_6 at room temperature

In compounds **1**, **2**, and **4** the two pairs of protons H2 and H3, H5 and H6 are easy to be distinguished from each other by their different coupling constants, and H6, in turn, is easy distinguished from H5 by its resonance in the upfield region. The assignment of the signals of H2 and H3, as well as of H101 and H41 can be achieved with combination of one and two dimensional NMR techniques (^{1}H, ^{1}H-^{1}H COSY).

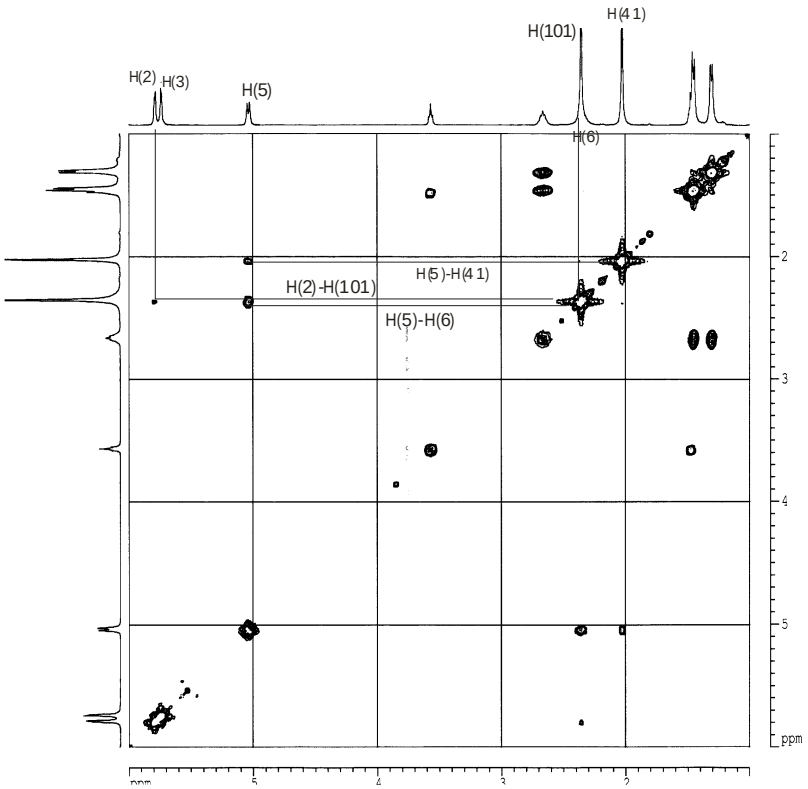

Spe. 2 2D COSY of $(thf)_4$K(6-Hyp-Hgual) (2a) (^{1}H-^{1}H correlation)

Based on the short spatial distances of H2 to H101 as well as H5 to H41 (Fig. 18), their ^{1}H-^{1}H correlations can be observed in the two dimensional ^{1}H-^{1}H COSY spectrum (Spe. 2). Since the doublet of H5 is easy to be identified according to the chemical shift of H6 and the coupling constant between them, from the correlation of H5 with the singlet of the methyl protons of the guaiazulene ring in the two dimensional ^{1}H-^{1}H COSY spectrum the singlet of H41 is readily to be assigned. In the following, the singlet of H101 is distinguished from that of H41, and the doublet of H2 from that of H3.

As shown in Spe. 1, the doublet of H6 is covered by the singlet of H101 in the one dimensional spectrum. However, its correlation with H5 in the two dimensional spectrum implies clearly its resonance position. As can be seen from Spe. 1, the coupling constant between H5 and H6 ($J>8.0$) is much larger than that between H2 and H3 ($2.0<J<3.0$).

The ^{1}H NMR spectra of **1**, **2** and **4** with the same ligand of 6-Hyp-Hgual are similar to each other, but much different from that of **3** with the ligand of 8-Hyp-Hgual. The significant differences of the signals in two ligands are illustrated by the spectra of **2a** and **3a** (Spe. 3).

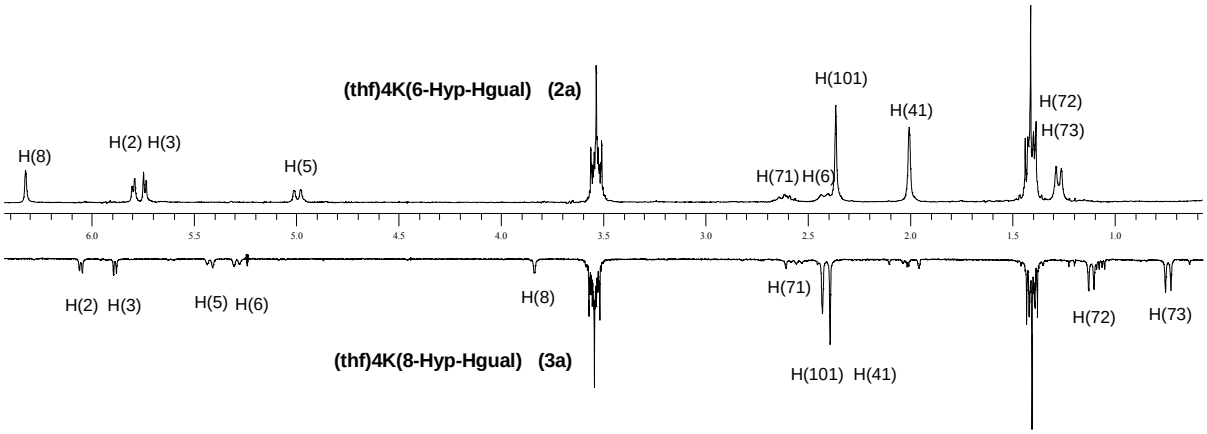

Spe. 3 Comparison of ^{1}H NMR spectra of $(thf)_4K$(6-Hyp-Hgual) (2a) and $(thf)_4K$(8-Hyp-Hgual) (3a) (C_6D_6, 298K, 250.133MHz)

In the spectrum of compound **2a** the signal of the *olefinic* proton H8 appears as singlet at the lowest field, whereas in the spectrum of **3a** as *aliphatic* proton it appears as singlet in the high field region with δ=3.84. On the other hand, although H5 and H6 in **2a** and **3a** couple with each other and show two doublets, in **2a** the doublet of the *aliphatic* proton H6 appears in the high field region ($\delta<4.0$), in **3a** the doublet of the *olefinic* proton H6 appears at low field ($\delta>5.0$). Thus, different from compound **2a**, in compound **3a** *four* doublets at δ 6.05 ($^3J_{HH}$ =3.7Hz), 5.88($^3J_{HH}$ =3.7Hz), 5.42 ($^3J_{HH}$ =6.6Hz), and 5.29($^3J_{HH}$ =6.6Hz) are found in the low field region for the olefinic protons of H2, H3, H5 and H6, which is very similar to the ^{1}H NMR spectral signals for compounds rac-[8,8´-diguaiazulenide]Ca(THF)$_2$ [85] and rac-[8,8´-diguaiazulenide] $TiCl_2$ [84] (Tab.1).

The differences between two types of ligands are also reflected by the different resonance of H101 and H41 as well as those of H72 and H73. Obviously, these shifts are related to the

better delocalized π-electrons in C4 and C5 in compound **3a**. All above results are consistent with the molecular structures established by X-ray diffraction analyses.

The influences of the coordinated THF in compound **2a** to the ^{1}H NMR chemical shifts are shown in Spe.4. In the THF saturated adduct **2a** the signals of H2 and H3 nearly overlap, thus they should be treated as AB-spin system. The signal of H6 is close to that of H71. Moreover, the two doublets of H72 and H73 are located at high field from the multiplets of THF.

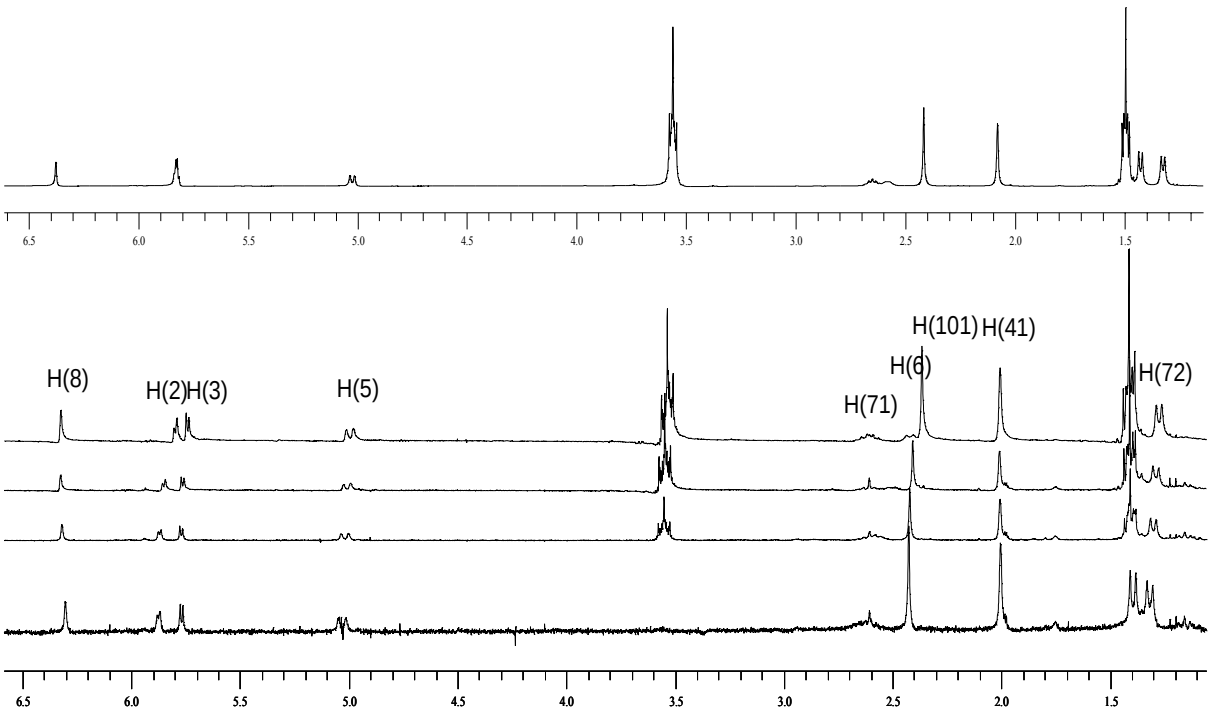

Spe. 4 ^{1}H NMR spectra of 2a and 2 in C_6D_6 at 298K

By gradually removing the coordinated THF, the resonances of H2 and H101 shift down-field, whereas those of H3 and H6 show an upfield shift. Owing to the opposite shift directions the signals of H2 and H3 separated from each other step by step, finally in the THF-free system they can be considered as AX-spin system. On the other hand, the opposite shift directions of H101 and H6 make them meet to each other when THF is nearly completely removed away. In the THF-free compound **2** the signal of H6 is covered by the signal of H101, and the former can be detected only from its correlation with H5 in the two dimensional spectrum. The same case occurs in compound **4** (Spe.1).

The ^{1}H NMR spectra of **1**, **2** and **4** are very similar to that reported for some lithium- and sodium-(6-R)-azulenide, and that of **3** is similar to lithium-, and sodium-(4-R)-azulenide[87]. A comparison of the ^{1}H NMR shifts of these Meisenheimer-Type complexes of azulene- and guaiazulene-1-id is compiled in Table 1.

Tab. 1 NMR spectral data for the Meisenheimer-Type complexes of azulene- and guaiazulene-1-id anions. Chemical shifts are in δ(ppm) and coupling constants are given in hertz. S=singlet, d=doublet, t=triplet, m=multiplet.

Product	*solvent*	*H1*	*H3*	*H2*	*H4*	*H8*	*H5*	*H7*	*H6*
1[e]	*d_8-benzene*	-	*5.73(d) $J_{2,3}$=3.0*	*5.89(d) $J_{5,6}$=3.0*	-	*6.24(s)*	*4.87(d) $J_{5,6}$=8.9*	-	*2.87(d) $J_{5,6}$=8.9*
2[e]	*d_8-benzene*	-	*5.77(d) $J_{2,3}$=3.0*	*5.88(d) $J_{2,3}$=3.0*	-	*6.30(s)*	*5.04(d) $J_{5,6}$ =8.3*	-	*2.43(d) $J_{5,6}$=8.3*
4[f]	*d_8-benzene*	-	*5.84(d) $J_{2,3}$=2.9*	*5.90(d) $J_{2,3}$=2.9*	-	*6.29(s)*	*5.00(d) $J_{5,6}$=7.9*	-	*2.40(d) $J_{5,6}$=7.9*
Li(6-N(C_6H_{11})$_2$-azul)[d]	*d_8-THF*	*5.61(s)*[a]			*6.24 (d,$J_{4,5}$=10.5)*		*4.86 (dd) $J_{4,5}$=10.5; $J_{5,6}$=4.5*		*b*
Li(6-NMe_2-azul)[d]	*d_8-THF*	*5.85(m)*[a]			*6.65 (d, $J_{4,5}$=10.5)*		*4.97(dd) $J_{4,5}$=10.5; $J_{5,6}$=4.5*	*b*	*b*
Li(6-Me-azul)[d]	*d_8-THF*	*5.51-5.61(m)*[a]			*6.26(dd) $J_{4,5}$=9.5; $J_{4,6}$=1.5*		*4.62(dd) ($J_{4,5}$=9.5; $J_{5,6}$=4.0)*		*b*
Na(6-C(ph)$_3$-azul)[d]	*d_8-THF*	*5.88(s)*[a]			*6.49 (d, $J_{4,5}$=9.5)*		*4.79(dd)($J_{4,5}$=9.5; $J_{5,6}$=4.0)*		*b*
Na(6-CD_2SOCD_3)-azul)[d]	*DMSO-d_6*	*5.50-5.60(m)*[a]			*6.34(d, $J_{4,5}$=9.5)*		*5.90 (d, $J_{4,5}$=9.5)*		*b*
Li(4-NMe_2-azul)[d]	*d_8-THF*	*5.83(d) $J_{1,2}$=2.0)*		*5.57(d) $J_{1,2}$=2.0*	*b*	*6.71(d) $J_{7,8}$=10.5*	*5.18(dd) $J_{5,6}$=10.5; $J_{4,5}$=7.5*	*5.32(dd) $J_{7,8}$=10.5; $J_{6,7}$=7.5*	*6.07(dd) $J_{5,6}$=10.5; $J_{6,7}$=7.5*
Li(4-Me-azul)[d]	*d_8-THF*	*5.20(d) $J_{1,2}$=2.5*		*5.54(t) $J_{1,2}$=2.5*	*b*	*6.60(d), $J_{7,8}$=10.5*	*5.10(dd) $J_{5,6}$=10.5; $J_{4,5}$=5.2*	*5.36(dd) $J_{7,8}$=10.5; $J_{6,7}$=6.2*	*5.65(dd) $J_{5,6}$=10.5; $J_{4,7}$=6.2*
Na(4-CD_2SOCD_3)-azul)[d]	*DMSO-d_6*	*5.54(d) $J_{1,2}$=2.5*		*5.13(t) $J_{1,2}$=2.5*	*3.57(d) $J_{4,5}$=6.5*	*6.55(d) $J_{7,8}$=10.5*	*4.98(dd) $J_{4,5}$=6.5, $J_{5,6}$=10.0*	*c*	*5.67(dd) $J_{6,7}$=7.0, $J_{5,6}$=10.0*
3[e]	*d_8-benzene*	-	*6.05(d), 5.88(d) $^3J_{2,3}$ =3.7*		-	*3.84 (s)*	*5.42 (d) $^3J_{5,6}$=6.6*	-	*5.29 (d) $^3J_{5,6}$=6.6*
rac-[8,8´-diguaiazulenide]Ca(THF)$_2$[g 85]	*d_8-THF*	-	*5.63(d), 5.57(d) $^3J_{2,3}$=3.35*		-	*4.13 (s)*	*5.69(d) $^3J_{5,6}$=6.73*	-	*5.52(d) $^3J_{HH}$=6.73*
rac-[8,8´-diguaiazulenide]$TiCl_2$[e 84]	*$CDCl_3$*	-	*7.05(d), 6.60(d) $^3J_{2,3}$=2.5*		-	*4.61 (s)*	*6.31(d) $^3J_{5,6}$=7.0*	-	*5.92(d) $^3J_{HH}$=7.0*

[a] Signals could not be resolved; [b] Signals could not be observed because of overlap with solvent absoptions; [c] Signals could not be observed because of overlap with signals of the major isomer; [d] Recorded on XL-100 spectrometer. [e] Recorded on AM 250 spectrometer; [f] Recorded on AM 400 spectrometer. [g] Recorded on AVANCE 500 spectrometer.

* 6-R-azul = 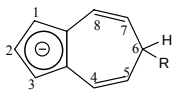 4-R-azul = 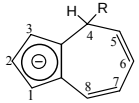

2.2.2.2 ^{13}C NMR Spectroscopy

The experimental data of the chemical shifts in the ^{13}C NMR spectra for all of the compounds **1**, **2**, **3** and **4** are consistent with their structures established by single crystal X-ray diffraction analyses.

In compounds **1**, **2**, and **4** the sixteen different carbon atoms in the ligand 6-Hyp-Hgual anion fall into three groups. The seven aliphatic carbon atoms (C_{Hyp}, C101, C41, C71, C72, C73, and C6) give rise to seven signals in the high field region ($\delta < 40$), of which the carbon atoms in the hypersilyl group show one signal in the expected range ($2.30 < \delta < 2.70$). The four secondary olefinic carbon atoms (C2, C3, C8, and C5) give rise to signals in the low field region ($100 < \delta < 120$), and the five tertiary olefinic carbon atoms (C1, C4, C7, C9, and C10) give rise to signals at even lower field ($114 < \delta < 145$).

The combination of DEPT 135 and ^{13}C-^{1}H correlated spectroscopy yielded following diagram for compound **2a**.

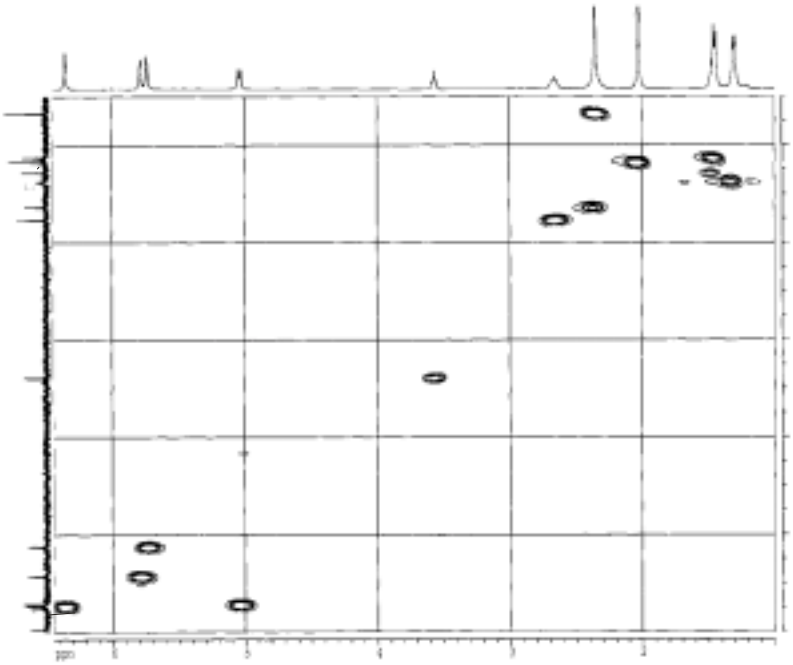

Spe. 5 2D COSY of 2a (^{1}H-^{13}C correlation)

As can be seen in Spe. 5, the ^{13}C NMR order deviates from the corresponding ^{1}H NMR order. The ^{13}C NMR order for **2a** from high-field to low-field has the sequence of C_{Hyp}, C101, C72, C41, C73, C6, C71, C3, C2, C5 and C8.

The ^{13}C NMR spectrum of **3** is different from those of **1**, **2** and **4**. The significant differences between them are reflected again with the signals of C6 and C8. While the carbon atoms C8 and C6 in all of compounds **1**, **2**, and **4** show olefinic- and aliphatic-features, respectively, in compound **3** the properties is inversed, the carbon atom C8 is aliphatic-, while C6 olefinic-carbon atom (see Tab. 2).

Tab. 2 Selected ^{13}C NMR spectral data for 1, 2, 4 and 3 recorded in C_6D_6 at 300K (δ, ppm)

	C1, C4, C7, C9, C10	C5	C2	C3	C6	C8
Li(6-Hyp-Hgual) (1)	134.0; 132.6; 121.4; 117.5; 114.2	115.0	106.1	101.0	32.8;	117.6
K(6-Hyp-Hgual) (2)	134.3; 130.5; 123.1; 119.5; 115.3	114.3	108.6	102.5	32.7	114.6
Cs(6-Hyp-Hgual) (4)	133.3; 131.5; 124.8; 121.1; 116.4	112.2	111.4	105.1	32.6	115.5
K(8-Hyp-Hgual) (3)	143.5; 139.1; 122.2; 119.7; 107.7	117.7; 112.9; 110.8; 101.4				35.6

Compare to the ^{13}C NMR spectral data for the known dominantly ionic complexes LiCp and NaCp [92] (Tab. 3), the interaction between the alkali metal cation and the C_5 ring in complexes **1**, **2**, **3**, and **4** can be also interpreted as predominantly ionic bonds, since the five olefinic carbon atoms, namely C1, C2, C3, C9, and C10, in the five-membered ring in complexes **1**, **2**, **3**, and **4** (Fig. 18) give rise to signals also in the low field region (δ>100) as for compounds LiCp and NaCp.

Tab. 3 ^{13}C NMR spectral data of several compounds [92]

Dominant bond type	Ionic			Covalent
Compound	LiCp	NaCp	$MgCp_2$	$FeCp_2$
^{13}C NMR δ (ppm)	103.6	103.4	108.0	68.2

2.2.2.3 ^{29}Si NMR Spectroscopy

Two different silicon atoms in the hypersilyl group, namely the central α-Si and three peripheral β-Si atoms in -$^{\alpha}Si(^{\beta}SiMe_3)_3$, give rise to two signals. The signals of the β-Si in compounds **2** and **4** measured in C_6D_6 at room temperature appear at about -12 ppm as a strong signal, and those of α-Si at about -77 ppm as a weak signal. Due to the poor solubility of compound **1** in C_6D_6, its ^{29}Si NMR spectrum missed. Instead, the ^{29}Si NMR spectrum for compound $(thf)_nLi$(6-hyp-Hgual) **1a** was recorded in d_8-THF, showing -6.7 ppm for the peripheral silicon atoms and -69.9ppm for the central silicon atom. These ^{29}Si NMR spectral data for **1a**, **2**, and **4** are similar to those of other hypersilyl substituted compounds with C-$Si(SiMe_3)_3$ bonds (Table 4).

Tab. 4 Chemical shifts δ of ^{29}Si (ppm) and coupling constants J(Hz) in C_6D_6

Compound	δ ^{29}Si (-Si(<u>Si</u>Me$_3$)$_3$)	δ ^{29}Si (-<u>Si</u>(SiMe$_3$)$_3$)	$^1J_{(\beta\text{-Si-C})}$
(thf)$_n$Li(6-Hyp-Hgual) (**1a**)	(-6.68*)	(-69.9*)	(43.5)*
(thf)$_4$K(6-Hyp-Hgual) (**2**) (**2a**)	-12.1(-6.75*)	-76.3(-70.9*)	43.3
(thf)$_n$Cs(6-Hyp-Hgual) (**4**)	-12.0	-77.6	
4-isopropyl-benzyl-hypersilane[93]	-12.7	-76.6	44.2
4-propyl-1-Hyp-benzene [93]	-12.8	-77.3	44.2
PhSi(SiMe$_3$)$_3$ [94]	-12.8	-76.8	
[PhSi(SiMe$_3$)$_2$]$_2$ [94]	-11.3	-70.7	

* Data in bracket are recorded in d_8-THF.

Compare to the ^{29}Si NMR data in compounds MSi(SiMe$_3$)$_3$ with bond M-Si, in Si(SiMe$_3$)$_4$ with Si-Si, in HSi(SiMe$_3$)$_3$ with H-Si, and in XSi(SiMe$_3$)$_3$ with X-Si, the ^{29}Si NMR spectral data in compounds **1a**, **2** and **4** with bond C-Si fall into the expected region (Tab. 5).

Tab. 5 Comparison of ^{29}Si NMR spectral data

compounds	δ(ppm) for α-Si	δ(ppm) for β-Si
M-Si(SiMe$_3$)$_3$ [24, 95] (M=Li, Na, K, Rb, Cs)	-189 ~ -179	-8.9 ~ -5.3
R$_2$M-Si(SiMe$_3$)$_3$ [96, 97] (M=Al, R=Me, Et) (M=Ga, In, R=Me)	-169 ~ -137	-8.6 ~ -7.5
Me$_3$Si-Si(SiMe$_3$)$_3$	-134.3	-9.8
H-Si(SiMe$_3$)$_3$	-115.6	-11.6
1a, **2**, **4** as well as other compounds with C-Si(SiMe$_3$)$_3$	-90 ~ -70	-13.0 ~ -11.0
X-Si(SiMe$_3$)$_3$ [97] (X=F,Cl,Br,I)	-5.78 ~ 33.4	-13.7 ~ -11.5

2.2.2.4 ^{7}Li NMR Spectroscopy

As deduced from the ^{13}C NMR spectral data, in compound **1** the interaction between Li-C_5(ring) is dominantly ionic. In solution the ion pair of cation and the anion can exist either in contact ion pair or solvent separated ion pair, which can be reflected from the ^{7}Li NMR data. According to literature[98, 99], the contact ion pair show often ^{7}Li NMR signal at much higher field than the solvent separated ion pair (Tab. 6). The ^{7}Li NMR spectrum recorded in d_8-THF for compound **1a** displays a singlet at -3.63ppm. Compare the value with those of LiCp and LiC(C_6H_5)$_3$ it can be supposed that compound **1a** in tetrahydrofuran should behave mainly as solvent-separated ion pair.

Tab. 6 Comparison of chemical shifts in ^{7}Li NMR spectra

Complex	^{7}Li (δ, ppm)	Type
(thf)$_n$Li(6-Hyp-Hgual) (**1a**)	-3.63(THF)	between solvent-separated ion pair and contact ion pair
$Li^+C(C_6H_5)_3^-$	-1.11(THF)	solvent-separated ion pair
$Li^+C_5H_5^-$	-8.37(THF)	contact ion pair
	-0.88(HMPA)	solvent-separated ion pair

2.2.3 Molecular Structures of Compounds 1 and 2a

By slowly cooling of the hot saturated solution of compound **1** in toluene colourless rod-shaped single crystals suitable for X-ray diffraction analysis was obtained. The light yellow rod-shaped single crystal of **2a** was obtained from tetrahydrofuran. Selected crystallographic data are listed in Tab. 7.

Tab. 7 Selected crystallographic data for 1 and 2a

	1	**2a**
Empirical formula	$C_{24}H_{45}LiSi_4$	$C_{40}H_{77}KO_4Si_4$
Formula weight (g/mol)	452.90	773.48
Temperature (K)	293(2)	293(2)
Crystal system	monoclinic	monoclinic
Space group	$P2_1/c$	$P2_1/n$
Unit cell dimensions (Å, deg)	a=18.878(4) b=9.870(2) c=15.866(3) β=103.24(3)	a=9.9317(14) b=22.913(2) c=20.6591(19) β=95.766(9)
V(Å^3)	2881.3(10)	4677.5(9)
Z	4	4
$\rho_{calc.}$ (Mg/m^3)	1.044	1.098
λ (Å)	0.71073	0.71073
Absorption coefficient (mm^{-1})	0.215	0.250
Number of reflections collected	13318	11770
Number of independent reflections	6623 [R(int)=0.0647]	11153 [R(int)=0.0628]
Data / restraints / parameters	6623 / 0 / 442	11153 /117 / 526
Goodness-of-fit on F^2	1.027	0.801
$R(F_o)$ [I>2σ(I)]	0.0501	0.0522
$wR(F_o^2)$ [I>2σ(I)]	wR2=0.1047	0.1181

2.2.3.1 Molecular Structure of [Li(6-Hyp-Hgual)]$_2$ (1)

The X-ray diffraction analysis showed that compound **1** has $C_{24}H_{45}Si_4$ as asymmetric unit. In the unit cell four of these moieties form two pairs of dimeric sandwich structure as [6R, (6A)S]-[(μ-Li-η^5:η^6-(6-Hyp-1,6-dihydro-guaiazulene-1-id)]$_2$ (Fig. 19).

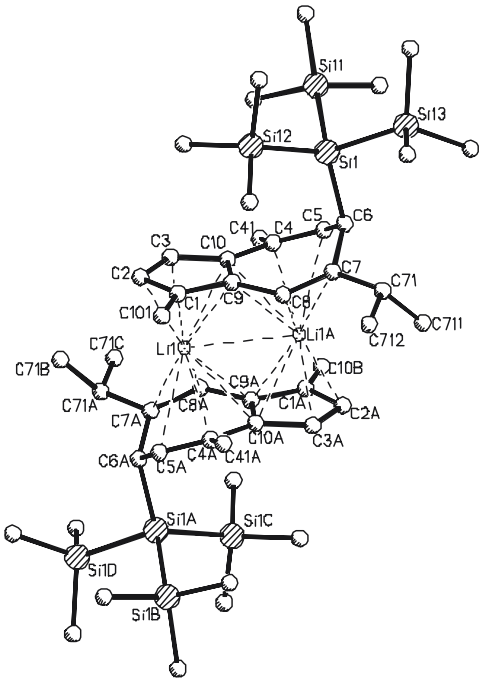

Selected bonds lengths(pm) and bond angles(deg)

Li(1)-C(2)	219.4(5)	Li(1)-C(8A)	240.9(5)
Li(1)-C(3)	223.9(4)	Li(1)-C(4A)	243.7(5)
Li(1)-C(1)	228.9(5)	Li(1)-C(9A)	252.2(5)
Li(1)-C(10)	239.3(4)	Li(1)-C(10A)	252.8(5)
Li(1)-C(9)	242.1(4)	Li(1)-C(5A)	262.6(4)
Li(1)-Li(1A)	281.5(8)	Li(1)-C(7A)	266.4(4)
C(2)-C(1)	140.6(3)	C(2)-C(3)	140.8(4)
C(3)-C(10)	141.9(3)	C(10)-C(9)	143.6(3)
C(9)-C(1)	142.6(3)	C(10)-C(4)	146.2(3)
C(6)-C(7)	151.6(3)	C(4)-C(5)	134.9(3)
C(7)-C(8)	134.8(3)	C(5)-C(6)	151.3(3)
C(8)-C(9)	146.4(3)	C(6)-Si(1)	197.4(2)
Me_3Si-C	187.6(4)	Si-Si(aver.)	236.7

Li(1)-$C_{5(cent.)}$	196.9	Li(1)-$C_{6(cent.)}$	195.6

$C_{5(cent)}$-Li(1)-C_6(cent) 161.3°

Fig. 19 Molecular structure of meso-[6R, (6A)S]-[(μ-Li-η^5:η^6-(6-Hyp-1,6-dihydro-guaiazulene-1-id)]$_2$. Atoms are represented by spheres of arbitrary radii; dashed lines are used to symbolize interatomic distances markedly smaller than the sum of the corresponding van der Walls radii; hydrogen atoms are omitted for clarity.

In the dimer the two ligands take anti-parallel orientation. Two chiral carbon atoms C6 and C6A possess S- and R-configuration, respectively. With this configuration the methyl and isopropyl groups in both guaiazulene frameworks are directed away from each other. The two bulky hypersilyl groups stretch away from the central lithium cations in opposite directions and locate above and below the seven-membered rings of the guaiazulene frameworks, respectively, shielding them like two umbrellas, thus preventing the formation of an infinite chain structure formed for many other lithium cyclopentadienide derivatives[100, 101, 102]. Due to the inversion center a meso-dimer is constructed.

Two lithium cations are encapsulated by two anti-parallel arranged carbanions. Each lithium cation is η^5:η^6-coordinated by the C_5-ring from one guaiazulene moiety and six olefinic carbon atoms of the seven-membered ring from the other guaiazulene moiety. The lithium cations show close contacts with a Li-Li distance of 281.5(8)pm, which is only about 6pm longer than for the base-free precursor α-[$LiSi(SiMe_3)_3]_2$ [24]. The bridgehead carbon atoms C9, C9A, C10, C10A have interaction to both of the two Li cations, forming two tetrahedrons with Li-Li as a common edge.

The structural parameters in **1** are similar to that of some chain structural compounds $(LiCp^R)_n$. For convenient comparison the related parameters for these compounds are summarized in Tab.8.

In compound **1** the Li-$C_{5(cent.)}$[I] distance is 196.9pm, the average value of Li-$C_{5,(aver.)}$[I] is 230.7pm, ranging from 219.4 to 242.1pm, being similar to corresponding distances in

[I] M-$C_{5(cent.)}$ means the distance of the metal cation to the centroid of the coordinated C_5 ring.

compound $[LiCp]_n$. In the seven-membered ring the Li-$C_{6(cent.)}$[II] distance is 195.6pm, the average Li-$C_{6,\,(aver.)}$[III] distance is 253.1pm, ranging from 240.9 to 266.4pm, of which the C8 and C4 are closest to the lithium atom, while C5 and C7 are further apart from it. The average bond lengths of the delocalized C-C bonds are 141.9 and 141.2pm for the five-membered ring and seven-membered ring, respectively.

Tab. 8 Bond distances (pm) in lithium cyclopentadienide complexes

Compound	Li-$C_{5(cent.)}$ (pm)	Li-$C_{6(cent.)}$ (pm)	$C_{5(cent.)}$-Li-$C_{5(cent.)}$ (deg)	Li-$C_{5,(aver.)}$ (pm)	C-C (aver.) (pm)	Li1-Li2	Ref
1	196.9	195.6	161.3	230.7 (Li-$C_{5,\,(aver.)}$) 253.1 (Li-$C_{6,(aver.)}$)	141.9(C_5) 141.2 (C_7, sp^2-C)	281.5(8)	this work
$[LiCp]_n$	196.9			230.7	141.3		[100]
$[LiCp^*]_n$	191.1			225.5			[101]
$[Li(Flu)]_2$ (Flu=Fluorenyl)		195.7 195.1	~180	240.8 (Li-C_6)	141.0	434.5(9)	[103]
[Li(dimethylfluo-renylsilyl)(C_5H_4)]$_n$	196.0; 197.3			230.4	141.3		[104]
{[μ-η^5:η^5-$C_5H_4(SiMe_3)$]Li}$_n$	195.7~ 198.2 (average 196.7)			230.6	141.6		[105]
$[LiInd]_n$ (Ind=Indenyl)	198.3			232.0 (Li-C_5)	141.6		[105]
15	188.5; 186.6			224.5; 222.7 (Li-C_5) 241.8; 244.4 (Li-C_7)	143.0 143.8	339.7(10)	this work
{$Li_2(THF)_2[C_{24}H_{14}](SiMe_3)_2$}$_2$	204 (external Li) 205, 209 (internal Li)		163.1	239.7		449.9	[106]

During last decade two kinds of lithiumcyclopentadienide derivatives with similar dimeric sandwich structure as for **1** have been reported. One is lithium fluorenide $[LiFlu]_2$ (Flu=Fluorenyl)[103], where the lithium cation is η^6:η^6-coordinated, the other is a compound with the formula {$Li_2(THF)_2[C_{24}H_{14}](SiMe_3)_2$}$_2$ [106], where two internal lithium cations are η^5:η^5-coordinated and two external lithium cations are coordinated with one η^5-Cp and two tetrahydrofuran molecules (Fig. 20).

[I] M-$C_{5,(aver.)}$ means the average bond distance of the five M-C distances, C is the carbon atoms in the C_5 ring.
[II] M-$C_{6(cent.)}$ means the distance of the metal cation to the centroid of the six olefinic carbon atoms in the seven-membered ring.
[III] M-$C_{6,(aver.)}$ means the average bond distance of six M-C distances, C is the olefinic carbon atoms in the seven-membered ring.

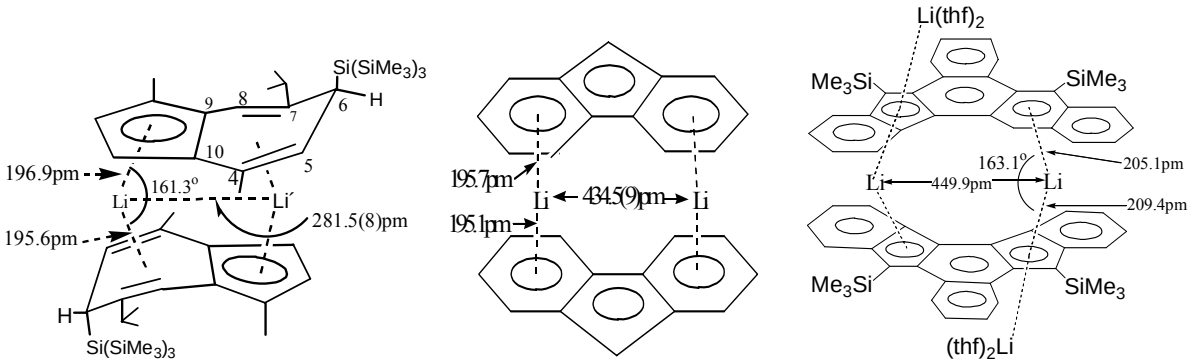

Fig. 20 Pictorial representation of selected bonding parameters: Left, 1; Middle, $[Li(Flu)]_2$; Right, $\{Li_2(THF)_2[C_{24}H_{14}](SiMe_3)_2\}_2$

As shown in Fig. 20, among the three compounds, the ligands in $\{Li_2(THF)_2[C_{24}H_{14}](SiMe_3)_2\}_2$ and $[LiFlu]_2$ are coplanar. In compound **1** only the aromatic C_5 rings are coplanar, the seven-membered rings are neither aromatic nor co-planar, instead they fold in boat-like shape owing to the influence of the bulky hypersilyl group.

Some parameters are shown in Fig. 20 and Fig.21. Here the folding angle α (2.0°) is defined as the dihedral angle between the C_5-ring plane and the best plane through the atoms C9, C10, C4, C8; the folding angle β (19.8°) represents the dihedral angle between the best plane through the atoms C9, C10, C4, C8 and the best plane through the atoms C4, C5, C7, C8; and the folding angle γ (39.9°) is the dihedral angle between the best plane through the atoms C4, C5, C7, C8 and the best plane through the atoms C5, C6, C7. All folding angles in the following compounds, if not specially mentioned, are defined in the same way as for this compound.

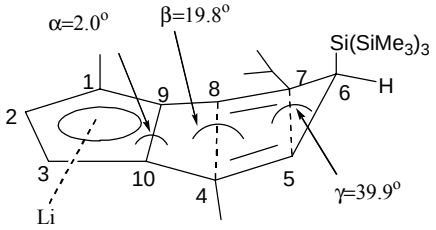

Fig. 21 Folding angle for compound 1

In compound **1** the folding angles increase along the sequence α, β, γ. Apparently the steric demand of the bulky hypersilyl group plays a key role. It stretches severely away from the seven-membered ring, resulting in the largest folding angle γ. C5 and C7 are drawn together with the hypersilyl group away from the lithium atom, resulting in a folding angle β smaller than γ, but larger than α, which is consistent with the larger bond distances of Li-C5′ and Li-C7′.

Considering the interactions of Li-Li′ and Li-C_5(ring) or Li-C_6′(ring) in above three sandwich compounds, compound **1** has the shortest Li-Li distance, since in it the two coordinated parts

within one ligand are annelleted neighbour rings, in other two compounds they are separated by one C_5- or C_6-ring. On the other hand, the Li-$C_{5(cent.)}$ distances in **1** are similar to the Li-$C_{6(cent.)}$ distance in compound Li(Flu), but much shorter than that found in $\{Li_2(THF)_2[C_{24}H_{14}](SiMe_3)_2\}_2$. The found angle of $C_{5(cent.)}$-Li-$C_{6(cent.)}$ in **1** (161.3°) has nearly the same value as in $\{Li_2(THF)_2[C_{24}H_{14}](SiMe_3)_2\}_2$ (163.1°).

The bond distances and bond angles in the hypersilyl group -$Si(SiMe_3)_3$ in **1** are generally within normal range [107]. The bond distance of C6-Si is about 10 pm longer than that of C-Si within hypersilyl group.

2.2.3.2 Molecular Structure of $(thf)_4 \cdot$K(6-Hyp-Hgual) (2a)

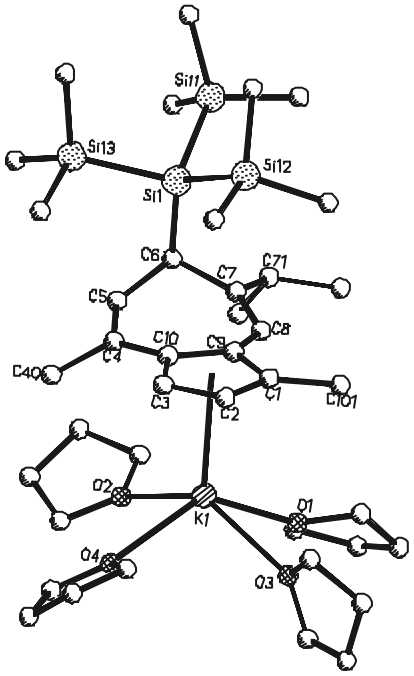

Selected bond lengths(pm) and bond angles(deg)

K1-C3	305.2(3)	K1-O1	279.1(2)
K1-C10	307.0(3)	K1-O2	278.0(2)
K1-C2	307.3(3)	K1-O3	279.4(2)
K1-C9	307.6(3)	K1-O4	275.4(5)
K1-C1	308.2(3)	C2-C3	138.7(4)
K1-$C_{5(cent.)}$	282.4	C2-C1	139.5(4)
C3-C10	141.6 (4)	C10-C9	142.4(3)
C9-C1	142.3(4)	C10-C4	145.6(4)
C4-C5	133.1(4)	C5-C6	150.0(4)
C6-C7	151.4(4)	C7-C8	133.8(3)
C8-C9	144.9(3)	Si1-C6	194.9(3)
average Si-C in -$Si(SiMe_3)_3$		186.8	
average Si-Si		235.5	

O4-K1-O2	87.6(11)	O2-K1-O1	83.65(7)
O4-K1-O1	136.2(3)	O2-K1-O3	141.39(7)
O4-K1-O3	83.4(6)	O3-K1-O1	78.03(8)
$C_{5(cent.)}$-K1-O1	116	$C_{5(cent.)}$-K1-O3	106
$C_{5(cent.)}$-K1-O2	112	$C_{5(cent.)}$-K1-O4	107

Fig. 22 Molecular structure of 2a. Atoms are represented by spheres of arbitrary radii; hydrogen atoms are omitted for clarity (one molecule of THF is in disorder)

The X-ray diffraction analysis of compound **2a** acquired from THF showed that four molecules, each of them as shown in Fig. 22, are arranged in the unit cell. In these monomers the potassium cation is η^5-coordinated with a planar five-membered ring, its coordination sphere is complemented by four oxygen atoms from four tetrahydrofuran molecules. The five-membered ring is not parallel to the best plane through the atoms O1, O2, O3 and O4, but is tilted a little toward O(3) and O(4) (5.7°), which is consistent with the smaller angles of $C_{5(cent.)}$–K(1)-O(3) and $C_{5(cent.)}$-K(1)-O(4) (Fig. 22). The bulky hypersilyl group shields the seven-membered ring from the other side of the ring against potassium cations. The whole molecule exhibits a swivel chair geometry, in which four coordinated tetrahydrofuran molecules serve as “feet”, and the upwards folded seven-membered ring as “chair backs”.

The average bond distance of K-$C_{5,(aver.)}$ in **2a** (306.8pm) is much longer than that of Li-$C_{5,(aver.)}$ in **1** (230.7pm) owing to the larger ionic radius of potassium atom. However, the average C-C bond distance in the five-membered ring is 140.9pm, being similar to that in compound **1**.

The seven-membered ring in **2a** is also folded as in **1**, leading to somewhat different folding angles: 7.1°, 20.8° and 41.2° (cf. **1**: 2.0°, 19.8° and 39.9°). Apparently this is related to the different aggregation states of these two compounds. In the monomer **2a** the seven-membered ring has no strong interaction with the potassium cation, it folds away from the potassium cation freely, resulting in larger folding angles. On the other hand, the hypersilyl group itself in **2a** is less restricted than in **1**, therefore all Si-C and Si-Si bonds are deformed slighter and show shorter bond distances, which is reflected in the dramatically variation of the bond distances of Si-C6 (Fig. 23).

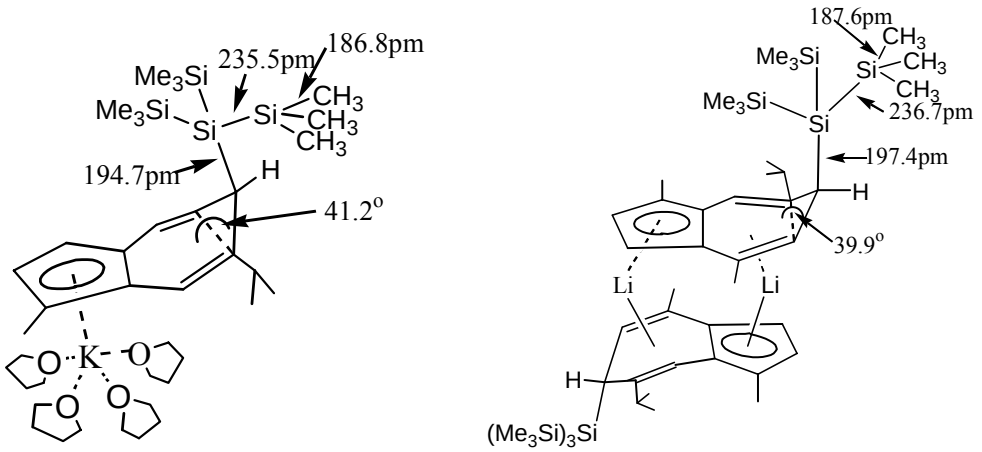

Fig. 23 Bond distances in the hypersilyl group in 1 and 2a

Overall, the bond parameters within the hypersilyl group in compound **2a** are still within the normal range, only the bond distance of Si-C6 (194.7pm) in compound **2a** is still exceptionally long even in comparison with the bond distance of C-Si (190.7pm) in the overcrowded compound $CH_2[Si(SiMe_3)_3]_2$ [108].

A similar structure to **2a** is formed for the monomer $K(C_5Bz_5)\cdot 3THF$ (Bz = $-CH_2(C_6H_5)$) [109] with a "Klavierstuhl" (piano chair) geometry. The related parameters are listed in the following table.

Tab. 9 Bond distances in 2a and similar complexes

complex	K-$C_{5(cent.)}$ (pm)	K-$C_{5,(aver.)}$ (pm)	K-O (aver.) (pm)	C-C (aver.) (pm)	Ref.
2a	282.4	306.8	278.1	140.9	This work
$K(C_5Bz_5)\cdot 3THF$	279	303.5	273.5	140.8	109
KCp	282				110
$K\{C_5Me_4[SiMe_2(NCMe_3)]\}\cdot THF$	281				111
$K[Cp(SiMe_3)]$	278				112
$(Et_2O)_2KCp$	277				113
$(py)_2KCp^*$	279				114

Compare to the parameters in compound $K(C_5Bz_5)\cdot 3THF$, all of the distances of K-$C_{5(cent.)}$, K-$C_{5,(aver.)}$ and K-O in **2a** are 3~4 pm longer. However, their average C-C distances in the C_5 ring are similar to each other. The K-$C_{5(cent.)}$ distances in all other structurally characterized compounds with K···Cp moieties are shorter than that in **2a** [115].

2.3 Mono-Hyp Substituted Metallocene Derivatives

As potential precursors for synthesis of metallocene derivatives, the reactivity of the complexes **1**, **2** as well as **3** with metal halides such as $MnBr_2$, $FeCl_2$, $NiCl_2$, $CoCl_2$, VCl_3 etc. have been investigated. The NMR spectroscopy and the structures of the derived metallocene complexes are discussed in detail.

2.3.1 Reactions

2.3.1.1 Metathesis of M(6-Hyp-Hgual) (M=Li, K) with $MnBr_2$, $FeCl_2$

When compound M(6-Hyp-Hgual) (M=Li **1**, K **2**) and $MnBr_2$(s) or $FeCl_2$(s) are mixed in tetrahydrofuran at ambient temperature in a 2:1 molar ratio, a brown-red solution of manganese bis(6-hypersilyl-1,6-dihydro-guaiazulene-1-id), abbreviated as $Mn(6\text{-Hyp-Hgual})_2$ (**5**) or an orange solution of $Fe(6\text{-Hyp-Hgual})_2$ (**6**) is observed in half an hour. Through re-crystallization in toluene both of compounds **5** and **6** can be purified with yield of about 40%.

Eq.16

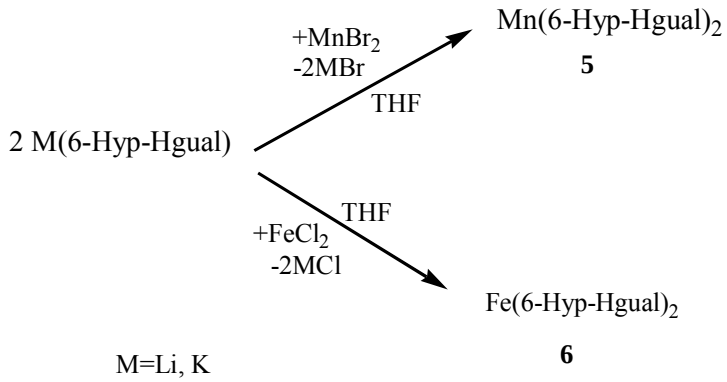

It is observed that if $MnBr_2$ is stoichiometric surplus in the mixture of $MnBr_2$ and **2**, white gleam crystalline compound was formed. X-ray diffraction analysis showed that the white needle crystal is THF solvated manganese bromide with foumula $(thf)_2MnBr_2$ and chain structure[I].

Each compound **5** and **6** comprises two diastereomers: the rac-diastereomers [(R, R) or (S, S)-racemic enantiomers] and meso-diastereomer [(R, S)-isomer] (Fig. 24). The synthetic approach employed in this study produces the statistical almost 50:50 rac:meso diastereomer ratio.

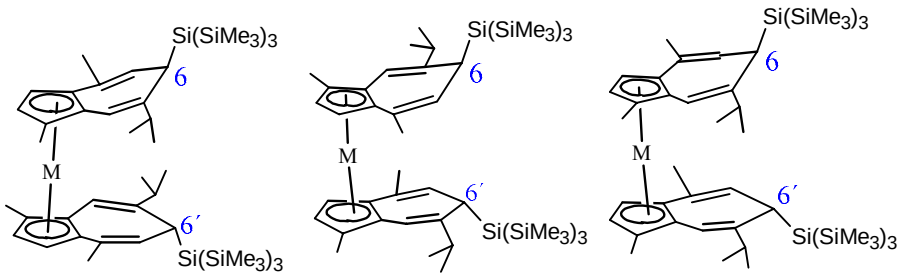

Fig. 24 Representation of the rac- and meso-isomers in the sandwich structure of 5 and 6

I

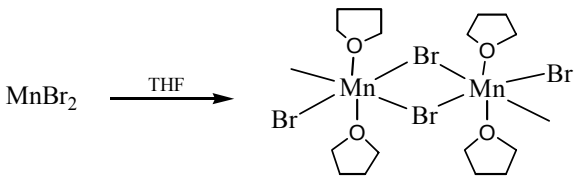

According to the different physical properties of two diastereomers it is possible to separate them by fractional crystallization. Depending on the nature of the ligand, different solvents had to be used to achieve successful separation of their diastereomers. From toluene the partly separation of the diastereomers could be accomplished. However, the many fractional-crystallization steps undertaken for the purification of the metallocenes incurred a heavy product-loss penalty.

It is noteworthy that the new produced ferrocene derivative **6**, similar to ferrocene, fulfils 18-valence electrons and is no more air- and moisture sensitive. Therefore, all characterization procedures of **6** can be performed in atmosphere. Compound **5**, however, is still air- and moisture sensitive.

2.3.1.2 Metathesis of K(8-Hyp-Hgual) with $FeCl_2$

In the same way, the metathesis between K(8-Hyp-Hgual) (**3**) and $FeCl_2$(s) takes place in tetrahydrofuran, and a red solution of Fe(8-Hyp-Hgual)$_2$ (**7**), a structural isomer of **6**, is formed.

Eq.17

$$2\ \text{K(8-Hyp-Hgual)} + \text{FeCl}_2 \xrightarrow{\text{THF}} \underset{\mathbf{7}}{\text{Fe(8-Hyp-Hgual)}_2} + 2\text{KCl}$$

Through recrystallization from toluene the X-ray diffraction quality red crystals of **7** were obtained. Similar to **6**, the two diastereomers in complex **7** can be partly separated from toluene.

2.3.1.3 Reaction of K(6-Hyp-Hgual) with $NiCl_2$ or other Metal Halides

The reaction between compound **2** and $NiCl_2$ in tetrahydrofuran in 1:1 or 1:2 molar ratio result in at room temperature immediately black powder of nickel. From the filtrated solution colourless hexangular platelets and red rod-shaped crystals were isolated. X-ray diffraction analysis showed that the colourless substance is an organic silicon compound **9** with structure shown in Eq. 18, and the red crystal is nickelocene derivative Ni(6-Hyp-Hgual)$_2$ (**8**).

Eq.18

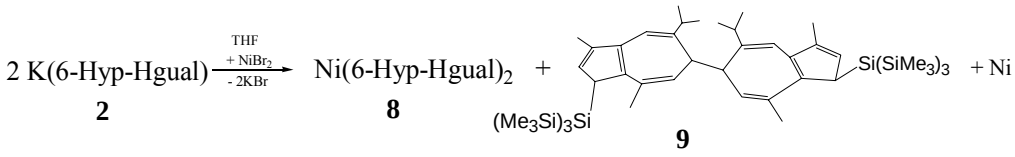

The occurrence of **9** is probably resulted from the decomposition of **8**, since Ni(II) is more easy to be reduced than Mn(II) and Fe(II). After the formation of Ni the two guaiazulenyl groups would rearrange and couple with each other to 6-6´-dimer **9**.

Eq. 19

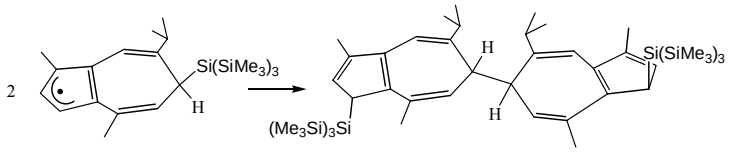

9

The formation of compound **9** was observed alongside several further reactions (Eq. 20-23).

Eq. 20

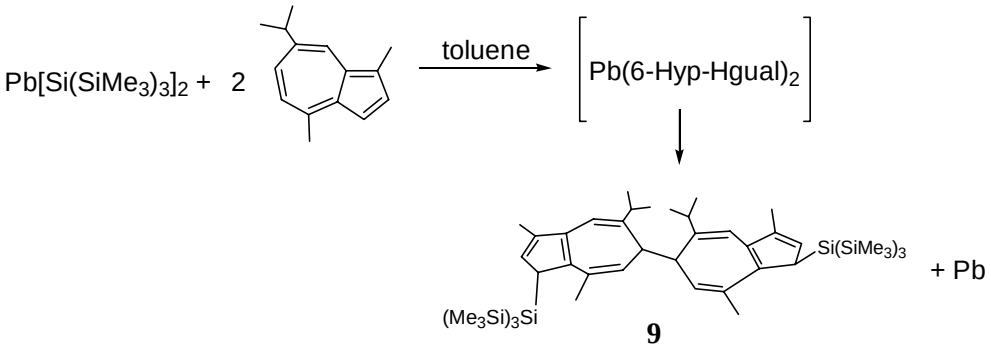

9

(In this reaction an intermediate complex Pb(6-Hyp-Hgual)$_2$ might exist, which decomposed immediately to product **9**).

Eq.21

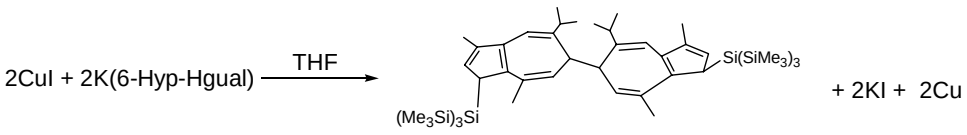

9

Eq.22

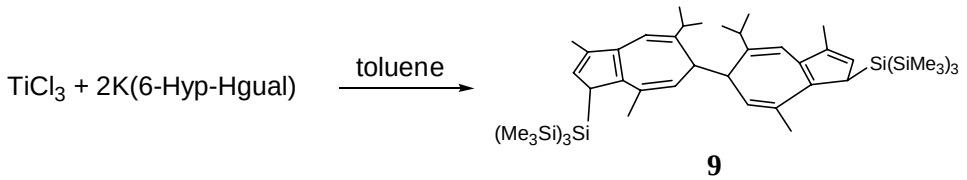

9

Eq.23

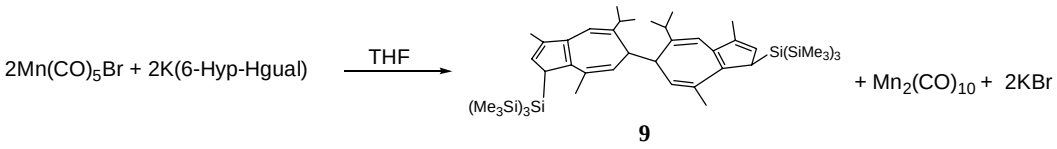

9

It is noticeable that in toluene and n-pentane the reactions between MX_2 ($MnBr_2$, $NiCl_2$, $FeCl_2$) and **2** or **3** do not take place. The same result was observed with VCl_3 as reactant. In DME at room temperature $CoCl_2$ does not react with **2**, instead, the element analysis showed that the Co(II) coordinated with DME and gave rise to red powder of $Co(DME)_3Cl_2$.

2.3.2 NMR Spectroscopy

In this section we will only discuss the NMR spectra of two iron complexes Fe(6-Hyp-Hgual)$_2$ (**6**), and Fe(6-Hyp-Hgual)$_2$ (**7**), as well as the NMR spectra of an organic silicon compound (3-Hyp-6-Hgua)$_2$ (**9**), since compounds Mn(6-Hyp-Hgual)$_2$ (**5**) and Ni(6-Hyp-Hgual)$_2$ (**8**) possess paramagnetic properties.

2.3.2.1 NMR Spectra of Fe(6-Hyp-Hgual)$_2$ (6) and Fe(8-Hyp-Hgual)$_2$ (7)

As mentioned, the batches of **6** and **7** isolated from the reaction mixtures comprises two diastereomers, *i.e.* the rac-diastereomer (R,R)- and (S,S)-L_2Fe, and the meso-diastereomer (R,S)-L_2Fe (L=6-Hyp-Hgual in **6**, 8-Hyp-Hgual in **7**), which are shown in Fig. 24 and Fig. 25 for **6** and **7**, respectively.

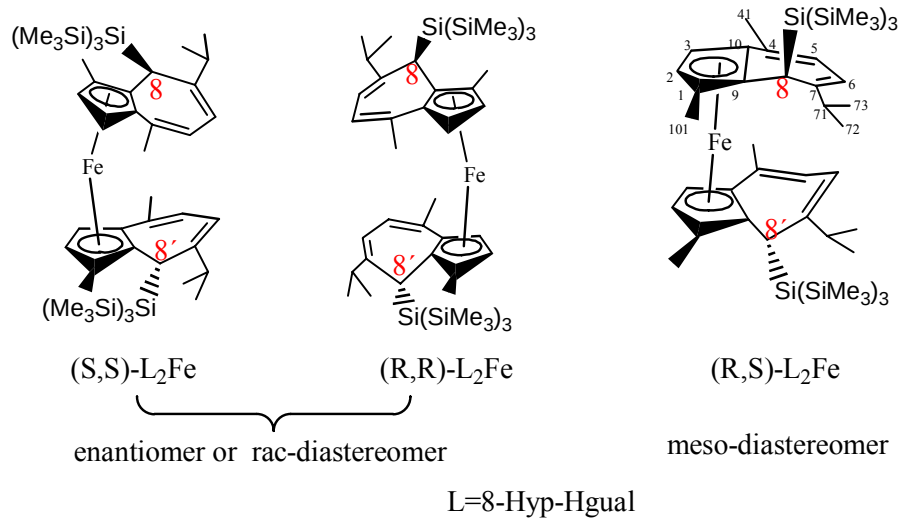

Fig. 25 Isomeric Structure and Numbering of carbon atoms in complex 7

Firstly, the two rac-enantiomers possess same physical and chemical properties, giving rise to same NMR signals, whereas the meso-diastereomer gives rise to different NMR signals from the rac-diastereomer. Thus, the rac- and meso-diastereomer will produce totally only two sets of signals. Next, the corresponding atoms on two guaiazulene moieties within one molecule, such as H2, H12, or C1, C11 etc., are equivalent, as the two rac-diastereomers have C_2-symmetry, and the meso-diastereomer has a mirror-plane bisecting and perpendicular to the axis of $C_{5(cent.)}$-M-$C'_{5(cent.)}$, thus, the two ligands moieties within one molecule give rise to same NMR spectra.

2.3.2.1.1 ^{1}H NMR Spectroscopy

At lower temperature both of two diastereosmers (rac- and meso-diastereomer) crystallize from toluene solution at the same time. The ^{1}H NMR spectrum of the crystals shows a mixture of two sets of signals (Spe. 6, **a**). If the saturated toluene solution of **6** is allowed to stay at room temperature, by slow evaporation of toluene one diastereomer crystallizes at first, followed by another, gives rise to ^{1}H NMR spectrum with one set of signals each (Spe. 6, **b** and **c**). In combination with the stereo-chemical assignments made by X-ray crystallography, it is possible to assign the two sets of proton signals to each particular diastereomer. The spectrum shown in Spe.6, **b** for the pure diastereomer was recorded with the same single crystal used for X-ray measurement. According to its solved structure of (R,R)- and (S,S)-Fe(6-Hyp-Hgual)$_2$ it is known immediately that this set of signals is from the rac-diastereomer. Obviously, another set of signals in Spe. 6, **c** can be undoubtedly assigned to the meso-diastereomer.

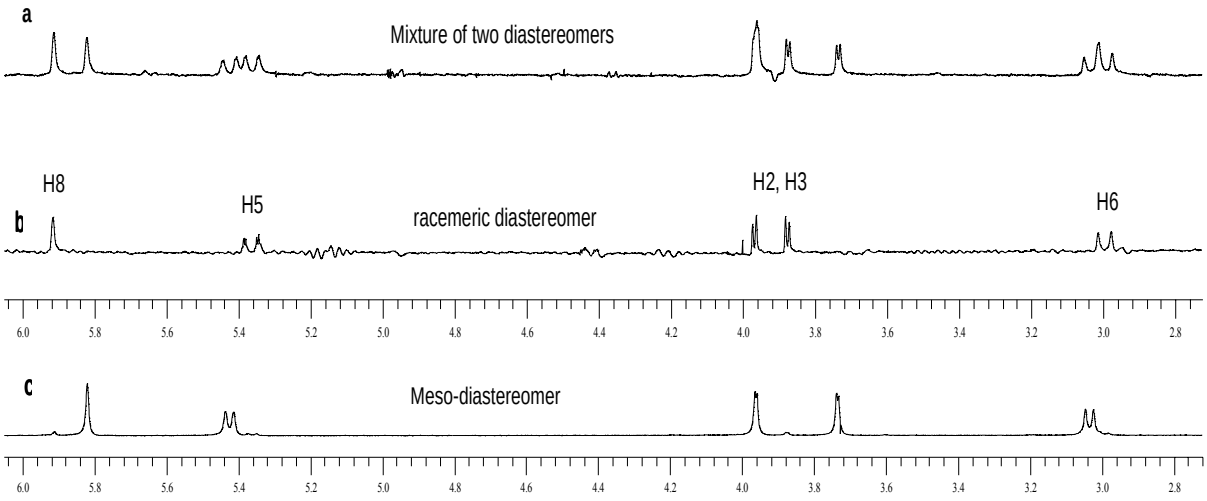

Spe. 6 Part of the ^{1}H NMR spectra of 6 recorded in C_6D_6 at 298K (250.133MHz).

a: mixture of rac- and meso-diastereomer ; b: rac-diastereomer; c: meso-diastereomer

Compare to the ^{1}H NMR spectrum of K(6-Hyp-Hgual) (**2**), the iron atom and the sandwich structure in **6** have greatly affect the resonances of the protons in the guaiazulene framework. In compound **2** the interaction between K^+ and the C_5-ring is dominantly *ionic*, whereas in compound **6** the interaction between Fe(II) and the C_5-ring is dominantly *covalent*, which results in the resonances of the olefinic protons H2, H3 in the coordination sphere to Fe(II) in **6** moving dramatically to upfield as shown in Spe.7.

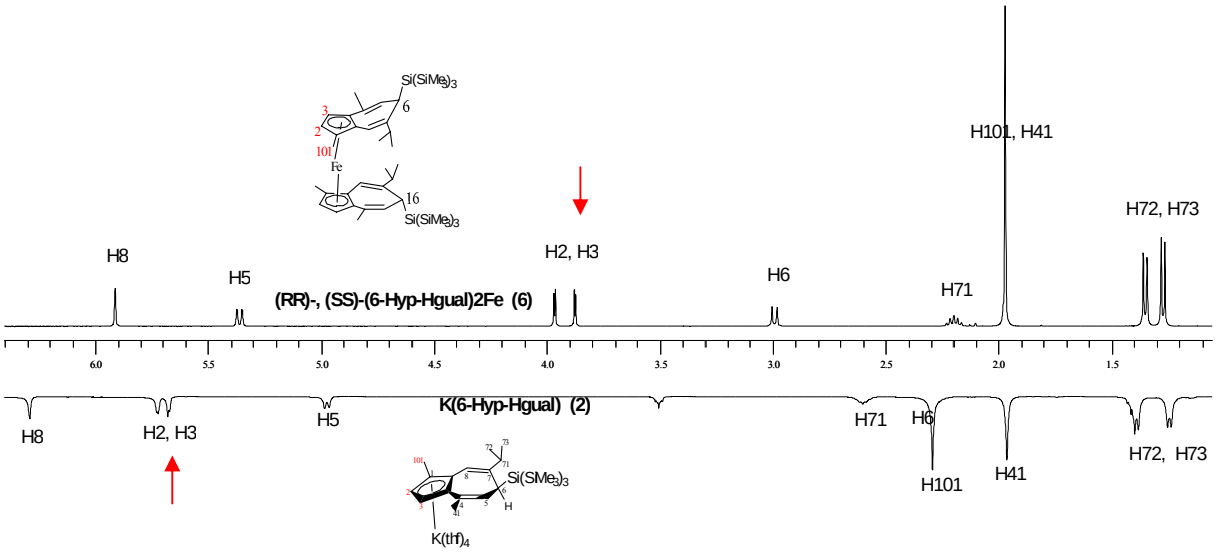

Spe. 7 Comparison of spectra of K(6-Hyp-Hgal) (2) and rac-[6-Hyp-Hgual]$_2$Fe (6)

Compare to the ^{1}H NMR spectrum of K(6-Hyp-Hgual) (**2**), in the ^{1}H NMR spectrum of **6** not only the resonances of H2 and H3, which are directly bonded to the coordinating carbon atoms C2, C3, moved upfield dramatically, but also the resonances of H8 and H101, which are close to the coordination sphere, move upfield about 0.5ppm, finally the signal of H101 overlaps nearly with the signal of H41. On the other hand, the signals of H5 and H6 shift down-field. All of these changes indicate the total different chemical environment of H atoms between two compounds.

Similar change can be observed between compounds Fe(8-Hyp-Hgua)$_2$ (**7**) and K(8-Hyp-Hgual) (**3**). The resonance changes of H atoms in or near to the coordination sphere for these two pairs of compounds are summarized in Tab. 10.

Tab. 10 Comparison of selected ^{1}H NMR spectral data for compound 6, 7 with 2 and 3, respectively

Compound	***H2, H3***	***H101***	*H8*		*Compound*	***H2, H3***	***H101***	*H8*
K(6-Hyp-Hgual) **(2)**	***5.88(d), 5.77(d) $J_{2,3}$=3.0***	***2.43(s)***	*6.30 (s)*		*K(8-Hyp-Hgual)* **(3)**	***6.05(d), 5.88(d) $J_{2,3}$ =3.7***	***2.42(s)***	*3.84 (s)*
rac-[6-Hyp-Hgual]$_2$Fe **(6)**	***3.98(d), 3.88(d) $^3J_{2,3}$=2.6***	***1.98(s)***	*5.92 (s)*		*rac-[8-Hyp-Hgual]$_2$Fe* ***(7)***	***3.61(d), 4.54(d) $^3J_{2,3}$=2.0***	***1.97(s)***	*3.31 (s)*
meso-[6-Hyp-Hgual]$_2$Fe **(6)**	***3.97(d) 3.73(d) J=2.4***	***1.97(s)***	*5.82 (s)*					

2.3.2.1.2 ^{13}C NMR Spectroscopy

The ^{13}C NMR spectral data recorded in C_6D_6 for compounds **6** and **7** are consistent with their ^{1}H NMR spectral data. All aliphatic carbon atoms give rise to signals within the expected range, but five of the olefinic carbon atoms show signals in the high field region with $67 < \delta < 88$. The selected ^{13}C NMR spectral data for all olefinic carbon atoms are summarized in Tab. 11.

Tab. 11 ^{13}C NMR spectral data of isomers in 6 and 7 in C_6D_6 at 300K (62.896MHz)

^{13}C NMR, *δ(ppm)*		**C1, C9, C10**	**C2, C3**	**C4, C7**	**C5, C8**
6	**meso-**	87.6; 83.8; 82.4	72.0; 68.5	145.1; 129.6	126.1; 115.1
	rac-	86.5; 83.7; 83.4	73.5; 67.3	145.5; 129.4	126.2; 115.0
		C1, C9, C10	**C2, C3**	**C4, C7**	**C5, C6**
7	**rac-**	85.6; 83.0; 82.3	73.7; 67.4	147.2; 135.6	128.6; 122.5
	meso-	85.4; 82.9; 83.8	73.6; 66.9	147.8; 135.2	125.7; 123.0

As mentioned above, in compounds **1**, **2**, **3** and **4** all olefinic carbon atoms give rise to ^{13}C NMR signals at low field with $\delta > 100$. When comparing with the known dominantly covalent compound $FeCp_2$, which has ^{13}C NMR signal at $\delta = 68.2$ppm, and considering the similar linkage of Fe-C_5(ring) in **6** and **7**, it can be deduced that the five upfield shifted ^{13}C NMR signals in **6** and **7** should be assigned to the coordinated carbon atoms C1, C9, C10, C3 and C2. Thus, these five olefinic carbon atoms in the C_5-ring coordinate to Fe(II) in dominantly covalent mode as shown in Fig. 26.

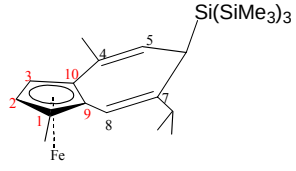

Fig.26 Coordinated carbon atoms in the ligand

The experiment has partly verified this deduction. In the DEPT-135 NMR spectrum three of these five *upfield shifted signals* disappear, indicating that in the five tertiary carbon atoms *C1*, *C9*, *C10*, C4 and C7, three of them possess upfield shifts. In combination with the ^{1}H-^{13}C correlated spectroscopy, two secondary carbon atoms with upfield shifted signals are assigned undoubtedly to *C2* and *C3*.

2.3.2.1.3 ^{29}Si NMR Spectroscopy

The ^{29}Si NMR data recorded in C_6D_6 for compound **6** shows two pairs of signals for the two diastereomer.

-$^{\alpha}Si(SiMe_3)_3$	-Si($^{\beta}SiMe_3)_3$
-70.5	-12.2
-70.7	-12.3

Compared to **1**, **2** and **4**, no change in the peripheral ^{29}Si NMR spectral data has been observed for **6 (**β-Si NMR data: in **2** -12.1, in **4** -12.1). However, the central Si atom in **6** shows slightly down-field shift (central Si NMR data: in **2** -76.3; in **4** -77.6). This is consistent with the structure.

2.3.2.2 NMR Spectroscopy of (3-Hyp-6-Hgua)$_2$ (9)

Compound **9** is formed through two 3-hypersilyl substituted guaiazulenyle coupling with each other in 6, 6´-position. Its structure was identified with ^{1}H-, ^{13}C- and ^{29}Si-NMR spectroscopy and X-ray diffraction analysis. Owing to its C2 symmetry the two equivalent moieties in one molecule of **9** give rise to same NMR signals. Without the influence of metal atoms all of its NMR spectral data are within expected range.

2.3.2.2.1 ^{1}H NMR Spectroscopy

The numbering of the protons in compound **9** and its ^{1}H NMR spectrum recorded in C_6D_6 at 300K are found in Spe. 8.

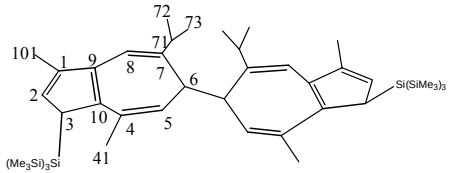

9

Spe. 8 ^{1}H NMR spectrum of 9

In Spe. 8 all signals for olefinic and aliphatic H atoms fall into the normal range. An interesting observation is that no significant coupling between H5 and H6, H2 and H3, respectively, can be observed; instead, two broad and two lightly broad singlets are formed. H8 shows, however, a relative sharp singlet. Similarly, the coupling constant $^3J_{H71\text{-}H72}$ (5.4Hz) in the isopropyl group is also smaller when compare with that of **2**. The signals of H101 and H41 overlap.

Although according to experience, namely, the coupling between H5 and H6 is always stronger than that of H2 and H3, from the two broad singlets in Spe.8 we can immediately assign the resonances of H5 and H6, H2 and H3 as well as H8, after all, the identification must be consistent either with theoretical calculation or experimental data.

The identification of the five singlets of H2, H3, H5, H6 and H8 in **9** was carried out according to the ^{1}H-^{1}H correlation (Spe. 9) and calculated NMR chemical shifts. From the two dimensional NMR spectrum the two pairs of protons, namely H5 and H6, H2 and H3, can be easy classified based on their different correlations. Since the signals of H101 and H41 overlap, the correlation between H2 and H101, H5 and H41 can not help us to distinguish H2 and H5. However, according to the calculated ^{1}H NMR chemical shifts[1] (-Si(SiMe$_3$)$_3$ was replaced by SiH$_3$ by the calculation) the signals of H2, H5, H8, H3 and H6 can be rationally assigned, which is consistent with the stronger coupling between H5 and H6. By the way, from the 2D spectrum it was observed that H8 had weak correlation with H3, and H3, in turn, has also correlations with H41, even with H101.

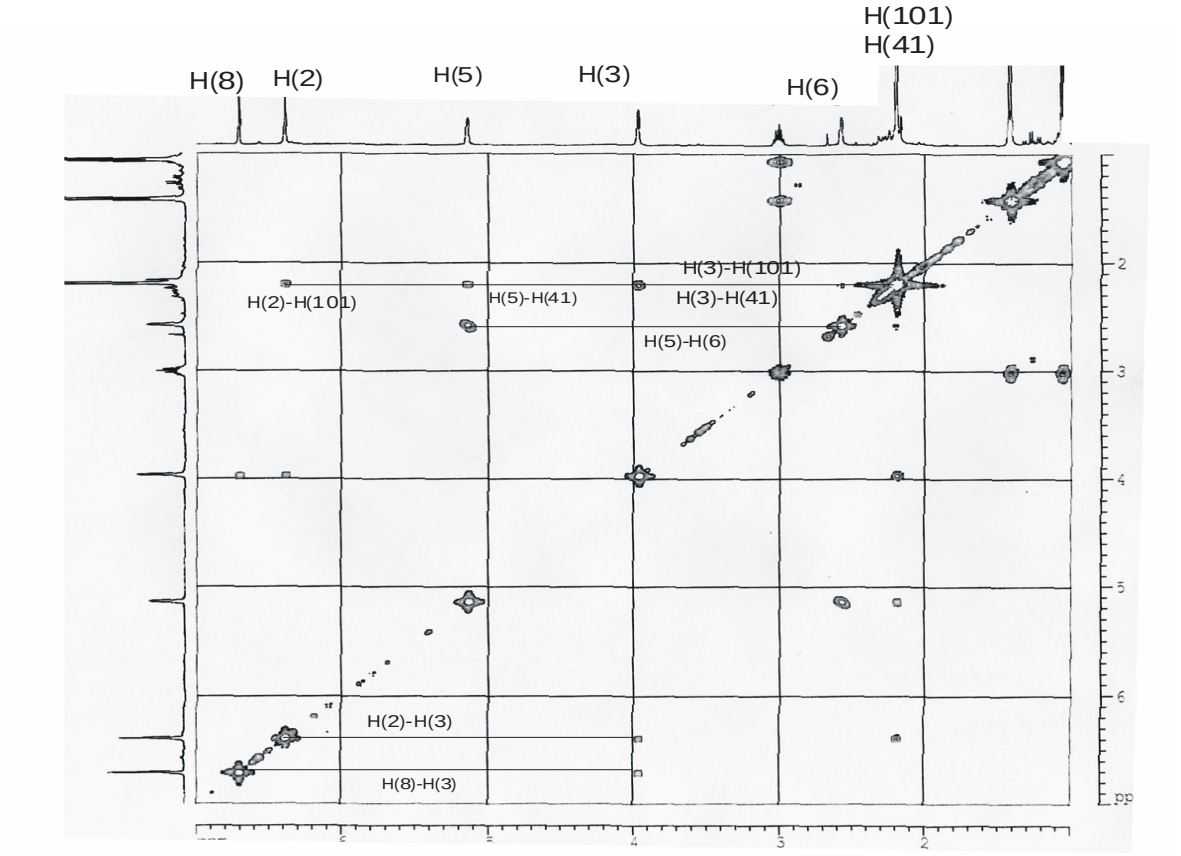

Spe. 9 2D COSY of 9 (^{1}H-^{1}H correlation)

[1] B3LYP(6-31G*):61AO

Compare with the ^{1}H NMR spectrum of compound **2** (Spe. 3), except the difference of the chemical shift of H3 (in **9** it is aliphatic proton, in **2** it is olefinic proton), all other signals in two compounds are actually in the same order.

2.3.2.2.2 ^{13}C NMR Spectroscopy

The ^{13}C NMR spectrum recorded in C_6D_6 at 300K for compound **9** revealed signals for all olefinic carbon atoms in the low field region, and for all of the eight aliphatic carbon atoms in the high field region, which is consistent with its molecular structure. The ^{13}C spectral data of **9** are compiled in the experimental section.

Via one and two dimensional NMR spectroscopy (^{1}H-^{13}C correlation) assisted by theoretical calculations, all ^{13}C NMR signals can be assigned. As shown in Spe. 10, some of the ^{13}C signals are in opposite order compared to the ^{1}H NMR date.

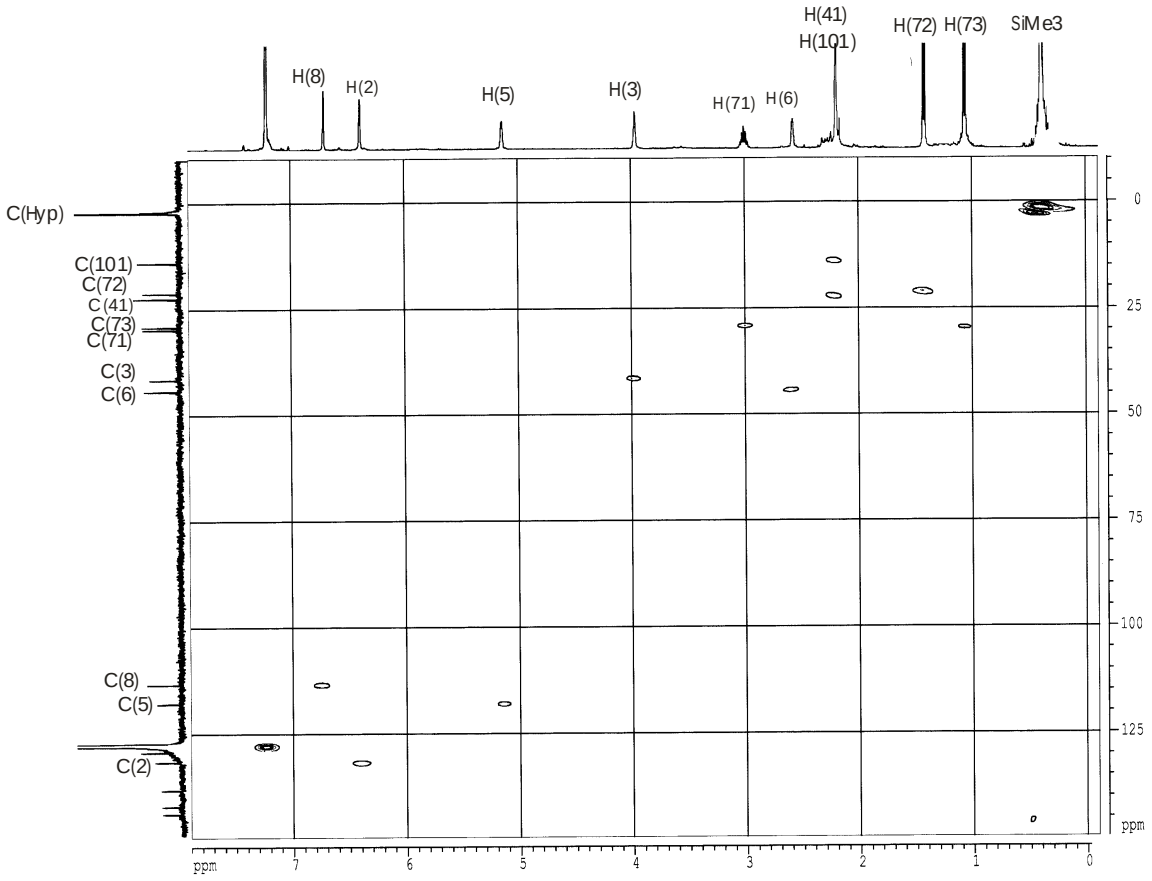

Spe. 10 2D COSY of 9 (^{1}H-^{13}C correlation)

2.3.2.2.3 ^{29}Si NMR Spectroscopy

The ^{29}Si NMR spectrum for compound **9** shows that the six β-Si atoms (peripheral silicon atoms) give rise to a strong singlet at -12.2ppm, which is close to the value for compounds **2**, however, the two α-Si atoms (central silicon atoms) bonding directly with the C_5-ring show a weak signal at much higher field at –90.2 ppm.

Compound	-$^{\alpha}Si(SiMe_3)_3$	-Si($^{\beta}Si$Me$_3$)$_3$
K(6-Hyp-Hgual) (**2**)	-76.3	-12.1
(3-Hyp-6-Hgua)$_2$ (**9**)	-90.2	-12.2

Obviously, the probably higher electronic density in the relative smaller five-membered ring and the special position of the central silicon atom (nearly normal to the best plane through the atoms C1, C2, C9 and C10) (Fig. 36) should make contribution to the upfield shift of α-Si..

2.3.3 Molecular Structures of Compounds 5, 6, 7, 8, and 9

2.3.3.1 Molecular Structures of (RR)- and (SS)-M(6-Hyp-Hgual)$_2$ (M=Mn 5, Fe 6, and Ni 8)

From toluene at a temperature range +5°C/-20°C complex Mn(6-Hyp-Hgual)$_2$ (**5**) crystallizes as red-brown rod-shaped, Fe(6-Hyp-Hgual)$_2$ (**6**) as orange rod-shaped, and Ni(6-Hyp-Hgual)$_2$ (**8**) as red rod-shaped crystals. All crystal structures reveal the presence of the (R,R)- and (S,S)- racemic enantiomers in equimolar ratio. The metal atoms in these compounds are in a sandwich environment formed by the two η^5:η^5-bonded ligands moieties.

The selected crystallographic data for the rac-diastereomer of complexes **5**, **6** and **8** are listed in Tab. 12, and the molecular diagrams for these three structures are depicted in Fig. 27.

Tab. 12 Crystallographic data and structure refinement for rac-diastereomer of 5, 6 and 8

empirical formula	Rac-$C_{48}H_{90}MnSi_8$ (**5**)	Rac-$C_{48}H_{90}FeSi_8$ (**6**)	Rac-$C_{48}H_{90}NiSi_8$ (**8**)
fw(g/mol)	946.86	947.77	950.63
crystal system	Triclinic	Triclinic	orthorhombic
space group	Pī	Pī	Pbca
unit cell constants (Å, deg)	a=9.5472(18) α=102.635(8) b=16.441(2) β=91.222(11) c=18.562(3) γ=96.696(12)	a=9.5990(10) α=102.891 b=16.524(2) β=91.357(8) c=18.772(3) γ=96.984(9)	a=17.284(2) b=18.002(3) c=36.972(4)
colour	red-brown	orange	red
Z	2	2	8
GOF	0.891	1.010	0.672
μ, mm^{-1}	0.433	0.462	0.533
F(000)	1030	1032	4144
no. of refl. collct	10404	8059	10614
no. of ind. refls	9771	7314	8953
no. of params	514	514	515
R_1 und wR_2 [I>2σ(I)]	0.0580/0.1449	0.0506/0.1172	0.0461/ 0.0689
R_1 und wR_2(all data)	0.0863/0.1543	0.0853/0.1339	0.0827/ 0.1451

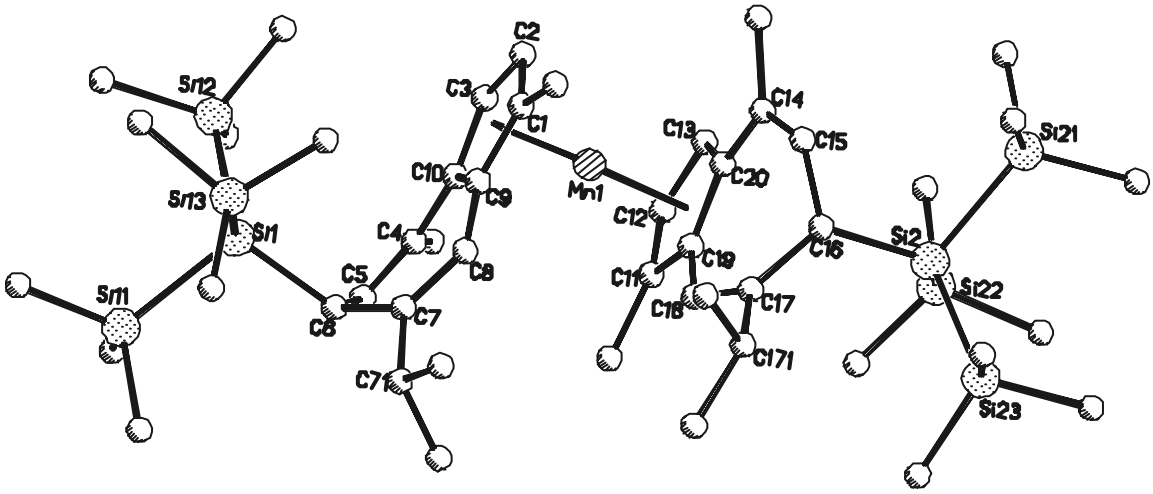

5 (SS)

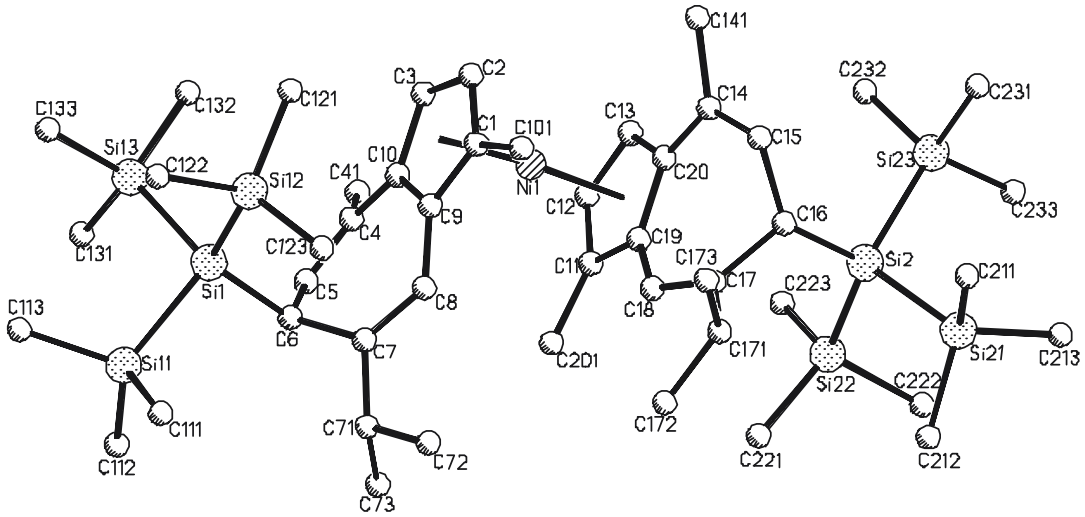

8 (SS)

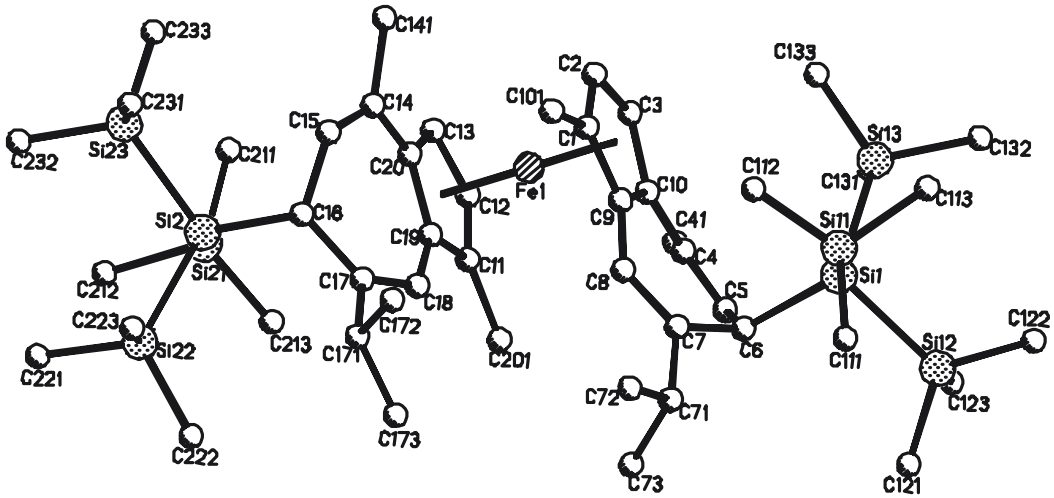

6 (RR)

Fig. 27 Molecular structures of rac-diastereomer of 5, 6 and 8, Atoms are represented by spheres of arbitrary radii; hydrogen atoms are omitted for clarity.

As shown in Fig. 27, with the (S, S)- or (R, R)-configuration both of the two ligands moieties within each molecule are staggered. The whole molecule seems like twisted tweezers, in which the uplift hypersilyl group as “free terminal” and the down putting side around C2 or C2´ as “riveted terminal”. The metal atom acts as the “rivet”.

The following parameters are therefore of main interest for the discussion of the structures: torsion angle τ of the two guaiazulene skeletons (Fig. 28, a); torsion angle τ_{cp} of the two coordinated C_5-rings (Fig. 28, b); tilt angle φ of two C_5 planes, which reflect their parallelism (Fig. 28, c); folding angles α, β, γ in each skeletons, which have same definitions as for compound **1** (Fig. 21); bending angle δ of the substituents from the bonded rings; and the metal to ring distances M-$C_{5(cent.)}$ as well as M-C_5(ring).

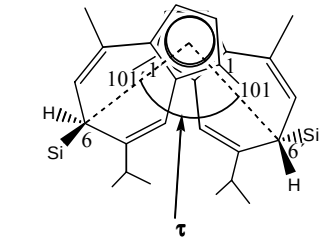

torsion angle between two ligand moieties

a

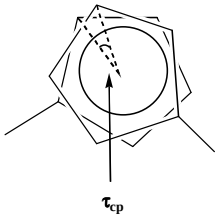

torsion angle between two C_5-rings

b

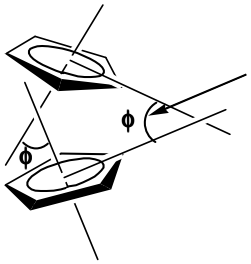

tilt angle ϕ between two C_5 rings

c

Fig. 28 Definition of torsion angles τ, τ_{cp} and tilt angle φ

Conformation Analysis

If we define the conformation as “overlap” position (Fig. 30, **a1** and **b1**), in which the two guaiazulene skeletons are overlapped, with two hypersilyl groups stretching away from the central metal atom, and without consideration of the relative positions of methyl and isopropyl groups, then we fix one ligand (the one below the paper plane) and rotate the other ligand (the one above the paper plane) around the axis $C_{5(cent.)}$-M-C´$_{5(cent.)}$ clockwise (symbol “-”) or anticlockwise(symbol “+”), the rotational angle is defined as the torsion angle of these two guaiazulene skeletons, and written as τ. The staggering degree of two guaiazulene

skeletons within one molecule can be evaluated with the torsion angle **τ** of C6-$C_{5(cent.)}$-$C'_{5(cent.)}$-C(6′) (Fig. 28).

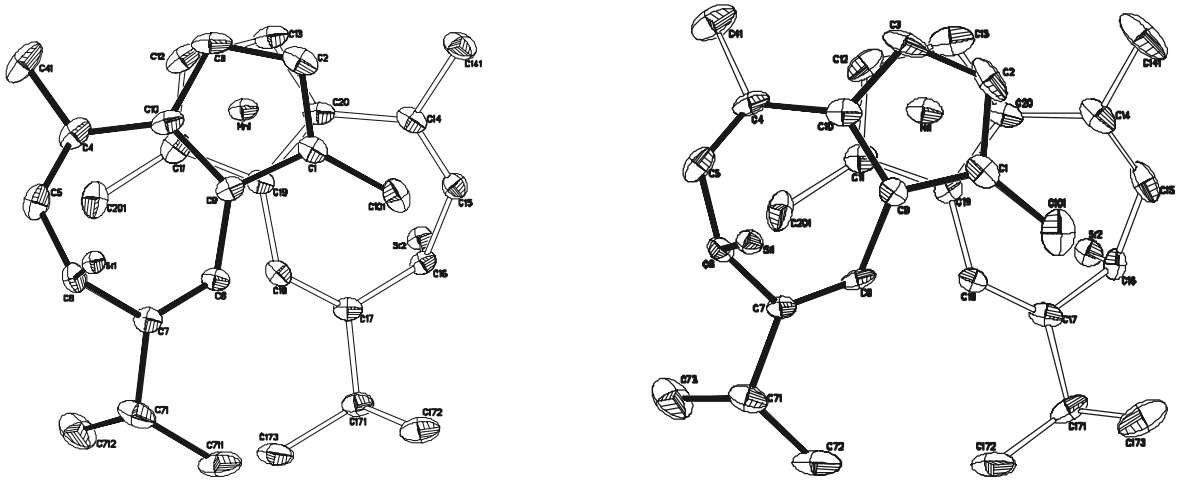

5 (SS, **τ** = -95.2°; τ_{Cp} = -24.4°)

8 (SS, **τ** = -108.7°; τ_{Cp}= 32.7°)

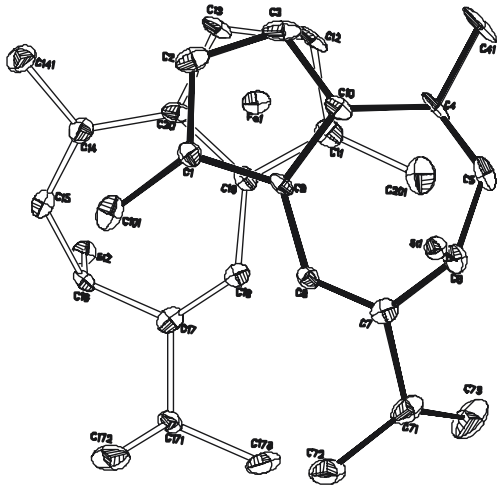

6 (RR, **τ** = 95.8°; τ_{Cp}= 25.0°)

Fig. 29 View along the axes $C_{5,\ cent.}$-M-$C_{5,cent.}$ in 5, 6 and 8, -$SiMe_3$ and H are omitted for clarity

As shown in Fig. 29, in the two compounds **5** and **8** with (S,S)-configuration the ligand moiety above the paper plane rotated anti-clockwise for about 100°, whereas in **6** with (R,R)-configuration the ligand moiety above the paper plane rotated clockwise for about 100°. Such geometry as stable conformation in the solid state can be understood through comparison of the following depicted conformations.

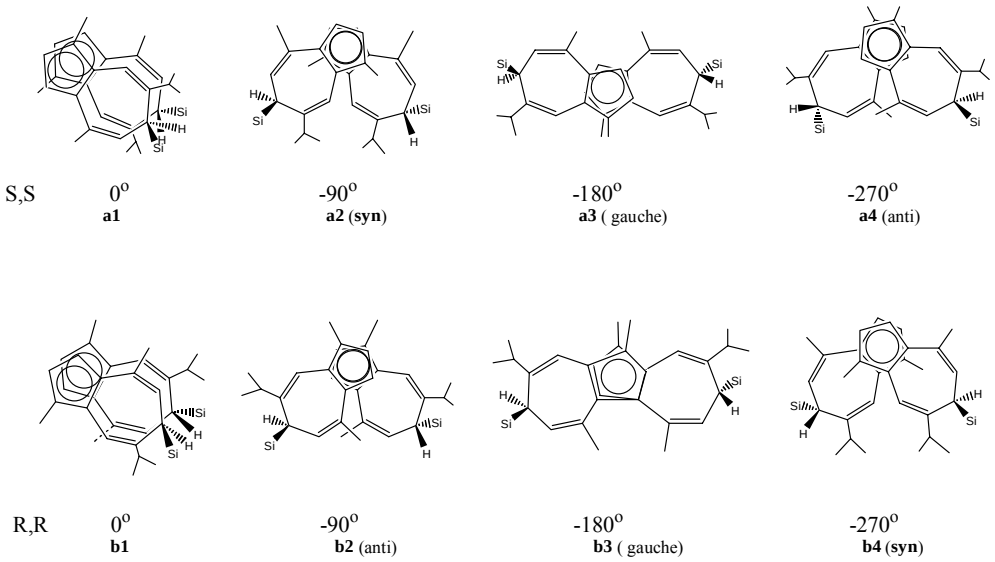

Fig. 30 Analysis of stable conformations of (R,R)- and (S,S)-configurations in 5, 6 and 8 in the solid states

In Fig. 30 four ideal conformations in staggering angles of 0°, -90°, -180° and -270° for each of (S,S)- and (R,R)-configuration are depicted, respectively. As mentioned above, conformations **a1** and **b1** are so called overlap-conformations, they are unstable because of the large steric effect. The conformations **a2** for (S,S)- and **b4** for (R,R)-configuration are enantiomer to each other, the other two pairs of enantiomers are **a3** and **b3**, as well as **a4** and **b2**. Analogue to literature[116, 117], in the following we will define **a2** for (S,S)- and **b4** for (R,R)-conformation as "*syn*"-conformations, since where the stretch direction from C1 to C101 in one ligand moiety is arranged along the same direction as from $C'_{5(cent.)}$ to C6´ in the second ligand moiety, the same is true for C1´-C101´ and $C_{5(cent.)}$-C6 (Fig. 28). Overall, the two 1-methyl groups in two guaiazulene moieties fall into the two seven-membered rings (Fig. 29). On the other hand, the **a4** for (S,S)- and **b2** for (R,R)-configurations will be defined as "*anti*"-conformations, since where the stretch direction from C1 to C101 in one ligand moiety is arranged in the anti-direction as from $C'_{5(cent.)}$ to C(6´) in the second ligand moiety (Fig. 30, Fig. 32). In **a3** or **b3** the two nearly overlapped bonds C1-C101 and C(1´)-C(101´) are arranged to the $C'_{5(cent.)}$-C(6´) and $C_{5(cent.)}$-C6 in a torsion angle of about 90°, we define them as "*gauche*"-conformations[I].

Obviously, in the syn-conformation **a2** for (S,S)- and **b4** for (R,R)-configuration, all of the methyl, isopropyl, and hypersilyl groups between two ligands moieties are staggered away from each other, thus they should be the most stable conformations in the solid. As can be

[I] The concept "syn" and "anti" conformer have been once used by Erker. He has proposed three possible solid state conformers for un-bridged, rac-bis(1-R-indenyl)-zirconium (titanium, hafnium)dichloride metallocenes, where the concept of "syn" and "anti" are defined by *the relative positions of two substituents R*. The ligand with extreme large R would select anti-conformer, the ligand with small R can keep syn-conformer, and the moderate large R let two ligands in molecule adopt gauche conformation.

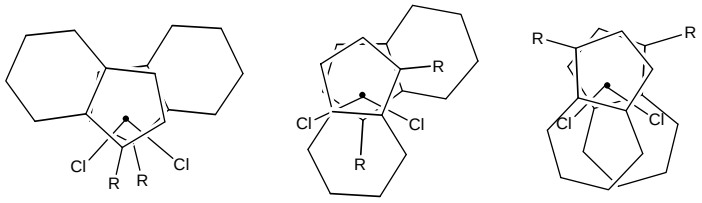

seen in Fig. 29, compounds **5** and **8** with (S,S)-configuration show just the geometry as **a2**, and compound **6** with (R,R)-configuration shows just the geometry as **b4**.

Since in the metallocene derived from azulene or guaiazulene the two seven-membered rings in one sandwich unit do not coordinate to the metal atom, they are often staggered due to the steric effect. Such case is observed also in the mentioned examples, *i.e.* in compounds **VIII** (Eq. 7), **IX** (Eq. 9), **XI** (Eq. 11), **XIII** (Eq. 12), all coupling between the two seven-membered rings either in 4,4´- or 8,8´-mode are not endo-endo´-coupling as in overlap positions, instead, the two seven-membered rings are staggered. To compare the coupling more conveniently these coupling modes are collected in the following figure.

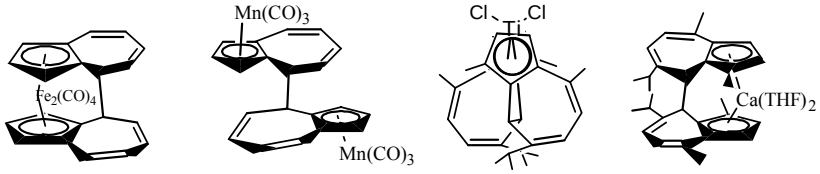

	VIII	**IX**	**XI**	**XIII**
Coupling	4, 4´-	4, 4´-	8, 8´-	8, 8´-

However, their staggered angles τ are not found in literature, thus no quantitative comparison can be executed between them and complexes **5**, **6** and **8**.

The project diagrams in Fig. 29 shows that the ten carbon atoms in two C_5 rings are staggered also. The data given there for the torsion angles of τ_{Cp} of two C_5 rings are the average value of the five smallest torsion angles. It rises up from -24.4° in **5**, 25.0° in **6**, to 32.7° in **8** (the ideal torsion angle τ_{Cp} for a staggered conformation is 36°).

Coplanarity

The sp^3-C atom in the 1-methyl group is nearly coplanar with the five sp^2-C atoms in the aromatic five-membered ring, the deviation are less than 0.0083 angstrom in all of the three compounds **5**, **6** and **8**. The 4-methyl and 7-isopropyl groups in the seven-membered ring stretch toward the centre metal atom, thus the steric hindrance exerted on them by the hypersilyl group could be possibly weakened.

The geometry of the two seven-membered rings is influenced greatly by the hypersilyl group. Due to the large steric demand the two bulky hypersilyl groups stretch always away from the metal centre and away from each other, thus each of the seven-membered rings folds to a boat form with its two bows stretch away from the metal centre, just as in compound **1** and **2a**. The folding angles of α, β and γ are 2.6˚, 24.1˚, 38.8˚ for **5**; 2.6˚, 24.3˚, 36.8˚ for **6** and 4.3˚, 24.6˚, 41.5˚ for **8**, respectively, being similar to those in **1** and **2a**. The nickelocene derivative **8** has the largest folding angles owing to the larger atom radius of nickel. The smallest value for the compound **6** shows its least deformed structure among three compounds.

The X-ray diffraction analysis revealed that the two C_5 rings in each sandwich unit are not parallel; instead, they tilt a little with their C2 and C3 closer to the metal centre. The tilt angle

φ of two C_5 rings is 2.2˚ in **5**, 1.4˚ in **6** and 1.9˚ in **8**, of which compound **6** has the smallest value, exhibits its normalized structural mode.

Bond Parameters

The two independent Fe-$C_{5(cent.)}$ distances in **6** amount to 166.0pm and 166.3pm, and the angle of $C_{5(cent.)}$ (1)-Fe-$C_{5(cent.)}$ (2) is 179.4°, indicating that the Fe(II) is nearly in the midst between the two C_5 rings. Overall, the ten Fe-C_5(ring) distances in **6** vary only in small range from 203.7 to 209.1pm, and the two independent Fe-$C_{5,(aver.)}$ bond lengths amount to 205.8 and 206.3(4)pm, respectively. Some other ferrocene derivatives with bulky substituents have similar Fe-$C_{5,(aver.)}$ bond distances [118, 119]. In the recent reported compound 1,1´,3,3´-tetrakis(1,1-dimethyl-3-butenyl)ferrocene the Fe-$C_{5,(aver.)}$ distance is 206.6(4)pm and the two Fe-$C_{5(cent.)}$ distances are 167.0 and 166.0pm), respectively [120]. In contrast, the dipentamethylcyclopentadienyl iron(II) Fe($Me_5Cp)_2$ has slightly shorter Fe-$C_{5,(aver.)}$ distance (205.0(2)pm) [121].

In both of the manganocene derivative **5** and nickelocene derivative **8** the M-C_5(ring) as well as M-$C_{5(cent.)}$ distances are significantly longer than those in **6**. However, the as in **6**, Mn(II) in **5** is still nearly in the midst between two C_5 rings, but Ni(II) in **8** slipped a little away from the middle point of the line $C_{5(cent.)}$(1) -$C_{5(cent.)}$(2). The Mn-$C_{5(cent.)}$ distances are 173.2 and 173.3pm with the angle of $C_{5(cent.)}$ (1)-Mn-$C_{5(cent.)}$ (2) in 179.0°, and both of the two Mn-$C_{5,(aver.)}$ distances are 211.1(4)pm, ranging from 208.1pm to 214.8pm. The Ni-$C_{5(cent.)}$ distances are even longer with 181.2 and 180.5pm with the angle of $C_{5(cent.)}$ (1)-Ni-$C_{5(cent.)}$ (2) in 174.1°, and the Ni-$C_{5,(aver.)}$ distances are 217.7(5) and 217.1(5)pm, ranging from 209.9 to 224.5pm.

Tab. 13 Selected bonds lengths and angles for compounds 5, 6 and 8

parameters	M=Mn(II) 5	M=Fe(II) 6	M=Ni(II) 8
M1-C2	208.2(4)	203.7(4)	209.9(5)
M1-C3	208.8(4)	203.9(4)	213.7(5)
M1-C1	210.3(4)	205.8(6)	217.1(5)
M1-C10	213.5(4)	207.4(4)	223.3(4)
M1-C9	214.8(4)	208.2(4)	224.5(5)
M1-$C_{5(cent.)}$ (1)	173.2	166.0	181.2
M1-C12	208.1(4)	205.7(5)	211.8(5)
M1-C13	209.2(4)	204.6(4)	215.3(5)
M1-C11	209.7(4)	204.1(4)	214.4(5)
M1-C19	213.6(4)	207.8(4)	220.3(4)
M1-C20	214.7(3)	209.1(4)	223.7(5)
M1-$C_{5(cent.)}$(2)	173.3	166.3	180.5
$C_{5(cent.)}$ (1)-M- $C_{5(cent.)}$ (2)	179.0	179.4	174.1
C-C (C_5 (1) ring aver.)	142.0 (140.8~143.1)	143.0 (140.4~144.8)	142.0 (140.2~144.1)
C4-C5	132.8(6)	134.3(6)	132.4(6)
C7-C8	133.0(5)	134.2(5)	134.2(6)
C6-C7	151.3(5)	150.3(6)	151.5(6)
C8-C9	144.3(5)	146.2(5)	145.2(6)
C5-C6	148.3(6)	149.6(7)	149.9(6)
C10-C4	145.7(6)	145.5(7)	144.1(6)
Si1-Si (aver.)	235.0	236.5	235.6
Si-C(aver.) in –Si1[($SiMe_3)_3$]	186.4 (184.5~187.9)	187.2 (185.6~188.3)	187.0 (185.2~188.2)
Si1-C6	196.8(4)	198.0(4)	195.4(5)
Si2-C16	195.4(3)	196.8(4)	194.0(5)
torsion angle τ_{Cp}(˚)	-24.4	25.0	32.7
torsion angle τ (˚)	-95.2	95.8	-108.7
folding angle α, β, γ(˚)	2.6, 24.1, 38.8	2.6, 24.3, 36.8	4.3, 24.6, 41.5
tilt angle φ (˚)	2.2	1.4	1.9

Compare to compound **6**, evidently the relative smaller bond orders in **5** and **8** as well as the larger Ni(II) radius should be responsible for the lengthening of the M-C bond distances.

According to the relationship between bond distances and spin states, *i.e.* the longer distances of M-C corresponds to high spin electronic configuration of the metal atom or cation, and the shorter distances of M-C corresponds to low spin configuration of the metal atom or cation, the spin states of Mn(II) and Ni(II) in **5** and **8** can be deduced by comparison of the corresponding Mn-C and Ni-C distances with those in literature.

Tab. 14 The relationship between bond distances and spin configurations

	Mn-C (pm)	Ni-C (pm)
$NiCp_2$		219.6(4) (low spin) [122]
Ni(6-Hyp-Hgual)$_2$ (**8**)		217.4(5) (low spin)
$(C_5H_4Me)_2Mn$	243.3(8) (high spin) [123]	
$(C_5H_5)_2Mn$	238.0 (high spin) [123]	
$(C_5H_4Me)_2Mn$	214.4(12) (low spin) [124]	
$(C_5Me_5)_2Mn$	211.2(2) (low spin) [121]	
Mn(6-Hyp-Hgual)$_2$ (**5**)	211.1(4) (low spin)	

As shown in Tab. 14, the Ni(II) in **8** should have low spin electronic configuration $^3A_2'$($a_1'^2$, $e_2'^4$, $e_1''^2$), since the low spin nickelocene $NiCp_2$ has even a little longer average Ni-Cp distance than that in **8**. Similarly, in compound **5** due to the shorter Mn-C distances the Mn(II) should be also in low spin state with electronic configuration $^2E_2'(a_1'^2, e_2'^3)$.

Thus, in compound Mn(6-Hyp-Hgual)$_2$ (**5**) the bond order is 2.5, in Ni(6-Hyp-Hgual)$_2$ (**8**) it is 2, in Fe(6-Hyp-Hgual)$_2$ (**6**) it is 3, which is consistent with the variation of M-C bond distances in three complexes.

Compound	Electronic Configuration	Bond Order
Mn(6-Hyp-Hgual)$_2$ (**5**)	$^2E_2'(a_1'^2, e_2'^3)$	2.5
Ni(6-Hyp-Hgual)$_2$ (**8**)	$^3A_2'$ $(a_1'^2, e_2'^4, e_1''^2)$	2
Fe(6-Hyp-Hgual)$_2$ (**6**)	$^1A_{1g}$ $(a_1'^2, e_2'^4)$	3

Within each compound the bridgehead atoms C9 and C10, due to the larger steric hindrance, are always a little bit far away from the central M(II) than C1, C2 and C3 (Tab. 13). This regular variation of the M-C distances results in the tilt of the C_5-ring.

The average C-C distances in the C_5 ring in all of the three compounds are found to be in the normal region (142.0pm). In the seven-membered ring the shorter bond distances C4-C5 and C7-C8 (132.8 ~134.2pm) indicate the double bond characters, whereas the longer bond distances C6-C7 and C5-C6 (148.3 ~151.5pm) show single bond characters. The C9-C8 and C10-C4 are delocalized with bond distances ranging from 144.1 to 145.7pm. The Si-Si and Si-C distances in the hypersilyl group are also in the expected region.

2.3.3.2 Molecular Structure of Fe(8-Hyp-Hgual)$_2$ (7)

Compound **7** crystallized from toluene as deep red rod-shaped crystals. It possesses triclinic crystal system with the rare space group P1. Selected crystallographic data are compiled in Tab. 15.

Tab. 15 Selected crystallographic data and structure refinement for 7

Empirical formula	$C_{48}H_{90}FeSi_8$
Formula weight (g/mol)	947.77
Temperature (K)	293(2)
Wavelength (Å)	0.71073
Crystal system	Triclinic
space group	P1
Unit cell dimensions (Å, deg)	A=10.390(3) α=72.113(14) b=19.181(2) β=86.80(2) c=23.436(5) γ=76.305(19)
Volume (Å^3)	4317.7(17)
Z	3
calc. density (Mg/m^3)	1.093
Absorption coefficient (mm^{-1})	0.457
F(000)	1548
Reflections collected / unique	6206 / 6206[R(int)=0.0000]
Data / restraints / parameters	6206 / 3 / 821
(Goodness-of-fit on F^2)	1.257
Final R indices [I>2σ(I)]	R1=0.0710, wR2=0.1728
R indices (all data)	R1=0.0864, wR2=0.1803

X-ray diffraction analysis revealed three independent molecules in the unit cell. Two of them have (S,S)-, and the third one has (R,R)-configuration, marked with **7$_A$**, **7$_C$** and **7$_B$**, respectively.

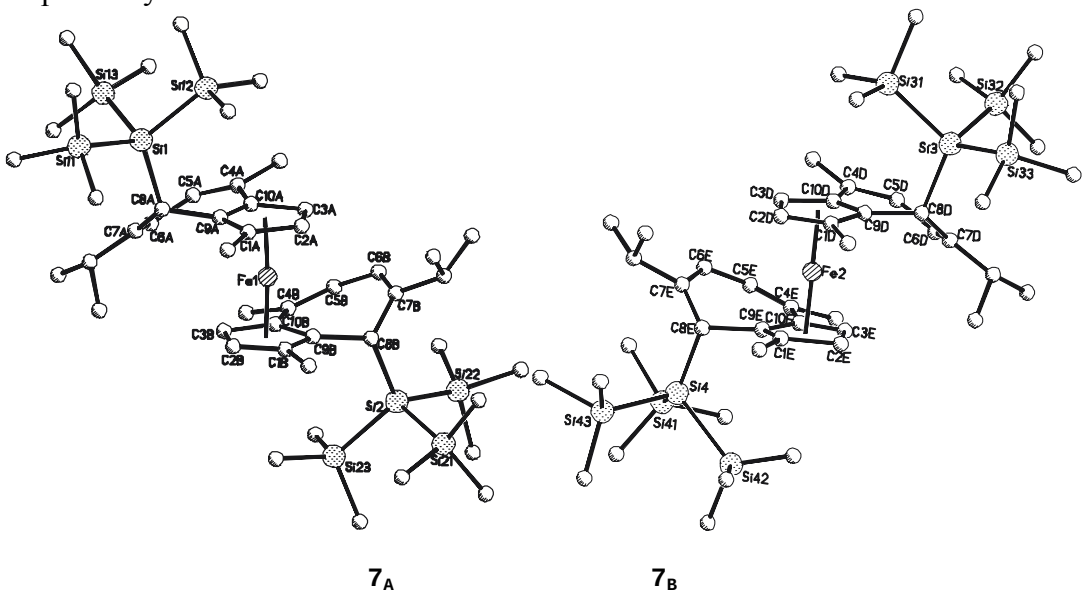

Fig. 31 Molecules of 7$_A$ [(S, S)-L$_2$Fe] and 7$_B$ [(R,R)-L$_2$Fe], L=[(8-Si(SiMe$_3$)$_3$)(C$_{15}$H$_{18}$)]. Atoms are represented by spheres of arbitrary radii; hydrogen atoms are omitted for clarity.

Overall, as in compound Fe(6-Hyp-Hgial)$_2$ (**6**), the two ligands moieties in compound Fe(8-Hyp-Hgual)$_2$ (**7**) are also staggered, but the project diagram along the axis of $C_{5(cent.)}$-Fe-$C'_{5(cent.)}$ looks totally different from that of **6** (Fig. 32).

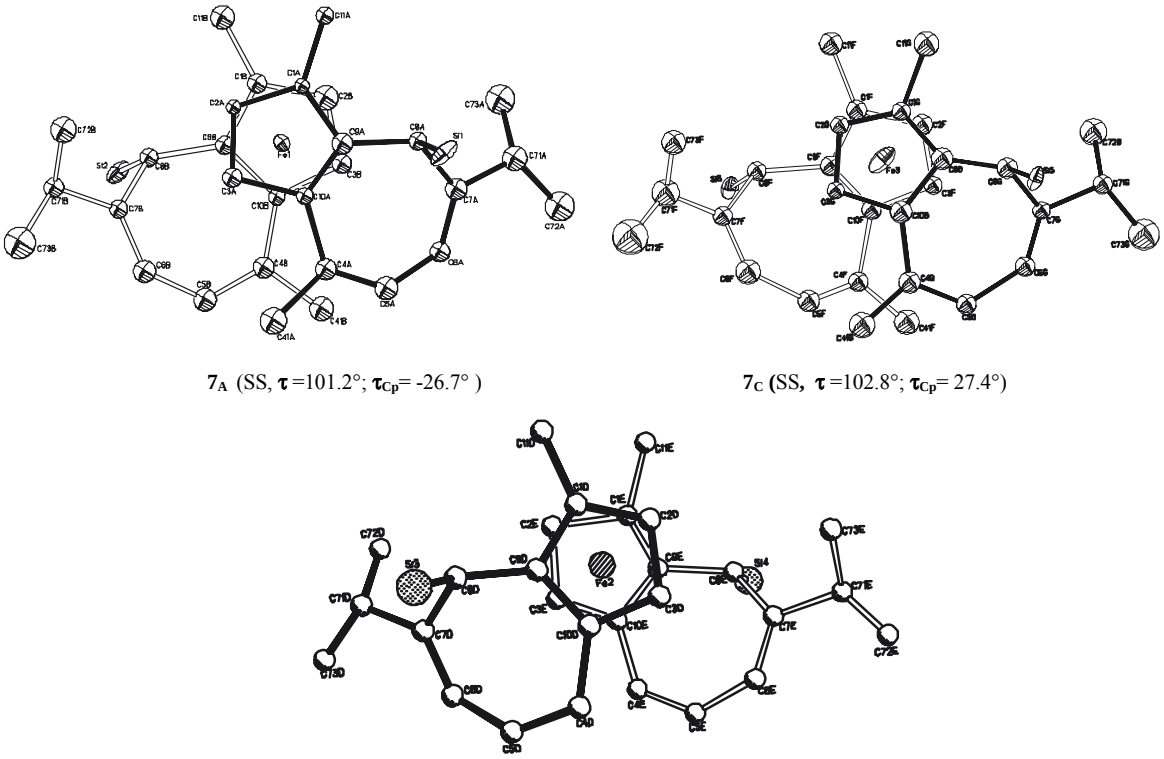

7$_A$ (SS, τ =101.2°; τ_{Cp}= -26.7°) **7$_C$** (SS, τ =102.8°; τ_{Cp}= 27.4°)

7$_B$ (RR, τ = -102.0°; τ_{Cp}= 27.3°)

Fig. 32 Projection along the axis $C_{5,cent.}$-Fe-$C'_{5,cent.}$ Hydrogen atoms and $SiMe_3$ are omitted for clarity

Conformation Analysis

As shown in Fig. 32, the two ligands moieties in each molecule of compound **7** are staggered for about 100° clockwise for R,R- and anticlockwise for S,S-configuration. Instead of the syn-conformation **a2** and **b4** taking up by compounds **5**, **6** and **8** (Fig. 29), in compound **7** the two ligands moieties are arranged in anti-conformation. A top view of **7** along the $C_{5(cent.)}$-M-$C'_{5(cent.)}$ axis (Fig. 32) show clearly the anti-type structure.

The selection of the "anti"-conformation in compound **7** as stable conformation in solid state can also be understood with following conformation analysis.

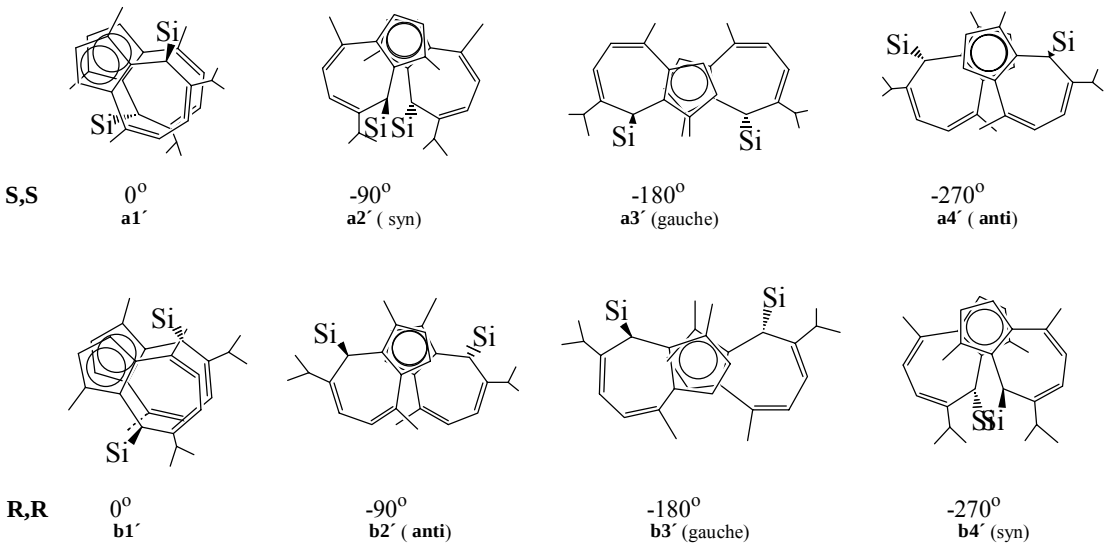

Fig. 33 Conformation analysis of (S,S)- and (R,R)-configurations for 7

Evidently, the syn-conformation **a2´** for (S,S)-configuration is not stable due to the great steric hindrance of the two bulky hypersilyl groups connected in C8 and C(8´), although all other substituents are staggered away from one another. In the anti-conformation **a4´** for (S,S)-configuration the two hypersilyl groups are staggered far away from each other, only the two 4-methyl groups are close to each other. In the gauche-conformations **a3´** for (S,S)-configuration the two 1-methyl groups overlap, indicating higher energy state than the anti-conformations. Consequently, the anti-conformations **a4´** for (S,S)-configuration should be the most stable conformation in the solid state. Similarly, the stable conformation for (R,R)-configuration should be also the anti-conformation symbolized as **b2´**, which is an enantiomer of **a4´**. Thus, it is the different position of the large hypersilyl group in the seven-membered ring which results in the conformation difference of **6** and **7**.

The results of the conformation analysis agree with that of the X-ray diffraction analysis. The molecule $\mathbf{7_A}$ and $\mathbf{7_C}$ with (S,S)-configuration take up conformation similar to **a4´**, and molecule $\mathbf{7_B}$ with (R,R)-configuration takes up similar conformation as **b2´** (Fig 32). In the anti-conformation in compound **7** the two hypersilyl groups stretch away from each other with staggered angle of C8-$C_{5(cent.)}$(1) -$C'_{5(cent.)}$(2)-C8´ close to 180° (171.9° in $\mathbf{7_A}$, 171.8° in $\mathbf{7_B}$, and 170.6° in $\mathbf{7_C}$).

The two C_5 rings are staggered nearly in the same degree with -26.7˚ in $\mathbf{7_B}$, 27.4˚ in $\mathbf{7_C}$ and 27.3˚ in $\mathbf{7_A}$, the data are still given as the average value of the five smallest torsion angles.

Coplanarity of 7

Compare to compound **6**, the co-planarity of the C_5 rings in compound **7** is poor, the deviation of them in three unique molecules varies from 0.0083 to 0.0169 angstrom. The methyl group in the C_5 ring bends toward to or away from the central Fe atom without regularity, with bending angles δ ranging from 1.4 to 7.3˚ in three independent molecules. Similarly, the seven-membered rings distort severely (Scheme 6). The atoms C5, C6, C7 fold strongly toward Fe(II), whereas C8, affected by the hypersilyl group, folds away from the Fe(II).

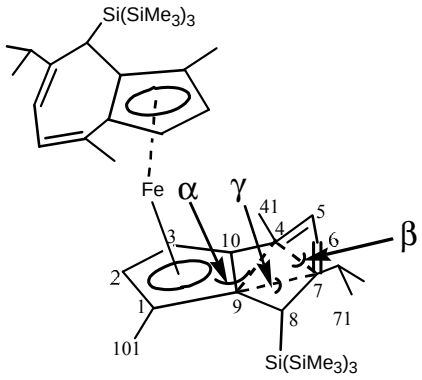

Scheme 6 Definition of the folding angle in 7

We write similarly the dihedral angle between the C_5 (ring) and the best plane through the atoms C4, C9, C10 as α, the dihedral angle between the best plane through the atoms C10, C9, C4, C7 and the best plane through the atoms C4, C5, C6, C7 as β, and the dihedral angle between the best plane through the atoms C10, C9, C7, C4 and the best plane through the atoms C7, C8, C9 as γ. Three molecules in **7** possess three series of independent data, *i.e.* 1.0˚, 11.4˚, 49.6˚ for (S,S)-$\mathbf{7_A}$; 1.5˚, 11.7˚, 50.8˚ for (S,S)-$\mathbf{7_C}$, and 2.4˚, 5.2˚, 47.2˚ for (R,R)-$\mathbf{7_B}$. The two same configurations (S,S)-$\mathbf{7_A}$ and (S,S)-$\mathbf{7_C}$ have similar data, but showing large difference from those for the (R,R)-$\mathbf{7_B}$. Compare to **5**, **6** and **8**, the folding angle γ in **7** is much larger, displaying the stronger bending action of the hypersilyl group in C8 than that in C6.

The two C_5 rings are not parallel with tilt angles in three independent molecules ranging from 2.6 to 3.2˚ (Tab.16). As in **8**, the Fe(II) centre in **7** in three unique molecules slipped a little away from the middle point of the line $C_{5(cent.)}(1)$-$C_{5(cent.)}(2)$ with the angle of $C_{5(cent.)}(1)$-Fe-$C_{5(cent.)}(2)$ in 174.7, 170.5, and 177.8° for $\mathbf{7_A}$, $\mathbf{7_B}$, and $\mathbf{7_C}$, respectively.

Bond Parameters

Three pairs of Fe-$C_{5(cent.)}$ parameters in three independent molecules of **7** vary from 164.4 to 168.9pm. Fe(II) is often much closer to one C_5 ring than to the other (Tab.16), showing again the irregularity. The Fe-C_5(ring) distances in **7** vary in larger range from 198.0 to 214.0pm than in **6**. The bonds C4-C5 and C6-C7 have double bond characters (119.3 ~ 134.8pm), whereas bonds C7-C8, C8-C9 are typical single bonds. It is noticeable that the bonds C4-C10 and C5-C6 with bond distances ranging from 142.0 to 158.5pm are not fully delocalized.

The irregular variation of parameters in **7** is easily rationalized as the result of the great steric demand of the bulky hypersilyl group bonded to C8 atom. Actually in **7** the hypersilyl group locates so close to the C_5 ring that the latter can not keep co-planarity any more. Owing to the poor coplanar properties the C_5 ring has no certain tilt direction in three independent molecules. The bond lengths and related parameters for **7** are collected in Tab. 16.

Tab. 16 Selected parameters of compound Fe(8-Hyp-Hgual) 7

parameters	(S,S)-FeL_2 (7_A)	(R,R)-FeL_2 (7_B)	(S,S)-FeL_2 (7_C)
Fe-C2	207.2(14)	199.8(19)	199.0(3)
Fe-C3	206.0(3)	206.0(3)	210.0(2)
Fe-C1	206.0(3)	203.0(3)	205.9(19)
Fe-C10	205.5(18)	205.1(19)	205.0(2)
Fe-C9	207.0(2)	211.2(19)	206.0(2)
Fe-$C_{5(cent.)}$(1)	167.1	169.9	168.9
Fe-C12	208.0(3)	211.0(3)	201.2(16)
Fe-C13	210.0(2)	201.9(17)	198.0(3)
Fe-C11	208.4(19)	201.9(17)	198.0(2)
Fe-C19	206.0(2)	209.4(19)	214.0(2)
Fe-C20	205.5(2)	206.0(2)	207.0(2)
Fe-$C_{5(cent.)}$(2)	167.7	167.5	164.4
$C_{5(cent.)}$(1)-Mn-$C_{5(cent.)}$(2) (deg)	174.7	170.5	177.8
C-C (C_5 (1) ring aver.)	130.0~151.0		
C4-C5	134.0(4); 141.0(5)	131.0(5); 139.0(4)	119.0(5); 135.0(4)
C7-C8	156.0(2); 152.0(4)	145.0(4); 152.4(18)	154.0(4); 146.0(2)
C6-C7	134.0(5); 137.0(3)	135.0(3); 136.0(5)	134.0(3); 128.0(5)
C8-C9	155.0(4); 156.0(4)	160.0(5); 150.0(4)	161.0(4); 142.0(3)
C5-C6	142.0(5); 148.0(3)	147.0(3); 145.0(5)	157.0(3); 160.0(5)
C10-C4	155.0(4); 145.0(5)	150.0(5); 152.0(4)	159.0(5); 153.0(5)
Si-Si	235.9(5)-239.0(5)	232.8(4)-243.5(4)	230.4(3)-240.8(3)
Si-C in –Si1[($SiMe_3$)$_3$]	183.0(5)-192.0(5)		
(Me_3Si)$_3$Si-C	195.7(4) ; 201.0(3)	195.3(3); 199.3(4)	196.2(4); 201.6(5)
torsion angle τ_{Cp}(°)	27.3	-26.7	27.4
torsion angle τ (°)	101.2	-102.0	102.8
folding angle α, β, γ(°)	1.0, 11.4, 49.6	2.4, 5.2, 47.2	1.5, 11.7, 50.8
tilt angle φ (°)	2.6	3.2	3.2

2.3.3.3 Conformation Analysis of (R,S)-Fe(6-Hyp-Hgual)$_2$ (6) and (R,S)-Fe(8-Hyp-Hgual)$_2$ (7)

All of the above discussed structures of the rac-diastereomers possess (R,R)- or (S,S)-configurations. The information of the meso-diastereomer with (S,R)- or (R,S)-configuration has been acquired firstly only through NMR spectra[I]. The four extreme conformations for (S,R)- or (R,S)-configurations in **6** are depicted in the following scheme. It seems that both of **c2** and **c4** should be the possible stable conformations in the solid state.

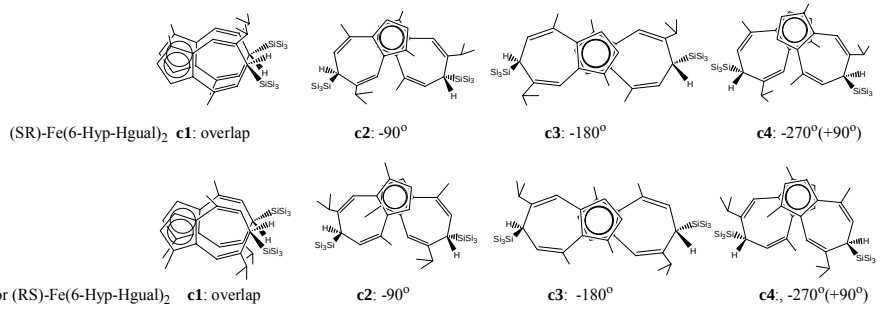

Fig. 34 Four ideal conformations of (S, R)- or (R,S)-conformers in 5, 6 and 8

[I] The meso-diastereomer of of (S,R)- or (R,S)-Fe(6-Hyp-Hgual)$_2$ has been successfully isolated and its crystal structure was obtained after I just submitted this dissertation. It has similar conformation to **c4**, but the torsion angle of C6-$C_{5(cent.)}$-C′$_{5(cent.)}$-C6′ is only 60°. According to the space group Pī, the molecule with confomation similar to **c2** must exist also in the meso-diastereomer. It is then consistent with above depicted conformations.

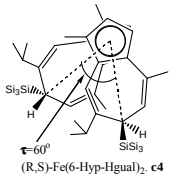

Similarly, the possible stable conformations for R,S-configuration in compound **7** in solid state might be a mixture of **c2´**and **c4´**.

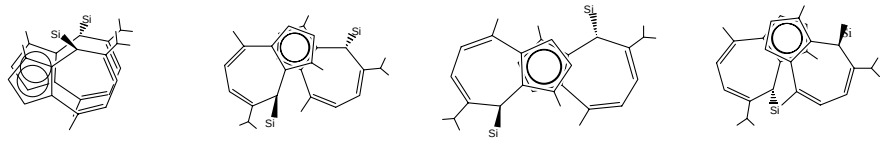

c1´: SR, overlap **c2´**: SR, -90° **c3´**: SR, -180° **c4´**: SR, -270°

Fig. 35 Four ideal conformations of (S, R)-conformers in compound 7

2.3.3.4 Molecular Structure of (3-Hyp-6-Hgual)$_2$ (9)

Compound **9** crystallizes from toluene as colourless hexangular platelets with monoclinic crystal system, space group C2/c. The selected crystallographic data are summarized in Tab. 17.

Tab. 17 Selected crystallographic data and structure refinement for 9

Empirical formula	$C_{24}H_{45}Si_4$
Formula weight (g/mol)	445.96
Temperature (K)	173(2)
Wavelength(Å)	0,71073
Crystal system	Monoclinic
Space group	C2/c
Unit cell dimensions (Å, deg)	a=25.989(2) b=19.2622(16) β=105.100(6) c=11.8707(12)
Volume (Å^3)	5737.4(9)
Z	8
calc. density (Mg/m^3)	1.033
Absorption coefficient (mm^{-1})	0.215
F(000)	1960
Reflections collected / unique	7700 / 6839[R(int)=0.0455]
Data / restraints / parameters	6839 / 0 / 284
(Goodness-of-fit on F^2)	1.002
Final R indices [I>2σ(I)]	R1=0.0603, wR2=0.1199
R indices (all data)	R1=0.1447, wR2=0.1533

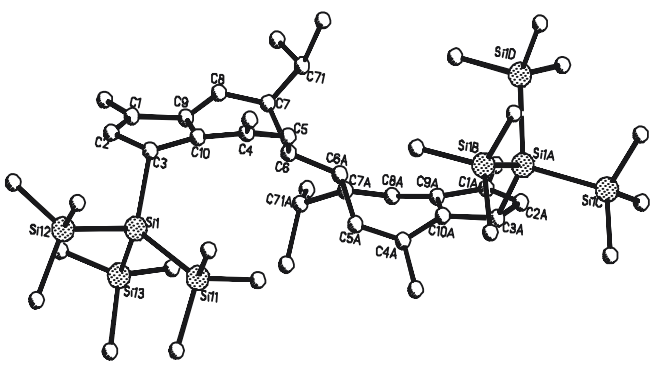

Selected bond distances(pm) and bond angles(deg)
C(1)-C(2) 133.7(5) C(2)-C(3) 148.9(4)
C(3)-C(10) 150.1(4) C(10)-C(9) 138.9(4)
C(9)-C(1) 146.3(4) C(4)-C(10) 145.3(4)
C(4)-C(5) 134.2(4) C(5)-C(6) 150.0(4)
C(6)-C(7) 152.3(4) C(7)-C(8) 134.7(4)
C(8)-C(9) 143.6(4) C(6)-C(6A) 153.8(5)
Si(1)-C(3) 195.4(3) Si(1)-Si 236.14(13)
Si-C(Me) 186.9(4)
C(5)-C(6)-C(6A) 111.8 C(7)-C(6)-C(6A) 116.7
C(6)-C(6)-C(7) 106.3
line Si(1)-C(3) to plane Cp(1) 33.6
folding angle α=13.6, β=27.2, γ=57.8

Fig. 36 Molecular structure of 9. Atoms are represented by spheres of arbitrary radii; hydrogen atoms are omitted for clarity.

Several interesting structural characters in the molecule of **9** (Fig. 36) can be observed: firstly, each hypersilyl group is connected to C3 or C3A instead of to C2 or C2A as in compound **14** (Fig. 45); secondly, both of the two bulky hypersilyl groups locate at the same side of the two five-membered rings, although stretching away from each other, thus the whole molecule has C_2-symmetry with C_2-axis through the midpoint of C6-C6A and perpendicular to the paper plane; thirdly, the hypersilyl group and the chiral carbon atoms C6 in the same guaiazulene moiety stretch along same direction, resulting always different configurations of chiral carbon atoms C3 and C6. The bending angle of the line C3-Si($SiMe_3$)$_3$ from the best plane through the atoms C2, C3 and C10 is 36.4°, and the folding angle of γ in the seven-membered ring is 57.8°, which is much larger than that in **2a**.

The same bending direction of hypersilyl group and C6 can be understood with Fig. 37. In compounds **2a**, **5**, **6**, and **8** the metal atoms M, corresponding to C6 in **9**, must coordinate still with ligand L. Owing to the steric effect of L, the hypersilyl group prefers to stretch away from the metal atoms, whereas in compound **9** the small atom H6 locates in the axial position, which gives rise to the possibility for the hypersilyl group and C6 to stretch along same direction.

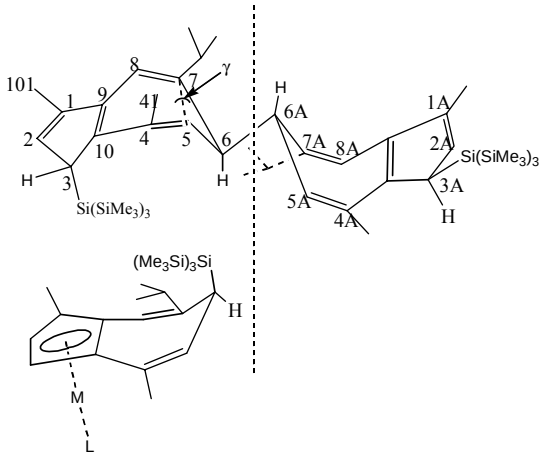

L=THF, M=K, **2a**
L= 6-Hyp-Hgual, M=Mn, **5**; M=Fe, **6**; M=Ni, **8**

Fig. 37 Comparison of the molecular structures of 9 and 2a, 5, 6, and 8

The related bending angles and folding angle in the five- and seven-membered rings for compound **9** are depicted in Scheme 7.

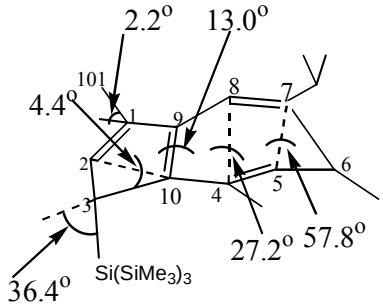

Scheme 7 Structural parameter of 9

As shown in Scheme 7, the bond C1-C101 bends away from the best plane through the atoms C1, C2, C9 and C10 in 2.2°. The dihedral angle between the best plane through the atoms C2, C1, C9, C10 and the best plane through the atoms C2, C3 and C10 is 4.4°. The folding angle β in the seven-membered ring is 27.2°. The folding angle α, which is between the best plane through the atoms C1, C2, C9 and C10 and the best plane through the atoms C4, C8, C9 and C10 is 13.0°.

The non-aromatic five-membered ring in compound **9** result in the single bond character of C3-C10 and C2-C3 with bond distances of 150.1 and 148.9pm, respectively. The bond distances in the hypersilyl group are similar to those in compound **2a** with Me-Si distances ranging from 185.5 to 187.8pm, and Si-Si from 235.6 to 236.8pm. The C6-Si distance is in the expected range as 195.4pm. All other C-C bond distances are consistent with the molecular structure.

2.4 Mono-Hyp Substituted Metallocene Dichloride Derivatives

2.4.1 Reactions

A characteristic properties of the reaction between $TiCl_3$, $ZrCl_4$ or $HfCl_4$ and compound **2** is that the reaction takes place not only in dipolar solvents like tetrahydrofuran but also in non-dipolar solvents such as toluene, this is much different from the metal halides of $MnBr_2$, $FeCl_2$ and $NiBr_2$, $CoCl_3$ VCl_3 etc., which in toluene do not react with complex **2**.

2.4.1.1 Reaction of $TiCl_3$ with K(6-Hyp-Hgual)(2)

Although the reaction of $TiCl_3$ with **2** can take place in both of toluene and tetrahydrofuran, the resulted products are much different. In toluene the ligand is oxidized to compound **9**, whereas in tetrahydrofuran the metal cation Ti(III) is oxidized to Ti(IV). Both of these processes implied that the probable intermediate Ti(6-Hyp-Hgual)$_2$Cl is not stable, it would react further and gives rise to the final products, either **9** or **10**, depending on the used solvent.

Eq.24

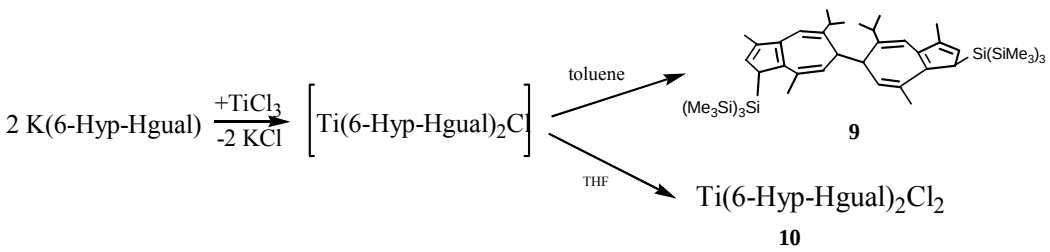

In toluene a yellowish intermediate was once captured as crystalline compound at 5°C, showing paramagnetic properties in ^{1}H NMR spectrum with very broad peaks similar neither to those of compound **9**, nor to those of compound **10**. The attempts to acquire X-ray quality single crystals through recrystallization of it at 5°C from toluene resulted in further reaction in several weeks, and furnished colourless compound **9**, which was demonstrated by NMR spectroscopic- and crystallographic methods.

In tetrahydrofuran the reaction of $TiCl_3$ with **2** is much different from that in toluene. The anhydrous red powder of $TiCl_3$ will form at first with THF to greenish complex of $(THF)_3 \cdot TiCl_3$, which reacts slowly with the yellow-green solution of compound **2a** and gives rise to brown solution. Through recrystallization the red needle-shaped crystals appear after several days. X-ray diffraction analysis revealed it to be the Ti(IV)-species of Ti(6-Hyp-Hgual)$_2$Cl$_2$ (Fig. 40). Similar oxidation of Ti(III) to Ti(IV) is reported [125] (Fig. 38).

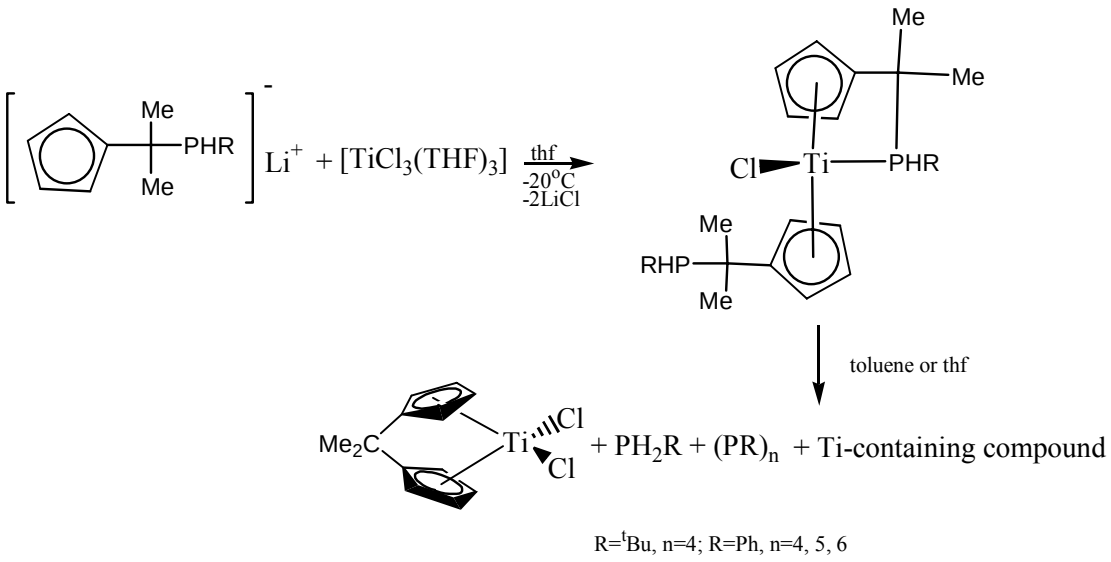

Fig. 38 Formation and decomposition of Ti{Cp[CMe$_2$(PHR)]}$_2$Cl

2.4.1.2 Reactions of MCl_4 (M=Zr(IV), Hf(IV)) with K(6-Hyp-Hgual) (2)

Different from the red-ox reaction of $TiCl_3$ with **2**, the metathesis between $ZrCl_4$, $HfCl_4$ and K(6-Hyp-Hgual) (**2**) in both of toluene and tetrahydrofuran results in always metallocene dichloride derivatives with yield in about 40%. Due to the heterogeneous character the reaction mixtures were allowed to stir for about 24 hours.

Eq.25

$$2\ \text{K(6-Hyp-Hgual)} + MCl_4 \xrightarrow{\text{toluene or THF}} M(\text{6-Hyp-Hgual})_2Cl_2 + 2\ \text{KCl}$$

M=Zr **11**, Hf **12**

Both of the products **11** and **12** can be purified with toluene and are observed as yellow and light yellow crystals, respectively.

*2.4.1.3 Reaction of ZrCp*Cl$_3$ with K(6-Hyp-Hgual)*

In toluene at room temperature the equimolar reaction of ZrCp*Cl$_3$ with **2** gave rise to clear yellow solution after overnight stirring. Without separation of the potassium chloride, rhombus-shaped platelets (not well shaped single crystals) grew up in one night at room temperature from the fresh prepared clear solution. The re-crystallization of the crystalline compound resulted in only powder instead of crystals, since it is difficult to dissolve in toluene again. This indicates that either the inorganic salt KCl precipitates or the product contains KCl unit. The element analysis of the crystalline compound showed its components as 1:1 molar ratio of ZrCp*(6-Hyp-Hgual)Cl$_2$ and KCl. The ^{1}H-, ^{13}C- and ^{29}Si NMR spectroscopy revealed the existences of 1:1 molar ratio of Cp* and the 6-Hyp-Hgual unit. Unfortunately all attempts to isolate and unambiguously identify the mixed sandwich compound failed.

Eq.26

$$\text{K(6-Hyp-Hgual)} + \text{ZrCp*Cl}_3 \xrightarrow{\text{toluene}} \underset{\textbf{13}}{\text{ZrCp*(6-Hyp-Hgual)Cl}_2} + \text{KCl}$$

2.4.2 NMR Spectroscopy

2.4.2.1 ^{1}H NMR Spectroscopy

The selected ^{1}H NMR spectral data for metallocene dichloride derivatives **10**, **11**, **12** and **13** are listed in the following table.

Tab. 18 Selected ^{1}H NMR data in C_6D_6 at 297K (250.133MHz) (s=singlet, d=doublet)

	Cp*	H8	H2	H3	H5	H6
ZrCp*(6-Hyp-Hgual) Cl$_2$ (13)	1.8 (s)	6.23 (s)	5.24(d) $^3J_{HH}$=2.8 (AB)	5.16(d) $^3J_{HH}$=2.8 (AB)	5.49(d) $^3J_{HH}$ =9.2	3.07(d) $^3J_{HH}$=9.2
Hf(6-Hyp-Hgual)$_2$Cl$_2$ (rac-12)		6.02 (s)	5.45(d) $^3J_{HH}$=3.2	5.33(d) $^3J_{HH}$=3.2	5.39(d) $^3J_{HH}$=8.7	3.06(d) $^3J_{HH}$=8.7
Zr(6-Hyp-Hgual)$_2$Cl$_2$ (rac-11)		6.03 (s)	5.55(d) $^3J_{HH}$=2.9	5.54(d) $^3J_{HH}$=2.9	5.38(d) $^3J_{HH}$=9.0	3.03(d) $^3J_{HH}$=9.0
Ti(6-Hyp-Hgual)$_2$Cl$_2$ (rac-10)		6.13 (s)	5.55(d) $^3J_{HH}$=2.8 (AB)	5.45(d) $^3J_{HH}$=2.8 (AB)	5.48(d) $^3J_{HH}$=9.0)	3.09(d) $^3J_{HH}$=9.0

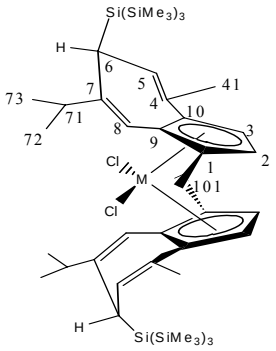

M=Ti(IV), Zr(IV), Hf(IV)

Fig. 39 Numbering of Carbon atoms for compounds 10, 11, 12

The rac- and meso-diastereomers in compounds **10**, **11** and **12** could be readily distinguished from one another by the differing positions of their ^{1}H NMR signals. It is notably that the NMR spectra recorded from the crystals of compounds **10** and **12** gave rise to only signals of the rac-diastereomers. The NMR spectra of Zr(6-Hyp-Hgual)$_2$Cl$_2$ (**11**) recorded with the firstly obtained crystalline compound was very complicate, indicating the presence of both diastereomers, but the NMR spectrum recorded with the crystals of **11** obtained through many fractional recrystallization steps showed nearly only the signals of the rac-diastereomer. Similar to compound **2a**, compound **13** had only rac-diastereomer, which gives rise to one set of NMR signals.

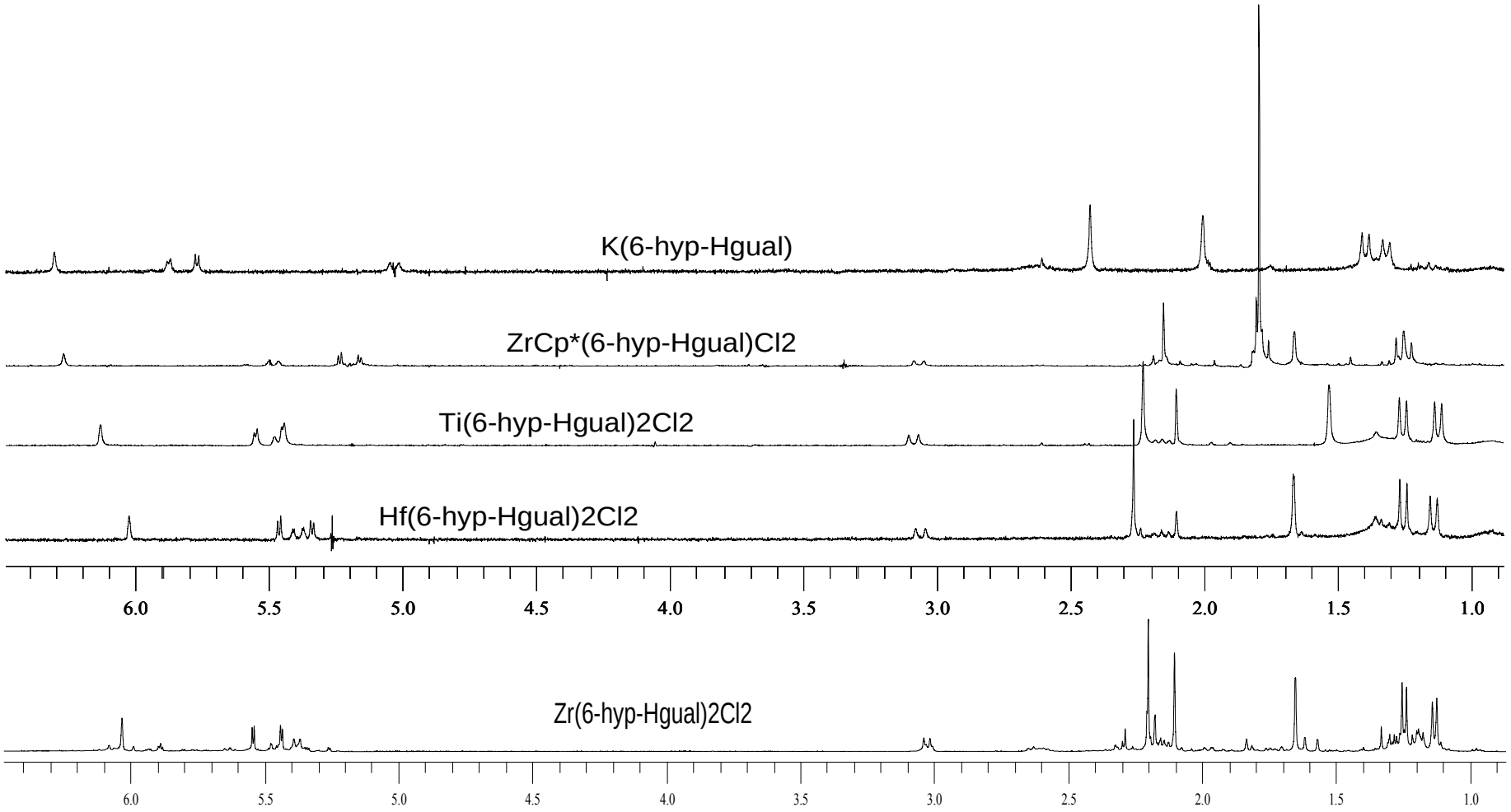

Spe. 11 ^{1}H NMR spectra of K[6-Hyp-Hgual], rac-[6-Hyp-Hgual]$_2$MCl$_2$, M=Ti(IV) (10), Zr(IV) (11), Hf(IV) (12) and ZrCp*(6-Hyp-Hgual)Cl$_2$·KCl (13). The signal at 2.10ppm is from the methyl group in the used solvent toluene

Compare to K(6-Hyp-Hgual) (**2**), in compounds **10**, **11**, **12** and **13** the signals of olefinic protons H8, H2, H3 and all of aliphatic protons showed upfield shifts, whereas the signals of H5 and H6 showed low-filed shifts. This caused the signals of H2, H3 and H5 are more and more close to each other, and the signals of H6 and H101 separated from each other. In compound **2** the signal of H6 was nearly covered with that of H101, but in **10**, **11**, **12** and **13** the signal of H6 moved to about 3.0ppm, and that of H101 located under 2.5ppm. The variation was shown clearly in the ^{1}H NMR spectra in Spe. 11.

2.4.2.2 ^{13}C NMR Spectroscopy

The selected ^{13}C NMR data recorded in C_6D_6 at room temperature for the rac-diastereomer of complexes **10**, **11**, **12** and **13** are collected in Tab .19.

Tab. 19 Selected ^{13}C NMR data in C_6D_6 at 297-300K

Compound	C1, C4, C7, C9, C10	C5	C8	C2	C3
Ti(6-Hyl-Hgual)$_2$Cl$_2$ (**10**)	151.6; 139.0; 135.9; 129.6; 127.0	134.0	115.4	109.0	107.1
Zr(6-Hyl-Hgual)$_2$Cl$_2$ (**11**)	149.6;134.6;130.6; 126.6; 125.5	131.3	113.8	106.9	105.2
Hf(6-Hyl-Hgual)$_2$Cl$_2$ (**12**)	149.6; 133.2; 129.2; 126.5; 123.5	131.5	113.8	105.3	104.2
ZrCp*(6-Hyl-Hgual)$_2$Cl$_2$ (**13**)	148.6; 138.6; 131.2; 126.8; 125.9; 123.2 (5C in the ring of Cp*); 12.50(Me in Cp*)	131.9	114.4	107.7	103.6

Similar to compounds **1**, **2** and **3**, all olefinic carbon atoms C1, C2, C3, C9 and C10 in the five-membered ring in compounds **10**, **11**, **12** and **13** give rise to signals above 100ppm, indicating the dominantly ionic character of M-C_5 (M=Ti(IV), Zr(IV) and Hf(IV)).

All aliphatic ^{13}C NMR spectral data for compounds **10**, **11**, **12** and **13** are compiled in the experimental section. Each of them falls into the corresponding expected region.

2.4.2.3 ^{29}Si NMR Spectroscopy

The peripheral silicon atom (β-Si) in all four kinds of metallocene dichloride derivatives have chemical shift in about -12.1ppm, and the resonance of the central Si atom (α-Si) in three similar compounds **10**, **11** and **12** are in about -70ppm, but in **13** it is in upfield (-86.3ppm).

Tab. 20 ^{29}Si NMR spectral data recorded in C_6D_6 at room temperature

δ(ppm)	**10**	**11**	**12**	**13**
α-Si	-68.6	-69.9	-69.2	-86.3
β-Si	-12.5	-12.1	-12.1	-12.1

2.4.3 Molecular Structures of 10, 11 and 12

Single crystals suitable for X-ray diffraction analysis for three metallocene dichloride derivatives M(6-Hyp-Hgual)$_2$Cl$_2$ (M=Ti **10**, Zr **11**, Hf **12**) are obtained from toluene. The selected crystallographic data are presented in Table 21.

Tab. 21 Crystallographic data and structure refinement for M(6-Hyp-Hgual)$_2$Cl$_2$ (M=Ti 10, Zr 11, Hf 12).

complex	**10**	**11**	**12**
empirical formular	$C_{48}H_{90}Cl_2TiSi_8$	$C_{48}H_{90}Cl_2Si_8Zr$	$C_{48}H_{90}Cl_2HfSi_8$
formula weight	1010.71	1054.05	1141.32
crystal system and space group	Triclinic, P $\bar{1}$	Triclinic, P $\bar{1}$	Triclinic, P $\bar{1}$
colour and shape of crystals	red rod-shaped	yellow needle	light yellow needle
unit cell constant (Å, deg)	a=9.2842(17), b=17.558(3) c=20.755(3), α=88.166(8) β=85.941(12),γ=78.459(11)	a=9.2207(18),b=17.480(4) c = 20.729(4),α=88.04(3) β= 85.83(3), γ=78.83(3)	a=9.208(3), b=17.480(3) c=20.605(4),α=88.771(12) β=85.612(19),γ=79.03(3)
V (Å^3)	3306.1(10)	3268.4(11)	3246.4(13)
Z, ρ(Mg/m^3)	2, 1.108	2, 1.165	2, 1.247
μ (mm^{-1})	0.387	0.428	1.868
F(000)	1192	1228	1276
Reflections collected / unique	13694 / 12863 [R(int) = 0.0346]	13717 / 12871 [R(int) = 0.0338	11053 / 10350 [R(int) = 0.0513]
Data / restraints / parameters	12863 / 143 / 660	12871 / 86 / 684	10350 / 0 / 612
Goodness-of-fit on F^2	0.845	1.048	0.945
Final R indices [I>2σ(I)]	R1 = 0.0455 wR2 = 0.1024	R1 = 0.0511 wR2 = 0.1145	R1 = 0.0519 wR2 = 0.1186
R indices (all data)	R1 = 0.0822 wR2 = 0.1095	R1 = 0.0803 wR2 = 0.1318	R1 = 0.0821 wR2 = 0.1276

Refinement method: Full-matrix least-squares on F^2

As can be seen by very similar cell parameters, the three complexes are iso-structural. In the crystal the complexes **10**, **11** and **12** are present as racemic mixture, *i.e.* as (R,R)- and (S,S)-racemic enantiomers, respectively. Thus, the chiral carbon atoms C6 and C(6´) exhibit the same configuration. The metal centre adopts a pseudo tetrahedral geometry with respect to the two chloride ligands and the two Cp centroids from η^5-coordinated ligands (Fig. 43). The seven-membered ring folds away from the metal centre, the folding angles α (2.2-3.9°), β(24.0-25.3°) and γ(37.0-40.9°) are similar to those found in compounds M(6-Hyp-Hgual)$_2$ (M=Mn(II) **5**, Fe(II) **6**, and Ni(II) **8**). The methyl groups bonded with C1 and C1´, due to the effect of chloride anion, stretch a little bit away from the metal centre (4.8-6.5°), but the methyl groups in C4 and C4´ and the isopropyl groups in C7 and C7´, which are close to the hypersilyl group, bend toward the metal centre.

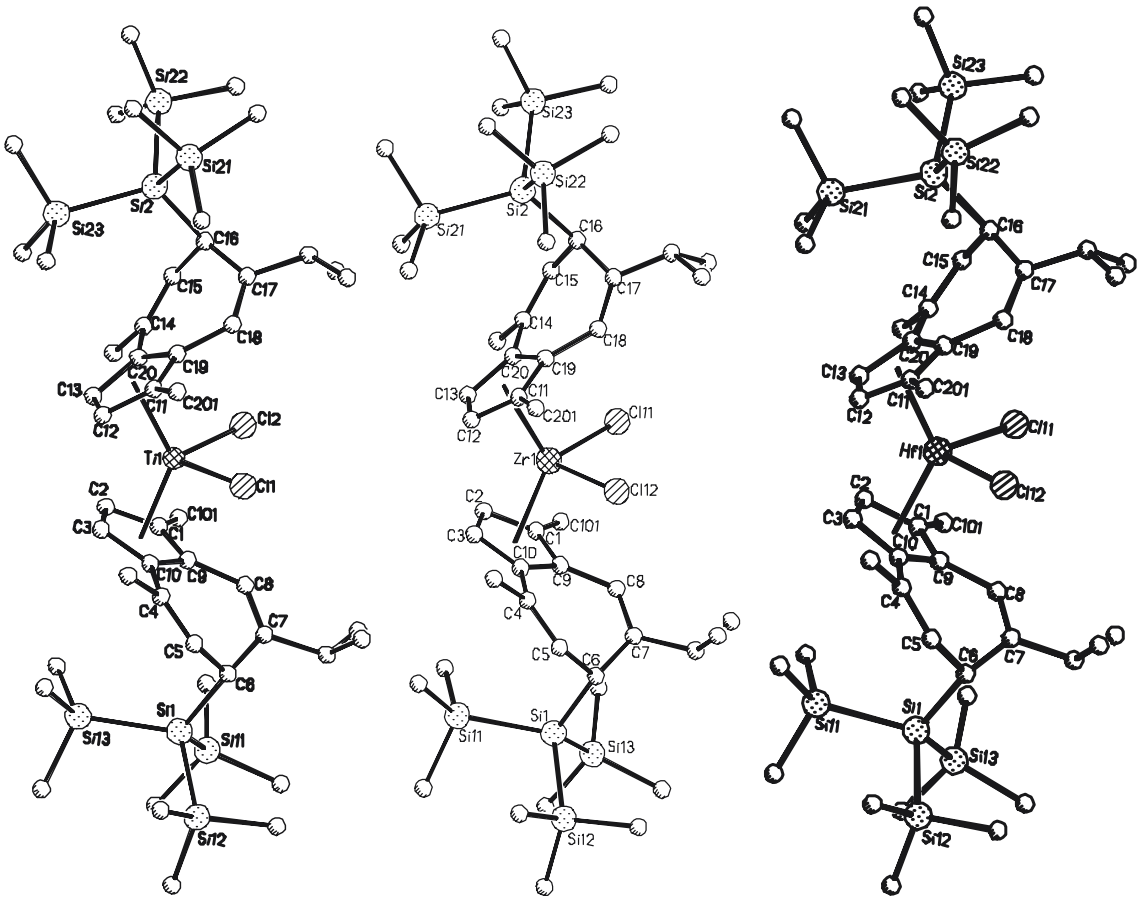

Fig. 40 Structures of M(6-Hyp-Hgual)$_2$Cl$_2$, M=Ti(IV) 10, Zr(IV) 11 and Hf(IV) 12. Atoms are represented by spheres of arbitrary radii; hydrogen atoms are omitted for clarity

The ligand looks just like small gold fish (Fig. 40), two of them in one molecule wag tails in different directions. Fig.41 shows clearly the staggered conformations with the molecules projected onto their Cl-M-Cl planes (top view of the enantiomer, looking down on the two five-membered rings of the hypersilyl substituted guaiazulene ligands). In each stable conformation of the projected diagrams, the two methyl groups bonded with C1 and C1´, and two chloride anions fall into the two seven-membered rings, namely the syn-conformation in all three compounds is adopted.

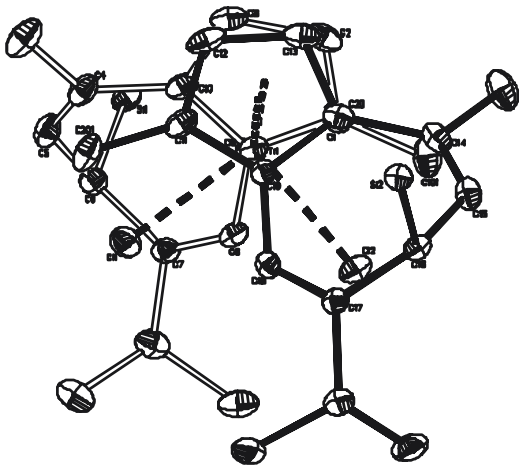

10(τ=107.0°, τ_{Cp}=15.7°)

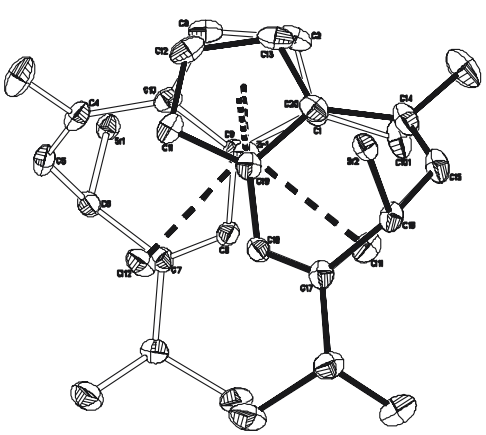

11(τ=105.9°, τ_{Cp}=14.3°)

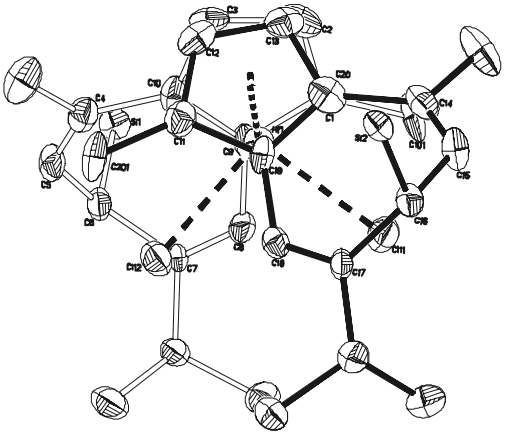

12(τ=104.4, τ_{Cp}=12.2°)

Fig. 41 Projections for M(6-HypHgual)$_2$Cl$_2$, M=Ti(IV) 10, Zr(IV) 11 and Hf(IV) 12. Atoms are represented by spheres of arbitrary radii; hydrogen atoms and SiMe$_3$ are omitted for clarity

Similar conformation analysis as by compound of Fe(6-Hyp-Hgual)$_2$ **6** (Fig. 30) can be executed for complexes of **10**, **11** and **12**.

In the syn-conformers of **10**, **11** and **12**, due to the existence of two chloride ligands, the two 1-methyl groups are staggered farther away from each other than those in M(6-Hyp-Hgual)$_2$ (M=Mn **5**, Fe **6**, and Ni **8**), this can be quantified by the torsion angles of C101-Cp-Cp´-C101´. They are about 20° larger than those in **5**, **6** and **8** (106.7 ~119.2°).

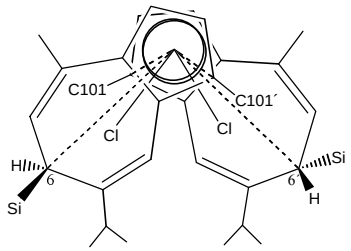

	10	**11**	**12**
C6-$C_{5(cent.)}$-C´$_{5(cent.)}$-C6´	107.0	105.9	104.4
C101-$C_{5(cent.)}$-C´$_{5(cent.)}$-C101´	-137.2	-138.2	-140.7
Cl-M-Cl	93.51(3)	95.61(5)	94.33(7)

Fig. 42 Structural parameters in complexes of 10, 11 and 12 (deg)

Based on the same reason, the two non-chloride ligand frameworks in these three complexes, when measured with the torsion angles of C6-Cp-Cp´-C6´, are staggered away from each other in general also a little bit larger than those in M(6-Hyp-Hgual)$_2$ (M=Mn(II) **5**, Fe(II) **6**, **τ**= ~96°) (Fig.42), and larger than that in similar compound $(C_9Me_7)_2ZrCl_2$ (**τ**=98.5°)[126].

The two C_5 rings in each molecule are staggered with dramatically smaller staggering angles (15.7° **10**, 14.3° **11**, 12.2° **12**) than those in the complexes M(6-Hyp-Hgual)$_2$ (M=Mn **5**, Ni **8**, Fe **6**, ranged from 24.4° to 32.7°). Compare to literature, in $(C_9Me_7)_2ZrCl_2$ [126] and $(Ind)_2ZrCl_2$ [127] the two C_5 rings are staggered also, but in $[MeCp(CH_2)_5]_2ZrCl_2$ [128] the two C_5 rings are eclipsed.

Due to the tetrahedral geometry (Fig.43), the two C_5 rings in compounds **10**, **11** and **12** tilt severely with tilt angle **φ** ranging from 58.3 to 58.6°. Similar metallocene dichloride derivatives such as Ti(8, 8´-bigua)Cl_2 (**XI**) (**φ**=50.3°) [84] and $(Ind)_2ZrCl_2$ (**φ**=62.07°) [127] show relative close tilt angles.

In the distorted tetrahedral geometry the bond angle of Cl-M-Cl ranges from 93.51(3) to 95.61(5)°, whereas the angle of $C_{5(cent.)}$-M-C´$_{5(cent.)}$ ranges from 129.4 to 132.3° (Fig. 43). Compare with other metallocene dichloride derivatives (Tab. 23) reported in literature, all these value fall into the normal range.

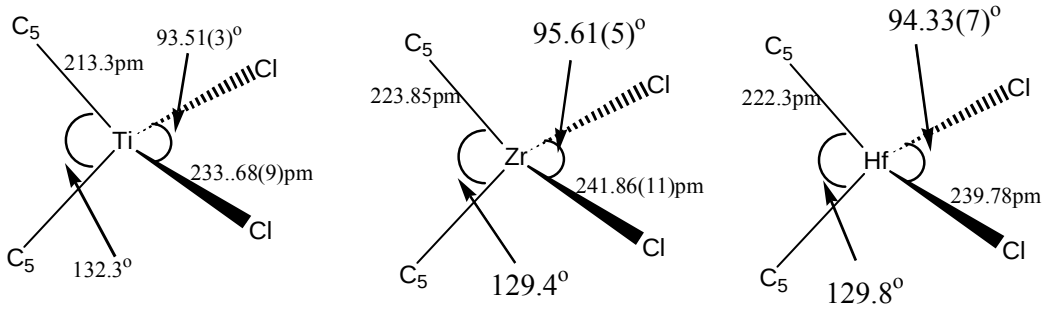

Fig. 43 Pseudo-tetrahedral geometries of M(IV), (M=Ti, 10, Zr, 11, Hf 12)

The two independent M-Cl bond distances in each compound of **10**, **11**, and **12** are slightly different from each other, but are close to the value reported in literature for corresponding

Ti(IV), Zr(IV) and Hf(IV) complexes, respectively (Tab. 23). Due to the different ionic radii of Ti(IV) (74.5pm), Zr(IV) (86.0pm) and Hf(IV) (85.0pm)[129] , the distances of Ti-Cl are the shortest with 233.04(9) and 234.32(10)pm, Hf-Cl with value 239.92(19) and 239.90(2)pm are longer, and Zr-Cl possesses the largest bond distances with value 241.34(11) and 242.30(11)pm. As shown in Tab. 23, the Ti-Cl distances in all Ti(IV) complexes are always smaller than 237pm, and the Hf-Cl distances are around 240pm, whereas the Zr-Cl distances are always larger than 241pm.

The distances of M-$C_{5(cent.)}$ vary in same tendency, *i.e.* Zr-$C_{5(cent.)}$ have the largest value (224.2 and 223.5pm), Ti-$C_{5(cent.)}$ have the smallest value (213.3 and 213.4 Å), and leaving Hf-$C_{5(cent.)}$ inbetween with 223.0 and 221.6pm, each of them falls into the corresponding bond distance range cited in Tab. 23.

The selected important parameters for compounds **10**, **11** and **12** are gathered in the following Table.

Tab. 22 Selected parameters for complexes M(6-Hyp-Hgual)$_2$Cl$_2$·C$_7$H$_8$, M=Ti, Zr, Hf

	Ti(6-Hyp-Hgual)$_2$Cl$_2$ (**10**)	Zr(6-Hyp-Hgual)$_2$Cl$_2$ (**11**)	Hf(6-Hyp-Hgual)$_2$Cl$_2$ (**12**)
M1-Cl(2)	233.04(9)	241.34(11)	239.22(19)
M1-Cl(1)	234.32(10)	242.30(11)	239.9(2)
M1-C3	235.6(3)	247.4(4)	245.6(6)
M1-C2	237.0(3)	248.6(4)	247.9(7)
M1-C10	249.1(3)	257.0(3)	254.8(7)
M1-C1	250.3(3)	258.9(3)	258.7(7)
M1-C9	253.7(3)	260.9(3)	259.4(7)
M1-C_5 (aver.)	245.1(3)	254.6(3)	253.3(7)
M1-C13	236.2(3)	246.5(4)	244.9(6)
M1-C12	237.0(3)	248.3(4)	244.8(8)
M1-C20	248.9(3)	256.1(3)	254.8(7)
M1-C11	249.7(3)	258.0(4)	255.9(8)
M1-C19	254.2(3)	259.9(3)	257.4(7)
M1-C_5(aver.)	245.2(3)	253.8(4)	251.6(7)
C6-Si1	197.8(3)	196.8(3)	198.1(7)
C16-Si2	197.5(3)	197.0(4)	197.8(8)
Cl(1)-M1-Cl(2)	93.51(3)	95.61(5)	94.33(7)
M1-$C_{5(cent)}$(1)	213.3	224.2	223.0
M1-$C_{5(cent)}$(2)	213.4	223.5	221.6
$C_{5(cent)}$(1) -M1-$C_{5(cent)}$(2)	132.3	129.4	129.8
torsion angle $\tau_{gua\text{-}gua}$ (°) C6-$C_{5(cent)}$(1)-$C_{5(cent)}$(2)-C16	107.0	105.9	104.4
torsion angle (°) C101-$C_{5(cent)}$(1)-$C_{5(cent)}$(2)-C201	-137.2	-138.2	-140.7
folding angle α, β, γ (°)	3.80, 24.2, 39.2 gua(2) 2.70, 24.6, 37.0 gua(1)	3.90, 24.3, 40.2 gua(1) 2.50, 24.0, 38.9 gua(2)	3.30, 24.0, 40.9 gua(1) 2.20, 25.3, 40.7 gua(2)
tilt angle φ(C_5-C_5) (°)	58.6	58.5	58.3
torsion angle $\tau_{C5\text{-}C5}$(°)	15.7(14.1-17.1)	14.3(12.8-16.1)	12.2(10.3-13.8)
bending angle δ (°)	5.60(Me to C_5(1) 5.70(Me to C_5(2)	4.80(Me to C_5(1) 4.80(Me to C_5(2)	5.20(Me to C_5(1) 6.50(Me to C_5(2)

A collection of geometric parameters for some similar metallocene dichloride derivatives resulted from fused-ring systems are developed in Tab. 23.

Tab. 23 Geometric parameters in the L_2MCl_2, L=Cp, Cp^R, Ind, Ind^R, bisgua and so on

	M-Cl (pm)	Cl-M-Cl (deg)	M-$C_{5(cent.)}$ (pm)	$C_{5(cent.)}$-Zr-$C'_{5(cent.)}$ (deg)	$\varphi_{C5\text{-}C5}$* (deg)	$\tau_{L\text{-}L}$** (deg)	$\tau_{C5\text{-}C5}$ (deg)	ref
$Ti(Cp^R)_2Cl_2$	236.51(11)	92.54(6)	208.6(2)	132.4				130
$TiCp_2Cl_2$	236.4(2)	94.53(6)	205.9	130.97				131
$(Binap\text{-}Cp)_2TiCl_2$	232.8(1)	95.88(6)						132
Ti(8,8´-bigua)Cl_2	235.5(1)	95.0(1)	208.3	128.5	50.3			84
Ti(6-Hyp-Hgual)$_2Cl_2$ (**10**)	233.69(10)	93.51(3)	213.3	132.3	58.6	107.6	15.7	this work
$Zr(Cp^R)_2Cl_2$	245.46(6)	93.95(3)	222.3	129.4				130
Zr(1-ethylindenyl)$_2Cl_2$	244.1(5)	96.45(16)	222.4	132.72				133
Zr(1-phenylindenyl)$_2Cl_2$	242.9(7)	98.98(2)	223.1(0)	128.66(6)				133
$[MeCp(CH_2)_5]_2ZrCl_2$	244.5(1) 253.6(2)	97.74(2)	223.0	132.2			eclip.	128
$(Me_3Si)(Hind)_2ZrCl_2$	244.4	93.70(6)	223.3(4)	129.9(2)				134
$(Ind)_2ZrCl_2$	244.0(2)	94.71(7)	223.0(8)	128.3(5)	62.07(15)	46.5(3)	stag.	127
$(C_9Me_7)_2ZrCl_2$	244.0(1) 241.9(1)	93.1	225.7(4)	128.3(5)	28.8	98.5	stag.	126
Zr(6-Hyp-Hgual)$_2Cl_2$ (**11**)	241.34(11) 242.30(11)	95.61(5)	223.8	129.4	58.5	106.9	14.3	this work
$Hf(Cp^R)_2Cl_2$	242.81(4)	93.49(2)	220.3(2)	129.8				130
Hf(6-Hyp-Hgual)$_2Cl_2$ (**12**)	239.92(19) 239.9(2)	94.33(7)	222.3	129.8	58.3	104.4	12.2	this work

* φ : tilt angle of $C_{5(cent)}(1)$ and $C_{5(cent)}(2)$
** τ: torsion angle of ligands

2.5 Bis-Hyp Substituted Lithium Guaiazulenide

In order to investigate the possibility to introduce a hypersilyl group to the five-membered ring, compound **2** and chlorohypersilane $ClSi(SiMe_3)_3$ were brought together for reaction, and the subsequent metallation was carried out.

2.5.1 Bis-Hyp Substituted Guaiazulene

2.5.1.1 Reaction

The metathesis between compound **2** and chlorotris(trimethylsilyl)silane $ClSi(SiMe_3)_3$ can take place in tetrahydrofuran. After 24 hours stirring colourless (greenish) rhombus-shaped crystals from the jade green viscous filtrate formed. X-ray diffraction analysis showed that the second hypersilyl group is connected to C2 instead of to C3 as in compound **9**, which can be understood only with the steric demand of the hypersilyl group.

Eq.27

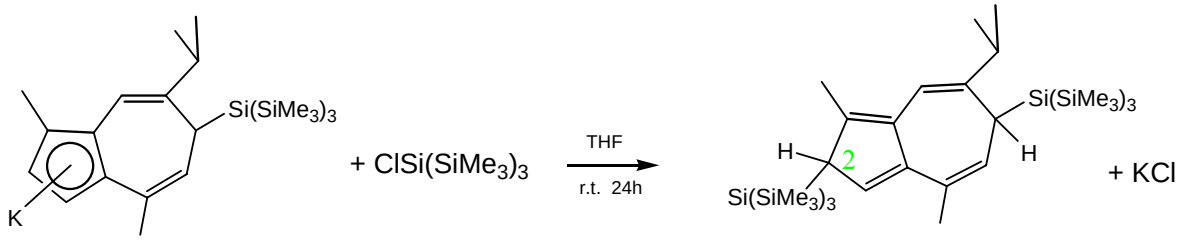

2,6-bis(Hyp)-H_2gua **14**

If the reaction is performed in toluene, the whole reaction mixture becomes to gel-like form. As a result tetrahydrofuran is the preferable solvent. Product **14** can crystallize either from tetrahydrofuran, toluene, or n-pentane at temperature range of +5˚C ~ -20C˚ with yield of about 50%.

2.5.1.2 NMR Spectroscopy

Similar to compound **9**, compound **14** is also hypersilyl substituted guaiazulene. However, different from **9**, in **14** in both of the five- and seven-membered rings there is a hypersilyl group. Moreover, in the five-membered rings the hypersilyl group is not connected to same carbon atom as in compound **9** (Fig.44). Their NMR spectral data demonstrated the structure difference.

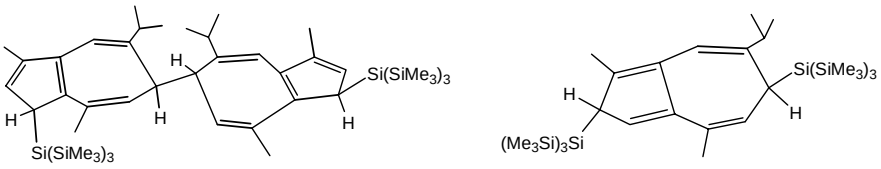

9 **14**

Fig. 44 Structure of compound 9 and 14

2.5.1.2.1 ^{1}H NMR Spectroscopy

At room temperature in C_6D_6 recorded ^{1}H NMR spectrum for compound **14** is shown in the following spectrum.

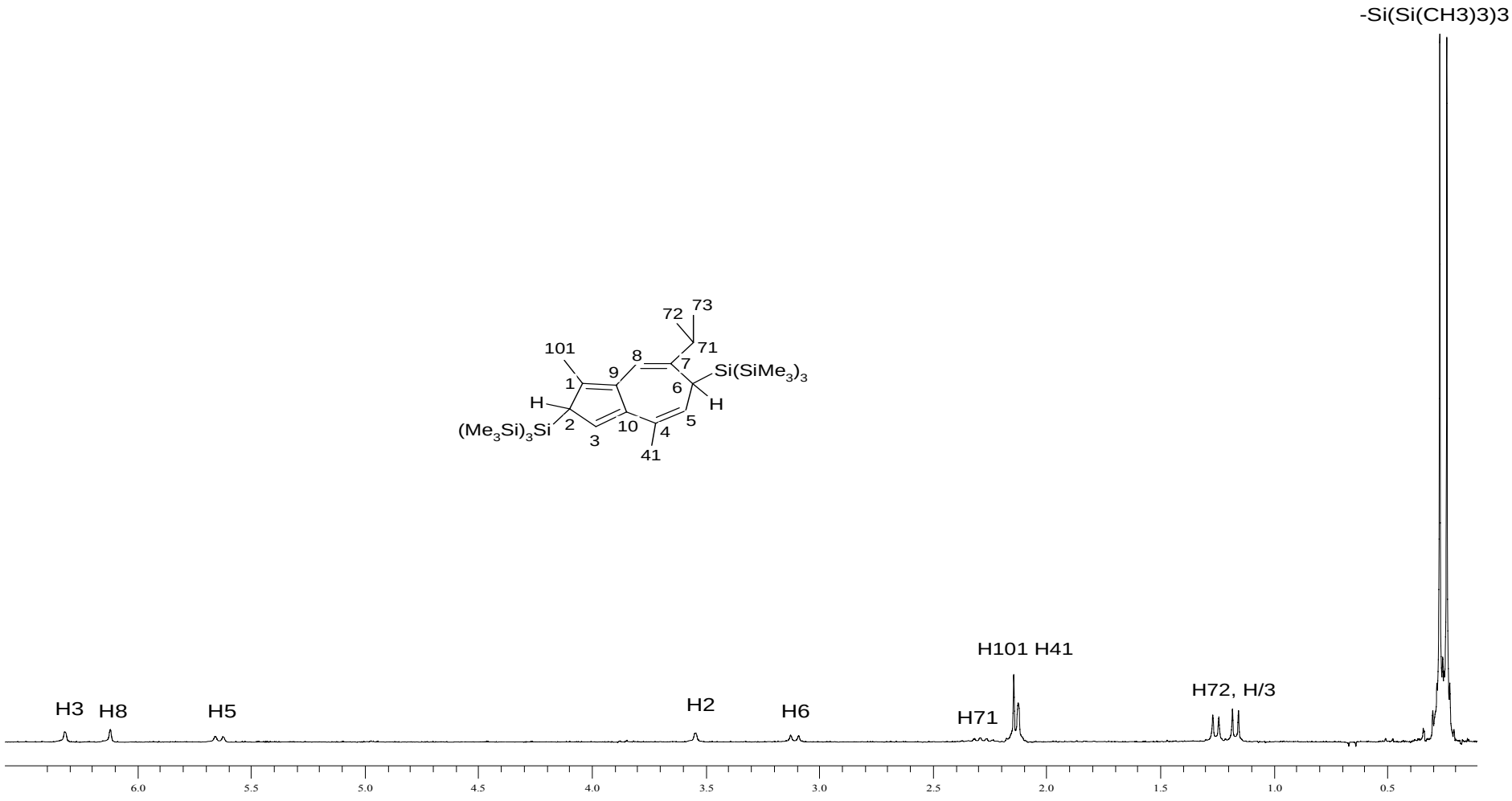

Spe. 12 ^{1}H NMR spectrum of 2,6-bis(Hyp)-H_2gua 14 recorded in C_6D_6 at room temperature (250MHz)

Compare with the ^{1}H NMR spectrum of **2** (Spe. 1 and Spe. 3), in Spe. 12 in the upfield region a new broad singlet appears, whereas in the down field region only three, instead of four signals as in the spectrum of precursor **2**, remain, indicating one olefinic proton is changed to aliphatic proton in the metathesis. The X-ray diffraction analysis revealed that this proton is H2. The coupling between H5 and H6 is similar to the value in **2** with coupling constant J=8.4Hz. However, the coupling between H2 and H3 is very weak. Only in the enlarged ^{1}H NMR spectrum of **14** the weak coupling between H2 and H3 as well as H5 and H41 can be observed with coupling constant J=1.6 and 1.1Hz, respectively. Thus, the signal of H5 shows a doublet of doublets. Two strong singlets from two hypersilyl groups locate side by side very close in the upfield region with chemical shifts of 0.24 and 0.27ppm, respectively. All other aliphatic protons give signals in the normal range.

From the two dimensional ^{1}H-^{1}H correlation diagram (Spe. 13) the coupling between H2 and H3, as well as H5 and H41 can be more clearly observed. However, the correlation of H2 and H101 can still not be seen. An interesting observation is that the correlation of H6 and H41 is a little bit strong, which reflects their short spatial distance to each other.

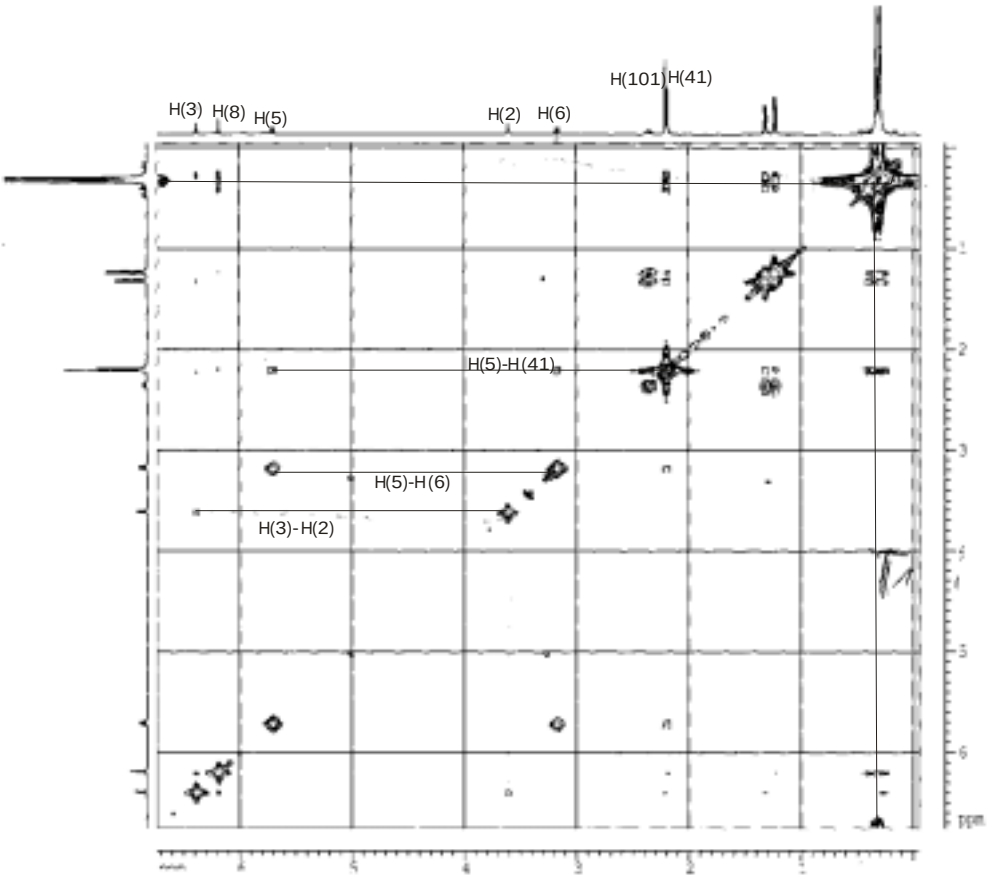

Spe. 13 2D COSY of 2,6-bis(Hyp)-H_2gua

2.5.1.2.2 ^{13}C NMR Spectroscopy

In combination with the 2D COSY and theoretical calculation of NMR data the ^{13}C NMR signals from high field to low field for compound **14** have the sequence of C_{Hyp}, C101, C72, C73, C41, C6, C71, C2, C8, C5, C3, C4, C9, C1, C10 and C7. All value fall within the expected range, *i.e.* eight olefinic carbon atoms possess chemical shift above 114ppm, and eight aliphatic carbon atoms, instead of seven as in **2**, show chemical shifts under 46ppm. Many of the ^{13}C NMR signals are still opposite to the corresponding ^{1}H NMR order.

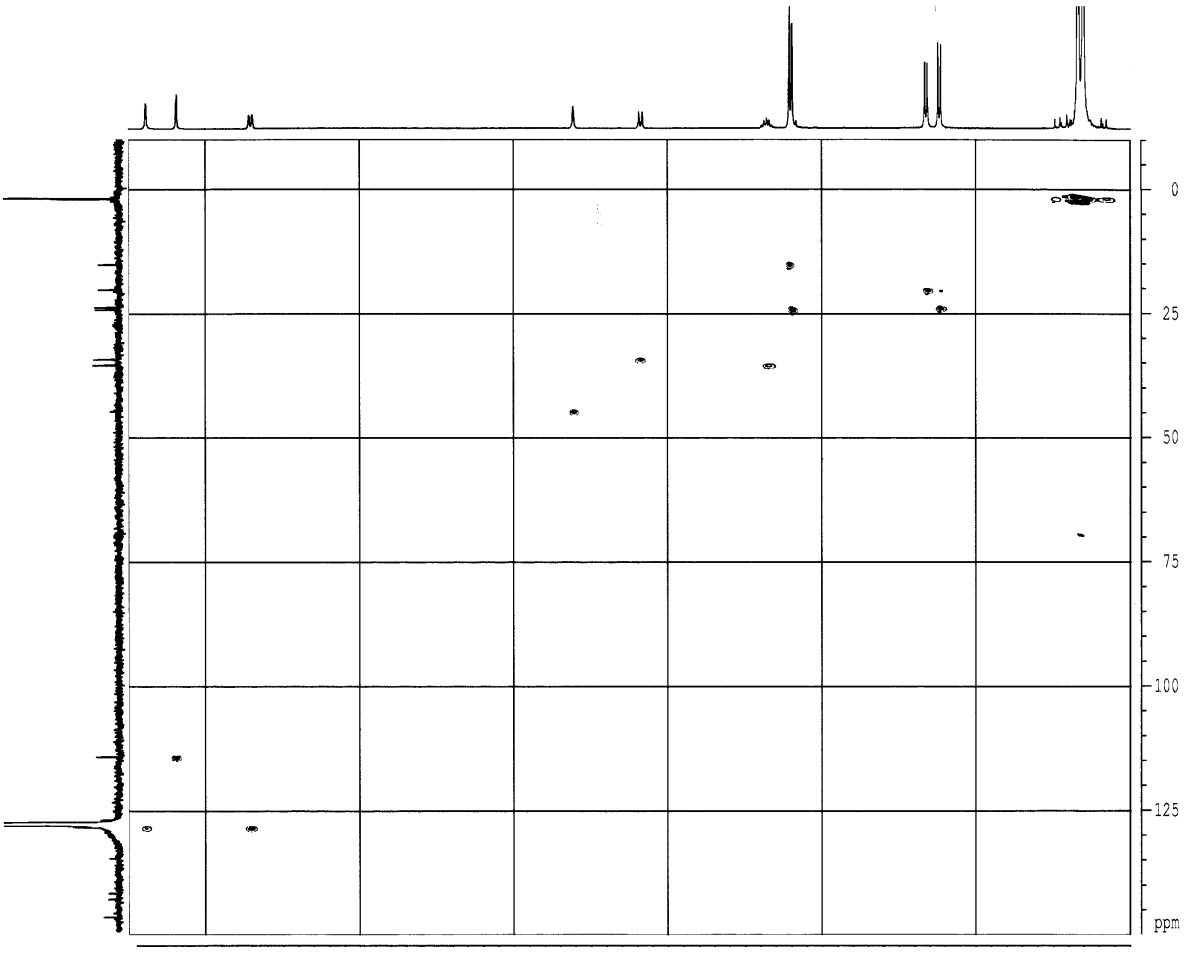

Spe. 14 2D COSY of 2,6-bis(Hyp)-H_2gua (^{1}H-^{13}C correlation)

2.5.1.2.3 ^{29}Si NMR Spectroscopy

The two kinds of β-Si atoms from two hypersilyl groups -Si($SiMe_3$)$_3$ give rise to two singlets nearly with same chemical shifts (-12.1 and -12.2 ppm) and show little influence resulted from the seven- or five-membered rings. The two kinds of α-Si atoms, on the other hand, show large difference with singlets in -72.5 and -90.5ppm, respectively. Compare to the absorptions of α-Si in the hypersilyl group in **9**, the signal in -90.5ppm should be assigned to the hypersilyl group bonded with C2 in **14**, and the hypersilyl group bonded with C6 has

similar absorptions (-72.5ppm) as ligand 6-Hyp-Hgual in compounds of **2a**, **4**, **6**, **10**, **11** and **12**.

2.5.1.3 Molecular structure of 2,6-bis(Hyp)-H_2gua (14)

The X-ray diffraction quality rhombus-shaped colourless crystal of compound **14** was obtained from toluene. It possesses monoclinic system with space group $P2_1/c$. The selected crystallographic data are summarized in Tab. 24.

Tab. 24 Selected crystallographic data for 14

Empirical formula	$C_{33}H_{72}Si_8$
Formula weight (g/mol)	693.62
Temperature (K)	173(2)
Wavelength(Å)	0.71073
Crystal system	monoclinic
space group	$P2_1/c$
Unit cell dimensions (Å, deg)	a=19.904(3) b=12.529(2) c=18.748(5) β=109.479(14)°
Volume (Å^3)	4407.9(17)
Z	4
calc. density (Mg/m^3)	1,045
Absorption coefficient (mm^{-1})	0.264
F(000)	1528
Reflections collected / unique	9799 / 9506[R(int)=0.0527]
Data / restraints / parameters	9506 / 0 / 385
(Goodness-of-fit on F^2)	0.857
Final R indices [I>2σ(I)]	R1=0.0441, wR2=0.0975
R indices (all data)	R1=0.0933, wR2=0.1059
Largest diff. peak and hole	0.421 und –0.230 e.Å^{-3}

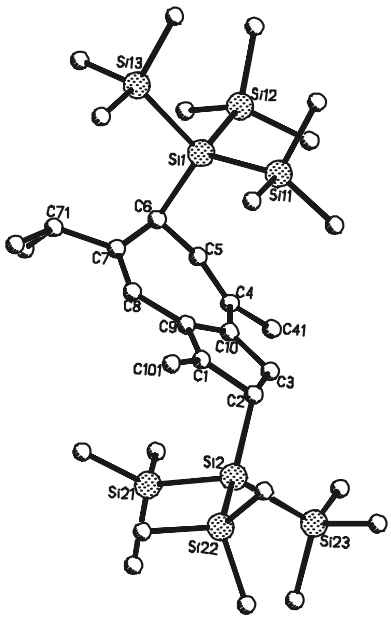

Selected bond distances(pm) and bond angles(deg)

Si(1)-C(6)	194.8(3)
Si(2)-C(2)	194.3(3)
Si(1)-Si(11)	234.82(11)
Si(1)-Si(12)	235.35(11)
Si(1)-Si(13)	235.38(12)
Si(2)-Si(21)	234.28(12)
Si(2)-Si(22)	236.28(12)
Si(2)-Si(23)	235.44(11)
Si(1x)-C	186.5(185.8-187.3)
Si(2x)-C	186.6(186.3-187.3)
C(1)-C(2)	147.4(4)
C(2)-C(3)	146.7(4)
C(3)-C(10)	134.7(4)
C(10)-C(9)	146.6(4)
C(9)-C(1)	135.0(3)
C(10)-C(4)	146.4(4)
C(4)-C(5)	132.5(4)
C(5)-C(6)	149.4(4)
C(6)-C(7)	150.5(4)
C(7)-C(8)	133.6(4)
C(8)-C(9)	144.8(4)
C(5)-C(6)-C(7)	118.8(2)
C(5)-C(6)-Si(1)	108.29(18)
C(7)-C(6)-Si(1)	114.66(18)
C(3)-C(2)-Si(2)	106.35(19)
C(3)-C(2)-C(1)	102.9(2)
C(1)-C(2)-Si(2)	111.49(18)

Fig. 45 Molecular structure of [(2S,6S)]-2,6-bis(Hyp)-H_2gua 14. Atoms are represented by spheres of arbitrary radii; hydrogen atoms are omitted for clarity.

As shown in Fig.45 and Fig.46, due to the steric demand the two hypersilyl groups extend in opposite directions above and below the guaiazulene fragment, respectively, with bending angle of 31.8° for C2-Hyp to the best plane through the atoms C1, C2 and C3, and of 46.2° for C6-Hyp to the best plane through the atoms C5, C6 and C7. The two chiral carbon atoms C2 and C6 have same configurations (S,S- or R,R-configurations). All methyl and isopropyl groups in the guaiazulene framework stretch away from the corresponding nearby hypersilyl group. The 1-methyl group deviates 2.9° away from the best plane through the atoms C1, C3, C9 and C10. All other folding angles are shown in the following figure.

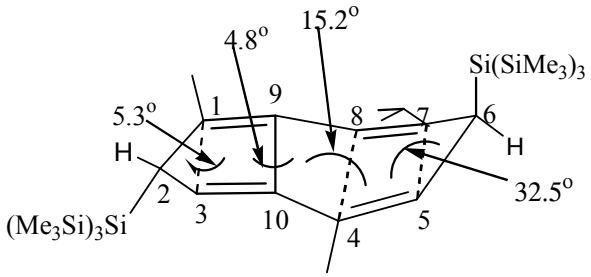

Fig. 46 Folding angles in compound 14

In **14** no metal cation coordinates to the C_5 ring, and thus the substituents especially the hypersilyl group in the seven-membered ring obtain smaller repulsions when compare with that of in **1**, **2a** and **4**, resulting in smaller folding angles in the seven-membered ring in **14**. Based on same reason, the bond distances of Si-Si, Si-Me and Si-C2 as well as Si-C6 in the hypersilyl group are shorter than those of in **1** and **2a**.

The condensed ring system shows evidence of partly delocalized bond characters. The bonds C4-C5, C10-C3, C7-C8 and C9-C1 (range from 132.6pm to 135.1pm) are typical double bonds, whereas the bond distances of C10-C4 and C8-C9 behave as delocalized bonds (146.4 and 144.8pm). It is noticeable that the bond distances of C1-C2 (147.8pm) and C2-C3 (146.5pm) are much shorter than that for typical single bonds, indicating their conjugated single-double bond character or the ambi-aromatic properties of the C_5 ring. C6-C7 and C5-C6 are typical single bonds.

2.5.2 Bis-Hyp Substituted Lithium Guaiazulenide

2.5.2.1 Reaction

Considering the possible formation of an aromatic five-membered ring system the proton H2 in compound **14** is expected to be markedly acidic. Therefore, a metallation with strong carbanion bases should be feasible. With ^{n}BuLi as metallation reagent at about 60˚C in toluene compound **14** can indeed be converted to lithium{2,6-bis[tris(trimethylsilyl)silyl]-2,6-dihydro-guaiazulene-2-id}(**15**), abbreviated as Li[2,6-bis(Hyp)-Hgual].

Eq.28

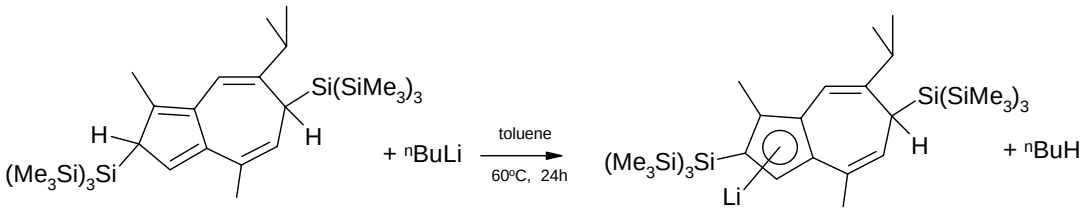

2,6-bis(Hyp)-H_2gua **14** Li[2,6-bis(Hyp)-Hgual)] **15**

As mentioned, though recrystallization the isolated yield of the precursor **14** only reached 50%, much of compound **14** remains still in solution with some impurities and thus can not be isolated. The impurities, being testified by experiment, do not interrupt the metallation shown in Eq. 28. Thus, in large-quantity synthesis of **15**, a one-pot synthesis is used, *i.e.* after the reaction (Eq. 27) finished (controlling with ^{1}H NMR), it is only necessary to change the solvent from tetrahydrofuran to toluene so that a metallation of tetrahydrofuran with ^{n}BuLi is avoided. In the subsequent procedure the ^{n}BuLi solution in hexane can be directly added to the toluene solution. Warming the green and turbid solution of **14** with ^{n}BuLi to 60°C the reaction slowly takes place and gives rise to a clear orange solution. From the concentrated toluene solution deep yellow rod-shaped crystals of **15** are formed at 5°C after one day (Scheme 8). The product **15** is extremely air- and moisture sensitive. On exposure to air the *yellow* powder of **15** immediately changes its colour to *red*.

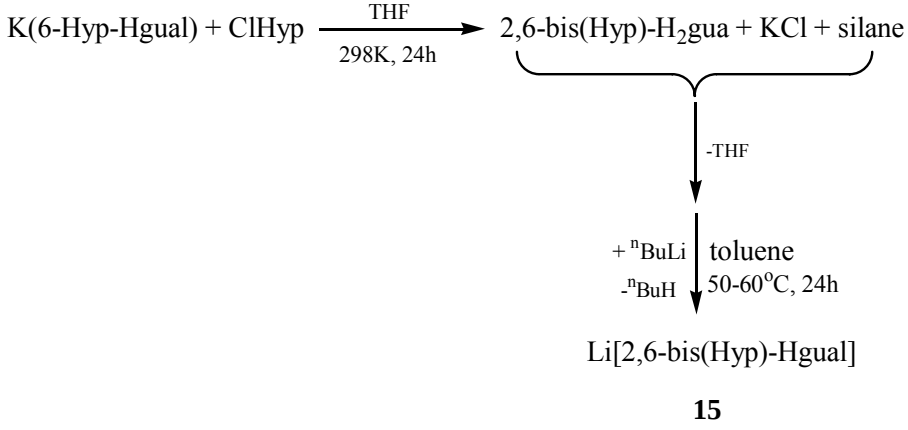

Scheme 8 One pot synthesis of Li[2,6-bis(Hyp)-Hgual]

If lithium bis(tris(trimethylsilyl)silyl)amide LiN[Si(SiMe$_3$)$_3$]$_2$ is used instead of ^{n}BuLi, no conversion of **14** to **15** has been observed.

2.5.2.2 NMR Spectroscopy

2.5.2.2.1 ^{1}H NMR Spectroscopy

The typical change in the ^{1}H NMR spectrum of Li(2,6-bis(Hyp)-Hgual) (**15**) is that the signal of H2 disappears, when compared with the ^{1}H NMR spectrum of 2,6-bis(Hyp)-H_2gua (**14**) (Spe. 15), indicating the success of metallation.

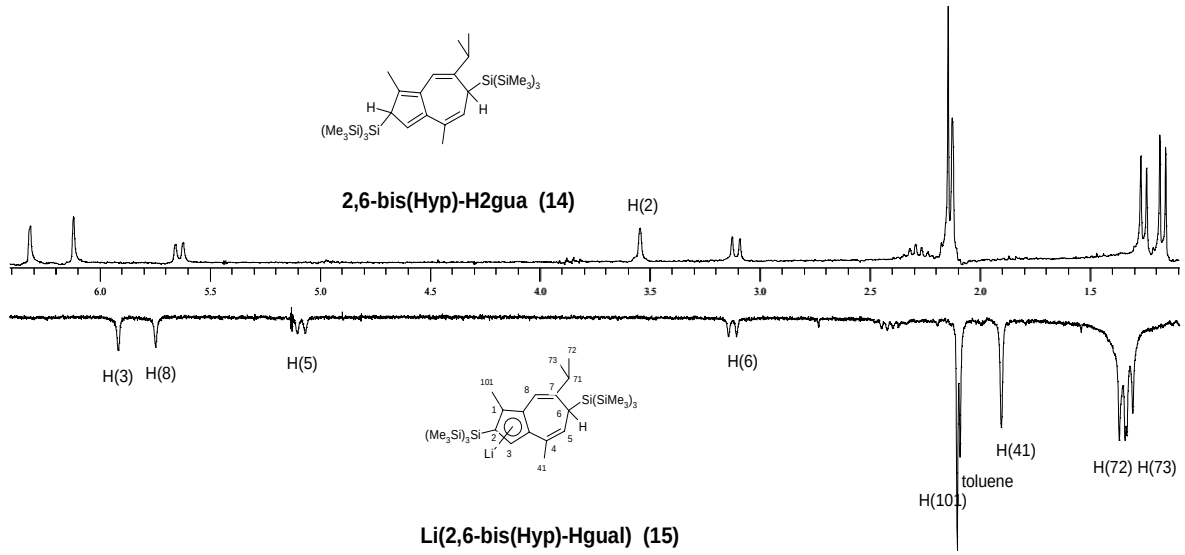

Spe. 15 Compare of ^{1}H NMR spectra of 14 and 15

The signals of H5, H6, H101 and H41 are always in the same order as in many other compounds such as **1**, **2a**, **4**, **5**, **6**, **8** etc. They are easy to identify with the ^{1}H-^{1}H correlation experiment. Since the doublet of H5 in the down field region has correlation with H41, thus, the signal of H101 is distinguished from that of H41. The singlet of H3 and H8 can be assigned through theoretical calculation. In Spe. 15 it shows that the signals of H3, H8, H5 and H41 move to upfield in **15**. However, all of the proton signals are in the same order as in compound **14**.

2.5.2.2.2 ^{13}C NMR Spectroscopy

The selected ^{13}C NMR data measured in C_6D_6 at room temperature for compound **15** are compiled in the following table.

Tab. 25 Selected ^{13}C NMR data for 15 measured at 298K in C_6D_6

Carbon atom	Tertiary olefinic carbon atom	Secondary olefinic carbon atom		
	C1, C4, C7, C9, C10, C2	C5	C3	C8
δ (ppm)	136.5; 124.1; 122.3; 120.6; 120.3; 99.0	118.2	115.8	112.7

All olefinic carbon atoms gave rise to signals above 99.0ppm, indicating the dominantly ionic character of Li-$C_{5(ring)}$ in compound **15**. All aliphatic carbon atoms gave rise to signals under 36.0 ppm at upfield as shown in Spe. 16. The ^{13}C NMR order from high field to low field is: C_{Hyp}, C101, C72, C41, C73, C6, C71, C8, C3 and C5. The assignment of the signals of five tertiary olefinic carbon atoms has been referred to the theoretical calculation of NMR data.

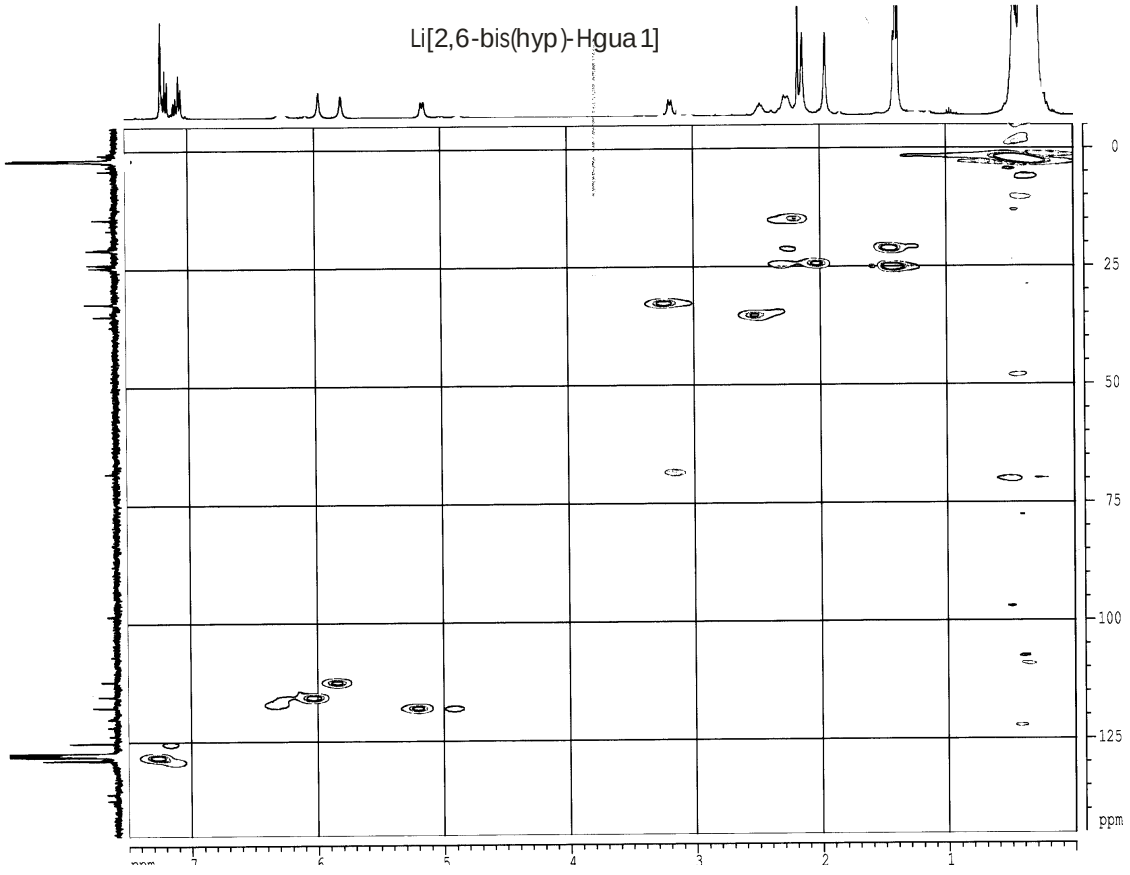

Spe. 16 2D COSY of 15 (^1H-^{13}C correlation)

2.5.2.2.3 ^{29}Si NMR Spectroscopy

As shown in Tab. 26, the central silicon atoms in compounds **14** and **15** have similar chemical shifts, only one of the peripheral silicon atom shows resonance in higher-field, and this peripheral silicon atom should belong to the hypersilyl group bonded with C2, since they

might locate above or below the five-membered ring, and therefore immersed in the π-electron cloud of the C_5-ring.

Tab. 26 Comparison of ^{29}Si NMR spectral data recorded at C_6D_6

compound		δ(ppm) β-Si	α-Si
2,6-bis(Hyp)-H_2gua	**(14)**	-12.1 -12.2	-72.5 (C6-Si) -90.5 (C2-Si)
Li(2,6-bis(Hyp)-Hgual)	**(15)**	-12.2 -13.4	-72.9 (C6-Si) -90.5 (C2-Si)
(-Hyp-6-Hgua)$_2$	**(9)**	-12.2	-90.2 (C3-Si)

2.4.2.2.4 ^{7}Li NMR Spectroscopy

The ^{7}Li NMR spectrum for complex Li[2,6-bis(Hyp)-Hgual] (**15**) shows one signal at -1.36ppm, it moves to down-field when compare to Li(6-Hyp-Hgual) (**1**) (^{7}Li: δ=-3.63ppm). Compare to data in Tab. 6, obviously in compound **15** in tetrahydrofuran the Li^+ cation and the ligand [2,6-bis(Hyp)-Hgual]$^-$ anion behave as typically solvent separated ion pair.

2.5.2.3 Molecular Structure of [Li(2,6-bis(Hyp)-Hgual)]$_2$ (15)

From toluene at temperature range -20~+5°C compound **15** crystallized as deep yellow rod-shaped crystals. X-ray crystal structure analysis showed triclinic crystal system with space group Pī. The selected crystallographic data are compiled in the following table.

Tab. 27 Selected crystallographic data for 15

Empirical formula	$C_{33}H_{71}Si_8Li$
Formula weight (g/mol)	699.55
Temperature (K)	173(2)
Wavelength(Å)	0.71073
Crystal system	Triclinic
space group	Pī
Unit cell dimensions	a=16.835(4)Å α=103.004(14)° b=18.894(3)Å β=112189(13)° c=20.054(4)Å γ=107.613(16)°
Volume (Å^3)	5196.9(17)
Z	2
calc. density (Mg/m^3)	1.011
Absorption coefficient (mm^{-1})	0.230
F(000)	1734
Reflections collected / unique	18111 / 17473[R(int)=0.0384]
Data / restraints / parameters	17473 / 536 / 976
(Goodness-of-fit on F^2)	0.861
Final R indices [I>2σ(I)]	R1=0.0564, wR2=0.0952
R indices (all data)	R1=0.1395, wR2=0.1164

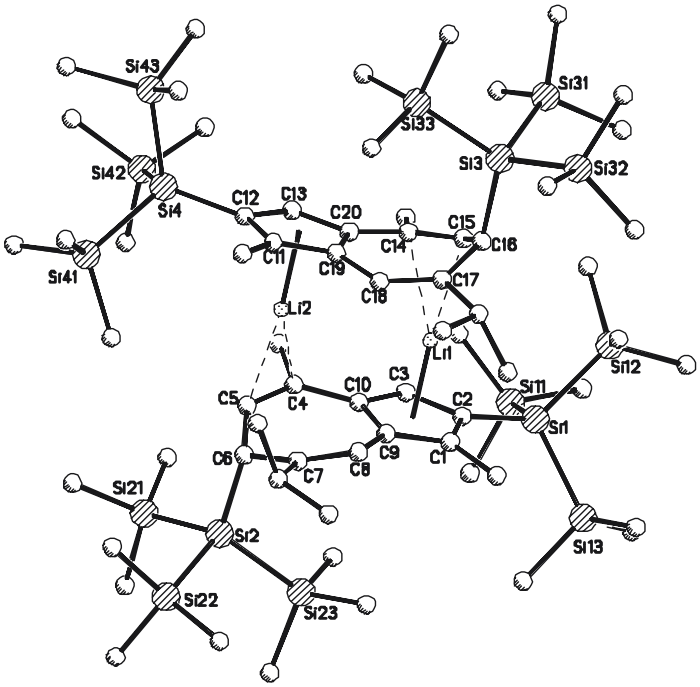

Selected bond distances (Å) and bond angles (deg)

Li(1)-C(3)	222.2(8)	Li(2)-C(13)	220.3(8)
Li(1)-C(10)	223.0(8)	Li(2)-C(19)	221.3(8)
Li(1)-C(9)	224.3(8)	Li(2)-C(20)	223.5(7)
Li(1)-C(1)	225.2(8)	Li(2)-C(12)	223.7(8)
Li(1)-C(2)	226.1(8)	Li(2)-C(11)	224.5(8)
Li(1)-C(14)	241.2(8)	Li(2)-C(5)	244.5(8)
Li(1)-C(15)	244.5(8)	Li(2)-C(4)	245.6(8)
Li(2)-Li(1)	339.7(10)		
C(2)-C(3)	140.8(5)	C(12)-C(13)	143.5(5)
C(2)-C(1)	144.1(5)	C(12)-C(11)	142.6(5)
C(3)-C(10)	141.6(5)	C(13)-C(20)	142.3(5)
C(10)-C(9)	142.6(5)	C(20)-C(19)	144.0(5)
C(9)-C(1)	143.7(5)	C(19)-C(11)	142.3(5)
C(10)-C(4)	146.4(5)	C(20)-C(14)	146.4(5)
C(8)-C(9)	147.3(5)	C(18)-C(19)	145.1(5)
C(4)-C(5)	136.8(5)	C(14)-C(15)	134.4(5)
C(5)-C(6)	151.1(5)	C(15)-C(16)	150.8(5)
C(6)-C(7)	151.5(5)	C(16)-C(17)	152.8(5)
C(7)-C(8)	136.0(5)	C(17)-C(18)	135.8(5)
Li(1)-$C_{5(cent.)}$	188.5	Li(2)-$C_{5(cent.)}$	186.6
C(14)-Li(1)-$C_{5(cent.)}$	148.2		
C(15)-Li(1)-$C_{5(cent.)}$	171.1		
C(4)-Li(2)-$C_{5(cent.)}$	147.7		
C(5)-Li(2)-$C_{5(cent.)}$	172.5		

Fig. 47 Molecular structure of [Li(2,6-bis(Hyp)-Hgual)]$_2$ (15), Atoms are represented by spheres of arbitrary radii; hydrogen atoms are omitted for clarity.

Similar to compound **1**, two molecules in **15** build dimeric sandwich-like metal-ring unit with formula $(C_{33}H_{71}LiSi_8)_2$ (Fig. 47). Due to the two new introduced bulky hypersilyl groups in the C2 and C2´ the two guaiazulene fragments are situated not just anti-parallel as in **1**(Fig. 48).

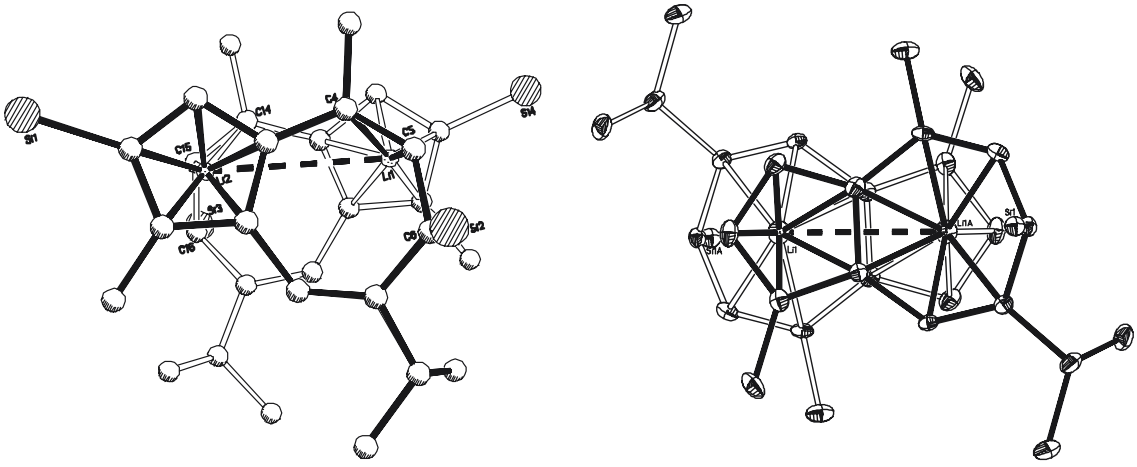

a **b**

Fig. 48 Projection of two guaiazulene fragments in 15 (left a) and 1(right b) along the axis of Li-C_5(ring). Hydrogen atoms and $SiMe_3$ are omitted for clarity.

As can be seen in Fig. 48, **a**, the two lines between $C_{5(cent.)}$-C6 and $C'_{5(cent.)}$-C6′ are in an angle for about 135°. Furthermore, the two guaiazulene fragments slide a little bit away from each other along their own pseudo axes C2-C6 or C2′-C6′. The result is that each C_5-coordinated Li^+ cation is spatially only close to two olefinic carbon atoms of the seven-membered ring of the second guaiazulene moiety, *i.e.* C4-C5···Li2 as well as C4′-C5′···Li1, respectively. Indeed the angles of C5′-Li1-$C_{5(cent)}$ and C5-Li2-$C'_{5(cent)}$ are 171.1° and 172.5°, and the angles $C_{5(cent)}$-Li1-C4′ and $C'_{5(cent)}$-Li2-C4 are 148.2° and 147.6°, respectively. The lithium cation in **15** is therefore μ-η^5:η^2 coordinated by a C_5-ring at one guaiazulene fragment and by two olefinic carbon atoms from the seven-membered rings at the other guaiazulene moiety. The distances of Li1-C4′ and Li2-C4 are similar to those in compound **1**, but the distances of Li1-C5′ and Li2-C5 are c.a. 20pm shorter than that in compound **1** (Li1-C5A 262.6pm). On the other hand, due to the slipping of the two ligand moieties the distance of Li1-Li2 (339.7(10)pm) is about 60pm longer than that of in **1**.

The seven-membered ring in **15** is also folded, but the corresponding folding angles β and γ become much smaller than those in **1** (α=1.5°, β=6.2° γ=30.3° in **15**; 2.0°, 19.8° 39.9° in **1**). Evidently, the stronger interaction of Li2-C5 and Li1-C5′ results in the contraction of β as well as γ.

As for the coordination of C_5-ring to Li^+ cations, the two independent average distances of Li1-C_5 (ring) and Li2-C_5' (ring) in **15** are 224.5pm and 222.7pm, and the Li1-$C_{5(cent)}$ as well as Li2-$C_5'_{(cent.)}$ distances are 188.9pm and 186.7pm, respectively, being significantly shorter than those in **1** and in all other compounds shown in Tab. 8. Obviously in compound **15** the lower coordination numbers of Li^+ cations to the seven-membered rings let it in some way similar to that of the solvated lithium cyclopentadienide. Actually some base adducts possess the similar even shorter Li-$C_{p(cent.)}$ distances, *e.g.* for [η^5-$C_5H_2(SiMe_3)_3$]Li·L, L=quinuclidine, 179.0pm[135]; L=THF, 180.0pm[136]. However, in compounds with TMEDA as co-ligand, the Li-$C_{5(cent.)}$ is longer, such as in [η^5-$C_5H_4(SiMe_3)$]Li·TMEDA (192.0pm) [137], and in [η^5-C_5H_4Me]Li·TMEDA (191.0pm)[138].

The selected Si-Si, Si-C bond distances and bond angles for the hypersilyl group in **15** are delivered in the following Table.

Tab. 28 Data for hypersilyl group in compound 15 (pm and deg)

bonds	Bond distances	bonds	Bond distances	bonds	Bond distances
Si1-C2	190.3(4)	C11-C12-Si(4)	128.4(3)	C1-C2-Si1	129.0(3)
Si(4)-C12	189.4(4)	C15-C16-Si(3)	112.0(3)	C5-C6-Si2	109.0(3)
Si2-C6	198.1(4)	C13-C12-Si(4)	124.4(3)	C3-C2-Si1	124.5(3)
Si(3)-C16	197.8(4)	C17-C16-Si(3)	112.5(3)	C7-C6-Si2	114.2(3)
Si1-Si	236.6(17)	C15-C16-C17	118.2(3)	C5-C6-C7	118.1(3)
Si(4)-Si	237.4(17)	C11-C12-C13	107.0(3)	C3-C2-C1	106.3(3)
Si2-Si	238.0(17)	Si[Si(11), Si(12), Si(13)]-C (aver.)	188.4(4) (186~190)	Si[Si(21), Si(22), Si(23)]-C (aver.)	187.8(5) (186~191)
Si(3)-Si	236.9(18)	Si[Si(41), Si(42), Si(43)]-C(aver.)	188.0(5) (186~190)	Si[Si(31), Si(32), Si(33)]-C(aver.)	188.4(5) (186~190)

It is noticeable that the distances of Si-C_{sp2} (190.3(4)pm and 189.4(4)pm) in **15** are about 8pm shorter than that of Si-C_{sp3} (198.1(4)pm and 197.8(4)pm). Nevertheless all of the other Si-Si and Si-C bonds in four hypersilyl- groups in **15** have nearly no significant difference.

Si1 and Si(4) are with the C_5-ring in one plane, but the angles C1-C2-C3 and C1´-C2´-C3´ are compressed to 106.3° and 106.9°, respectively. Otherwise, the especially short distances of C4-C5, C8-C7 in **15**, ranging from 134 to 137pm, show their pure double bond characters.

The introduction of a second hypersilyl group to the C_5-ring changed the chemical properties of the compound **15** greatly. Compare to complex **1**, complex **15** is extremely air- and moisture sensitive. The former is a good precursor for synthesis of metallocene derivatives, whereas the latter in our hands, did not lead to isolable complexes sofar. We have also examined whether a third hypersilyl group could be introduced to the guaiazulene moiety, but were not successful to date.

3 Experiment Section

3.1 General Comments

All experiments manipulations described below were performed under an inert atmosphere of purified dry argon gas using standard Schlenk techniques. The solvents toluene and tetrahydrofuran were dried over sodium and potassium (Na/K) alloy, and n-pentane was dried over lithiumaluminiumtetrahydride($LiAlH_4$), distilled prior to use. Guaiazulene, trichlorosilane $HSiCl_3$, trimethylchlorosilane Me_3SiCl were purchased by ACRÖS co., and $ClSi(SiMe_3)_3$, $ZrCp^*Cl_3$, (-)-sparteine, (1R)-(-)fenchone, ^nBuLi, KO^tBu, $ZrCp^*Cl_3$, by Aldrich, lithium by Chemetall GmbH, All anhydrous metal salts were commercially obtained.

3.2 Characterization

3.2.1 Element Analysis

The carbon- and hydrogen-contents were decided using combustion analysis with an instrument from Perkin Elmer Company, model PE 2400. The contents of metals, *i.e.* lithium, potassium, manganese, iron, nickel, zirconium, hafnium and titanium, were measured according to suitable atom-emission-spectroscopic method with an instrument Optima 3000 Array-ICP from Perkin-Elmer Company. Due to the extremely air- and moisture sensitivity of some lithium-, potassium-, and cesium compounds their element analysis results are only in limit extent reliable.

3.2.2 Melting Point

The melting points were recorded in sealed capillary with a small melting point determination apparatus.

3.2.3 NMR-Spectroscopy

1D NMR Spectroscopy: Most of the ^1H-, ^{13}C-, ^{29}Si- and ^7Li NMR spectra were recorded with an instrument of Brucker AM 200, AC250 and AM 400, respectively, at University of Stuttgart. Several spectra were complemented with Brucker AM 400 at Johannes Gutenberg University of Mainz. In all measurement either d_6-benzene or d_8-THF was used as internal standard. The following ^1H- and ^{13}C-NMR data were referred to the signals of solvents: ^1H in d_5-benzene with δ=7.15ppm; ^{13}C in d_5-benzene with δ=128.02ppm. As external reference $SiMe_4$ was used for ^1H-, ^{13}C- and ^{29}Si NMR, and 14.4M LiCl in D_2O was used for ^7Li NMR spectroscopy.

2D NMR Spectroscopy: ^1H-^1H, ^1H-^{13}C correlation experiments were carried out with an instrument of Bruker AM 400 at Johannes Gutenberg University of Mainz. The internal- and external references are the same as by the 1D NMR measurements.

3.2.4 X-ray diffraction analysis

Each single crystal of suitable dimension was immersed under argon into Nujol or Paratone-N (Exxon) oil, the oil-coated crystal was then manipulated onto a glass fiber and transferred to a nitrogen stream of Siemens P3 four-circle diffractometer which is equipped with a low-temperature record system. Mo-Kα radiation (λ=71.073pm) was used for all measurements. The structures (phase problem) were solved by direct method with program SHELXS-86 [139a] and refined by full matrix least squares techniques based on F_o^2 data with software packages SHELXL-93 and SHELXL-97 [139b]. The data with $F_o^2 \geq -3\sigma(F_o^2)$ were used. The residuals R-factor were calculated with formula $R1=\sum||F_o|-|F_c|| / \sum|F_o|$, where F_o means the measured (observed) structure factor, and F_c means the theoretical (calculated) structure factor. The weighted R-factor was calculated with $wR_2=\{\sum[w(F_o^2-F_c^2)^2]/\sum w(F_o^2)^2\}^{1/2}$, in which $w=1/(\sigma^2(F_o^2)+(a\cdot P)^2+bP)$ and $P=[\max(0, F_o^2)+2F_c^2]/3$. Goodness of fit on S were calculated with $S=\{\sum[w(F_o^2-F_c^2)^2]/N_o-N_p\}^{1/2}$, where N_o is the number of reflections, and N_p is the number of parameters. The positions of H-atoms were calculated in terms of the expected ideal geometry of their environment and then refined together with carbon atoms to which they are bonded as rigid groups with d(C-H)=0.96Å and U(iso)=0.08Å). Anisotropic displacement parameters were introduced for all non-hydrogen atoms.

3.3 Synthesis and Characterization

3.3.1 Syntheses of Reactants

3.3.1.1 Synthesis of $Si(SiMe_3)_4$

The synthesis of $Si(SiMe_3)_4$ is according to literature[140]. A mixture of 150ml of THF, 59.00ml of $HSiCl_3$ (0.584mol, d=1.342g/ml) and 334.00ml of Me_3SiCl (2.63mol, d=0.856) was added dropwise through a drip-funnel to a three-neck flask with 42.00g (6.10mol) of Li and 800ml of THF with intensive stirring under cooling with ice bath. After the dropping finished, the reaction mixture was allowed to warm slowly to room temperature and stirred overnight. The supernatant liquid was decanted to a glass frit (G3), and the mud was washed with tetrahydrofuran. The collected filtrate was dried under reduced pressure (1×10^{-3} torr) at room temperature for 24h. Via sublimation of the yellowish residue at reduced pressure (1.0×10^{-3} torr) at 80°C white beautiful wax-form crystals was obtained. The together collected product weighted 105.6g (0.329mol) with yield 56.3%. Formula $C_{12}H_{36}Si_5$, M=320.84g/mol.

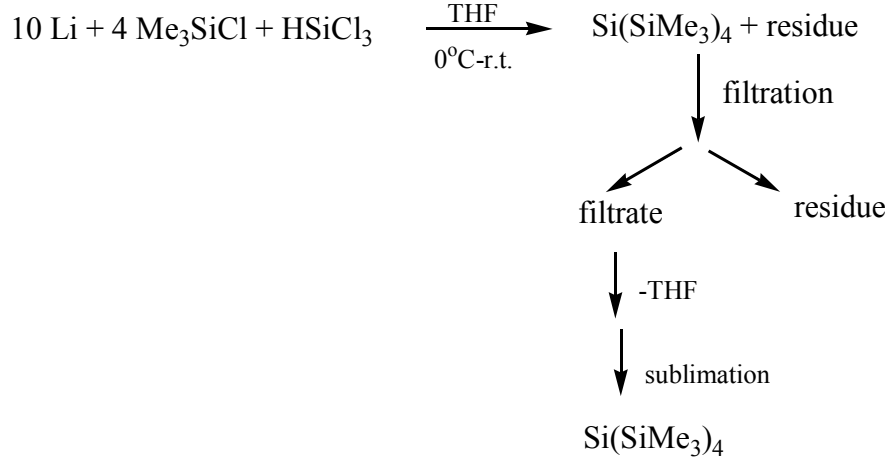

NMR in C_6D_6 at 298K

^{1}H (250.133MHz):δ=0.26ppm

^{13}C{^{1}H} (62.896MHz): δ=2.85ppm

^{29}Si{^{1}H} (39.761MHz): δ= -9.80ppm; -134.3ppm. $J_{C\text{-}Si}$=44.5Hz.

3.3.1.2 Synthesis of $KSi(SiMe_3)_3$

The synthesis process of $KSi(SiMe_3)_3$ is manipulated according to Christoph Marschner´s method [25]. At room temperature 37.30g (116.2mmol) of tetrakis(trimethylsilyl)silane $Si(SiMe_3)_4$ in 80ml of tetrahydrofuran was added to a solution of 13.00g (116.0mmol) of potassium-tert.-butoxylate KO^tBu in 70ml of tetrahydrofuran with stirring. After 12 h the solvent tetrahydrofuran as well as the volatile by-product Me_3SiO^tBu were removed at 40°C under reduced pressure (1.0×10^{-3} torr). The residue was washed with n-pentane and dried at reduced pressure. White powder yielded 25.70g (89.60mmol), 77.10%. It has formula $KC_9H_{27}Si_4$ with M=286.75g/mol.

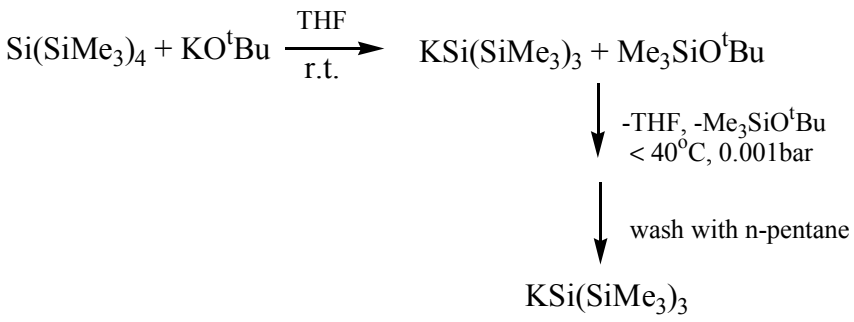

NMR in C_6D_6 at 298K

^{1}H NMR(250.133MHz): δ=0.54~0.58ppm (vary with the content of tetrahydrofuran)

^{13}C{^{1}H} NMR(62.896MHz): δ=7.40ppm

^{29}Si {^{1}H} NMR(39.761MHz): δ= -5.80ppm; -185.7ppm.

3.3.1.3 Synthesis of $LiSi(SiMe_3)_3$

$LiSi(SiMe_3)_3$ was synthesized according to R. E. Wochele´s dissertation.[23] At room temperature a solution of 25.00g of $ClSi(SiMe_3)_3$ (88.30mmol) in 50ml of toluene was added to a suspension of 4.30g of Li(619.6mmol) and 0.20g (8.70mmol) of Na in 200ml of toluene. The temperature was then controlled in range 80~85°C and stirred for 3.5 hours. After the reaction finished (controlling with ^{1}H NMR spectrum), the excess solid lithium, sodium and the produced LiCl or NaCl were separated away from the solution with glass frit G3. To the filtrate 2.00 g of lithium was added and the reaction mixture was brought to reaction at the same condition (80~85°C) for 1.5 h, in order to convert the formed $NaSi(SiMe_3)_3$ to $LiSi(SiMe_3)_3$. After the filtration the solvent in the filtrate was carefully distilled under reduced pressure at 30~60°C. The crude product was purified through re-crystallization in n-pentane at temperature range -10°C~20°C. The pure product $[LiSi(SiMe_3)_3]_2$ showed as colourless rod-shaped crystals. Yield: 19.20g (75.40mmol), 85.40%.

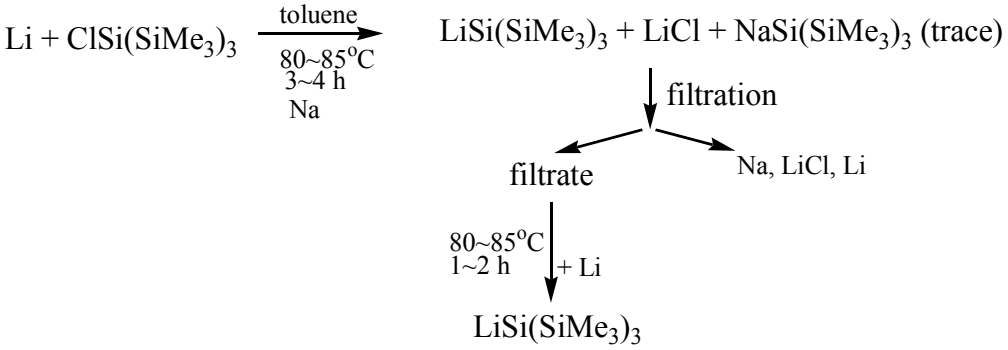

NMR in C_6D_6 at 298K

^{1}H NMR(250.133MHz): δ=0.34ppm

^{13}C{^{1}H} NMR(62.896MHz): δ=5.73ppm

^{13}Si {^{1}H} NMR(39.761MHz): δ= -7.15ppm; -181.9ppm.

3.3.1.4 Synthesis of $CsSi(SiMe_3)_3$

The synthesis of $CsSi(SiMe_3)_3$ is similar to that of $KSi(SiMe_3)_3$. At room temperature the equivalent tetrakis(trimethylsilyl)silane $Si(SiMe_3)_4$ and cesium tertiary-butoxylate CsO^tBu were mixed in tetrahydrofuran with stirring. After 12 h the solvent tetrahydrofuran as well as the volatile by-product Me_3SiO^tBu were removed at 40°C under reduced pressure (1.0×10^{-3} torr). The residue was washed with n-pentane and dried at reduced pressure. Yield: about 70~80%. It has formula $CsC_9H_{27}Si_4$ with M=380.56g/mol.

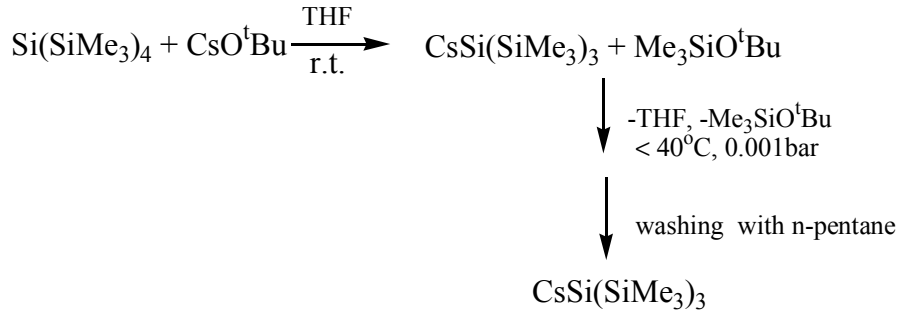

NMR in C_6D_6 at 298K

^{1}H NMR(250.133MHz): δ=0.47ppm

^{13}C{^{1}H} NMR(62.896MHz): δ=7.9ppm

^{13}Si {^{1}H} NMR(39.761MHz): δ= -5.3ppm; -179.4ppm.

3.3.2 Syntheses and Characterization of New Compounds

3.3.2.1 $[Li(6\text{-}Hyp\text{-}Hgual)]_2$ (1)

Preparation

A blue solution of 2.44g (12.30mmol) of guaiazulene in 10ml of n-pentane was dropped into a solution of 2.59g (10.17mmol) of $LiSi(SiMe_3)_3$ in 10ml of n-pentane at room temperature with stirring. The reaction took place immediately and yellowish precipitate formed instantaneously. One hour later the reaction mixture was filtrated and washed with n-pentane until the colour of the excess guaiazulene disappeared. The precipitate was dried under reduced pressure (1.0×10^{-3} torr) at room temperature. It afforded 3.29g (7.26mmol) light yellow powder with yield 71.4%.

Product Properties

The light yellow powder of **1** in solid state is thermally stable, but is air-, moisture, and light sensitive. Exposure to air or under ambient light the colour of **1** will deepen slowly. It is soluble in tetrahydrofuran, on heating also soluble in toluene and C_6D_6, but insoluble in n-pentane. Above 150°C it will decompose. By gradual cooling of its hot toluene solution colourless needle crystals could be obtained.

Element Analysis

Formula: $LiC_{24}H_{45}Si_4$, M =452.90g/mol

	C	H	Si	Li
Calc.(%)	63.64	10.01	24.80	1.532
Found(%)	63.65	9.57		1.480

NMR spectral data

^{1}H NMR (C_6D_6, 298K, 250.133MHz, δ: ppm, J: Hz)

δ=6.24(s, 1H, H8)
δ=5.89(d, $^3J_{HH}$ =3.0, 1H, H2)
δ=5.73(d, $^3J_{HH}$ =3.0, 1H, H3)
δ=4.87(d, $^3J_{HH}$ =8.9, 1H, H5)
δ=2.87(d, $^3J_{HH}$ =8.9, 1H, H6)
δ=2.27(m, $^3J_{HH}$ =6.9, 1H, H71)
δ=2.22(s, 3H, H101)
δ=2.01(s, 3H, H41)
δ=1.22(d, $^3J_{HH}$ =6.9, 3H, -CH(C$\underline{H}_3$)$_2$)
δ=1.21(d, $^3J_{HH}$ =6.9, 3H, -CH(C$\underline{H}_3$)$_2$)
δ=0.17(s, 27H, -Si(Si(C$\underline{H}_3$)$_3$)$_3$)

^{13}C{^{1}H} NMR (C_6D_6, 298K, 62.896MHz, δ: ppm)

δ=134.0; 132.6; 121.4; 117.5; 114.2 (5 tert.-C: C1, C4, C7, C9 and C10)
δ=117.6 (1C, C8)
δ=106.1 (1C, C2)
δ=36.0 (1C, C71)
δ=25.2 (1C, C72)
δ=21.1 (1C, C73)
δ=2.40 (9C, -Si(Si(C$\underline{H}_3$)$_3$)$_3$)
δ=115.0 (1C, C5)
δ=101.0 (1C, C3)
δ=32.8(1C, C6)
δ=24.6 (1C, C41)
δ=13.6 (1C, C101)

^{29}Si {^{1}H} NMR(d_8-THF, 39.761MHz, 302K)

δ= -6.7(3 β-Si, -Si($\underline{Si}$Me$_3$)$_3$, $^1J_{C\text{-}Si}$ = 43.5Hz)
δ= -69.9(1 α-Si, -$\underline{Si}$(SiMe$_3$)$_3$)

^{7}Li NMR(d_8-THF, 77.779MHz, 302K)

δ= -3.63ppm

3.3.2.2 K(6-Hyp-Hgual) (2) and K(8-Hyp-Hgual) (3)

Preparation

At room temperature a deep blue solution of 25.0g (126.1mmol) of guaiazulene in 30ml of tetrahydrofuran was added dropwise to a yellow solution of 36.0g (125.5mmol) of $KSi(SiMe_3)_3$ in 70ml of tetrahydrofuran with stirring. Three hours later the solution was concentrated to about 50ml and cooled in -20°C. Several hours later product **2a** formed as yellowish rod-shaped crystals. The rest solution could be either concentrated further or cooled at lower temperature. The purity of **2a** should be always controlled through ^1H NMR spectroscopy so that the compound **3a** did not co-crystallized with **2a**. The pure product of **2a** was collected together and dried at room temperature at reduced pressure (1.0×10^{-3} torr) for 24 hours. After the crystallized tetrahydrofuran was removed, pure yellow powder of **2** remained. Yield: 48.7g (100.4mmol), 80.0%.

The rest solution was further concentrated to 15-20ml and cooled at 5°C. Deep-yellow rod-shaped crystals of **3a** would form in several hours. Again the crystallized tetrahydrofuran could be removed away. It afforded 4.87g (10.04mmol) deep-yellow powder of **3** (yield 8.00%).

If only exclusive compound **2** is needed, a simple purifying method is to store the tetrahydrofuran solution for several weeks at room temperature or heat the solution until the signals of the **3a** in the ^1H NMR spectrum disappear. Compound **2a** can be then separated from the tetrahydrofuran solution and dried at reduced pressure. Another alternative method for synthesis of **2** is that the reaction was allowed to take place in n-pentane or toluene, and purified in tetrahydrofuran.

Product Properties

The light yellow powder of compound **2** is extremely air- and moisture sensitive. In tetrahydrofuran it is easy to dissolve and easy to form crystals. In toluene and C_6D_6 it is soluble, but the solution will become to gel-like form. Above 150°C it will decompose.

Similar to compound **2**, the yellow powder of compound **3** is also extremely air- and moisture sensitive. It is easy to dissolve in tetrahydrofuran, but in one or two weeks it will change to isomer **2**. Above 150°C it will decompose.

Element Analysis of 2

Formula: $KC_{24}H_{45}Si_4$, M =485.06g/mol

	C	H	Si	K
Calc.(%)	59.42	9.350	23.16	8.060
Found(%)	55.56	8.830		7.370

NMR Spectral Data of Compound 2

^{1}H NMR (C_6D_6, 298K, 250.133MHz, δ: ppm, J: Hz)

δ=6.30(s, 1H, H8)
δ=5.88(d, $^{3}J_{HH}$ =3.0, 1H, H2)
δ=5.77(d, $^{3}J_{HH}$ =3.0, 1H, H3)
δ=5.04(d, $^{3}J_{HH}$ =8.3, 1H, H5)
δ=2.43(d, $^{3}J_{HH}$ =8.3, 1H, H6)
δ=2.61(m, $^{3}J_{HH}$ =6.6, 1H, H71)
δ=2.43(s, 3H, H101)
δ=2.00(s, 3H, H41)
δ=1.40(d, $^{3}J_{HH}$ =6.6, 3H, -CH(C$\underline{H}_3$)$_2$)
δ=1.32(d, $^{3}J_{HH}$=6.6, 3H, -CH(C$\underline{H}_3$)$_2$)
δ=0.34(s, 27H, -Si(Si(C$\underline{H}_3$)$_3$)$_3$)

^{13}C{^{1}H} NMR (C_6D_6, 298K, 62.896MHz, δ: ppm)

δ=134.3; 130.5; 123.1; 119.5; 115.3 (5 tert.-C: C1, C4, C7, C9 and C10)
δ=114.6 (1C, C8)
δ=108.6 (1C, C2)
δ=35.2 (1C, C71)
δ=27.6 (1C, C72)
δ=22.6 (1C, C73)
δ=2.36 (9C, -Si(Si(C$\underline{H}_3$)$_3$)$_3$)
δ=114.5 (1C, C5)
δ=102.5 (1C, C3)
δ=32.7(1C, C6)
δ=23.4 (1C, C41)
δ=13.4 (1C, C101)

^{29}Si {^{1}H} NMR(39.761MHz, 302K)

In d_8-THF: δ= -6.75 (3 β-Si, -Si($\underline{Si}$Me$_3$)$_3$, $^{1}J_{C\text{-}Si}$ = 43.5Hz)
δ= -70.9 (1 α-Si, -$\underline{Si}$(SiMe$_3$)$_3$)

in C_6D_6: δ= -12.1 (3 β-Si, -Si($\underline{Si}$Me$_3$)$_3$, $^{1}J_{C\text{-}Si}$ = 43.5Hz)
δ= -76.3 (1 α-Si, -$\underline{Si}$(SiMe$_3$)$_3$)

NMR Spectral Data of Compound 3

^{1}H NMR (C_6D_6, 298K, 250.133MHz, δ: ppm, J: Hz)

δ=3.84(s, 1H, H8)
δ=6.05 (d, $^{3}J_{HH}$ =3.7, 1H); δ=5.88(d, $^{3}J_{HH}$ =3.7, 1H): H2 and H3, AB spin system
δ=5.42 (d, $^{3}J_{HH}$ =6.6, 1H); δ=5.29(d, $^{3}J_{HH}$ =6.6, 1H, H6): H5 and H6, AB spin system
δ=2.61(m, $^{3}J_{HH}$ =6.6, 1H, H71)
δ=2.42(s, 3H, Me of guaiazulenyl)
δ=2.39(s, 3H, Me of guaiazulenyl)
δ=1.12(d, $^{3}J_{HH}$ =6.6, ; 5.883H, -CH(C$\underline{H}_3$)$_2$)
δ=0.74(d, $^{3}J_{HH}$ =6.6, 3H, -CH(C$\underline{H}_3$)$_2$)
δ=0.40(s, 27H, -Si(Si(C$\underline{H}_3$)$_3$)$_3$)

$^{13}C\{^{1}H\}$ NMR (C_6D_6, 298K, 62.896MHz, δ: ppm)

δ=143.5; 139.1; 122.2; 119.7; 107.7 (5 tert.-C: C1, C4, C7, C9 and C10)

δ=117.7; 112.9; 110.8; 101.4 (4 sp^2-C: C5, C2, C3, C6)

δ=35.6; 30.2; 24.9; 24.6; 20.9; 14.5 (6 sp^3-C: C71, C8, C72, C73, C41, C101)

δ=2.60 (9C, -Si(Si($\underline{C}H_3)_3)_3$)

3.3.2.3 Cs(6-Hyp-Hgual) (4)

Preparation

At room temperature a deep blue solution of 0.54g (2.72mmol) of guaiazulene in 8ml of tetrahydrofuran was added to a brown solution of 1.03g (2.71mmol) of $CsSi(SiMe_3)_3$ in 8ml of tetrahydrofuran with stirring. Ten minutes later the solvent tetrahydrofuran was removed away under reduced pressure at room temperature. The residue was re-crystallized in toluene at -30°C.

Product Properties

The yellow crystal of **4** is air- and moisture sensitive. It is soluble in tetrahydrofuran and toluene, but insoluble in n-pentane.

Element Analysis

Formula: $CsC_{24}H_{45}Si_4$, M=578.87g/mol

	C	H	Si	Cs
Calc.(%)	49.79	7.835	19.40	22.95
Found(%)	47.08	7.540		

NMR Spectral Data of 4

^{1}H NMR (C_6D_6, 298K, 400.131MHz, δ: ppm, J: Hz)

δ=6.29(s, 1H, H8)
δ=5.90 (d, $^3J_{HH}$ =2.9, 1H); δ=5.84(d, $^3J_{HH}$ =2.9, 1H): H2 and H3, AB spin system
δ=5.00 (d, $^3J_{HH}$ =7.9, 1H, H5);
δ=2.40(d, $^3J_{HH}$ =7.9, 1H, H6)
δ=2.69(m, $^3J_{HH}$ =6.4, 1H, H71)
δ=2.37(s, 3H, Me of guaiazulenyl)

δ=1.99(s, 3H, Me of guaiazulenyl)
δ=1.42(d, $^{3}J_{HH}$ =6.4, ; 5.883H, -CH(C<u>H</u>$_3$)$_2$)
δ=1.25(d, $^{3}J_{HH}$ =6.4, 3H, -CH(C<u>H</u>$_3$)$_2$)
δ=0.37(s, 27H, -Si(Si(C<u>H</u>$_3$)$_3$)$_3$)

^{13}C{^{1}H} NMR (C_6D_6, 298K, 100.613MHz, δ: ppm)

δ=133.3; 131.5; 124.8; 121.1; 116.4 (5 tert.-C: C1, C4, C7, C9 and C10)
δ=115.5 (1C, C8) δ=112.2 (1C, C5)
δ=111.4 (1C, C2) δ=105.1 (1C, C3)
δ=35.6 (1C, C71) δ=32.6(1C, C6)
δ=28.3 (1C, C72) δ=23.7 (1C, C41)
δ=23.3 (1C, C73) δ=14.0 (1C, C101)
δ=2.64 (9C, -Si(Si(<u>C</u>H$_3$)$_3$)$_3$)

^{29}Si {^{1}H} NMR(39.761MHz, 302K)

In C_6D_6: δ= -12.1 (3 β-Si, -Si(<u>Si</u>Me$_3$)$_3$, $^{1}J_{C\text{-}Si}$ = 46.50Hz)
δ= -77.6 (1 α-Si, -<u>Si</u>(SiMe$_3$)$_3$)

3.3.2.4 Mn(6-Hyp-Hgual)$_2$ (5)

Preparation

To a flask containing 0.37g (1.72mmol) of solid $MnBr_2$ and 5ml of tetrahydrofuran was added a solution of 1.67g (3.44mmol) of **2** in 10ml of tetrahydrofuran at room temperature with stirring. The colour of the initially greenish-yellow solution of **2** turned in about ten minutes to brown-yellow. The mixture was stirred overnight. After removal of the solvent tetrahydrofuran, 8ml of toluene was added into the residue. The produced KBr and the excess $MnBr_2$ were separated away from the solution via filtration, and the precipitate was washed with toluene for two times (2x5ml). The concentrated filtrate afforded 0.66g (0.70mmol, 40.6% yield) of brown-red crystals of **5** at -20°C.

Product Properties

The red-brown rod-shaped crystals are air- and moisture sensitive. It is soluble in tetrahydrofuran, toluene and n-pentane. Above 98°C it will decompose. It has paramagnetic properties.

Element Analysis

Formula: $MnC_{48}H_{90}Si_8$, M = 946.86g/mol

	C	H	Si	Mn
Calc.(%)	60.88	9.580	23.72	5.802
Found(%)	58.80	9.850		5.820

3.3.2.5 Fe(6-Hyp-Hgual)$_2$ (6)

Preparation

At room temperature a greenish-yellow solution of **2** (1.00g, 2.06mmol) in 10ml of tetrahydrofuran was added to a flask with 0.13g (1.03mmol) of solid $FeCl_2$ in 8ml of tetrahydrofuran with stirring. One hour later the initially greenish-yellow colour turned to red. The mixture was allowed to be stirred overnight. After removal of the solvent tetrahydrofuran at reduced pressure, 8ml of toluene was added into the residue. Via filtration the produced salt KCl and the excess $FeCl_2$ were separated away. The product was obtained from the concentrated filtrate (about 5ml) through recrystallization at +5 ~ -20°C. 0.39g (0.41mmol, 39.9%) of orange rod-shaped crystals of **6** was collected.

Product Properties

The orange rod-shaped crystal of **6** is air- and moisture stable. It is soluble in toluene and C_6D_6, but insoluble in acetone. Above 209°C it will decompose.

Element Analysis

Formula: $FeC_{48}H_{90}Si_8$, M = 947.77g/mol

	C	H	Si	Fe
Calc.(%)	60.82	9.571	23.70	5.892
Found(%)	60.99	9.990		5.090

NMR Spectral Data

Racemic Diastereomer

^{1}H NMR (C_6D_6, 298K, 250.133MHz, δ: ppm, J: Hz)

δ=5.92(s, 1H, H8)
δ=3.98(d, $^3J_{HH}$ =2.6, 1H, H2)
δ=3.88(d, $^3J_{HH}$ =2.6, 1H, H3)
δ=5.37(dd, $^3J_{HH}$ =9.1, $^4J_{HH}$=1.2, 1H, H5)
δ=1.98(s, 3H, H101)
δ=1.98(s, 3H, H41)
δ=1.36(d, $^3J_{HH}$ =6.7, 3H, -CH(C$\underline{H}_3$)$_2$)
δ=1.28(d, $^3J_{HH}$ =6.7, 3H, -CH(C$\underline{H}_3$)$_2$)

δ=3.00(d, $^{3}J_{HH}$ =9.1, 1H, H6)
δ=2.21(m, $^{3}J_{HH}$ =6.7, 1H, H71)
δ=0.24(s, 27H, -Si(Si(C$\underline{H}_3$)$_3$)$_3$)

^{13}C{^{1}H} NMR (C_6D_6, 298K, 62.896MHz, δ: ppm)

δ=145.5; 129.4 (2 tert.-C: C4 and C7)
δ=86.5; 83.7; 83.4 (3 tert.-C: C1, C9 and C10)
δ=126.2 (C5)
δ=115.0 (C8)
δ=67.3 (C2)
δ=23.8(CH_3 in isopropyl)
δ=23.5C(41)
δ=35.9(C71)
δ=73.5(C3)
δ=33.1(C6)
δ=21.1(CH_3 in isopropyl)
δ=11.2 (C101)
δ=2.30 (9C, -Si(Si(C$\underline{H}_3$)$_3$)$_3$, J_{C-H}=120; J_{Si-H}=6.2)

^{29}Si {^{1}H} NMR(C_6D_6, 39.761MHz, 302K)

δ= -12.3 (3 β-Si, -Si($\underline{Si}Me_3$)$_3$, $^{1}J_{C-Si}$ = 43.5Hz)
δ= -70.8 (1 α-Si, -$\underline{Si}$(SiMe$_3$)$_3$)

Meso-diastereomer

^{1}H NMR (C_6D_6, 298K, 250.133MHz, δ: ppm, J: Hz)

δ=5.82(s, 1H, H8)
δ=3.97(d, $^{3}J_{HH}$ =2.5, 1H, H2)
δ=3.73(d, $^{3}J_{HH}$ =2.5, 1H, H3)
δ=5.43(d, $^{3}J_{HH}$ =9.2, 1H, H5)
δ=3.03(d, $^{3}J_{HH}$ =9.2, 1H, H6)
δ=2.17(m, $^{3}J_{HH}$ =6.4, 1H, H71 in -C*H*(CH$_3$)$_2$)
δ=1.97(s, 3H, H101)
δ=1.97(s, 3H, H41)
δ=1.30(d, $^{3}J_{HH}$ =6.4, 3H, -CH(C*H*$_3$)$_2$)
δ=1.28(d, $^{3}J_{HH}$ =6.4, 3H, -CH(C*H*$_3$)$_2$)
δ=0.22(s, 27H, -Si(Si(C*H*$_3$)$_3$)$_3$)

^{13}C{^{1}H} NMR (C_6D_6, 298K, 62.896MHz, δ: ppm)

δ=145.1; 129.6 (2 tert.-C: C4 and C7)
δ=87.6; 83.8; 82.4 (3 tert.-C: C1, C9 and C10)
δ=126.1 (C5)
δ=115.1 (C8)
δ=68.5 (C2)
δ=24.2(CH_3 in isopropyl)
δ=23.5C(41)
δ=32.9(C6)
δ=72.0(C3)
δ=35.8(C71)
δ=20.9(CH_3 in isopropyl)
δ=12.8 (C101)
δ=2.30 (9C, -Si(Si(C$\underline{H}_3$)$_3$)$_3$), J_{C-H}=120)

^{29}Si {^{1}H} NMR(C_6D_6, 39.761MHz, 302K)

δ= -12.3(3 β-Si, -Si($\underline{Si}Me_3$)$_3$, $^{1}J_{C-Si}$ = 43.5Hz)
δ= -70.7(1 α-Si, -$\underline{Si}$(SiMe$_3$)$_3$)

3.3.2.6 Fe(8-Hyp-Hgual)$_2$ (7)

Preparation

Yellow solution of **3** (0.93g, 1.92mmol) in 10ml of tetrahydrofuran was added at room temperature to a flask with 0.12g (1.420mmol) of solid $FeCl_2$ in 8ml of tetrahydrofuran with stirring. One hour later the initially yellow colour turned to blood red. The mixture was allowed to be stirred overnight. After removal of the solvent tetrahydrofuran at reduced pressure, 8ml of toluene was added to the residue. Via filtration the produced salt KCl and the excess $FeCl_2$ were filtrated away. From the concentrated filtrate (about 5ml) at +5 ~ -20°C 0.365g (0.385mmol) red rod-shaped crystals of **7** formed. Yield: 40.1%.

Product Properties

The red rod-shaped crystal of **7** is air- and moisture stable. It has good solubility in toluene and C_6D_6, but insoluble in acetone. Above 183°C it will decompose.

NMR Spectral Data

Racemic Diastereomer

^{1}H NMR (C_6D_6, 298K, 250.133MHz, δ: ppm, J: Hz)

δ=3.31(s, 1H, H8)
δ=4.54(d, $^3J_{HH}$ =2.0, 1H, H2)
δ=3.61(d, $^3J_{HH}$ =2.0, 1H, H3)
δ=5.71(d, $^3J_{HH}$ =8.7, 1H, H5)
δ=5.41(d, $^3J_{HH}$ =8.7, 1H, H6)
δ=2.41(m, $^3J_{HH}$ =6.6, 1H, H71)
δ=1.97(s, 3H, H101)
δ=1.83(s, 3H, H41)
δ=1.16(d, $^3J_{HH}$ =6.6, 3H, -CH(C$\underline{H}_3$)$_2$)
δ=0.86(d, $^3J_{HH}$ =6.6, 3H, -CH(C$\underline{H}_3$)$_2$)
δ=0.22(s, 27H, -Si(Si(C$\underline{H}_3$)$_3$)$_3$)

^{13}C{^{1}H} NMR (C_6D_6, 298K, 62.896MHz, δ: ppm)

δ=147.2.5; 135.6 (2 tert.-C: C4 and C7)
δ=85.6; 83.0; 82.3 (3 tert.-C: C1, C9 and C10)
δ=128.6; 122.5 (2 sp^2-C: C5 and C8)
δ=73.7; 67.4 (C2 and C3)
δ=37.9; 32.3; 27.6; 22.8; 20.0; 13.7 (6 sp^3-C: C6, C71, C72, C73, C41, C101)
δ=2.66 (9C, -Si(Si(C$\underline{H}_3$)$_3$)$_3$)

Meso-diastereomer

^{13}C{^{1}H} NMR (C_6D_6, 298K, 62.896MHz, δ: ppm)

δ=147.8; 135.2 (2 tert.-C: C4 and C7)
δ=85.4; 83.8; 82.9 (3 tert.-C: C1, C9 and C10)
δ=125.7; 123.0 (2 sp^2-C: C5 and C8
δ=73.6; 66.9 (C2 and C3)
δ=38.6; 31.6; 25.8; 23.1; 20.5; 14.3 (6 sp^3-C: C6, C71, C72, C73, C41, C101)
δ=2.66 (9C, -Si(Si($\underline{C}H_3)_3)_3$)

3.3.2.7 Ni(6-Hyp-Hgual)$_2$ (8)

Preparation

At about -20°C a solution of 1.55g (3.19mmol) of **2** in 15 ml of tetrahydrofuran was added drop wise to a stirring suspension of 0.69g (3.16mmol) of $NiBr_2$ in 10ml of tetrahydrofuran. In half an hour dark fine powder appeared in the reaction mixture, indicating the formation of nickel. The mixture was allowed to be warmed slowly to room temperature and stirred overnight. After evacuation of the solvent tetrahydrofuran under reduced pressure at room temperature, the residue was extracted with 25ml mixture of toluene and n-pentane 1:1(v/v). The supernatant liquid was sucked carefully to another clean flask, and stored at 5°C. The oxidized colourless hexangular crystals of **9** crystallized at first with yield 30%.

By further re-crystallization of the extracting at -20°C it afforded 0.17g (1.78mmol, 24.2%) of red needle crystals of **8**.

Product Properties of 8

The red needle crystal of **8** is air- and moisture sensitive. It has good solubility in toluene and C_6D_6. Above 140°C it decomposes.

Element Analysis

Formula: $NiC_{48}H_{90}Si_8$, M = 950.62g/mol

	C	H	Si	Ni
Calc.(%)	60.64	9.542	23.64	6.174
Found(%)	60.45	9.870		

3.3.2.8 (3-Hyp-6-Hgua)$_2$ (9)

Preparation

To a flask containing 0.73g (1.04mmol) of $Pb(Hyp)_2$ and 10ml of toluene was added 0.50ml of guaiazulene solution in toluene (containing 0.21g, 1.11mmol guaiazulene, concentration:

21.18g/50ml toluene) at room temperature with stirring. The initially blue solution would change immediately to dark. The mixture was stirred for 20 minutes and then filtrated and washed with toluene. 0.623g (0.698mmol, 67.1%) of colourless hexangular crystals of **9** was afforded at -20°C from the concentrated filtrate.

The variation preparation of **9** can be followed by reaction of CuCl with **2** in tetrahydrofuran, or $TiCl_3$ with **2** in toluene (yield >50%) etc.

Product Properties

The colourless hexangular platelets have good solubility in tetrahydrofuran. It is soluble in toluene, but insoluble in n-pentane. Above 150°C it decomposes.

Element Analysis

Formula: $C_{48}H_{90}Si_8$, M = 891.93g/mol

	C	H	Si
Calc.(%)	64.64	10.17	25.19
Found(%)	64.37	10.09	

NMR

^{1}H NMR (C_6D_6, 297K, 250.133MHz, δ: ppm, J: Hz)

δ=6.64(s, 1H, H8)
δ=6.33(s, 1H, H2)
δ=5.07(s, 1H, H5)
δ=3.89(s, 1H, H3)
δ=2.93(m, $^3J_{HH}$ =5.4, 1H, H71)
δ=2.13(s, 6H, H101, H41)
δ=2.51(s, 1H, H6)
δ=1.37(d, $^3J_{HH}$ =5.4, 3H, -CH($C\underline{H}_3$)$_2$)
δ=1.01(d, $^3J_{HH}$ =5.4, 3H, -CH($C\underline{H}_3$)$_2$)
δ=0.33(s, 27H, -Si(Si($C\underline{H}_3$)$_3$)$_3$)

^{13}C{^{1}H} NMR (C_6D_6, 300K, 100.613MHz, δ: ppm)

δ=144.4; 141.1; 140.0; 124.0; 120.6 (5 tertiary C: C1, C4, C7, C9, C10)
δ=132.2 (1C, C2
δ=113.9 (1C, C8)
δ=42.2(1C, C3)
δ=29.7; 21.7 (C72, C73)
δ=14.6 (1C, C101)
δ=118.4 (1C, C5)
δ=44.1(1C, C6)
δ=30.3 (1C, C71)
δ=23.0 (1C, C41)
δ=2.72 (9C, -Si(Si($\underline{C}H_3$)$_3$)$_3$)

^{29}Si {^{1}H} NMR (C_6D_6, 79.495MHz, 297K)

δ= -11.5 (3 β-Si, -Si($\underline{Si}Me_3$)$_3$)
δ= -90.2 (1 α-Si, -$\underline{Si}$($SiMe_3$)$_3$)

3.3.2.9 Ti(6-Hyp-Hgual)$_2$Cl$_2$ (10)

Preparation

At room temperature 0.87g(1.79mmol) of **2** in 10ml of tetrahydrofuran was added to a stirring light green suspension of 0.14g(0.90mmol) of $TiCl_3$ in 10ml of tetrahydrofuran. 24 hours later the solvent tetrahydrofuran was removed under reduced pressure. To the residue 10ml of toluene was added. The produced KCl and the excess $TiCl_3$ were then separated away via filtration. At -20°C from the concentrated filtrate 0.30g (0.297mmol) of red-brawn crystals with yield 33% was afforded.

Product Properties

The red rod-shaped crystal of **10** is air- and moisture sensitive. It is soluble in toluene and C_6D_6. Above 230°C it will decompose.

Element Analysis

Formula: $TiC_{48}H_{90}Si_8Cl_2$, M = 1010.71g/mol

	C	H	Si	Ti	Cl
Calc.(%)	57.04	8.975	22.23	4.737	7.015
Found(%)	57.86	8.910		4.860	

NMR Spectral Data (Racemic Diastereomer)

^{1}H NMR (C_6D_6, 298K, 250.133MHz, δ: ppm, J: Hz)

δ=6.13(s, 1H, H8)
δ=5.55(d, $^3J_{HH}$ =2.8, 1H, H2)
δ=5.45(d, $^3J_{HH}$ =2.8, 1H, H3)
δ=5.48(d, $^3J_{HH}$ =9.0, 1H, H5)
δ=3.09(d, $^3J_{HH}$ =9.0, 1H, H6)
δ=2.16(m, $^3J_{HH}$ =6.7, 1H, H71)
δ=2.23(s, 3H, H101)
δ=1.53(s, 3H, H41)
δ=1.25(d, $^3J_{HH}$ =6.7, 3H, -CH(C$\underline{H}_3$)$_2$)
δ=1.12(d, $^3J_{HH}$ =6.7, 3H, -CH(C$\underline{H}_3$)$_2$)
δ=0.23(s, 27H, -Si(Si(C$\underline{H}_3$)$_3$)$_3$)

^{13}C{^{1}H} NMR (C_6D_6, 298K, 62.896MHz, δ: ppm)

δ=151.6; 139.0; 135.9; 129.6; 127.0 (5 tert.-C: C1. C4. C7, C9 and C10)
δ=134.0 (1C, C5)
δ=109.0 (1C, C2)
δ=34.3 (1C, C71)
δ=24.1 (1C, C72)
δ=23.1 (1C, C41)
δ=2.26 (9C, -Si(Si(C$\underline{H}_3$)$_3$)$_3$)
δ=115.4 (1C, C8)
δ=107.1 (1C, C3)
δ=30.2 (1C, C6)
δ=20.4 (1C, C73)
δ=16.4 (1C, C101)

^{29}Si {^{1}H} NMR (C_6D_6, 39.761MHz, 302K)

δ= -12.5(3 β-Si, -Si(<u>Si</u>Me_3)$_3$)
δ= -68.6(1 α-Si, -<u>Si</u>($SiMe_3$)$_3$)

3.3.2.10 Zr(6-Hyp-Hgual)$_2$Cl$_2$ (11)

Preparation

To a stirring suspension of 0.57g(2.45mmol) of $ZrCl_4$ in 25ml of tetrahydrofuran was added at room temperature 1.20g (2.48mmol) of **2**. The resulted solution turned immediately to yellow. The solution was allowed to be stirred overnight. The produced salt KCl and the excess of $ZrCl_4$ were separated from the solution via filtration. The filtrate was concentrated to about 8ml and cooled at 5°C. Several days later very beautiful yellow needle crystals formed. Yield: 0.86g (0.82mmol) 66.1%.

Product Properties

The yellow needle crystal of compound **11** is air- and moisture-sensitive. It has good solubility in toluene and C_6D_6. Above 234°C it will decompose.

Element Analysis

Formula: $ZrC_{48}H_{90}Si_8Cl_2$, M = 1054.05g/mol

	C	H	Si	Zr	Cl
Calc.(%)	54.69	8.606	21.31	8.654	6.726
Found(%)	54.68	8.620		7.940	

NMR Spectral Data (Racemic Diastereomer)

^{1}H NMR (C_6D_6, 298K, 250.133MHz, δ: ppm, J: Hz)

δ=6.03(s, 1H, H8)
δ=5.55(d, $^{3}J_{HH}$ =2.9, 1H, H2)
δ=5.54(d, $^{3}J_{HH}$ =2.9, 1H, H3)
δ=5.38(d, $^{3}J_{HH}$ =9.0, 1H, H5)
δ=3.03(d, $^{3}J_{HH}$ =9.0, 1H, H6)
δ=2.61(m, $^{3}J_{HH}$ =6.6, 1H, H71)
δ=2.10(s, 3H, H101)
δ=1.65(s, 3H, H41)
δ=1.24(d, $^{3}J_{HH}$ =6.6, 3H, -CH(C<u>H</u>$_3$)$_2$)
δ=1.13(d, $^{3}J_{HH}$ =6.6, 3H, -CH(C<u>H</u>$_3$)$_2$)
δ=0.22(s, 27H, -Si(Si(C<u>H</u>$_3$)$_3$)$_3$)

$^{13}C\{^1H\}$ NMR (C_6D_6, 298K, 62.896MHz, δ: ppm)

δ=149.6; 134.6; 130.6; 126.6; 125.5 (5 tert.-C: C1. C4. C7, C9 and C10)
δ=131.3 (1C, C5) δ=113.8 (1C, C8)
δ=106.9 (1C, C2) δ=105.2 (1C, C3)
δ=36.6 (1C, C71) δ=33.5 (1C, C6)
δ=24.0 (1C, C72) δ=20.4 (1C, C73)
δ=23.5 (1C, C41) δ=15.4 (1C, C101)
δ=2.23 (9C, -Si(Si($\underline{C}H_3)_3)_3$)

$^{29}Si\ \{^1H\}$ NMR (C_6D_6, 39.761MHz, 302K)

δ= -12.1(3 β-Si, -Si($\underline{Si}Me_3)_3$)
δ= -69.9(1 α-Si, -$\underline{Si}(SiMe_3)_3$)

3.3.2.11 Hf(6-Hyp-Hgual)$_2$Cl$_2$ (12)

Preparation

To a suspension of 0.456g (1.424mmol) of $HfCl_4$ in 15ml of tetrahydrofuran was added at room temperature 1.297g (2.674mmol) of **2** with stirring. The resulted solution turned immediately to light yellow. The solution was allowed to be stirred for 24 hours, the produced salt KCl and the excess of $HfCl_4$ were filtrated away from the solution. From the concentrated filtrate 0.93g (0.81mmol) (yield: 60.1%) of **12** was obtained at 5°C.

Product Properties

The light yellow needle crystal of **12** is air- and moisture sensitive. Similar to **11** it has good solubility in toluene and C_6D_6. Above 242°C it will decompose.

Element Analysis

Formula: $HfC_{48}H_{90}Si_8Cl_2$, M = 1141.32g/mol

	C	H	Si	Hf	Cl
Calc.(%)	50.51	7.948	19.68	15.63	6.212
Found(%)	50.50	7.960		13.77	

NMR Spectral Data (Racemic Diastereomer)

^1H NMR (C_6D_6, 298K, 250.133MHz, δ: ppm, J: Hz)

δ=6.02(s, 1H, H8)
δ=5.45(d, $^3J_{HH}$ =3.2, 1H, H2)
δ=5.33(d, $^3J_{HH}$ =3.2, 1H, H3)
δ=5.39(d, $^3J_{HH}$ =8.7, 1H, H5)
δ=3.06(d, $^3J_{HH}$ =8.7, 1H, H6)
δ=2.16(m, $^3J_{HH}$ =6.7, 1H, H71)
δ=2.26(s, 3H, H101)
δ=1.67(s, 3H, H41)
δ=1.25(d, $^3J_{HH}$ =6.7, 3H, -CH(C$\underline{H}_3$)$_2$)
δ=1.14(d, $^3J_{HH}$ =6.7, 3H, -CH(C$\underline{H}_3$)$_2$)
δ=0.23(s, 27H, -Si(Si(C$\underline{H}_3$)$_3$)$_3$)

^{13}C{^{1}H} NMR (C_6D_6, 298K, 62.896MHz, δ: ppm)

δ=149.6; 133.2; 129.2; 126.5; 123.5 (5 tert.-C: C1. C4. C7, C9 and C10)
δ=131.5 (1C, C5)
δ=113.8 (1C, C8)
δ=105.3 (1C, C2)
δ=104.2 (1C, C3)
δ=36.6 (1C, C71)
δ=33.2 (1C, C6)
δ=24.1 (1C, C72)
δ=20.4 (1C, C73)
δ=23.5 (1C, C41)
δ=15.2 (1C, C101)
δ=2.25 (9C, -Si(Si(C$\underline{H}_3$)$_3$)$_3$)

^{29}Si {^{1}H} NMR (C_6D_6, 39.761MHz, 302K)

δ= -12.1(3 β-Si, -Si($\underline{Si}$Me$_3$)$_3$)
δ= -69.2(1 α-Si, -$\underline{Si}$(SiMe$_3$)$_3$)

3.3.2.12 ZrCp(6-Hyp-Hgual)Cl$_2$ ·KCl (13)*

Preparation

At room temperature 0.355g (1.18mmol) of ZrCp*Cl$_3$ was added to a stirring solution of 0.574g (1.18mmol) of K(6-Hyp-Hgual) **2** in 45ml of toluene. After 12 h stirring the colour of the initially greenish-yellow solution turned to orange. The mixture was filtered and the filtrate was concentrated to about 30ml and cooled at 5°C. The collected crystalline compound of **13** weighted 0.38g (0.464mmol) (yield 39.3%).

Product Properties

The yellow powder of **13** is air- and moisture sensitive. It is soluble in toluene and C_6D_6. Above 262°C it will decompose.

Element Analysis

Formula: $C_{34}H_{60}Si_4ZrCl_2$·KCl, M=817.96/mol

	C	H	Si	Zr	Cl	K
Calc.(%)	49.93	7.394	13.73	11.15	13.00	4.780
Found(%)	49.16	7.490				

NMR Spectral Data

^{1}H NMR (C_6D_6, 298K, 250.133MHz, δ: ppm, J: Hz)

δ=6.27(s, 1H, H8)
δ=5.24(d, $^{3}J_{HH}$ =2.8, 1H, H2)
δ=5.16(d, $^{3}J_{HH}$ =2.8, 1H, H3)
δ=5.49(d, $^{3}J_{HH}$ =9.2, 1H, H5)
δ=3.07(d, $^{3}J_{HH}$ =9.2, 1H, H6)
δ=2.19(m, $^{3}J_{HH}$ =7.3, 1H, H71)
δ=2.15(s, 3H, H101)
δ=1.66(s, 3H, H41)
δ=1.27(d, $^{3}J_{HH}$ =7.3, 3H, -CH(C$\underline{H}_3$)$_2$)
δ=1.24(d, $^{3}J_{HH}$ =7.3, 3H, -CH(C$\underline{H}_3$)$_2$)
δ=0.24(s, 27H, -Si(Si(C$\underline{H}_3$)$_3$)$_3$)

^{13}C{^{1}H} NMR (C_6D_6, 298K, 62.896MHz, δ: ppm)

δ=148.6; 138.6; 131.2; 126.8; 125.9 (5 tert.-C: C1. C4. C7, C9 and C10)
δ=123.2 (5C, Cp (ring))
δ=131.9 (1C, C5)
δ=107.7 (1C, C2)
δ=36.8 (1C, C71)
δ=24.1 (1C, C72)
δ=23.6 (1C, C41)
δ=2.33 (9C, -Si(Si(C$\underline{H}_3$)$_3$)$_3$)
δ=114.4 (1C, C8)
δ=103.6 (1C, C3)
δ=33.8 (1C, C6)
δ=20.6 (1C, C73)
δ=15.6 (1C, C101)

^{29}Si {^{1}H} NMR (C_6D_6, 39.761MHz, 302K)

δ= -12.1(3 β-Si, -Si($\underline{Si}Me_3$)$_3$)
δ= -86.3(1 α-Si, -$\underline{Si}$(SiMe$_3$)$_3$)

3.3.2.13 2,6-bis(Hyp)-H_2gua (14)

Preparation

5.240g (10.80mmol) of **2** in 15 ml of tetrahydrofuran was added to a solution of 3.058g (10.80mmol) of ClSi(SiMe$_3$)$_3$ in 15ml of tetrahydrofuran at room temperature with stirring. The colour of the reaction mixture would slowly change to green. After 24h the reaction mixture became to jade green and turbid. The produced KCl was filtrated away and the filtrate was concentrated to about 8ml and cooled at 5°C. From toluene or tetrahydrofuran the product crystallized as colourless rhombus-shaped crystals. Yield: 3.74g (5.39mmol), 49.9%.

Product Properties

The pure product of **14** is light yellow powder. It is soluble in n-pentane, toluene, C_6D_6 and tetrahydrofuran. At 128±1°C it melts.

Elemental Analysis

Formula: $C_{33}H_{72}Si_8$, M=693.62g/mol

	C	H	Si
Calc.(%)	57.14	10.46	32.39
Found(%)	56.78	11.11	

NMR Spectral Data

^{1}H NMR (C_6D_6, 298K, 250.133MHz, δ: ppm, J: Hz)

δ=6.12(s, 1H, H8)
δ=6.31(d, $^3J_{HH}$=1.6, 1H, H3)
δ=5.64(d, $^3J_{HH}$ =9.0, 1H, H5)
δ=3.11(d, $^3J_{HH}$ =9.0, 1H, H6)
δ=2.29(m, $^3J_{HH}$ =2.1, 1H, -C<u>H</u>$(CH_3)_2$)
δ=2.14(s, 3H, H101)
δ=2.12(s, 3H, H41)
δ=3.54(d, $^3J_{HH}$ =1.6, 1H, H2)
δ=1.25(d, $^3J_{HH}$ =6.7, 3H, -CH(C<u>H</u>$_3)_2$)
δ=1.17(d, $^3J_{HH}$ =6.7, 3H, -CH(C<u>H</u>$_3)_2$)
δ=0.27(s, 27H, -Si(Si(C<u>H</u>$_3)_3)_3$)
δ=0.24(s, 27H, -Si(Si(C<u>H</u>$_3)_3)_3$)

^{13}C{^{1}H} NMR (C_6D_6, 298K, 62.896MHz, δ: ppm)

δ=146.8 (1C, C7)
δ=142.1(1C, C1)
δ=127.2(1C,C4)
δ=128.3 (1C, C5)
δ=45.2 (1C, C2)
δ=34.7 (1C, C6)
δ=24.3 (1C, C72)
δ=15.6 (1C, C101)
δ=2.30 (9C, -Si(Si(<u>C</u>$H_3)_3)_3$)
δ=143.2(1C, C10)
δ=135.1(1C, C9)
δ=128.7 (1C, C3)
δ=114.6(1C, C8)
δ=35.8 (1C, C71)
δ=24.6 (1C, C41)
δ=20.7 (1C, C73)
δ=2.40 (9C, -Si(Si(<u>C</u>$H_3)_3)_3$)

^{29}Si {^{1}H} NMR (C_6D_6, 39.761MHz, 302K)

δ= -12.1(3 β-Si, -Si(<u>Si</u>$Me_3)_3$)
δ= -12.2(3 β-Si, -Si(<u>Si</u>$Me_3)_3$)
δ= -72.5(1 α-Si, -<u>Si</u>$(SiMe_3)_3$)
δ= -90.5(1 α-Si, -<u>Si</u>$(SiMe_3)_3$)

3.3.2.14 [Li(2,6-bis(Hyp)-Hgual)]$_2$ (15)

Preparation

8.96g (18.47mmol) of **2** was added to a solution of 5.23g (18.47mmol) of $ClSi(SiMe_3)_3$ in 60ml of tetrahydrofuran at room temperature. With stirring the initially greenish-yellow

colour of the reaction mixture turned slowly to jade green. Keep stirring until the ^{1}H NMR signals of **2** and $ClSi(SiMe_3)_3$ completely disappeared. The solvent tetrahydrofuran was then removed in *vacuo* and replaced with 30ml of toluene, followed a solution of 7.40ml of ^{n}BuLi (2.5M in hexanes) was added into the reaction mixture. The molar ratio of ^{n}BuLi to compound **14** was calculated as 1:1, and the yield of **14** was regarded as 100%. The reaction mixture was heated to 60°C and stirred overnight. The turbid jade green solution of **14** would change to clear yellow solution. After the signals of **14** in the ^{1}H NMR spectra disappeared, solvent toluene was distilled under reduced pressure until the residue was completely dried. 25ml of toluene was added into the residue and the suspension was filtrated. The filtrate was concentrated to incipient crystallization and cooled at 5°C. One day later deep yellow rod-shaped crystals formed. Yield: 9.41g (13.45mmol), 72.8%.

Product Properties

The yellow powder of **15** is extremely air- and moisture sensitive. It is soluble in toluene, C_6D_6 and tetrahydrofuran. Above 128°C it decomposes.

Element Analysis

Formula: $C_{33}H_{71}Si_8Li$, M=699.55g/mol

	C	H	Si	Li
Calc.(%)	56.65	10.22	32.11	0.99
Found(%)	55.75	10.38		1.24

NMR Spectral Data

^{1}H NMR (C_6D_6, 298K, 250.133MHz, δ: ppm, J: Hz)

δ=5.74(s, 1H, H8)
δ=5.91(s, 1H, H3)
δ=5.08(d, $^{3}J_{HH}$ =8.7, 1H, H5)
δ=3.12(d, $^{3}J_{HH}$ =8.7, 1H, H6)
δ=2.42(m, $^{3}J_{HH}$ =6.7, 1H, -C<u>H</u>$(CH_3)_2$)
δ=2.10(s, 3H, H101)
δ=1.90(s, 3H, H41)
δ=1.35(d, $^{3}J_{HH}$ =6.7, 3H, -CH(C<u>H</u>$_3)_2$)
δ=1.32(d, $^{3}J_{HH}$ =6.7, 3H, -CH(C<u>H</u>$_3)_2$)
δ=0.34(s, 27H, -Si(Si(C<u>H</u>$_3)_3)_3$)
δ=0.30(s, 27H, -Si(Si(C<u>H</u>$_3)_3)_3$)

^{13}C{^{1}H} NMR (C_6D_6, 298K, 62.896MHz, δ: ppm)

δ=136.5; 124.1; 122.3; 120.6; 120.3; 99.0 (6 tert.-C: C1, C2, C4, C7, C9 and C10)
δ=118.2 (1C, C5)
δ=112.7(1C, H8)
δ=32.8 (1C, C6)
δ=115.8 (1C, C3)
δ=35.4 (1C, C71)
δ=25.1 (1C, C72)

δ=24.4 (1C, C41)
δ=15.0 (1C, C101)
δ=21.2 (1C, C73)
δ=2.50 (18C, in -Si(Si($\underline{C}H_3)_3)_3$)

^{29}Si {^{1}H} NMR (C_6D_6, 39.761MHz, 302K)

δ= -12.2(3 β-Si, -Si($\underline{Si}Me_3)_3$)
δ= -13.4(3 β-Si, -Si($\underline{Si}Me_3)_3$)
δ= -72.9(1 α-Si, -$\underline{Si}(SiMe_3)_3$)
δ= -90.5(1 α-Si, -$\underline{Si}(SiMe_3)_3$)

^{7}Li NMR(d_8-THF, 77.779MHz, 302K)

δ= -1.36ppm

4 Summary

The bulky tris(trimethylsilyl)silyl group, -Si($SiMe_3$)$_3$, which is named also hypersilyl, and in the following will be abbreviated as “Hyp”, due to its good electron releasing properties and large steric demand, can be employed as protection group in the synthesis of organic compounds to build *regio*- and *stereo*-selective collection of C-C bonds under mild reaction conditions. It can also stabilize some reactive intermediated state and/or metal centre in unusual oxidation state, which established its important positions in the organometallic synthesis of low valent main group- and transition- metal complexes. On the other hand, the π-electron rich azulene system can undergo not only electrophilic substitution, but also nucleophilic addition, red-ox reaction, resulting different complexes. The coordination chemistry of azulene system has been and is being a fascinating research area.

Within the framework of examining the regio- and stereo-selective effect of the hypersilyl group on the addition to the π-conjugated azulene system and of examining the reactivity of alkali metal hypersilanide, a number of novel hypersilyl substituted alkali metal guaiazulenide were developed. With these complexes as precursors a series of metallocene- and metallocene dichloride derivatives were synthesized and characterized.

At first, we investigated the addition of alkali metal hypersilanides M$Si(SiMe_3)_3$ (M=Li, K, Cs) to guaiazulene. Experiment showed that the bulky hypersilyl group has strong regio- and stereo-selectivity. However, the addition was greatly affected by the employed solvent. In tetrahydrofuran the addition of lithium-, potassium- and cesium- hypersilanide to guaiazulene resulted in two structural isomers: M(6-Hyp-Hgual) (80%) and M(8-Hyp-Hgual) (7%) (M=Li, K, Cs). Since those adducts with hypersilyl substituents at 6-position are more stable than those substituted at 8-position, the latter in tetrahydrofuran at room temperature even at 5°C completely convert to the former within two weeks.

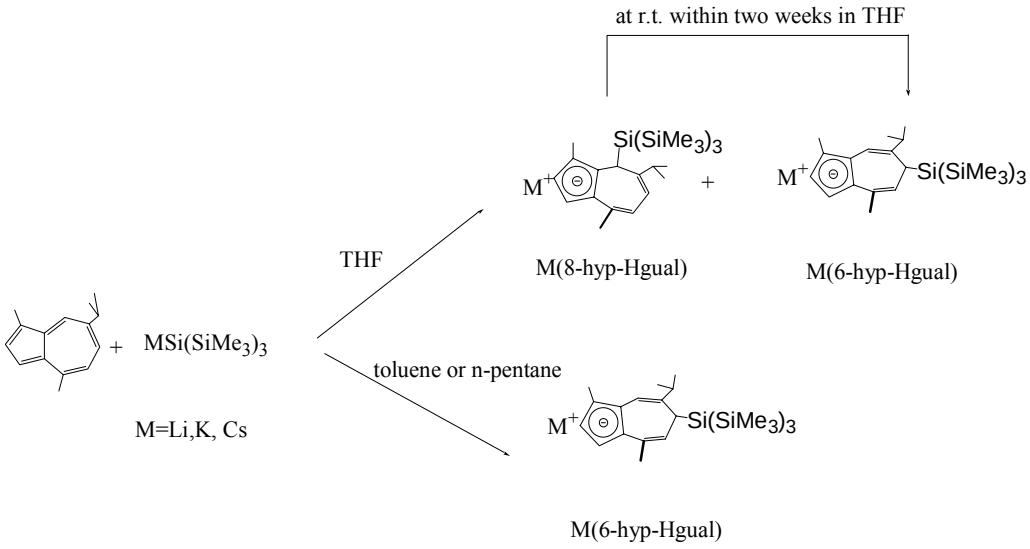

If the reaction is performed in non-coordinating solvents such as n-pentane or toluene, the product is exclusive 6-position adduct of η^5-M(6-hyp-Hgual) (M=Li **1**, K **2**, Cs **4**).

All compounds M(6-Hyp-Hgual) ($M=Li^+$, K^+, Cs^+) consist of one pair of rac-enantiomer. All attempts to separate them using chiral additives failed up to now, however.

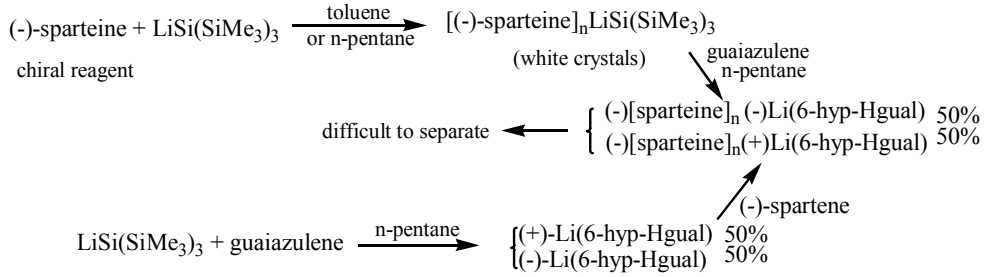

The compound Li(6-Hyp-Hgual) (**1**) crystallizes from toluene as colourless needles. X-ray diffraction analysis revealed the dimeric sandwich structure of the obtained meso-diastereomer.

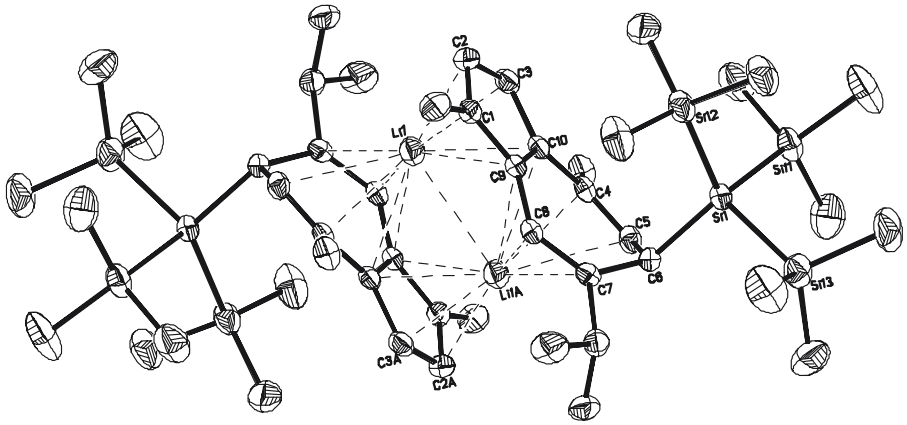

1

In the present isomers each lithium cation is μ-η^5:η^6-coordinated by eleven olefinic carbon atoms, five of them stemming from the five-membered ring of one guaiazulene moiety, and six from the seven-membered ring of the second guaiazulene moiety. The single aliphatic carbon atom C6 in the seven-membered ring is far away from the metal centre because of the bonded bulky hypersilyl group and therefore has no interaction with the lithium cation. It is just the large hypersilyl group which determine the dimeric sandwich structure of compound **1**, since its steric demand inhibits the attack of lithium cations from outside of the dimer and the formation of coordination polymers. In the dimer the Li-Li distance is 281.5(8) pm, which is the shortest value in all reported dimeric structures of lithium cyclopentadienides to date.

All of the ^{13}C NMR data for the five olefinic carbon atoms in the C_5-ring in the ligand of Li(6-Hyp-Hgual) (**1**) are similar with that of the ionic LiCp, demonstrating the dominantly ionic character of Li-$C_{5(ring)}$ in compound **1**.

Two structural isomers of compounds K(6-Hyp-Hgual) (**2**) and K(8-Hyp-Hgual) (**3**) are isolated. Very probably in toluene or n-pentane solution **2** and **3** should also possess similar oligomeric structures as found for **1**. However, all attempts to get crystals either from n-pentane or toluene, failed. In tetrahydrofuran they crystallize as monomer. The potassium cation is η^5-coordinated with a planar C_5-ring, and its coordination sphere is completed by four oxygen atoms from tetrahydrofuran molecules. The whole molecule looks like a swivel chair.

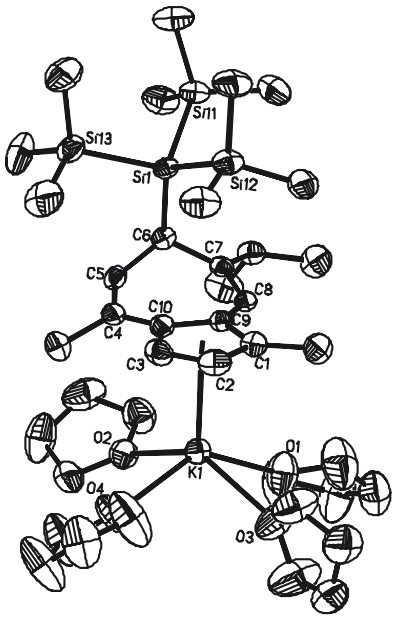

2a

Just like **1**, the ^{13}C NMR data of **2** and **3** implied still dominantly ionic structure of K-$C_{5(ring)}$ in the molecules.

Compound **2** is a valuable precursor for the syntheses of metallocenes derivatives due to it's simple synthesis, high yield (80%) and easy handling. The properties of Cs(6-Hyp-Hgual) (**4**) are in some way similar to those of Li(6-Hyp-Hgual) (**1**), in other way to those of K(6-Hyp-Hgual) (**2**). It can be purified through recrystallization from n-pentane or toluene. Unfortunately, its molecular structure could not be revealed so far.

In the subsequent experiments, we used the obtained compounds **1**, **2** and **3** as precursors for the syntheses of new chiral metallocene complexes. The resulting metallocene derivatives from these precursors lead to formation of two diastereomers: one pair of rac-enantiomer and one meso-diastereomer. By fractional crystallization the rac-diastereomer pair can be partly or completely separated from the meso-diastereomer.

Through reaction of **1** or **2a** with $MnBr_2$ or $FeCl_2$ in tetrahydrofuran in a molar ratio 2:1 metallocene derivatives Mn(6-Hyp-Hgual)$_2$ (**5**) and Fe(6-Hyp-Hgual)$_2$ (**6**) have been obtained.

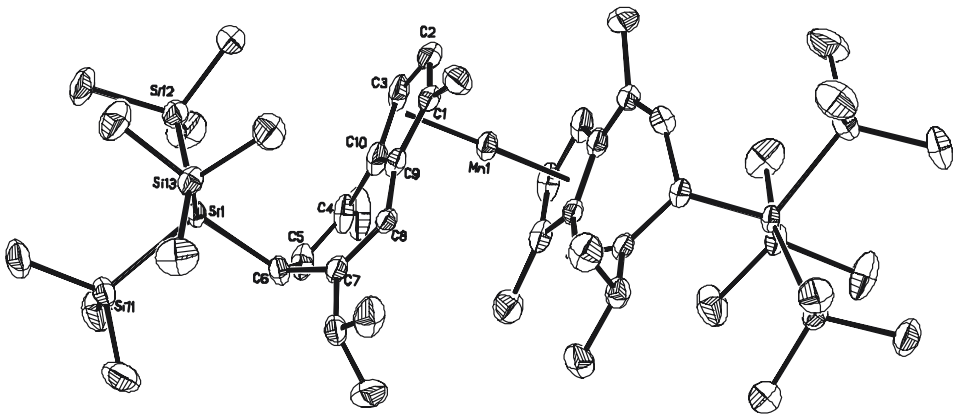

5

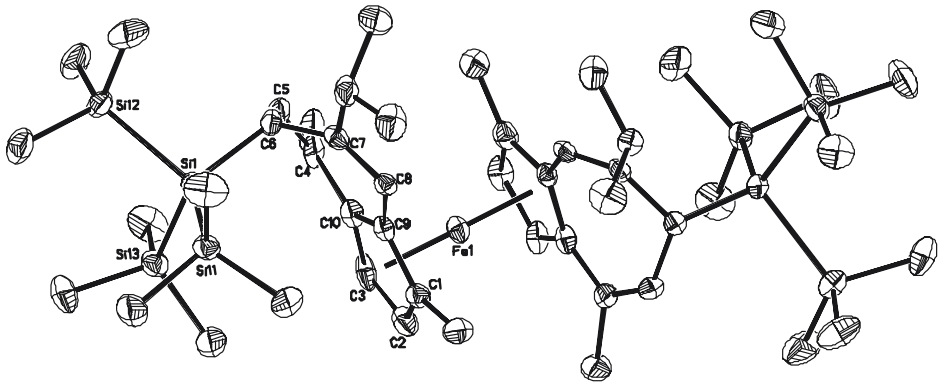

6

Nevertheless, not all reactions of compound **1**, **2a** and MX_2 proceed in the same way as with $MnBr_2$ and $FeCl_2$. For example, if **2a** reacts with $NiBr_2$ in tetrahydrofuran, two kinds of products are formed: one is the nickelocene derivative Ni(6-Hyp-Hgual)$_2$ (**8**) resulted from the metathesis, the another one is the red-ox product (3-Hyp-6-Hgua)$_2$ (**9**), where the hypersilyl group moved from C6 to C3, and the produced radicals were coupled to a 6-6´-dimer.

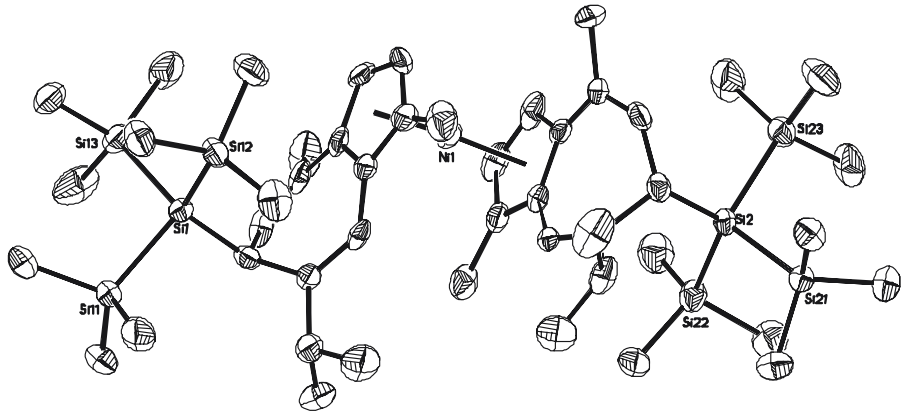

8

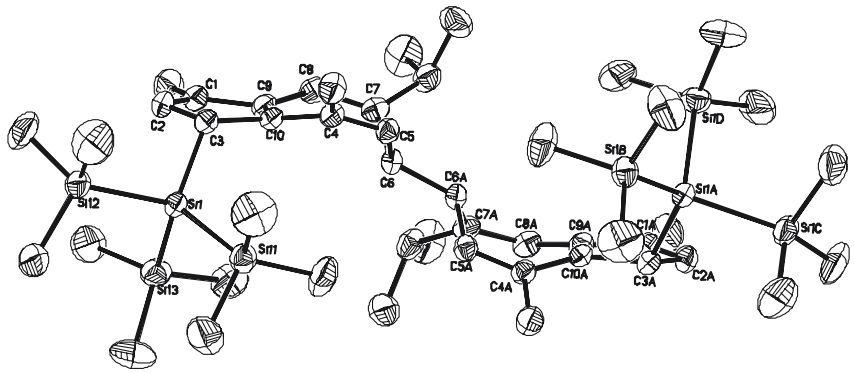

9

The solvent greatly influences the outcome of the metathesis. In toluene no metathesis reaction is observed between $MnBr_2$, $FeCl_2$ and $NiBr_2$ and compound **2**.

Among all of the metallocene derivatives mentioned above, only the structures of the rac-diastereomers were revealed by X-ray diffraction analyses, both chiral carbon atoms C6 and C6´ show the same configuration, either (R,R) or (S,S). The view along the $C_{5(cent.)}$-M-$C'_{5(cent.)}$ axis shows that the syn-conformation[I] is adopted in solid state. In these conformers the two guaiazulene frameworks are in a staggered conformation.

[I] syn-conformation: the two lines C1-C101 and $C'_{5(cent.)}$-C6´ as well as C1´-C101´ and $C_{5(cent.)}$-C6 stretch along same directions, respectively.

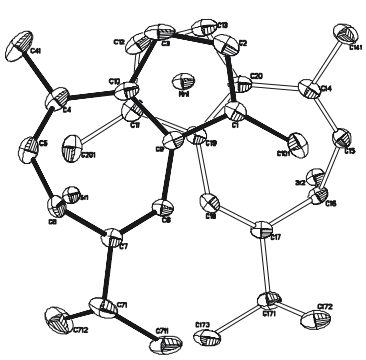

5 (SS, τ = -95.2°; τ_{Cp} = -24.4°)

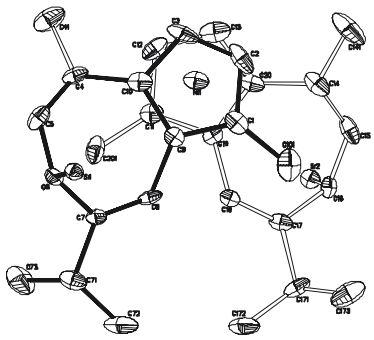

8 (SS, τ = -108.7°; τ_{Cp}= 32.7°)

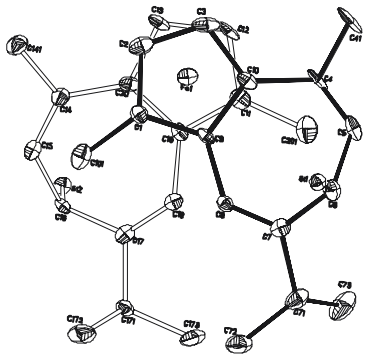

6 (RR, τ = 95.8°; τ_{Cp}= 25.0°)

The two five-membered rings are not parallel to each other, but tilted such, that C2 and C3 are closer to the central metal atom. The reason for this displacement may be found in the repulsive interaction of the methyl group on C1 with the seven-membered ring of the second guaiazulenide ligand. Together with the staggered conformation the whole molecule looks just like a pair of tweezers.

The average bond distances Ni-$C_{5,(aver.)}$ (217.4 pm) and Mn-$C_{5,(aver.)}$ (211.1pm) in the sandwich structures of **5** and **8** are much longer than the Fe-$C_{5,(aver.)}$ distance (206.0pm) in compound **6**, for compound **8** it is due to the large radius of Ni(II) and the lower bond order, for compound **5** it is only due to the lower bond order, when compare to compound **6**. However, compare to the data in corresponding nickelocene and manganocene derivatives these M-$C_{5,(aver.)}$ distances in **5** and **8** are even shorter. The short M-$C_{5,(aver.)}$ distances indicated that in both of compounds **5** and **8** the M(II) cation should possess low-spin states.

	Ni-C (pm)	Electronic Configuration	Bond Order
$NiCp_2$	219.6(4)		
$Ni(6\text{-Hyp-Hgual})_2$ (**8**)	217.4(5)	$^3A_2'$ ($a_1'^2$, $e_2'^4$, $e_1''^2$)	2
	Mn-C(pm)		
$(C_5H_4Me)_2Mn$	243.3(8) (high spin)		
$(C_5H_5)_2Mn$	238.0 (high spin)		
$(C_5H_4Me)_2Mn$	214.4(12) (low spin)		
$(C_5Me_5)_2Mn$	211.2(2) (low spin)		
$Mn(6\text{-Hyp-Hgual})_2$ (**5**)	211.1(4) (low spin)	$^2E_2'$ ($a_1'^2$, $e_2'^3$)	2.5
$Fe(6\text{-Hyp-Hgual})_2$ (**6**)		$^1A_{1g}$ ($a_1'^2$, $e_2'^4$)	3

For compounds **6** and **7** two sets of signals for the rac-diastereomer and meso-diastereomer have been found in the ^{1}H- and ^{13}C-NMR spectra. The two drastically upfield shifted ^{1}H NMR signals (H2 and H3) and five upfield ^{13}C NMR signals around 60~80ppm (C_5 ring) demonstrated that the interactions of Fe-C_5 are dominantly covalent when compare to ferrocene (^{13}C NMR: 68.8ppm [94]). The same situation is expected in compounds **5** and **8**.

In crystals of the corresponding ferrocene derivative Fe(8-Hyp-Hgual)$_2$ (**7**) resulted from **3a** there are three unique molecules, two of them possess (S,S)-, the third possesses (R,R)-configuration. The hypersilyl group at C8 deforms the seven-membered ring severely. C8 and C4 stretch away from the central metal atom, whereas C5, C6 and C7 are directed toward the metal centre.

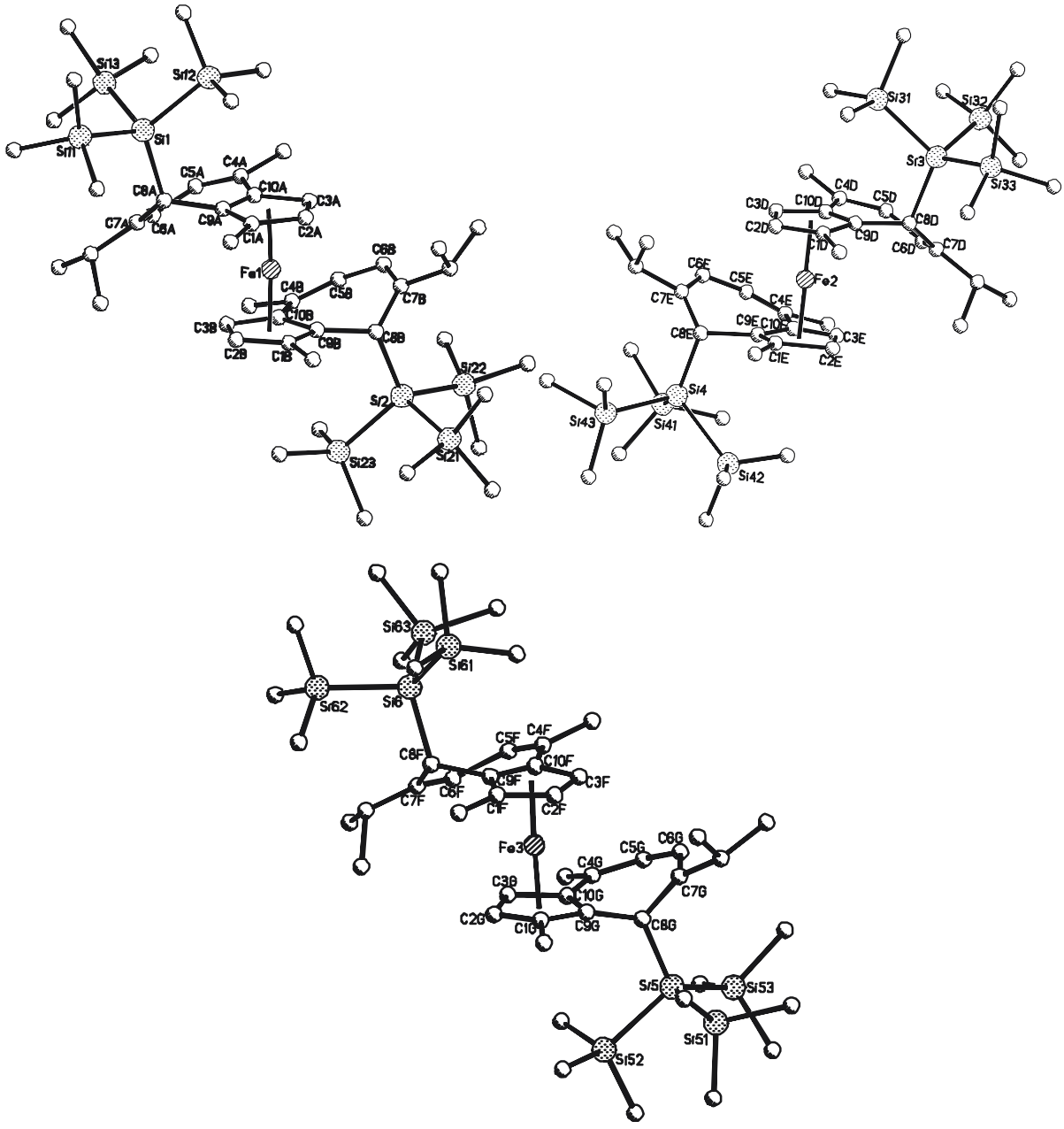

7

In each of the three independent molecules of **7** the two guaiazulene frameworks as well as the two five-membered rings are in a staggered conformation.

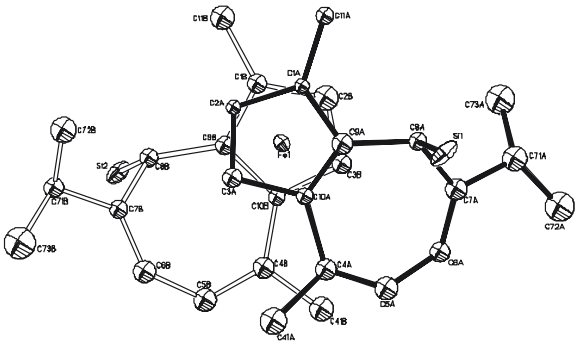

7_A (SS, τ =101.2°; τ_{Cp}= -26.7°)

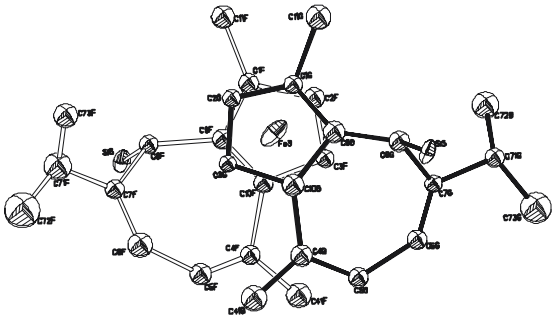

7_C (SS**,** τ =102.8°; τ_{Cp}= 27.4°)

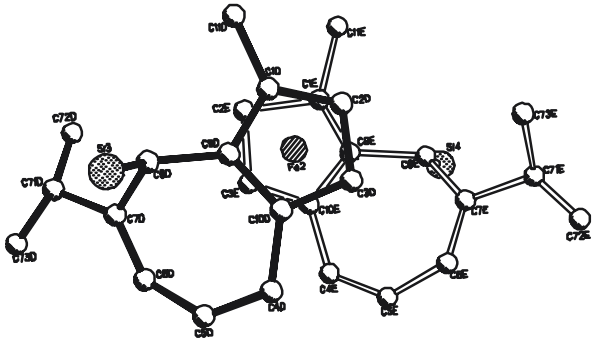

7_B **(**RR**,** τ = -102.0°; τ_{Cp}= 27.3° **)**

On the contrary to compound **6**, in compound **7** the top view of the enantiomers showed that the anti-conformations[I] are adopted for the stable conformers in solid states for the three unique molecules, in which two 1-methyl groups and two seven-membered rings in a molecule stretch in opposite directions. To understand this conformation difference for compounds **6** and **7**, the conformation analysis is helpful.

[I] anti-conformation: C1-C101 in one guaiazulene moiety and $C'_{5(cent.)}$-C6′ in another guaiazulene moiety within one molecule stretch in opposite direction; The same is true for C1′-C101′ and $C_{5(cent.)}$-C6

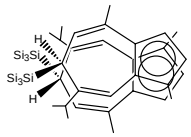

a1:SS, overlap, 0^o

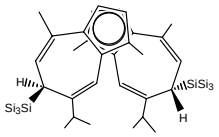

a2: SS, -90^o

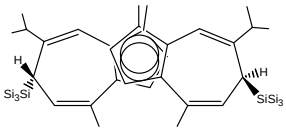

a3: SS,-180^o

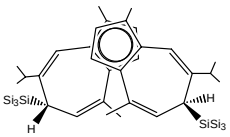

a4: SS, -270^o or $+90^o$

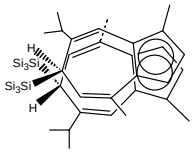

b1: RR, overlap

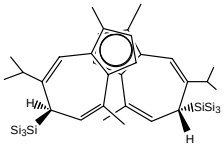

b2: RR, -90^o

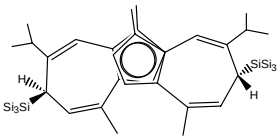

b3: RR, -180^o

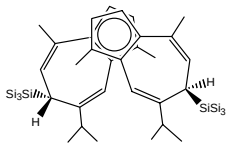

b4: RR, -270^o or $+90^o$

For compound **6**, the conformation of **a2** for (S,S)-, and **b4** for (R,R)-configuration are the most stable conformations in solid states, which are consistent with that found by X-ray diffraction analysis.

In compound **7** the hypersilyl group is bonded with C8. Owing to its large steric hindrance, conformation **a2´** for (S,S)- and **b4´** for (R,R)- are not stable conformations any more, instead, **a4´** and **b2´** are the most stable conformations in solid state for (S,S)- and (R,R)-configuration, respectively. This is consistent with the finding of the X-ray diffraction experiment.

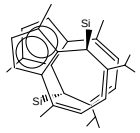

a1´:SS, overlap, 0^o

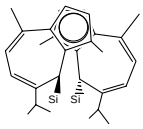

a2´: SS, 90^o

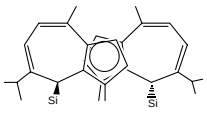

a3´: SS, -180^o

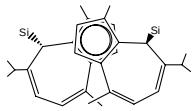

a4´: SS, -270^o or $+90^o$

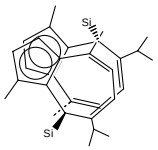

b1´: RR, overlap

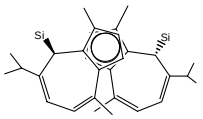

b2´: RR, -90^o

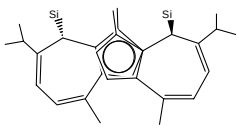

b3´: RR, -180^o

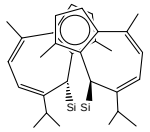

b4´: RR, -270^o or $+90^o$

SiH_4

The reaction of **2** with $TiCl_3$ can take place either in toluene or in tetrahydrofuran. In toluene the ligand is oxidized to compound **9**, whereas in tetrahydrofuran the metal cation Ti(III) is oxidized to Ti(IV). Both of these processes imply that the probable intermediate Ti(6-Hyp-Hgual)$_2$Cl is not stable, but would react further to give the final product, either (3-Hyp-6-Hgua)$_2$ (**9**) or Ti(6-Hyp-Hgual)$_2$Cl$_2$ (**10**), depending on the solvent employed. However, if compound **2** reacts with MCl_4 (M=Zr(IV), Hf(IV)) or with ZrCp*Cl_3 either in THF or in

toluene, three metallocene dichlorides Zr(6-Hyp-Hgual)$_2$Cl$_2$ (**11**), Hf(6-Hyp-Hgual)$_2$Cl$_2$ (**12**) and ZrCp*(6-Hyp-Hgual)Cl$_2$·KCl(**13**) are produced. The molecular structure of **13** could not be determined sofar.

The X-ray diffraction analysis revealed that the isolated crystals of the series of compounds **10**, **11** and **12** only contain the appropriate rac-diastereomer. An interesting observation is that in the NMR spectra of **10** and **12** recorded on the crystals only the signals of the pair of rac-diastereomer appear, indicating that from toluene the two diastereomers can be well separated, and the rac-diastereomer crystallizes more easily. In compound **11**, however, for non-obvious reasons, two diastereomers were detected, and by fractional recrystallization the rac-diastereomer can be at least partly separated from the meso-diastereomer.

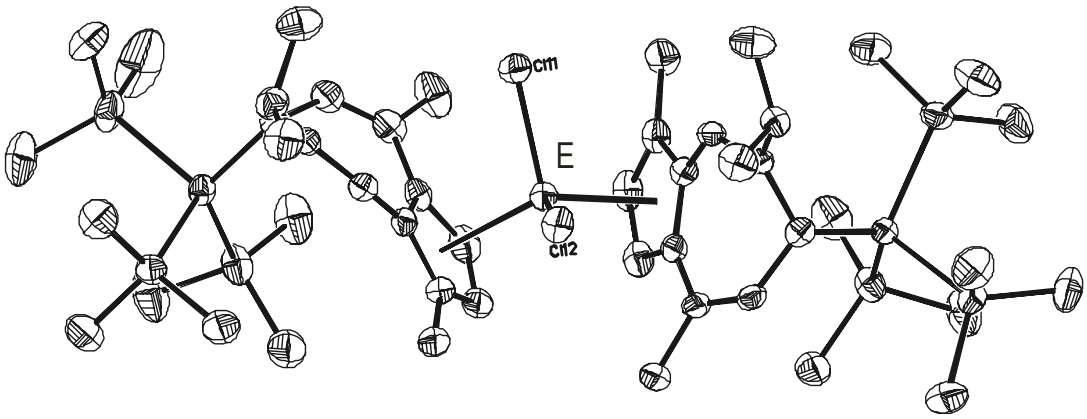

E=Ti(**10**), Zr(**11**), Hf(**12**)

Similar to the corresponding metallocene derivatives **5**, **6** and **8**, in all of the three metallocene dichlorides **10**, **11** and **12**, the two guaiazulene frameworks are also staggered, and in solid state the syn-conformation is adopted. The projection to the Cl-M-Cl plane shows that the two methyl groups bonded to C1 and C11, the two chloride anions, and the two non-chloro ligands are orientated almost along the same direction. The conformer analysis leads to the same conclusion.

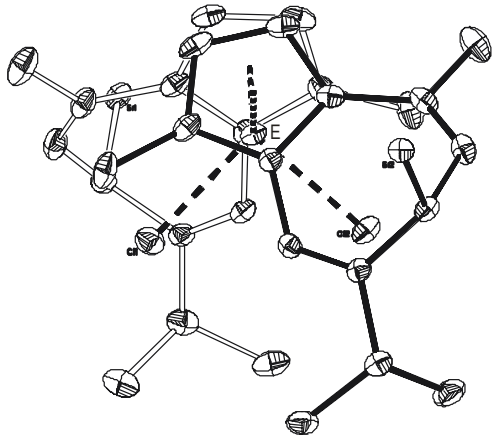

E=Ti, **10**(τ = -137.2°, τ_{Cp}=15.7°)
E=Zr, **11**(τ = -138.2°, τ_{Cp}=14.3°)
E=Hf, **12**(τ = -140.7, τ_{Cp}=12.2°)

In the syn-conformers of compounds **10**, **11** and **12**, owing to the presence of two chloride anions, the two methyl groups bonded with C1 and C1´ are staggered farther away from each other than for **5**, **6** and **8**, and the two seven-membered rings within one molecule staggered also slightly larger than 100°.

Owing to the tetrahedral geometry the two C_5 rings in compounds **10**, **11** and **12** tilt severely with tilt angles ranging from 58.3 to 58.6°, which is consistent with those of reported Ti(8, 8´-bigua)Cl_2 (50.3°) and $(Ind)_2ZrCl_2$ (62.07°). Compare with other metallocene dichloride derivatives reported in literature, all value in the distorted tetrahedral geometries of these three compounds fall into the normal range.

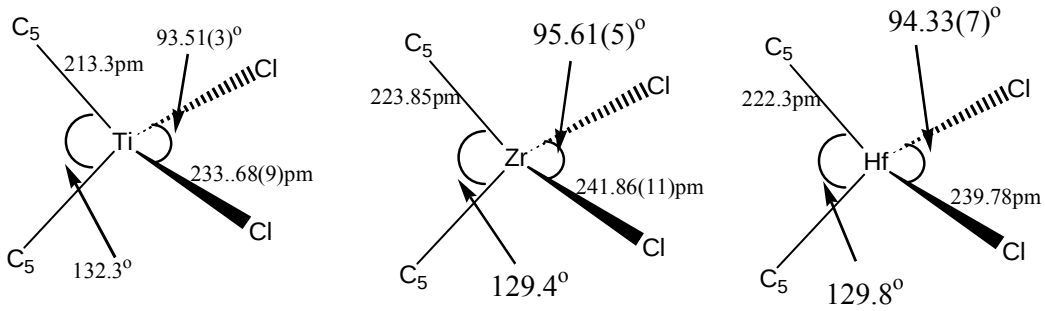

Similar to compounds **1**, **2**, **3** and **4**, the ^{13}C NMR data of **10**, **11**, **12** and **13** indicated that the interactions of M-$C_{5(ring)}$ (M=Ti(IV), Zr(IV) and Hf(IV)) are dominantly ionic.

Finally, in order to check the effect of hypersilyl group at the five-membered ring, a second hypersilyl group was introduced to the five-membered ring.

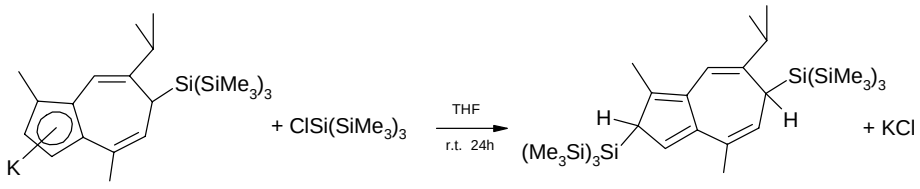

2,6-bis(hyp)-H_2gua **14**

At room temperature the metathesis between compound **2** and chlorohypersilane $ClSi(SiMe_3)_3$ in tetrahydrofuran can take place and gives rise to 2,6-bis(Hyp)-H_2gua (**14**). It was found that in the product the second hypersilyl substituent is bonded to C2 instead of C3. Such

connection can keep two hypersilyl groups far away from each other, so that the steric repulsion between them is drastically reduced.

In compound **14** the two hypersilyl groups stretch away from each other and are located above and below the guaiazulene framework, respectively. The two chiral carbon atoms have the same configuration.

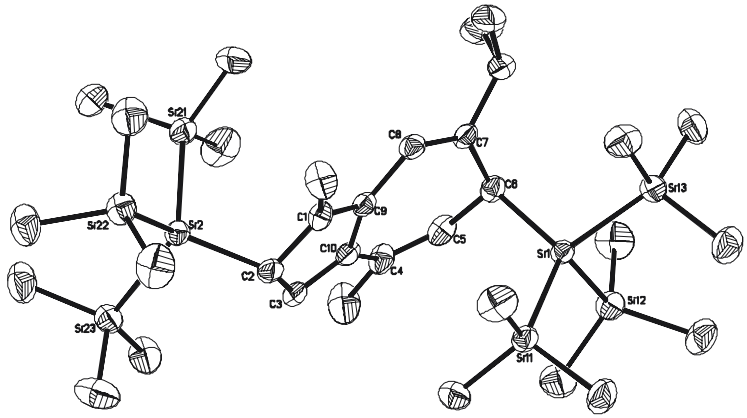

14

In toluene with ^{n}BuLi at 60°C compound **14** can be metallated and give a new kind of aromatic pseudo lithium cyclopentadienide Li(2,6-bis(Hyp)-Hgual) (**15**). X-ray diffraction analysis revealed its dimeric structure.

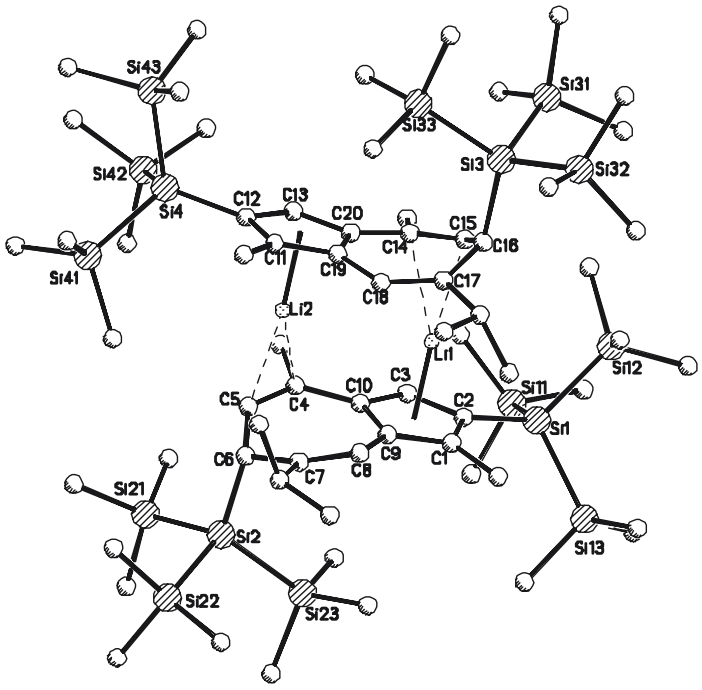

15

Compare to **1**, compound **15** has a staggered and slipped sandwich structure, owing to the existence of the two huge hypersilyl groups in C2 and C2´ position, respectively.

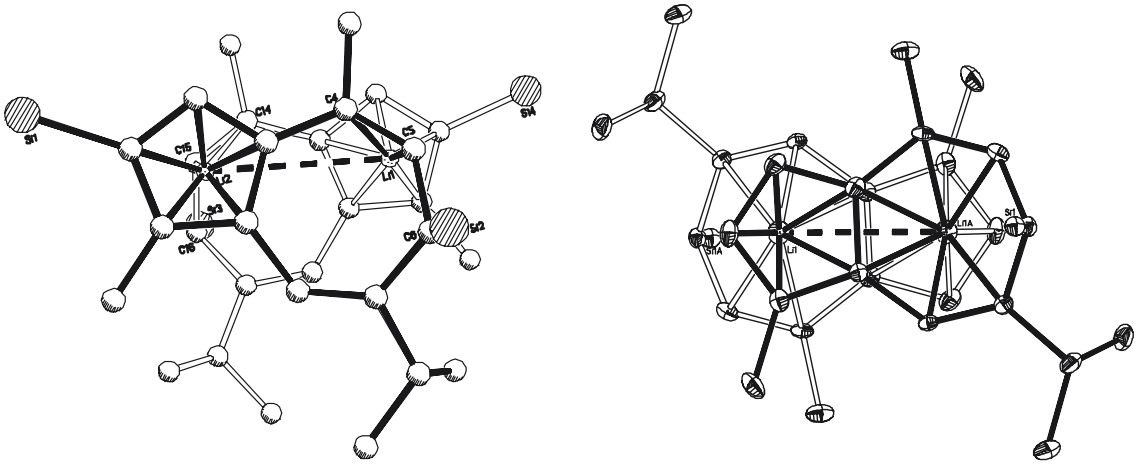

15 **1**

Each lithium cation in **15** is bonded in μ-η^5:η^2-mode to five olefinic carbon atoms from the C_5-ring of one ligand, and two carbon atoms (C4 and C5 or C4´ and C5´) from the seven-membered ring of the second ligand. The Li-Li distance in **15** (339.7(10)pm) is much larger than that for compound **1**(281.5(8)pm). However, the distances of Li1-C5´, and Li2-C5 in **15** are about 20pm shorter than those in compound **1**, which is consistent with the smaller folding angles of the seven-membered ring in compound **15** compared to those in **1**.

Compound	**1**	**15**
Li1-C15 (pm)	262.6(4)	244.5(8)
Folding angles		
α(°)	2.0	1.5
β(°)	19.8	6.2
γ(°)	39.9	30.3

Here, the folding angle α means the dihedral angle between the C_5-ring and the best plane through the atoms C9, C10, C4, C8; the folding angle β means the dihedral angle between the best plane through C9, C10, C4, C8 and the best plane through C4, C8, C5, C7; and the folding angle γ is the dihedral angle between the best plane through C4, C8, C5, C7 and the plane through C5, C6, C7.

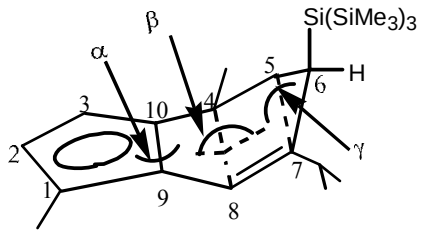

The introduction of a second hypersilyl group to the C_5-ring changed the chemical properties of the compound **15** greatly. Compare to complex **1**, complex **15** is extremely air- and moisture sensitive. The former is a good precursor for synthesis of metallocene derivatives, whereas the latter in our hands, did not lead to isolable complexes sofar. We have also examined whether a third hypersilyl group could be introduced to the guaiazulene moiety, but were not successful to date.

5 Appendix

5.1 Crystallographic data for Li(6-Hyp-Hgual)

5.1.1 Crystallographic data and structure refinement for Li(6-Hyp-Hgual)

Empirical formula	$C_{24}H_{45}LiSi_4$
Formula weight (g/mol)	452.90
Temperature (K)	173(2)
Wavelength(Å)	0.71073
Crystal system, space group	monoclinic, $P2_1/c$
Unit cell dimensions (Å ,deg)	a=18.878(4) α=90 b=9.870(2) β=103.24(3) c=15.866(3) γ=90
Volume ($Å^3$)	2881.3(10)
Z; calc. density (Mg/m^3)	4; 1.044
Absorption coefficient (mm^{-1})	0.215
F(000)	992
Theta range for data collection (deg)	2.22 ~ 27.51
Limiting indices	-24≤h≤23,-12≤k≤12,-20≤l≤20
Reflections collected / unique	13318 / 6623[R(int)=0.0647]
Completeness to θ	27.51; 100%
Refinement method	full-matrix least-squares on F^2
Data / restraints / parameters	6623 / 0 / 442
(Goodness-of-fit on F^2)	1.027
Final R indices [I>2σ(I)]	R1=0.0501,wR2=0.1047
R indices (all data)	R1=0.0952, wR2=0.1238
Largest diff. peak and hole ($e.Å^{-3}$)	0.298 und –0.272

5.1.2 Atomic coordinates ($\times 10^4$) and equivalent isotropic displacement parameters ($A^2 \times 10^3$) for Li(6-Hyp-Hgual), U(eq) is defined as one third of the trace of the orthogonalized U_{ij} tensor.

atom	x/a	y/b	z/c	U(eq)	atom	x/a	y/b	z/c	U(eq)
Li(1)	-339(2)	6013(4)	392(3)	29(1)	C(122)	2352(2)	4120(5)	2972(2)	54(1)
C(2)	427(1)	7178(3)	1374(2)	29(1)	C(123)	2422(2)	7032(4)	2317(2)	51(1)
C(3)	645(1)	7346(2)	591(2)	26(1)	Si(13)	3764(1)	2677(1)	1229(1)	37(1)
C(10)	924(1)	6091(2)	373(1)	22(1)	C(131)	3659(2)	1623(4)	227(3)	61(1)
C(4)	1202(1)	5821(2)	-397(1)	22(1)	C(132)	4719(2)	3343(4)	1484(4)	63(1)
C(41)	983(1)	6813(3)	-1136(2)	31(1)	C(133)	3682(2)	1532(4)	2144(3)	65(1)
C(5)	1650(1)	4785(2)	-470(2)	24(1)	C(7)	1530(1)	3060(2)	696(1)	21(1)
C(6)	2022(1)	3784(2)	210(1)	21(1)	C(71)	1646(1)	1525(2)	764(2)	28(1)
Si(1)	2912(1)	4485(1)	995(1)	23(1)	C(711)	1323(2)	844(3)	-107(2)	35(1)
Si(11)	3407(1)	6214(1)	269(1)	34(1)	C(712)	1362(2)	831(3)	1480(2)	42(1)
C(111)	2803(2)	7744(3)	55(3)	52(1)	C(8)	1045(1)	3693(2)	1065(1)	20(1)
C(112)	4309(2)	6852(5)	911(3)	64(1)	C(9)	860(1)	5135(2)	1034(1)	20(1)
C(113)	3541(2)	5528(5)	-785(3)	59(1)	C(1)	541(1)	5823(2)	1644(2)	25(1)
Si(12)	2837(1)	5299(1)	2368(1)	35(1)	C(101)	394(2)	5244(3)	2464(2)	35(1)
C(121)	3800(2)	5402(5)	3025(2)	51(1)					

5.1.3 Bond lengths [Å] for Li(6-Hyp-Hgual)

Bonds	Bond lengths	Bonds	Bond lengths	Bonds	Bond lengths
Li(1)-C(2)	2.194(5)	C(10)-C(4)	1.462(3)	Si(12)-C(123)	1.876(4)
Li(1)-C(3)	2.239(4)	C(10)-Li(1)#1	2.528(5)	Si(12)-C(121)	1.881(3)
Li(1)-C(1)	2.289(5)	C(4)-C(5)	1.349(3)	Si(13)-C(132)	1.874(3)
Li(1)-C(10)	2.393(4)	C(4)-C(41)	1.511(3)	Si(13)-C(131)	1.875(4)
Li(1)-C(8)#1	2.409(5)	C(4)-Li(1)#1	2.437(5)	Si(13)-C(133)	1.874(4)
Li(1)-C(9)	2.421(4)	C(5)-C(6)	1.513(3)	C(7)-C(8)	1.348(3)
Li(1)-C(4)#1	2.437(5)	C(5)-Li(1)#1	2.626(4)	C(7)-C(71)	1.530(3)
Li(1)-C(9)#1	2.522(5)	C(6)-C(7)	1.516(3)	C(7)-Li(1)#1	2.664(4)
Li(1)-C(10)#1	2.528(5)	C(6)-Si(1)	1.974(2)	C(71)-C(712)	1.527(4)
Li(1)-C(5)#1	2.626(4)	Si(1)-Si(12)	2.3593(10)	C(71)-C(711)	1.534(4)
Li(1)-C(7)#1	2.664(4)	Si(1)-Si(11)	2.3682(10)	C(8)-C(9)	1.464(3)
Li(1)-Li(1)#1	2.815(8)	Si(1)-Si(13)	2.3737(10)	C(8)-Li(1)#1	2.409(5)
C(2)-C(1)	1.406(3)	Si(11)-C(113)	1.876(4)	C(9)-C(1)	1.426(3)
C(2)-C(3)	1.408(4)	Si(11)-C(111)	1.877(3)	C(9)-Li(1)#1	2.522(5)
C(3)-C(10)	1.419(3)	Si(11)-C(112)	1.881(3)	C(1)-C(101)	1.504(3)
C(10)-C(9)	1.436(3)	Si(12)-C(122)	1.874(4)		

5.1.4 Bonds angles for Li(6-Hyp-Hgual) (deg)

Bond angle	parameter	Bond angle	parameter	Bond angle	parameter
C(2)-Li(1)-C(3)	37.02(11)	C(8)#1-Li(1)-C(7)#1	30.29(9)	C(6)-Si(1)-Si(13)	106.49(8)
C(2)-Li(1)-C(1)	36.47(11)	C(9)-Li(1)-C(7)#1	164.8(2)	Si(12)-Si(1)-Si(13)	107.03(4)
C(3)-Li(1)-C(1)	60.79(13)	C(4)#1-Li(1)-C(7)#1	78.01(13)	Si(11)-Si(1)-Si(13)	106.81(4)
C(2)-Li(1)-C(10)	59.73(13)	C(9)#1-Li(1)-C(7)#1	58.28(11)	C(113)-Si(11)-C(111)	109.2(2)
C(3)-Li(1)-C(10)	35.48(10)	C(10)#1-Li(1)-C(7)#1	76.11(13)	C(113)-Si(11)-C(112)	108.3(2)
C(1)-Li(1)-C(10)	59.12(12)	C(5)#1-Li(1)-C(7)#1	57.98(11)	C(111)-Si(11)-C(112)	105.41(19)
C(2)-Li(1)-C(8)#1	138.6(2)	C(2)-Li(1)-Li(1)#1	113.2(2)	C(113)-Si(11)-Si(1)	108.88(14)
C(3)-Li(1)-C(8)#1	108.85(19)	C(3)-Li(1)-Li(1)#1	91.9(2)	C(111)-Si(11)-Si(1)	112.10(12)
C(1)-Li(1)-C(8)#1	167.6(2)	C(1)-Li(1)-Li(1)#1	90.8(2)	C(112)-Si(11)-Si(1)	112.75(13)
C(10)-Li(1)-C(8)#1	108.50(18)	C(10)-Li(1)-Li(1)#1	57.40(14)	C(122)-Si(12)-C(123)	109.9(2)
C(2)-Li(1)-C(9)	59.16(12)	C(8)#1-Li(1)-Li(1)#1	82.41(19)	C(122)-Si(12)-C(121)	105.83(17)
C(3)-Li(1)-C(9)	58.98(12)	C(9)-Li(1)-Li(1)#1	57.01(14)	C(123)-Si(12)-C(121)	108.38(18)
C(1)-Li(1)-C(9)	35.11(9)	C(4)#1-Li(1)-Li(1)#1	81.14(19)	C(122)-Si(12)-Si(1)	113.68(13)
C(10)-Li(1)-C(9)	34.72(9)	C(9)#1-Li(1)-Li(1)#1	53.61(14)	C(123)-Si(12)-Si(1)	112.56(13)
C(8)#1-Li(1)-C(9)	134.89(19)	C(10)#1-Li(1)-Li(1)#1	52.88(14)	C(121)-Si(12)-Si(1)	106.04(12)
C(2)-Li(1)-C(4)#1	136.0(2)	C(5)#1-Li(1)-Li(1)#1	109.7(2)	C(132)-Si(13)-C(131)	106.6(2)
C(3)-Li(1)-C(4)#1	165.9(2)	C(7)#1-Li(1)-Li(1)#1	111.0(2)	C(132)-Si(13)-C(133)	106.9(2)
C(1)-Li(1)-C(4)#1	106.78(18)	C(1)-C(2)-C(3)	109.1(2)	C(131)-Si(13)-C(133)	108.2(2)
C(10)-Li(1)-C(4)#1	133.8(2)	C(1)-C(2)-Li(1)	75.45(18)	C(132)-Si(13)-Si(1)	110.73(13)
C(8)#1-Li(1)-C(4)#1	82.52(14)	C(3)-C(2)-Li(1)	73.24(17)	C(131)-Si(13)-Si(1)	110.38(13)
C(9)-Li(1)-C(4)#1	107.11(18)	C(2)-C(3)-C(10)	108.2(2)	C(133)-Si(13)-Si(1)	113.71(15)
C(2)-Li(1)-C(9)#1	158.8(2)	C(2)-C(3)-Li(1)	69.75(17)	C(8)-C(7)-C(6)	123.9(2)
C(3)-Li(1)-C(9)#1	122.06(19)	C(10)-C(3)-Li(1)	78.18(16)	C(8)-C(7)-C(71)	122.0(2)
C(1)-Li(1)-C(9)#1	143.1(2)	C(3)-C(10)-C(9)	107.3(2)	C(6)-C(7)-C(71)	114.06(19)
C(10)-Li(1)-C(9)#1	100.82(16)	C(3)-C(10)-C(4)	125.9(2)	C(8)-C(7)-Li(1)#1	64.32(15)
C(8)#1-Li(1)-C(9)#1	34.43(9)	C(9)-C(10)-C(4)	126.8(2)	C(6)-C(7)-Li(1)#1	91.81(15)
C(9)-Li(1)-C(9)#1	110.62(17)	C(3)-C(10)-Li(1)	66.34(16)	C(71)-C(7)-Li(1)#1	118.16(17)
C(4)#1-Li(1)-C(9)#1	62.98(12)	C(9)-C(10)-Li(1)	73.72(15)	C(712)-C(71)-C(7)	115.3(2)
C(2)-Li(1)-C(10)#1	156.4(2)	C(4)-C(10)-Li(1)	123.71(18)	C(712)-C(71)-C(711)	109.9(2)
C(3)-Li(1)-C(10)#1	143.8(2)	C(3)-C(10)-Li(1)#1	133.53(17)	C(7)-C(71)-C(711)	110.4(2)
C(1)-Li(1)-C(10)#1	120.03(19)	C(9)-C(10)-Li(1)#1	73.27(15)	C(7)-C(8)-C(9)	128.1(2)
C(10)-Li(1)-C(10)#1	110.28(17)	C(4)-C(10)-Li(1)#1	69.47(15)	C(7)-C(8)-Li(1)#1	85.39(17)
C(8)#1-Li(1)-C(10)#1	63.43(12)	Li(1)-C(10)-Li(1)#1	69.72(17)	C(9)-C(8)-Li(1)#1	77.04(16)
C(9)-Li(1)-C(10)#1	99.89(16)	C(5)-C(4)-C(10)	124.2(2)	C(1)-C(9)-C(10)	107.69(19)
C(4)#1-Li(1)-C(10)#1	34.20(9)	C(5)-C(4)-C(41)	119.4(2)	C(1)-C(9)-C(8)	125.1(2)
C(9)#1-Li(1)-C(10)#1	33.05(9)	C(10)-C(4)-C(41)	116.4(2)	C(10)-C(9)-C(8)	127.1(2)
C(2)-Li(1)-C(5)#1	126.75(19)	C(5)-C(4)-Li(1)#1	82.50(17)	C(1)-C(9)-Li(1)	67.38(15)
C(3)-Li(1)-C(5)#1	158.4(2)	C(10)-C(4)-Li(1)#1	76.33(15)	C(10)-C(9)-Li(1)	71.56(15)
C(1)-Li(1)-C(5)#1	116.01(18)	C(41)-C(4)-Li(1)#1	114.80(18)	C(8)-C(9)-Li(1)	123.68(17)
C(10)-Li(1)-C(5)#1	164.2(2)	C(4)-C(5)-C(6)	129.2(2)	C(1)-C(9)-Li(1)#1	133.31(17)
C(8)#1-Li(1)-C(5)#1	76.22(13)	C(4)-C(5)-Li(1)#1	66.89(15)	C(10)-C(9)-Li(1)#1	73.69(15)

C(9)-Li(1)-C(5)#1	132.32(19)	C(6)-C(5)-Li(1)#1	93.36(16)	C(8)-C(9)-Li(1)#1	68.53(15)
C(4)#1-Li(1)-C(5)#1	30.60(9)	C(5)-C(6)-C(7)	115.69(18)	Li(1)-C(9)-Li(1)#1	69.38(17)
C(9)#1-Li(1)-C(5)#1	74.32(13)	C(5)-C(6)-Si(1)	114.28(15)	C(2)-C(1)-C(9)	107.7(2)
C(10)#1-Li(1)-C(5)#1	57.60(11)	C(7)-C(6)-Si(1)	112.06(15)	C(2)-C(1)-C(101)	125.4(2)
C(2)-Li(1)-C(7)#1	127.0(2)	C(6)-Si(1)-Si(12)	118.72(7)	C(9)-C(1)-C(101)	126.8(2)
C(3)-Li(1)-C(7)#1	116.05(19)	C(6)-Si(1)-Si(11)	108.58(7)	C(2)-C(1)-Li(1)	68.08(17)
C(1)-Li(1)-C(7)#1	158.2(2)	Si(12)-Si(1)-Si(11)	108.61(4)	C(9)-C(1)-Li(1)	77.51(16)
C(10)-Li(1)-C(7)#1	132.51(19)	C(101)-C(1)-Li(1)	122.8(2)		

5.1.5 Anisotropic displacement parameters ($A^2 \times 10^3$) for Li(6-Hyp-Hgual). The anisotropic displacement factor exponent takes the form:

$-2\pi^2[h^2a^{*2}U11 + ... + 2hka^*b^*U12]$

atom	U11	U22	U33	U23	U13	U12
Li(1)	22(2)	33(2)	29(2)	-2(2)	4(2)	-1(2)
C(2)	26(1)	26(1)	34(1)	-11(1)	7(1)	0(1)
C(3)	23(1)	20(1)	35(1)	1(1)	4(1)	-3(1)
C(10)	17(1)	21(1)	26(1)	-2(1)	4(1)	-5(1)
C(4)	18(1)	23(1)	24(1)	3(1)	5(1)	-6(1)
C(41)	26(1)	36(2)	28(1)	9(1)	3(1)	-2(1)
C(5)	21(1)	30(1)	21(1)	1(1)	7(1)	-4(1)
C(6)	18(1)	22(1)	25(1)	-2(1)	7(1)	0(1)
Si(1)	17(1)	26(1)	24(1)	0(1)	4(1)	-2(1)
Si(11)	25(1)	35(1)	41(1)	9(1)	7(1)	-6(1)
C(111)	46(2)	33(2)	71(2)	12(2)	5(2)	-4(1)
C(112)	39(2)	62(2)	82(3)	21(2)	-4(2)	-21(2)
C(113)	58(2)	70(3)	57(2)	12(2)	32(2)	-3(2)
Si(12)	27(1)	52(1)	26(1)	-9(1)	5(1)	-10(1)
C(121)	37(2)	76(3)	36(2)	-11(2)	3(1)	-16(2)
C(122)	39(2)	91(3)	29(2)	1(2)	4(1)	-17(2)
C(123)	40(2)	62(2)	51(2)	-27(2)	7(2)	-3(2)
Si(13)	25(1)	35(1)	47(1)	7(1)	2(1)	6(1)
C(131)	56(2)	49(2)	79(3)	-13(2)	16(2)	17(2)
C(132)	23(1)	58(2)	100(3)	7(2)	3(2)	8(1)
C(133)	55(2)	56(2)	73(3)	29(2)	-4(2)	1(2)
C(7)	22(1)	18(1)	23(1)	0(1)	2(1)	-3(1)
C(71)	25(1)	21(1)	39(1)	4(1)	9(1)	2(1)
C(711)	42(2)	22(1)	47(2)	-6(1)	17(1)	0(1)
C(712)	60(2)	24(1)	47(2)	10(1)	20(2)	0(1)
C(8)	18(1)	22(1)	20(1)	1(1)	3(1)	-4(1)
C(9)	16(1)	21(1)	22(1)	-1(1)	3(1)	-3(1)
C(1)	20(1)	29(1)	25(1)	-7(1)	6(1)	-4(1)
C(101)	42(2)	42(2)	26(1)	-7(1)	16(1)	-2(1)

5.2 Crystallographic data for $(thf)_4$·[K(6-Hyp-Hgual)]

5.2.1 Crystallographic data and structure refinement for $(thf)_4$K(6-Hyp-Hgual)

Empirical formula	$C_{40}H_{77}KO_4Si_4$
Formula weight (g/mol)	773.49
Temperature (K)	173(2)
Wavelength(Å)	0.71073
Crystal system, space group	Monoclinic, $P2_1/n$
Unit cell dimensions (Å ,deg)	A=9.9317(14) b=22.913(2) c=20.6591(19) β=95.766(9)
Volume ($Å^3$)	4677.5(9)
Z; calc. density (Mg/m^3)	8; 1.098
Absorption coefficient (mm^{-1})	0.250
F(000)	1696

Theta range for data collection (deg)	1.78 ~28.01
Limiting indices	-13≤h≤12,-4≤k≤30,-27≤l≤27
Reflections collected / unique	11770 / 11153[R(int)=0.0628]
Completeness to θ	28.01; 98.8%
Refinement method	full-matrix least-squares on F^2
Data / restraints / parameters	11153 /117 / 526
(Goodness-of-fit on F^2)	0.801
Final R indices [I>2σ(I)]	R1=0,0522, wR2=0,1181
R indices (all data)	R1=0.1189, wR2=0.1338
Largest diff. peak and hole (e.$Å^{-3}$)	0.303 und –0.245

5.2.2 Atomic coordinates ($\times 10^4$) and equivalent isotropic displacement parameters ($A^2 \times 10^3$) for $(thf)_4K(6\text{-Hyp-Hgual})$, U(eq) is defined as one third of the trace of the orthogonalized Uij tensor.

atom	x/a	y/b	z/c	U(eq)	atom	x/a	y/b	z/c	U(eq)
K(1)	3177(1)	328(1)	8123(1)	36(1)	O(2)	890(2)	812(1)	7442(1)	50(1)
Si(1)	4331(1)	3085(1)	8999(1)	28(1)	C(21)	1156(4)	1319(2)	7081(2)	64(1)
Si(11)	5023(1)	3979(1)	8569(1)	38(1)	C(22)	-41(4)	1710(2)	7102(2)	73(1)
C(111)	5304(4)	4579(1)	9185(2)	63(1)	C(23)	-1149(4)	1322(2)	7257(2)	84(1)
C(112)	6636(3)	3903(2)	8183(2)	58(1)	C(24)	-534(3)	754(2)	7415(2)	76(1)
C(113)	3707(3)	4259(1)	7934(2)	54(1)	O(3)	4754(3)	-684(1)	8189(1)	72(1)
Si(12)	6273(1)	2709(1)	9599(1)	42(1)	C(31)	5695(5)	-810(2)	8736(2)	82(1)
C(121)	5883(4)	2132(1)	10182(2)	59(1)	C(32)	6525(4)	-1298(2)	8562(2)	81(1)
C(122)	7571(3)	2444(2)	9080(2)	60(1)	C(33)	5625(4)	-1611(2)	8066(2)	81(1)
C(123)	7103(3)	3327(1)	10096(2)	59(1)	C(34)	4664(5)	-1186(2)	7797(3)	118(2)
Si(13)	2693(1)	3302(1)	9712(1)	44(1)	O(1)	4163(3)	319(1)	6904(1)	73(1)
C(131)	3309(4)	3865(2)	10329(2)	81(1)	C(11)	3629(5)	514(2)	6295(2)	97(2)
C(132)	2195(4)	2662(2)	10192(2)	76(1)	C(12)	4571(5)	377(2)	5822(2)	109(2)
C(133)	1122(4)	3598(2)	9256(2)	74(1)	C(13)	5742(4)	101(2)	6203(2)	85(1)
C(2)	4900(3)	714(1)	9368(2)	42(1)	C(14)	5538(4)	257(3)	6868(2)	106(2)
C(3)	3658(3)	979(1)	9415(2)	41(1)	O(4)	1398(9)	-335(3)	8753(5)	70(2)
C(10)	3501(3)	1439(1)	8955(1)	32(1)	C(41)	49(5)	-440(3)	8758(3)	94(2)
C(4)	2281(3)	1783(1)	8795(1)	35(1)	C(42)	-136(6)	-849(4)	9281(4)	115(3)
C(40)	979(4)	1535(2)	9003(2)	55(1)	C(43)	1172(5)	-896(4)	9669(3)	93(2)
C(5)	2255(3)	2292(1)	8483(1)	34(1)	C(44)	2121(5)	-638(4)	9265(3)	109(3)
C(6)	3423(3)	2638(1)	8280(1)	27(1)	O(4)	1480(50)	-333(15)	8780(30)	82(10)
C(7)	4382(3)	2316(1)	7881(1)	27(1)	C(41A)	560(30)	-112(9)	9164(14)	97(8)
C(71)	4675(3)	2619(1)	7257(1)	33(1)	C(42A)	360(30)	-539(8)	9660(12)	83(7)
C(711)	3488(4)	2561(2)	6733(1)	56(1)	C(43A)	650(30)	-1109(8)	9355(14)	69(7)
C(712)	5975(4)	2434(2)	6992(2)	54(1)	C(44A)	1630(30)	-932(11)	8925(15)	106(8)
C(8)	4925(3)	1799(1)	8062(1)	28(1)	C(1)	5544(3)	986(1)	8879(1)	34(1)
C(9)	4681(3)	1441(1)	8616(1)	28(1)	C(101)	6887(3)	820(2)	8665(2)	47(1)

5.2.3 Bond lengths for $(thf)_4K(6\text{-Hyp-Hgual})$ [Å]

Bond	Bond Lengths	Bond	Bond Lengths	Bond	Bond Lengths
K(1)-O(4)	2.73(3)	Si(1)-Si(11)	2.3618(11)	C(10)-C(4)	1.456(4)
K(1)-O(4)	2.754(5)	Si(11)-C(112)	1.868(3)	C(4)-C(5)	1.331(4)
K(1)-O(2)	2.780(2)	Si(11)-C(113)	1.870(3)	C(4)-C(40)	1.514(4)
K(1)-O(1)	2.793(2)	Si(11)-C(111)	1.874(3)	C(5)-C(6)	1.500(4)
K(1)-O(3)	2.794(2)	Si(12)-C(121)	1.855(3)	C(6)-C(7)	1.514(4)
K(1)-C(3)	3.052(3)	Si(12)-C(122)	1.859(3)	C(7)-C(8)	1.338(3)
K(1)-C(10)	3.070(3)	Si(12)-C(123)	1.889(3)	C(7)-C(71)	1.517(3)
K(1)-C(2)	3.073(3)	Si(13)-C(132)	1.864(4)	C(71)-C(712)	1.513(4)
K(1)-C(9)	3.076(3)	Si(13)-C(133)	1.867(4)	C(71)-C(711)	1.524(4)
K(1)-C(1)	3.082(3)	Si(13)-C(131)	1.873(4)	C(8)-C(9)	1.449(3)
K(1)-C(44)	3.474(5)	C(2)-C(3)	1.387(4)	C(9)-C(1)	1.423(4)
Si(1)-C(6)	1.949(3)	C(2)-C(1)	1.395(4)	C(1)-C(101)	1.496(4)
Si(1)-Si(12)	2.3492(11)	C(3)-C(10)	1.416(4)		
Si(1)-Si(13)	2.3547(11)	C(10)-C(9)	1.424(3)		

5.2.4 Bond Angles for $(thf)_4$ K(6-Hyp-Hgual) (deg)

Bond angle	parameter	Bond angle	parameter	Bond angle	parameter
O(4)-K(1)-O(4)	1.8(17)	O(3)-K(1)-C(1)	89.17(8)	C(3)-C(2)-C(1)	109.3(3)
O(4)-K(1)-O(2)	87.6(11)	C(3)-K(1)-C(1)	43.43(8)	C(3)-C(2)-K(1)	76.10(18)
O(4)-K(1)-O(2)	85.9(2)	C(10)-K(1)-C(1)	43.89(7)	C(1)-C(2)-K(1)	77.26(17)
O(4)-K(1)-O(1)	137.2(13)	C(2)-K(1)-C(1)	26.20(7)	C(2)-C(3)-C(10)	108.5(3)
O(4)-K(1)-O(1)	136.2(3)	C(9)-K(1)-C(1)	26.72(7)	C(2)-C(3)-K(1)	77.73(18)
O(2)-K(1)-O(1)	83.65(7)	O(4)-K(1)-C(44)	20.7(12)	C(10)-C(3)-K(1)	77.31(16)
O(4)-K(1)-O(3)	83.4(6)	O(4)-K(1)-C(44)	22.4(2)	C(3)-C(10)-C(9)	107.0(2)
O(4)-K(1)-O(3)	84.37(14)	O(2)-K(1)-C(44)	108.11(10)	C(3)-C(10)-C(4)	126.1(3)
O(2)-K(1)-O(3)	141.39(7)	O(1)-K(1)-C(44)	139.92(17)	C(9)-C(10)-C(4)	126.4(2)
O(1)-K(1)-O(3)	78.03(8)	O(3)-K(1)-C(44)	69.12(14)	C(3)-C(10)-K(1)	75.95(16)
O(4)-K(1)-C(3)	83.6(14)	C(3)-K(1)-C(44)	75.47(16)	C(9)-C(10)-K(1)	76.88(14)
O(4)-K(1)-C(3)	84.7(3)	C(10)-K(1)-C(44)	99.77(16)	C(4)-C(10)-K(1)	106.49(16)
O(2)-K(1)-C(3)	107.20(8)	C(2)-K(1)-C(44)	78.21(14)	C(5)-C(4)-C(10)	124.0(3)
O(1)-K(1)-C(3)	138.92(9)	C(9)-K(1)-C(44)	118.22(15)	C(5)-C(4)-C(40)	119.5(3)
O(3)-K(1)-C(3)	108.96(9)	C(1)-K(1)-C(44)	103.55(13)	C(10)-C(4)-C(40)	116.5(3)
O(4)-K(1)-C(10)	102.6(11)	C(6)-Si(1)-Si(12)	120.14(9)	C(4)-C(5)-C(6)	128.4(3)
O(4)-K(1)-C(10)	103.2(2)	C(6)-Si(1)-Si(13)	106.96(9)	C(5)-C(6)-C(7)	116.1(2)
O(2)-K(1)-C(10)	89.27(7)	Si(12)-Si(1)-Si(13)	109.25(4)	C(5)-C(6)-Si(1)	112.17(18)
O(1)-K(1)-C(10)	118.99(8)	C(6)-Si(1)-Si(11)	107.36(9)	C(7)-C(6)-Si(1)	113.81(17)
O(3)-K(1)-C(10)	129.33(8)	Si(12)-Si(1)-Si(11)	105.18(4)	C(8)-C(7)-C(6)	122.5(2)
C(3)-K(1)-C(10)	26.74(7)	Si(13)-Si(1)-Si(11)	107.33(4)	C(8)-C(7)-C(71)	122.4(2)
O(4)-K(1)-C(2)	93.7(15)	C(112)-Si(11)-C(113)	107.56(16)	C(6)-C(7)-C(71)	115.1(2)
O(4)-K(1)-C(2)	95.3(3)	C(112)-Si(11)-C(111)	106.36(17)	C(712)-C(71)-C(7)	115.0(2)
O(2)-K(1)-C(2)	131.83(8)	C(113)-Si(11)-C(111)	105.69(16)	C(712)-C(71)-C(711)	110.3(3)
O(1)-K(1)-C(2)	122.73(9)	C(112)-Si(11)-Si(1)	111.98(11)	C(7)-C(71)-C(711)	111.2(2)
O(3)-K(1)-C(2)	86.30(8)	C(113)-Si(11)-Si(1)	110.62(11)	C(7)-C(8)-C(9)	128.9(2)
C(3)-K(1)-C(2)	26.17(8)	C(111)-Si(11)-Si(1)	114.20(12)	C(1)-C(9)-C(10)	107.7(2)
C(10)-K(1)-C(2)	43.48(8)	C(121)-Si(12)-C(122)	110.15(17)	C(1)-C(9)-C(8)	125.0(2)
O(4)-K(1)-C(9)	126.9(13)	C(121)-Si(12)-C(123)	106.80(15)	C(10)-C(9)-C(8)	127.0(2)
O(4)-K(1)-C(9)	127.9(3)	C(122)-Si(12)-C(123)	105.58(16)	C(1)-C(9)-K(1)	76.84(15)
O(2)-K(1)-C(9)	100.49(7)	C(121)-Si(12)-Si(1)	112.93(12)	C(10)-C(9)-K(1)	76.33(14)
O(1)-K(1)-C(9)	95.87(8)	C(122)-Si(12)-Si(1)	113.29(12)	C(8)-C(9)-K(1)	108.76(15)
O(3)-K(1)-C(9)	114.87(8)	C(123)-Si(12)-Si(1)	107.56(11)	C(2)-C(1)-C(9)	107.5(3)
C(3)-K(1)-C(9)	43.72(7)	C(132)-Si(13)-C(133)	107.5(2)	C(2)-C(1)-C(101)	126.1(3)
C(10)-K(1)-C(9)	26.79(7)	C(132)-Si(13)-C(131)	105.41(18)	C(9)-C(1)-C(101)	126.5(3)
C(2)-K(1)-C(9)	43.37(7)	C(133)-Si(13)-C(131)	106.98(19)	C(2)-C(1)-K(1)	76.53(17)
O(4)-K(1)-C(1)	119.9(15)	C(132)-Si(13)-Si(1)	113.82(13)	C(9)-C(1)-K(1)	76.44(15)
O(4)-K(1)-C(1)	121.5(3)	C(133)-Si(13)-Si(1)	110.85(12)	C(101)-C(1)-K(1)	112.6(2)
O(2)-K(1)-C(1)	127.20(7)	C(131)-Si(13)-Si(1)	111.84(13)	C(24)-O(2)-K(1)	138.1(2)
O(1)-K(1)-C(1)	98.15(8)			C(21)-O(2)-K(1)	113.97(19)

5.2.5 Anisotropic displacement parameters (A^2 x 10^3) for $(thf)_4$K(6-Hyp-Hgual). The anisotropic displacement factor exponent takes the form: $-2\pi^2[h^2a^{*2}U11+ ... +2hka^*b^*U12]$

atom	U11	U22	U33	U23	U13	U12
K(1)	36(1)	35(1)	36(1)	1(1)	1(1)	2(1)
Si(1)	33(1)	26(1)	24(1)	-3(1)	-2(1)	1(1)
Si(11)	46(1)	29(1)	38(1)	-1(1)	-3(1)	-7(1)
C(111)	90(3)	35(2)	63(2)	-9(2)	-1(2)	-11(2)
C(112)	53(2)	56(2)	63(2)	0(2)	6(2)	-18(2)
C(113)	63(2)	38(2)	57(2)	13(2)	-7(2)	-6(2)
Si(12)	43(1)	37(1)	41(1)	-4(1)	-17(1)	2(1)
C(121)	71(2)	53(2)	45(2)	8(2)	-26(2)	0(2)
C(122)	35(2)	56(2)	85(3)	-14(2)	-11(2)	2(2)
C(123)	63(2)	51(2)	56(2)	-7(2)	-26(2)	-6(2)
Si(13)	54(1)	44(1)	35(1)	-10(1)	12(1)	2(1)

C(131)	100(3)	86(3)	62(2)	-37(2)	26(2)	-8(3)
C(132)	115(3)	71(3)	48(2)	-2(2)	42(2)	-10(2)
C(133)	59(2)	91(3)	75(3)	-11(2)	18(2)	29(2)
C(2)	56(2)	33(2)	36(2)	8(1)	-3(2)	-2(2)
C(3)	50(2)	42(2)	35(2)	2(1)	12(2)	-13(2)
C(10)	35(2)	33(2)	28(1)	-5(1)	6(1)	-5(1)
C(4)	36(2)	36(2)	35(2)	-12(1)	10(1)	-8(1)
C(40)	44(2)	53(2)	70(3)	-9(2)	22(2)	-11(2)
C(5)	28(2)	40(2)	35(2)	-15(1)	2(1)	2(1)
C(6)	31(1)	27(1)	24(1)	1(1)	-2(1)	3(1)
C(7)	29(1)	28(1)	22(1)	-4(1)	-1(1)	-6(1)
C(71)	44(2)	28(2)	26(1)	3(1)	2(1)	-5(1)
C(711)	74(3)	63(2)	28(2)	10(2)	-9(2)	-15(2)
C(712)	72(2)	49(2)	46(2)	10(2)	29(2)	-2(2)
C(8)	28(1)	29(1)	27(1)	-7(1)	4(1)	-4(1)
C(9)	32(1)	25(1)	27(1)	-3(1)	3(1)	-2(1)
C(1)	38(2)	34(2)	31(1)	1(1)	2(1)	-3(1)
C(101)	42(2)	41(2)	58(2)	8(2)	0(2)	9(2)

5.3 Crystallographic data for 2,6-bis(Hyp)-H_2gua

5.3.1 Crystallographic data and structure refinement for 2,6-bis(Hyp)-H_2gua

Empirical formula	$C_{33}H_{72}Si_8$
Formula weight (g/mol)	693.62
Temperature (K)	173(2)
Wavelength(Å)	0.71073
Crystal system, space group	Monoclinic, $P2_1/c$
Unit cell dimensions (Å ,deg)	A=19.904(3) b=12.529(2) c=18.748(5) β=109.479(14)
Volume ($Å^3$)	4407.9(17)
Z; calc. density (Mg/m^3)	5; 1,045
Absorption coefficient (mm^{-1})	0.264
F(000)	1528
Theta range for data collection (deg)	1.95 ~27.00
Limiting indices	-25≤h≤23,-16≤k≤0, 0≤l≤23
Reflections collected / unique	9799 / 9506[R(int)=0.0527]
Completeness to θ	27.00; 98.9%
Refinement method	full-matrix least-squares on F^2
Data / restraints / parameters	9506 / 0 / 385
(Goodness-of-fit on F^2)	0.857
Final R indices [I>2σ(I)]	R1=0.0441, wR2=0.0975
R indices (all data)	R1=0.0933, wR2=0.1059
Largest diff. peak and hole ($e.Å^{-3}$)	0.421 und –0.230

5.3.2 Atomic coordinates ($\times 10^4$) and equivalent isotropic displacement parameters ($A^2 \times 10^3$) for 2,6-bis(Hyp)-H_2gua. U(eq) is defined as one third of the trace of the orthogonalized Uij tensor.

atom	x/a	y/b	z/c	U(eq)	atom	x/a	y/b	z/c	U(eq)
Si(1)	1365(1)	7358(1)	4212(1)	22(1)	C(133)	1158(2)	4559(2)	4096(2)	47(1)
Si(2)	3378(1)	11720(1)	6859(1)	24(1)	C(122)	-287(2)	8656(3)	3422(2)	51(1)
Si(11)	1137(1)	7407(1)	5362(1)	28(1)	C(232)	1860(2)	13423(3)	6132(2)	44(1)
Si(12)	281(1)	7599(1)	3217(1)	31(1)	C(71)	3191(1)	7748(3)	4076(2)	37(1)
Si(13)	1781(1)	5650(1)	4042(1)	29(1)	C(101)	3731(2)	8951(2)	6912(2)	41(1)
Si(21)	3899(1)	11988(1)	5922(1)	33(1)	C(121)	474(2)	7989(3)	2346(2)	49(1)

Si(22)	4283(1)	11580(1)	8051(1)	35(1)	C(112)	776(2)	8696(3)	5565(2)	43(1)
Si(23)	2681(1)	13190(1)	6968(1)	31(1)	C(211)	4454(2)	13220(3)	6181(2)	54(1)
C(6)	1988(1)	8452(2)	4037(2)	25(1)	C(123)	-260(2)	6345(3)	2988(2)	47(1)
C(7)	2765(1)	8315(2)	4490(1)	25(1)	C(233)	3204(2)	14451(3)	7073(2)	53(1)
C(9)	2804(1)	9387(2)	5642(2)	24(1)	C(231)	2384(2)	12992(3)	7802(2)	56(1)
C(2)	2772(2)	10463(2)	6630(2)	28(1)	C(213)	3222(2)	12208(3)	4970(2)	55(1)
C(10)	2200(1)	10120(2)	5358(2)	25(1)	C(111)	1930(2)	7033(3)	6181(2)	50(1)
C(1)	3122(1)	9560(2)	6390(2)	26(1)	C(222)	4483(2)	12915(3)	8520(2)	51(1)
C(3)	2171(1)	10715(2)	5946(2)	31(1)	C(223)	3993(2)	10686(3)	8686(2)	58(1)
C(8)	3080(1)	8687(2)	5190(2)	27(1)	C(132)	1859(2)	5522(3)	3081(2)	47(1)
C(5)	1647(2)	9514(2)	4035(2)	31(1)	C(41)	1249(2)	11204(3)	4417(2)	51(1)
C(212)	4489(2)	10871(3)	5844(2)	55(1)	C(711)	3923(2)	7354(3)	4564(2)	53(1)
C(113)	426(2)	6389(3)	5270(2)	53(1)	C(712)	3274(2)	8464(3)	3449(2)	62(1)
C(131)	2656(2)	5344(3)	4787(2)	46(1)	C(221)	5148(2)	11087(3)	8000(2)	52(1)
C(4)	1715(1)	10224(2)	4578(2)	31(1)					

5.3.3 Bond lengths [Å] for 2,6-bis(Hyp)-H_2gua

Bonds	Bond distance	Bonds	Bond distance	Bonds	Bond distance
Si(1)-C(6)	1.948(3)	Si(13)-C(132)	1.866(3)	C(7)-C(8)	1.336(4)
Si(1)-Si(11)	2.3482(11)	Si(13)-C(133)	1.871(3)	C(7)-C(71)	1.505(4)
Si(1)-Si(12)	2.3535(11)	Si(13)-C(131)	1.873(3)	C(9)-C(1)	1.350(3)
Si(1)-Si(13)	2.3538(12)	Si(21)-C(213)	1.863(3)	C(9)-C(8)	1.448(4)
Si(2)-C(2)	1.943(3)	Si(21)-C(212)	1.863(3)	C(9)-C(10)	1.466(4)
Si(2)-Si(21)	2.3428(12)	Si(21)-C(211)	1.867(3)	C(2)-C(3)	1.467(4)
Si(2)-Si(23)	2.3544(11)	Si(22)-C(223)	1.861(4)	C(2)-C(1)	1.474(4)
Si(2)-Si(22)	2.3628(12)	Si(22)-C(221)	1.861(3)	C(10)-C(3)	1.347(4)
Si(11)-C(112)	1.858(3)	Si(22)-C(222)	1.871(3)	C(10)-C(4)	1.464(4)
Si(11)-C(111)	1.858(3)	Si(23)-C(233)	1.865(3)	C(1)-C(101)	1.489(4)
Si(11)-C(113)	1.869(3)	Si(23)-C(231)	1.864(3)	C(5)-C(4)	1.325(4)
Si(12)-C(122)	1.863(3)	Si(23)-C(232)	1.873(3)	C(4)-C(41)	1.508(4)
Si(12)-C(121)	1.863(3)	C(6)-C(5)	1.494(4)	C(71)-C(711)	1.523(4)
Si(12)-C(123)	1.872(3)	C(6)-C(7)	1.505(4)	C(71)-C(712)	1.530(4)

5.3.4 Bond angles for 2,6-bis(Hyp)-H_2gua (deg)

Bond angle	parameter	Bond angle	parameter	Bond angle	parameter
C(6)-Si(1)-Si(11)	117.70(9)	C(132)-Si(13)-C(131)	110.18(15)	C(7)-C(6)-Si(1)	114.66(19)
C(6)-Si(1)-Si(12)	104.08(9)	C(133)-Si(13)-C(131)	106.19(15)	C(8)-C(7)-C(71)	120.8(2)
Si(11)-Si(1)-Si(12)	108.52(4)	C(132)-Si(13)-Si(1)	110.80(11)	C(8)-C(7)-C(6)	124.8(2)
C(6)-Si(1)-Si(13)	110.13(9)	C(133)-Si(13)-Si(1)	112.78(11)	C(71)-C(7)-C(6)	114.3(2)
Si(11)-Si(1)-Si(13)	109.41(4)	C(131)-Si(13)-Si(1)	111.56(11)	C(1)-C(9)-C(8)	124.6(2)
Si(12)-Si(1)-Si(13)	106.30(4)	C(213)-Si(21)-C(212)	108.02(17)	C(1)-C(9)-C(10)	108.6(2)
C(2)-Si(2)-Si(21)	110.34(9)	C(213)-Si(21)-C(211)	107.65(17)	C(8)-C(9)-C(10)	126.3(2)
C(2)-Si(2)-Si(23)	108.27(9)	C(212)-Si(21)-C(211)	107.93(15)	C(3)-C(2)-C(1)	103.2(2)
Si(21)-Si(2)-Si(23)	111.95(4)	C(213)-Si(21)-Si(2)	112.33(11)	C(3)-C(2)-Si(2)	106.4(2)
C(2)-Si(2)-Si(22)	111.68(10)	C(212)-Si(21)-Si(2)	113.53(12)	C(1)-C(2)-Si(2)	111.63(18)
Si(21)-Si(2)-Si(22)	109.34(4)	C(211)-Si(21)-Si(2)	107.14(11)	C(3)-C(10)-C(4)	125.1(3)
Si(23)-Si(2)-Si(22)	105.16(4)	C(223)-Si(22)-C(221)	108.82(17)	C(3)-C(10)-C(9)	107.6(2)
C(112)-Si(11)-C(111)	109.30(16)	C(223)-Si(22)-C(222)	107.40(17)	C(4)-C(10)-C(9)	127.3(2)
C(112)-Si(11)-C(113)	106.27(15)	C(221)-Si(22)-C(222)	105.39(16)	C(9)-C(1)-C(2)	109.6(2)
C(111)-Si(11)-C(113)	108.22(16)	C(223)-Si(22)-Si(2)	110.44(12)	C(9)-C(1)-C(101)	126.6(3)
C(112)-Si(11)-Si(1)	114.63(11)	C(221)-Si(22)-Si(2)	113.77(11)	C(2)-C(1)-C(101)	123.8(2)
C(111)-Si(11)-Si(1)	112.38(11)	C(222)-Si(22)-Si(2)	110.72(11)	C(10)-C(3)-C(2)	110.6(3)
C(113)-Si(11)-Si(1)	105.61(10)	C(233)-Si(23)-C(231)	110.22(17)	C(7)-C(8)-C(9)	129.9(3)
C(122)-Si(12)-C(121)	108.12(16)	C(233)-Si(23)-C(232)	104.85(15)	C(4)-C(5)-C(6)	131.7(3)
C(122)-Si(12)-C(123)	107.62(15)	C(231)-Si(23)-C(232)	106.86(15)	C(5)-C(4)-C(10)	125.0(3)
C(121)-Si(12)-C(123)	106.81(15)	C(233)-Si(23)-Si(2)	110.37(11)	C(5)-C(4)-C(41)	119.6(3)
C(122)-Si(12)-Si(1)	112.74(11)	C(231)-Si(23)-Si(2)	109.28(12)	C(10)-C(4)-C(41)	115.4(3)
C(121)-Si(12)-Si(1)	109.05(10)	C(232)-Si(23)-Si(2)	115.11(11)	C(7)-C(71)-C(711)	115.7(2)
C(123)-Si(12)-Si(1)	112.26(11)	C(5)-C(6)-C(7)	118.9(2)	C(7)-C(71)-C(712)	110.1(3)
C(132)-Si(13)-C(133)	105.04(15)	C(5)-C(6)-Si(1)	108.27(18)	C(711)-C(71)-C(712)	108.9(3)

5.3.5 Anisotropic displacement parameters ($A^2 \times 10^3$) for 2,6-bis(Hyp)-H_2gua. The anisotropic displacement factor exponent takes the form: $-2\pi^2[h^2a^{*2}U11 + ... +2hka^*b^*U12]$

atom	U11	U22	U33	U23	U13	U12	atom	U11	U22	U33	U23	U13	U12
Si(3)	23(1)	26(1)	30(1)	13(1)	10(1)	10(1)	C(211)	65(4)	44(3)	66(4)	19(3)	23(3)	3(3)
Si(31)	47(1)	48(1)	42(1)	28(1)	17(1)	28(1)	C(212)	74(4)	41(3)	64(4)	8(3)	22(3)	31(3)
C(311)	88(5)	96(5)	93(5)	69(4)	56(4)	43(4)	C(213)	69(4)	42(3)	43(3)	11(2)	17(3)	28(3)
C(312)	79(4)	82(4)	63(4)	39(3)	21(3)	60(4)	Si(22)	44(1)	40(1)	36(1)	24(1)	19(1)	23(1)
C(313)	83(4)	83(4)	39(3)	28(3)	11(3)	49(4)	C(221)	78(4)	54(3)	57(3)	38(3)	32(3)	42(3)
Si(32)	41(1)	29(1)	48(1)	9(1)	8(1)	15(1)	C(222)	64(4)	65(3)	44(3)	29(3)	15(3)	34(3)
C(321)	94(5)	66(4)	42(3)	0(3)	10(3)	42(4)	C(223)	72(4)	54(3)	57(3)	35(3)	44(3)	27(3)
C(322)	68(4)	37(3)	94(4)	25(3)	27(4)	27(3)	Si(23)	32(1)	34(1)	42(1)	20(1)	23(1)	16(1)
C(323)	40(3)	33(3)	92(4)	21(3)	11(3)	3(2)	C(231)	54(3)	55(3)	84(4)	42(3)	48(3)	36(3)
Si(33)	32(1)	41(1)	50(1)	18(1)	23(1)	16(1)	C(232)	52(3)	58(3)	52(3)	25(3)	32(3)	26(3)
C(331)	50(3)	71(4)	103(5)	38(3)	48(3)	39(3)	C(233)	34(3)	45(3)	52(3)	24(2)	22(2)	16(2)
C(332)	81(4)	80(4)	68(4)	43(3)	55(3)	41(3)	Li(2)	43(5)	34(4)	48(5)	24(4)	20(4)	25(4)
C(333)	40(3)	42(3)	85(4)	14(3)	30(3)	10(3)	Li(1)	35(4)	38(4)	31(4)	12(3)	11(4)	13(4)
Si(4)	25(1)	27(1)	32(1)	13(1)	14(1)	7(1)	C(2)	22(2)	22(2)	31(2)	15(2)	12(2)	4(2)
Si(41)	32(1)	34(1)	45(1)	24(1)	18(1)	11(1)	C(3)	23(2)	30(2)	26(2)	14(2)	11(2)	10(2)
C(411)	75(4)	44(3)	60(4)	31(3)	21(3)	10(3)	C(10)	25(2)	27(2)	32(2)	16(2)	15(2)	12(2)
C(412)	66(4)	67(3)	67(4)	46(3)	42(3)	29(3)	C(4)	23(2)	27(2)	29(2)	15(2)	15(2)	14(2)
C(413)	36(3)	65(3)	84(4)	43(3)	23(3)	26(3)	C(41)	23(2)	27(2)	31(2)	12(2)	5(2)	8(2)
Si(42)	33(1)	29(1)	37(1)	8(1)	19(1)	4(1)	C(5)	23(2)	21(2)	34(2)	13(2)	16(2)	9(2)
C(421)	80(4)	47(3)	37(3)	15(2)	29(3)	9(3)	C(6)	23(2)	27(2)	23(2)	12(2)	13(2)	10(2)
C(422)	31(3)	34(3)	46(3)	2(2)	15(2)	4(2)	C(7)	25(2)	26(2)	25(2)	10(2)	13(2)	13(2)
C(423)	35(3)	39(3)	84(4)	5(3)	32(3)	5(2)	C(71)	38(3)	33(2)	34(3)	19(2)	24(2)	15(2)
Si(43)	27(1)	34(1)	35(1)	15(1)	16(1)	12(1)	C(72)	43(3)	54(3)	34(3)	20(2)	22(2)	20(2)
C(431)	35(3)	44(3)	45(3)	23(2)	11(2)	15(2)	C(73)	46(3)	44(3)	32(3)	11(2)	17(2)	5(2)
C(432)	29(3)	40(3)	61(3)	19(2)	26(2)	8(2)	C(8)	21(2)	26(2)	24(2)	7(2)	10(2)	9(2)
C(433)	48(3)	44(3)	52(3)	15(2)	21(3)	23(3)	C(9)	21(2)	22(2)	25(2)	10(2)	11(2)	11(2)
Si(1)	25(1)	24(1)	26(1)	13(1)	12(1)	7(1)	C(1)	16(2)	28(2)	24(2)	13(2)	10(2)	11(2)
Si(11)	45(1)	37(1)	30(1)	12(1)	18(1)	7(1)	C(101)	28(2)	31(2)	34(2)	19(2)	12(2)	7(2)
C(111)	72(4)	75(4)	38(3)	22(3)	30(3)	4(3)	C(12)	23(2)	22(2)	38(3)	11(2)	15(2)	9(2)
C(112)	74(4)	52(3)	62(4)	-3(3)	34(3)	24(3)	C(13)	26(2)	26(2)	27(2)	7(2)	13(2)	10(2)
C(113)	54(3)	52(3)	32(3)	18(2)	10(3)	-2(3)	C(20)	17(2)	26(2)	31(2)	13(2)	13(2)	10(2)
Si(12)	28(1)	31(1)	37(1)	20(1)	13(1)	11(1)	C(14)	18(2)	32(2)	38(3)	20(2)	13(2)	12(2)
C(121)	41(3)	52(3)	51(3)	26(3)	21(3)	21(2)	C(141)	37(3)	29(2)	38(3)	17(2)	17(2)	8(2)
C(122)	42(3)	48(3)	73(4)	40(3)	26(3)	12(2)	C(15)	23(2)	27(2)	29(2)	15(2)	12(2)	9(2)
C(123)	47(3)	52(3)	52(3)	22(3)	20(3)	25(3)	C(16)	16(2)	28(2)	32(2)	15(2)	8(2)	9(2)
Si(13)	27(1)	33(1)	37(1)	17(1)	16(1)	12(1)	C(17)	19(2)	31(2)	31(2)	18(2)	6(2)	13(2)
C(131)	44(3)	48(3)	58(3)	26(3)	25(3)	24(2)	C(171)	34(3)	27(2)	35(3)	13(2)	8(2)	12(2)
C(132)	41(3)	54(3)	64(3)	25(3)	35(3)	14(3)	C(172)	48(3)	42(3)	30(3)	12(2)	4(2)	10(2)
C(133)	31(3)	43(3)	47(3)	19(2)	20(2)	14(2)	C(173)	23(3)	48(3)	39(3)	9(2)	-1(2)	6(2)
Si(2)	30(1)	25(1)	28(1)	13(1)	15(1)	12(1)	C(18)	23(2)	33(2)	23(2)	14(2)	6(2)	12(2)
Si(21)	44(1)	29(1)	37(1)	12(1)	17(1)	15(1)	C(19)	24(2)	24(2)	30(2)	12(2)	13(2)	12(2)
C(201)	35(3)	28(2)	40(3)	17(2)	18(2)	8(2)	C(11)	25(2)	24(2)	18(2)	5(2)	5(2)	10(2)

5.4 Crystallographic data for Li(2,6-bis(Hyp)-Hgual)

5.4.1 Crystallographic data and structure refinement for Li(2,6-bis(Hyp)-Hgual)

Empirical formula	$C_{33}H_{71}Si_8Li$
Formula weight (g/mol)	699.55
Temperature (K)	173(2)
Wavelength(Å)	0.71073
Crystal system, space group	triclinic, Pī

Unit cell dimensions (Å ,deg)	a=16.835(4) α=103.004(14) b=18.894(3) β=112189(13) c=20.054(4) γ=107.613(16)
Volume (Å^3)	5196.9(17)
Z; calc. density (Mg/m^3)	2; 1.011
Absorption coefficient (mm^{-1})	0.230
F(000)	1734
Theta range for data collection (deg)	2.11~25.00
Limiting indices	-10≤h≤19,-20≤k≤19,-23≤l≤22
Reflections collected / unique	18111 / 17473[R(int)=0.0384]
Completeness to θ	25.00; 95.4%
Refinement method	full-matrix least-squares on F^2
Data / restraints / parameters	17473 / 536 / 976
(Goodness-of-fit on F^2)	0.861
Final R indices [I>2σ(I)]	R1=0.0564, wR2=0.0952
R indices (all data)	R1=0.1395, wR2=0.1164
Largest diff. peak and hole (e.Å^{-3})	0.344 und –0.325

5.4.2 Atomic coordinates (×10^4) and equivalent isotropic displacement parameters (A^2×10^3) for Li(2,6-bis(Hyp)-Hgual). U(eq) is defined as one third of the trace of the orthogonalized Uij tensor.

atom	a/x	y/b	z/c	U(eq)	atom	a/x	y/b	z/c	U(eq)
Si(3)	-4259(1)	15553(1)	7948(1)	27(1)	C(212)	-2572(4)	8936(3)	7000(3)	64(2)
Si(31)	-4779(1)	15761(1)	6758(1)	43(1)	C(213)	-3852(3)	9574(3)	6144(2)	55(1)
C(311)	-3730(4)	16455(3)	6727(3)	81(2)	Si(22)	-1744(1)	10473(1)	9293(1)	37(1)
C(312)	-5662(4)	16217(3)	6650(3)	70(2)	C(221)	-1491(4)	9557(3)	9134(3)	56(1)
C(313)	-5396(4)	14813(3)	5872(3)	70(2)	C(222)	-630(3)	11296(3)	10158(3)	58(1)
Si(32)	-3327(1)	16864(1)	8934(1)	45(1)	C(223)	-2753(3)	10215(3)	9539(3)	54(1)
C(321)	-3235(4)	16916(3)	9906(3)	77(2)	Si(23)	-821(1)	11407(1)	8059(1)	33(1)
C(322)	-3842(4)	17585(3)	8681(3)	70(2)	C(231)	-113(3)	10786(3)	8253(3)	53(1)
C(323)	-2099(3)	17274(3)	9035(3)	66(2)	C(232)	-1119(3)	11440(3)	7073(3)	50(1)
Si(33)	-5612(1)	14929(1)	8071(1)	40(1)	C(233)	-5(3)	12449(2)	8807(2)	43(1)
C(331)	-6122(3)	15675(3)	8230(3)	66(2)	Li(2)	-4427(5)	12172(4)	7458(4)	38(2)
C(332)	-5338(4)	14642(3)	8946(3)	66(2)	Li(1)	-2800(5)	13636(4)	7325(4)	38(2)
C(333)	-6544(3)	14016(3)	7164(3)	60(2)	C(2)	-1678(3)	13503(2)	7017(2)	26(1)
Si(4)	-6974(1)	11126(1)	6895(1)	28(1)	C(3)	-2508(3)	12774(2)	6606(2)	26(1)
Si(41)	-6719(1)	10319(1)	7641(1)	37(1)	C(10)	-2714(3)	12458(2)	7129(2)	26(1)
C(411)	-7553(4)	9239(3)	7012(3)	66(2)	C(4)	-3509(3)	11704(2)	6914(2)	24(1)
C(412)	-6944(4)	10568(3)	8496(3)	60(2)	C(41)	-4248(3)	11305(2)	6060(2)	31(1)
C(413)	-5468(3)	10400(3)	8002(3)	60(2)	C(5)	-3591(3)	11322(2)	7404(2)	26(1)
Si(42)	-7566(1)	10313(1)	5574(1)	36(1)	C(6)	-2909(3)	11468(2)	8227(2)	23(1)
C(421)	-7616(4)	10887(3)	4914(2)	59(2)	C(7)	-2292(3)	12330(2)	8807(2)	24(1)
C(422)	-8819(3)	9562(2)	5174(2)	43(1)	C(71)	-2121(3)	12438(2)	9640(2)	31(1)
C(423)	-6856(3)	9742(3)	5454(3)	58(2)	C(72)	-2940(3)	12510(3)	9749(2)	42(1)
Si(43)	-8221(1)	11439(1)	6933(1)	32(1)	C(73)	-1179(3)	13152(2)	10278(2)	46(1)
C(431)	-8667(3)	11839(3)	6157(2)	44(1)	C(8)	-1900(3)	12973(2)	8652(2)	25(1)
C(432)	-9247(3)	10510(2)	6751(3)	44(1)	C(9)	-1993(3)	13003(2)	7900(2)	22(1)
C(433)	-7829(3)	12218(3)	7895(2)	49(1)	C(1)	-1350(2)	13650(2)	7832(2)	22(1)
Si(1)	-1084(1)	14076(1)	6541(1)	25(1)	C(101)	-459(3)	14339(2)	8487(2)	32(1)
Si(11)	-1694(1)	13234(1)	5236(1)	41(1)	C(12)	-5875(3)	12068(2)	7223(2)	28(1)
C(111)	-1321(4)	13831(3)	4687(3)	68(2)	C(13)	-5615(3)	12370(2)	6705(2)	27(1)
C(112)	-1208(4)	12453(3)	5226(3)	68(2)	C(20)	-4807(3)	13129(2)	7141(2)	23(1)
C(113)	-3038(3)	12682(3)	4667(2)	57(2)	C(14)	-4351(3)	13628(2)	6811(2)	28(1)
Si(12)	-1324(1)	15244(1)	6526(1)	32(1)	C(141)	-4667(3)	13244(2)	5951(2)	36(1)
C(121)	-2556(3)	14974(3)	5761(2)	47(1)	C(15)	-3742(3)	14409(2)	7196(2)	27(1)
C(122)	-467(3)	15893(3)	6282(3)	54(1)	C(16)	-3432(3)	14992(2)	7993(2)	26(1)
C(123)	-1182(3)	15831(3)	7478(3)	50(1)	C(17)	-3217(3)	14706(2)	8669(2)	27(1)
Si(13)	579(1)	14454(1)	7127(1)	31(1)	C(171)	-2384(3)	15332(2)	9432(2)	35(1)
C(131)	852(3)	13643(3)	7434(3)	47(1)	C(172)	-2383(3)	15217(3)	10173(2)	48(1)
C(132)	1050(3)	14597(3)	6422(3)	51(1)	C(173)	-1444(3)	15404(3)	9453(2)	46(1)
C(133)	1272(3)	15432(2)	7995(2)	40(1)	C(18)	-3738(3)	13970(2)	8618(2)	28(1)
Si(2)	-2201(1)	10809(1)	8170(1)	27(1)	C(19)	-4547(3)	13284(2)	7948(2)	25(1)
Si(21)	-3243(1)	9539(1)	7120(1)	38(1)	C(11)	-5209(3)	12645(2)	7996(2)	25(1)
C(211)	-4187(4)	8964(3)	7314(3)	67(2)	C(201)	-5229(3)	12608(2)	8734(2)	35(1)

5.4.3 Bond lengths [Å] for Li(2,6-bis(Hyp)-Hgual)

Bonds	Bond distances	Bonds	Bond distances	Bonds	Bond distances
Si(3)-C(16)	1.978(4)	Si(12)-C(123)	1.865(4)	Li(1)-C(15)	2.445(8)
Si(3)-Si(33)	2.3597(17)	Si(12)-C(121)	1.876(4)	C(2)-C(3)	1.408(5)
Si(3)-Si(32)	2.3672(18)	Si(12)-C(122)	1.886(4)	C(2)-C(1)	1.441(5)
Si(3)-Si(31)	2.3814(17)	Si(13)-C(133)	1.876(4)	C(3)-C(10)	1.416(5)
Si(31)-C(313)	1.869(5)	Si(13)-C(131)	1.891(4)	C(10)-C(9)	1.426(5)
Si(31)-C(311)	1.887(5)	Si(13)-C(132)	1.895(4)	C(10)-C(4)	1.464(5)
Si(31)-C(312)	1.903(5)	Si(2)-C(6)	1.981(4)	C(4)-C(5)	1.368(5)
Si(32)-C(321)	1.874(5)	Si(2)-Si(23)	2.3753(17)	C(4)-C(41)	1.514(5)
Si(32)-C(323)	1.886(5)	Si(2)-Si(21)	2.3785(18)	C(5)-C(6)	1.511(5)
Si(32)-C(322)	1.886(5)	Si(2)-Si(22)	2.3872(16)	C(6)-C(7)	1.515(5)
Si(33)-C(333)	1.881(5)	Si(21)-C(213)	1.862(4)	C(7)-C(8)	1.360(5)
Si(33)-C(332)	1.886(5)	Si(21)-C(211)	1.863(5)	C(7)-C(71)	1.537(5)
Si(33)-C(331)	1.888(5)	Si(21)-C(212)	1.869(5)	C(71)-C(72)	1.515(5)
Si(4)-C(12)	1.893(4)	Si(22)-C(222)	1.872(5)	C(71)-C(73)	1.540(5)
Si(4)-Si(43)	2.3697(18)	Si(22)-C(221)	1.892(4)	C(8)-C(9)	1.473(5)
Si(4)-Si(42)	2.3699(18)	Si(22)-C(223)	1.899(4)	C(9)-C(1)	1.437(5)
Si(4)-Si(41)	2.3836(16)	Si(23)-C(232)	1.868(4)	C(1)-C(101)	1.493(5)
Si(41)-C(411)	1.870(5)	Si(23)-C(233)	1.869(4)	C(12)-C(11)	1.426(5)
Si(41)-C(412)	1.883(5)	Si(23)-C(231)	1.911(4)	C(12)-C(13)	1.434(5)
Si(41)-C(413)	1.893(4)	Li(2)-C(13)	2.203(8)	C(13)-C(20)	1.424(5)
Si(42)-C(422)	1.872(4)	Li(2)-C(19)	2.213(8)	C(20)-C(19)	1.438(5)
Si(42)-C(423)	1.880(5)	Li(2)-C(20)	2.235(7)	C(20)-C(14)	1.464(5)
Si(42)-C(421)	1.885(4)	Li(2)-C(12)	2.237(8)	C(14)-C(15)	1.342(5)
Si(43)-C(433)	1.870(4)	Li(2)-C(11)	2.245(8)	C(14)-C(141)	1.514(5)
Si(43)-C(431)	1.884(4)	Li(2)-C(5)	2.445(8)	C(15)-C(16)	1.506(5)
Si(43)-C(432)	1.897(4)	Li(2)-C(4)	2.456(8)	C(16)-C(17)	1.528(5)
Si(1)-C(2)	1.901(4)	Li(2)-Li(1)	3.397(10)	C(17)-C(18)	1.358(5)
Si(1)-Si(11)	2.3546(18)	Li(1)-C(3)	2.222(8)	C(17)-C(171)	1.506(5)
Si(1)-Si(12)	2.3660(16)	Li(1)-C(10)	2.230(8)	C(171)-C(173)	1.531(5)
Si(1)-Si(13)	2.3780(17)	Li(1)-C(9)	2.243(8)	C(171)-C(172)	1.549(5)
Si(11)-C(111)	1.879(4)	Li(1)-C(1)	2.252(8)	C(18)-C(19)	1.451(5)
Si(11)-C(112)	1.893(5)	Li(1)-C(2)	2.261(8)	C(19)-C(11)	1.423(5)
Si(11)-C(113)	1.896(5)	Li(1)-C(14)	2.412(8)	C(11)-C(201)	1.510(5)

5.4.4 Bond angles for Li(2,6-bis(Hyp)-Hgual) [deg]

Bond angles	Parameter	Bond angles	Parameter	Bond angles	Parameter
C(16)-Si(3)-Si(33)	116.77(12)	C(211)-Si(21)-Si(2)	110.21(17)	C(3)-C(10)-Li(1)	71.1(3)
C(16)-Si(3)-Si(32)	108.34(13)	C(212)-Si(21)-Si(2)	110.33(16)	C(9)-C(10)-Li(1)	71.9(3)
Si(33)-Si(3)-Si(32)	108.79(7)	C(222)-Si(22)-C(221)	105.2(2)	C(4)-C(10)-Li(1)	123.4(3)
C(16)-Si(3)-Si(31)	109.70(12)	C(222)-Si(22)-C(223)	110.2(2)	C(5)-C(4)-C(10)	125.4(4)
Si(33)-Si(3)-Si(31)	107.90(7)	C(221)-Si(22)-C(223)	106.0(2)	C(5)-C(4)-C(41)	119.2(3)
Si(32)-Si(3)-Si(31)	104.66(6)	C(222)-Si(22)-Si(2)	112.67(15)	C(10)-C(4)-C(41)	115.3(3)
C(313)-Si(31)-C(311)	107.2(3)	C(221)-Si(22)-Si(2)	112.82(15)	C(5)-C(4)-Li(2)	73.3(3)
C(313)-Si(31)-C(312)	105.9(2)	C(223)-Si(22)-Si(2)	109.59(15)	C(10)-C(4)-Li(2)	102.3(3)
C(311)-Si(31)-C(312)	109.0(2)	C(232)-Si(23)-C(233)	108.3(2)	C(41)-C(4)-Li(2)	99.1(3)
C(313)-Si(31)-Si(3)	113.40(16)	C(232)-Si(23)-C(231)	109.7(2)	C(4)-C(5)-C(6)	132.3(3)
C(311)-Si(31)-Si(3)	110.02(18)	C(233)-Si(23)-C(231)	105.6(2)	C(4)-C(5)-Li(2)	74.3(3)
C(312)-Si(31)-Si(3)	111.07(17)	C(232)-Si(23)-Si(2)	112.18(16)	C(6)-C(5)-Li(2)	109.0(3)
C(321)-Si(32)-C(323)	109.6(3)	C(233)-Si(23)-Si(2)	113.20(15)	C(5)-C(6)-C(7)	118.3(3)
C(321)-Si(32)-C(322)	105.5(2)	C(231)-Si(23)-Si(2)	107.60(14)	C(5)-C(6)-Si(2)	108.4(2)
C(323)-Si(32)-C(322)	106.3(2)	C(13)-Li(2)-C(19)	62.3(2)	C(7)-C(6)-Si(2)	114.2(3)
C(321)-Si(32)-Si(3)	113.61(18)	C(13)-Li(2)-C(20)	37.43(17)	C(8)-C(7)-C(6)	126.4(3)
C(323)-Si(32)-Si(3)	110.03(17)	C(19)-Li(2)-C(20)	37.72(17)	C(8)-C(7)-C(71)	120.3(3)
C(322)-Si(32)-Si(3)	111.51(17)	C(13)-Li(2)-C(12)	37.68(18)	C(6)-C(7)-C(71)	113.3(3)
C(333)-Si(33)-C(332)	109.4(2)	C(19)-Li(2)-C(12)	62.5(2)	C(72)-C(71)-C(7)	111.5(3)
C(333)-Si(33)-C(331)	108.8(2)	C(20)-Li(2)-C(12)	63.1(2)	C(72)-C(71)-C(73)	110.0(4)

C(332)-Si(33)-C(331)	105.3(2)	C(13)-Li(2)-C(11)	62.2(2)	C(7)-C(71)-C(73)	113.6(3)
C(333)-Si(33)-Si(3)	111.21(16)	C(19)-Li(2)-C(11)	37.22(17)	C(7)-C(8)-C(9)	128.8(3)
C(332)-Si(33)-Si(3)	113.48(17)	C(20)-Li(2)-C(11)	62.7(2)	C(10)-C(9)-C(1)	107.4(3)
C(331)-Si(33)-Si(3)	108.32(16)	C(12)-Li(2)-C(11)	37.11(18)	C(10)-C(9)-C(8)	129.1(3)
C(12)-Si(4)-Si(43)	111.32(13)	C(13)-Li(2)-C(5)	141.3(4)	C(1)-C(9)-C(8)	123.5(3)
C(12)-Si(4)-Si(42)	110.05(13)	C(19)-Li(2)-C(5)	154.5(4)	C(10)-C(9)-Li(1)	70.9(3)
Si(43)-Si(4)-Si(42)	105.54(6)	C(20)-Li(2)-C(5)	149.2(4)	C(1)-C(9)-Li(1)	71.7(3)
C(12)-Si(4)-Si(41)	114.03(13)	C(12)-Li(2)-C(5)	140.0(3)	C(8)-C(9)-Li(1)	120.5(3)
Si(43)-Si(4)-Si(41)	107.88(6)	C(11)-Li(2)-C(5)	147.7(3)	C(9)-C(1)-C(2)	108.6(3)
Si(42)-Si(4)-Si(41)	107.61(6)	C(13)-Li(2)-C(4)	119.2(3)	C(9)-C(1)-C(101)	126.5(3)
C(411)-Si(41)-C(412)	106.1(2)	C(19)-Li(2)-C(4)	141.0(3)	C(2)-C(1)-C(101)	124.9(3)
C(411)-Si(41)-C(413)	107.3(2)	C(20)-Li(2)-C(4)	116.9(3)	C(9)-C(1)-Li(1)	71.0(3)
C(412)-Si(41)-C(413)	109.0(2)	C(12)-Li(2)-C(4)	145.2(4)	C(2)-C(1)-Li(1)	71.7(3)
C(411)-Si(41)-Si(4)	109.51(15)	C(11)-Li(2)-C(4)	177.6(4)	C(101)-C(1)-Li(1)	125.8(3)
C(412)-Si(41)-Si(4)	113.87(16)	C(5)-Li(2)-C(4)	32.40(15)	C(11)-C(12)-C(13)	106.9(3)
C(413)-Si(41)-Si(4)	110.71(15)	C(13)-Li(2)-Li(1)	92.7(3)	C(11)-C(12)-Si(4)	128.4(3)
C(422)-Si(42)-C(423)	107.78(19)	C(19)-Li(2)-Li(1)	75.3(2)	C(13)-C(12)-Si(4)	124.5(3)
C(422)-Si(42)-C(421)	105.6(2)	C(20)-Li(2)-Li(1)	62.0(2)	C(11)-C(12)-Li(2)	71.8(3)
C(423)-Si(42)-C(421)	107.1(2)	C(12)-Li(2)-Li(1)	125.1(3)	C(13)-C(12)-Li(2)	69.9(3)
C(422)-Si(42)-Si(4)	109.30(15)	C(11)-Li(2)-Li(1)	112.5(3)	Si(4)-C(12)-Li(2)	127.8(3)
C(423)-Si(42)-Si(4)	112.60(17)	C(5)-Li(2)-Li(1)	91.3(3)	C(20)-C(13)-C(12)	109.8(3)
C(421)-Si(42)-Si(4)	114.05(15)	C(4)-Li(2)-Li(1)	65.7(2)	C(20)-C(13)-Li(2)	72.5(3)
C(433)-Si(43)-C(431)	107.8(2)	C(3)-Li(1)-C(10)	37.10(17)	C(12)-C(13)-Li(2)	72.5(3)
C(433)-Si(43)-C(432)	107.7(2)	C(3)-Li(1)-C(9)	61.7(2)	C(13)-C(20)-C(19)	106.0(3)
C(431)-Si(43)-C(432)	108.6(2)	C(10)-Li(1)-C(9)	37.18(17)	C(13)-C(20)-C(14)	125.5(3)
C(433)-Si(43)-Si(4)	112.22(15)	C(3)-Li(1)-C(1)	61.2(2)	C(19)-C(20)-C(14)	128.5(3)
C(431)-Si(43)-Si(4)	109.72(15)	C(10)-Li(1)-C(1)	62.0(2)	C(13)-C(20)-Li(2)	70.0(3)
C(432)-Si(43)-Si(4)	110.76(15)	C(9)-Li(1)-C(1)	37.30(17)	C(19)-C(20)-Li(2)	70.3(3)
C(2)-Si(1)-Si(11)	109.27(13)	C(3)-Li(1)-C(2)	36.62(18)	C(14)-C(20)-Li(2)	123.9(3)
C(2)-Si(1)-Si(12)	114.00(13)	C(10)-Li(1)-C(2)	62.3(2)	C(15)-C(14)-C(20)	124.8(4)
Si(11)-Si(1)-Si(12)	107.18(6)	C(9)-Li(1)-C(2)	62.5(2)	C(15)-C(14)-C(141)	118.2(3)
C(2)-Si(1)-Si(13)	112.77(13)	C(1)-Li(1)-C(2)	37.26(17)	C(20)-C(14)-C(141)	116.7(3)
Si(11)-Si(1)-Si(13)	105.07(7)	C(3)-Li(1)-C(14)	119.9(3)	C(15)-C(14)-Li(1)	75.3(3)
Si(12)-Si(1)-Si(13)	108.03(6)	C(10)-Li(1)-C(14)	118.2(3)	C(20)-C(14)-Li(1)	101.9(3)
C(111)-Si(11)-C(112)	108.8(2)	C(9)-Li(1)-C(14)	142.0(3)	C(141)-C(14)-Li(1)	98.2(3)
C(111)-Si(11)-C(113)	106.4(2)	C(1)-Li(1)-C(14)	178.6(4)	C(14)-C(15)-C(16)	130.9(4)
C(112)-Si(11)-C(113)	107.7(2)	C(2)-Li(1)-C(14)	144.1(3)	C(14)-C(15)-Li(1)	72.6(3)
C(111)-Si(11)-Si(1)	110.61(16)	C(3)-Li(1)-C(15)	141.0(3)	C(16)-C(15)-Li(1)	109.2(3)
C(112)-Si(11)-Si(1)	108.56(17)	C(10)-Li(1)-C(15)	150.2(4)	C(15)-C(16)-C(17)	118.5(3)
C(113)-Si(11)-Si(1)	114.57(16)	C(9)-Li(1)-C(15)	155.8(4)	C(15)-C(16)-Si(3)	111.5(3)
C(123)-Si(12)-C(121)	107.0(2)	C(1)-Li(1)-C(15)	147.6(3)	C(17)-C(16)-Si(3)	112.4(3)
C(123)-Si(12)-C(122)	110.1(2)	C(2)-Li(1)-C(15)	138.8(3)	C(18)-C(17)-C(171)	121.2(3)
C(121)-Si(12)-C(122)	107.4(2)	C(14)-Li(1)-C(15)	32.07(15)	C(18)-C(17)-C(16)	124.6(3)
C(123)-Si(12)-Si(1)	111.55(15)	C(3)-Li(1)-Li(2)	93.8(3)	C(171)-C(17)-C(16)	114.1(3)
C(121)-Si(12)-Si(1)	110.85(15)	C(10)-Li(1)-Li(2)	63.3(2)	C(17)-C(171)-C(173)	111.0(4)
C(122)-Si(12)-Si(1)	109.86(16)	C(9)-Li(1)-Li(2)	75.6(2)	C(17)-C(171)-C(172)	115.5(3)
C(133)-Si(13)-C(131)	109.3(2)	C(1)-Li(1)-Li(2)	112.9(3)	C(173)-C(171)-C(172)	109.5(4)
C(133)-Si(13)-C(132)	106.2(2)	C(2)-Li(1)-Li(2)	125.6(3)	C(17)-C(18)-C(19)	130.0(4)
C(131)-Si(13)-C(132)	107.1(2)	C(14)-Li(1)-Li(2)	66.4(2)	C(11)-C(19)-C(20)	109.1(3)
C(133)-Si(13)-Si(1)	112.21(14)	C(15)-Li(1)-Li(2)	91.7(3)	C(11)-C(19)-C(18)	124.4(3)
C(131)-Si(13)-Si(1)	110.40(15)	C(3)-C(2)-C(1)	106.1(3)	C(20)-C(19)-C(18)	126.5(3)
C(132)-Si(13)-Si(1)	111.48(15)	C(3)-C(2)-Si(1)	124.5(3)	C(11)-C(19)-Li(2)	72.6(3)
C(6)-Si(2)-Si(23)	115.40(12)	C(1)-C(2)-Si(1)	129.1(3)	C(20)-C(19)-Li(2)	72.0(3)
C(6)-Si(2)-Si(21)	109.39(12)	C(3)-C(2)-Li(1)	70.2(3)	C(18)-C(19)-Li(2)	121.0(3)
Si(23)-Si(2)-Si(21)	109.82(7)	C(1)-C(2)-Li(1)	71.0(3)	C(19)-C(11)-C(12)	108.2(3)
C(6)-Si(2)-Si(22)	109.85(12)	Si(1)-C(2)-Li(1)	128.4(3)	C(19)-C(11)-C(201)	125.7(3)
Si(23)-Si(2)-Si(22)	108.15(6)	C(2)-C(3)-C(10)	110.7(3)	C(12)-C(11)-C(201)	126.1(3)
Si(21)-Si(2)-Si(22)	103.56(6)	C(2)-C(3)-Li(1)	73.2(3)	C(19)-C(11)-Li(2)	70.2(3)
C(213)-Si(21)-C(211)	107.0(2)	C(10)-C(3)-Li(1)	71.8(3)	C(12)-C(11)-Li(2)	71.1(3)
C(213)-Si(21)-C(212)	105.0(2)	C(3)-C(10)-C(9)	107.3(3)	C(201)-C(11)-Li(2)	126.7(3)
C(211)-Si(21)-C(212)	108.4(2)	C(3)-C(10)-C(4)	126.1(3)		
C(213)-Si(21)-Si(2)	115.59(15)	C(9)-C(10)-C(4)	126.6(3)		

5.4.5 Anisotropic displacement parameters ($A^2 \times 10^3$) for Li(2,6-bis(Hyp)-Hgual). The anisotropic displacement factor exponent takes the form: $-2\pi^2[h^2a^{*2}U11 + ... +2hka^*b^*U12]$

atom	U11	U22	U33	U23	U13	U12	atom	U11	U22	U33	U23	U13	U12
Si(3)	23(1)	26(1)	30(1)	13(1)	10(1)	10(1)	C(212)	74(4)	41(3)	64(4)	8(3)	22(3)	31(3)
Si(31)	47(1)	48(1)	42(1)	28(1)	17(1)	28(1)	C(213)	69(4)	42(3)	43(3)	11(2)	17(3)	28(3)
C(311)	88(5)	96(5)	93(5)	69(4)	56(4)	43(4)	Si(22)	44(1)	40(1)	36(1)	24(1)	19(1)	23(1)
C(312)	79(4)	82(4)	63(4)	39(3)	21(3)	60(4)	C(221)	78(4)	54(3)	57(3)	38(3)	32(3)	42(3)
C(313)	83(4)	83(4)	39(3)	28(3)	11(3)	49(4)	C(222)	64(4)	65(3)	44(3)	29(3)	15(3)	34(3)
Si(32)	41(1)	29(1)	48(1)	9(1)	8(1)	15(1)	C(223)	72(4)	54(3)	57(3)	35(3)	44(3)	27(3)
C(321)	94(5)	66(4)	42(3)	0(3)	10(3)	42(4)	Si(23)	32(1)	34(1)	42(1)	20(1)	23(1)	16(1)
C(322)	68(4)	37(3)	94(4)	25(3)	27(4)	27(3)	C(231)	54(3)	55(3)	84(4)	42(3)	48(3)	36(3)
C(323)	40(3)	33(3)	92(4)	21(3)	11(3)	3(2)	C(232)	52(3)	58(3)	52(3)	25(3)	32(3)	26(3)
Si(33)	32(1)	41(1)	50(1)	18(1)	23(1)	16(1)	C(233)	34(3)	45(3)	52(3)	24(2)	22(2)	16(2)
C(331)	50(3)	71(4)	103(5)	38(3)	48(3)	39(3)	Li(2)	43(5)	34(4)	48(5)	24(4)	20(4)	25(4)
C(332)	81(4)	80(4)	68(4)	43(3)	55(3)	41(3)	Li(1)	35(4)	38(4)	31(4)	12(3)	11(4)	13(4)
C(333)	40(3)	42(3)	85(4)	14(3)	30(3)	10(3)	C(2)	22(2)	22(2)	31(2)	15(2)	12(2)	4(2)
Si(4)	25(1)	27(1)	32(1)	13(1)	14(1)	7(1)	C(3)	23(2)	30(2)	26(2)	14(2)	11(2)	10(2)
Si(41)	32(1)	34(1)	45(1)	24(1)	18(1)	11(1)	C(10)	25(2)	27(2)	32(2)	16(2)	15(2)	12(2)
C(411)	75(4)	44(3)	60(4)	31(3)	21(3)	10(3)	C(4)	23(2)	27(2)	29(2)	15(2)	15(2)	14(2)
C(412)	66(4)	67(3)	67(4)	46(3)	42(3)	29(3)	C(41)	23(2)	27(2)	31(2)	12(2)	5(2)	8(2)
C(413)	36(3)	65(3)	84(4)	43(3)	23(3)	26(3)	C(5)	23(2)	21(2)	34(2)	13(2)	16(2)	9(2)
Si(42)	33(1)	29(1)	37(1)	8(1)	19(1)	4(1)	C(6)	23(2)	27(2)	23(2)	12(2)	13(2)	10(2)
C(421)	80(4)	47(3)	37(3)	15(2)	29(3)	9(3)	C(7)	25(2)	26(2)	25(2)	10(2)	13(2)	13(2)
C(422)	31(3)	34(3)	46(3)	2(2)	15(2)	4(2)	C(71)	38(3)	33(2)	34(3)	19(2)	24(2)	15(2)
C(423)	35(3)	39(3)	84(4)	5(3)	32(3)	5(2)	C(72)	43(3)	54(3)	34(3)	20(2)	22(2)	20(2)
Si(43)	27(1)	34(1)	35(1)	15(1)	16(1)	12(1)	C(73)	46(3)	44(3)	32(3)	11(2)	17(2)	5(2)
C(431)	35(3)	44(3)	45(3)	23(2)	11(2)	15(2)	C(8)	21(2)	26(2)	24(2)	7(2)	10(2)	9(2)
C(432)	29(3)	40(3)	61(3)	19(2)	26(2)	8(2)	C(9)	21(2)	22(2)	25(2)	10(2)	11(2)	11(2)
C(433)	48(3)	44(3)	52(3)	15(2)	21(3)	23(3)	C(1)	16(2)	28(2)	24(2)	13(2)	10(2)	11(2)
Si(1)	25(1)	24(1)	26(1)	13(1)	12(1)	7(1)	C(101)	28(2)	31(2)	34(2)	19(2)	12(2)	7(2)
Si(11)	45(1)	37(1)	30(1)	12(1)	18(1)	7(1)	C(12)	23(2)	22(2)	38(3)	11(2)	15(2)	9(2)
C(111)	72(4)	75(4)	38(3)	22(3)	30(3)	4(3)	C(13)	26(2)	26(2)	27(2)	7(2)	13(2)	10(2)
C(112)	74(4)	52(3)	62(4)	-3(3)	34(3)	24(3)	C(20)	17(2)	26(2)	31(2)	13(2)	13(2)	10(2)
C(113)	54(3)	52(3)	32(3)	18(2)	10(3)	-2(3)	C(14)	18(2)	32(2)	38(3)	20(2)	13(2)	12(2)
Si(12)	28(1)	31(1)	37(1)	20(1)	13(1)	11(1)	C(141)	37(3)	29(2)	38(3)	17(2)	17(2)	8(2)
C(121)	41(3)	52(3)	51(3)	26(3)	21(3)	21(2)	C(15)	23(2)	27(2)	29(2)	15(2)	12(2)	9(2)
C(122)	42(3)	48(3)	73(4)	40(3)	26(3)	12(2)	C(16)	16(2)	28(2)	32(2)	15(2)	8(2)	9(2)
C(123)	47(3)	52(3)	52(3)	22(3)	20(3)	25(3)	C(17)	19(2)	31(2)	31(2)	18(2)	6(2)	13(2)
Si(13)	27(1)	33(1)	37(1)	17(1)	16(1)	12(1)	C(171)	34(3)	27(2)	35(3)	13(2)	8(2)	12(2)
C(131)	44(3)	48(3)	58(3)	26(3)	25(3)	24(2)	C(172)	48(3)	42(3)	30(3)	12(2)	4(2)	10(2)
C(132)	41(3)	54(3)	64(3)	25(3)	35(3)	14(3)	C(173)	23(3)	48(3)	39(3)	9(2)	-1(2)	6(2)
C(133)	31(3)	43(3)	47(3)	19(2)	20(2)	14(2)	C(18)	23(2)	33(2)	23(2)	14(2)	6(2)	12(2)
Si(2)	30(1)	25(1)	28(1)	13(1)	15(1)	12(1)	C(19)	24(2)	24(2)	30(2)	12(2)	13(2)	12(2)
Si(21)	44(1)	29(1)	37(1)	12(1)	17(1)	15(1)	C(11)	25(2)	24(2)	18(2)	5(2)	5(2)	10(2)
C(211)	65(4)	44(3)	66(4)	19(3)	23(3)	3(3)	C(201)	35(3)	28(2)	40(3)	17(2)	18(2)	8(2)

5.5 Crystallographic data for Mn(6-Hyp-Hgual)$_2$

5.5.1 Crystallographic data and structure refinement for Mn(6-Hyp-Hgual)$_2$

Empirical formula	$C_{48}H_{90}MnSi_8$
Formula weight (g/mol)	946.86
Temperature (K)	173(2)
Wavelength(Å)	0,71073
Crystal system, space group	triclinic, P(-1)
Unit cell dimensions (Å ,deg)	a=9.5472(18) α=102.635(8)

	b=16.441(2) β=91.222(11)
	c=18.562(3) γ=96.696(12)
Volume (Å^3)	2820.2(8)
Z; calc. density (Mg/m^3)	2; 1.115
Absorption coefficient (mm^{-1})	0.433
F(000)	1030
Theta range for data collection (deg)	2.15 ~25.00
Limiting indices	0≤h≤11,-19≤k≤18,-22≤l≤22
Reflections collected / unique	10404 / 9771[R(int)=0.0468]
Completeness to θ	25.00; 98.3%
Refinement method	full-matrix least-squares on F^2
Data / restraints / parameters	9771 / 0 / 514
(Goodness-of-fit on F^2)	0.891
Final R indices [I>2σ(I)]	R1=0.0580, wR2=0.1449
R indices (all data)	R1=0.0863, wR2=0.1543
Largest diff. peak and hole (e.Å^{-3})	2.426 and –0.521

5.5.2 Atomic coordinates (×10^4) and equivalent isotropic displacement parameters (A^2×10^3) for Mn(6-Hyp-Hgual)$_2$, U(eq) is defined as one third of the trace of the orthogonalized ij tensor.

atom	x/a	y/b	z/c	U(eq)	atom	x/a	y/b	z/c	U(eq)
Mn(1)	6251(1)	3453(1)	4793(1)	25(1)					
C(2)	7303(5)	4614(2)	5333(2)	36(1)	C(12)	4471(4)	3041(3)	4082(2)	35(1)
C(3)	5957(5)	4499(3)	5618(2)	37(1)	C(13)	5536(4)	3442(3)	3717(2)	32(1)
C(10)	5898(4)	3791(2)	5946(2)	30(1)	C(20)	6707(4)	2983(2)	3667(2)	27(1)
C(4)	4681(4)	3437(3)	6286(2)	35(1)	C(14)	8048(5)	3204(2)	3363(2)	29(1)
C(41)	3268(5)	3606(4)	6030(2)	54(1)	C(141)	8410(5)	4113(2)	3331(2)	40(1)
C(5)	4799(4)	2999(3)	6802(2)	36(1)	C(15)	8938(4)	2650(2)	3106(2)	28(1)
C(6)	6084(4)	2788(2)	7148(2)	29(1)	C(16)	8780(4)	1723(2)	3022(2)	24(1)
Si(1)	6921(1)	3670(1)	7991(1)	21(1)	Si(2)	7892(1)	1188(1)	2050(1)	21(1)
Si(11)	5874(1)	3255(1)	9005(1)	29(1)	Si(21)	9169(1)	1831(1)	1211(1)	32(1)
C(111)	3937(5)	3347(3)	8968(2)	48(1)	C(211)	8835(6)	2931(3)	1252(3)	58(1)
C(112)	6057(6)	2125(3)	8968(3)	52(1)	C(212)	11117(5)	1872(4)	1411(3)	58(1)
C(113)	6674(5)	3875(3)	9913(2)	50(1)	C(213)	8745(7)	1245(4)	232(3)	69(2)
Si(12)	6445(1)	5049(1)	8026(1)	31(1)	Si(22)	5487(1)	1284(1)	1854(1)	27(1)
C(121)	7554(6)	5563(3)	7411(2)	47(1)	C(221)	4367(5)	906(3)	2543(2)	51(1)
C(122)	6830(6)	5697(3)	8986(2)	47(1)	C(222)	5156(5)	2368(3)	1823(3)	49(1)
C(123)	4547(5)	5107(3)	7800(3)	51(1)	C(223)	4865(5)	593(3)	944(2)	55(1)
Si(13)	9373(1)	3720(1)	8176(1)	28(1)	Si(23)	8307(1)	-232(1)	1759(1)	31(1)
C(131)	10372(5)	3856(3)	7355(3)	47(1)	C(231)	10242(5)	-292(3)	1862(3)	44(1)
C(132)	10036(5)	4649(3)	8927(3)	48(1)	C(232)	7735(6)	-774(3)	789(2)	49(1)
C(133)	9857(5)	2774(3)	8471(3)	52(1)	C(233)	7328(6)	-878(3)	2339(3)	50(1)
C(7)	7146(4)	2413(2)	6621(2)	27(1)	C(17)	8260(4)	1377(2)	3667(2)	25(1)
C(71)	7579(5)	1605(3)	6757(2)	42(1)	C(171)	9077(4)	710(2)	3848(2)	30(1)
C(711)	9029(6)	1412(3)	6489(3)	51(1)	C(172)	10508(5)	1106(3)	4227(2)	46(1)
C(712)	6458(6)	874(3)	6422(3)	58(1)	C(173)	8324(5)	150(3)	4303(2)	42(1)
C(8)	7635(4)	2729(2)	6061(2)	24(1)	C(18)	7223(4)	1640(2)	4090(2)	24(1)
C(9)	7224(4)	3465(2)	5850(2)	24(1)	C(19)	6363(4)	2296(2)	4004(2)	24(1)
C(1)	8084(4)	3978(2)	5458(2)	28(1)	C(11)	4977(4)	2342(3)	4278(2)	32(1)
C(101)	9561(4)	3862(3)	5243(2)	38(1)	C(201)	4217(5)	1728(3)	4673(2)	42(1)

5.5.3 Bond lengths [Å] for Mn(6-Hyp-Hgual)$_2$

Bonds	Bond lengths	Bonds	Bond lengths	Bonds	Bond lengths
Mn(1)-C(12)	2.081(4)	Si(11)-C(113)	1.865(4)	C(15)-C(16)	1.487(5)
Mn(1)-C(2)	2.082(4)	Si(11)-C(112)	1.874(5)	C(16)-C(17)	1.503(5)
Mn(1)-C(3)	2.089(4)	Si(11)-C(111)	1.874(5)	C(16)-Si(2)	1.954(3)
Mn(1)-C(13)	2.092(4)	Si(12)-C(121)	1.845(5)	Si(2)-Si(22)	2.3460(15)
Mn(1)-C(11)	2.097(4)	Si(12)-C(123)	1.870(5)	Si(2)-Si(21)	2.3522(15)
Mn(1)-C(1)	2.103(4)	Si(12)-C(122)	1.869(4)	Si(2)-Si(23)	2.3608(15)

Mn(1)-C(10)	2.135(4)	Si(13)-C(131)	1.856(4)	Si(21)-C(211)	1.858(5)
Mn(1)-C(20)	2.136(4)	Si(13)-C(133)	1.859(5)	Si(21)-C(213)	1.872(5)
Mn(1)-C(19)	2.147(3)	Si(13)-C(132)	1.866(4)	Si(21)-C(212)	1.880(5)
Mn(1)-C(9)	2.148(4)	C(7)-C(8)	1.330(5)	Si(22)-C(221)	1.848(5)
C(2)-C(3)	1.408(6)	C(7)-C(71)	1.506(5)	Si(22)-C(223)	1.858(4)
C(2)-C(1)	1.409(6)	C(71)-C(712)	1.524(7)	Si(22)-C(222)	1.860(5)
C(3)-C(10)	1.423(6)	C(71)-C(711)	1.526(7)	Si(23)-C(233)	1.864(5)
C(10)-C(9)	1.430(5)	C(8)-C(9)	1.443(5)	Si(23)-C(232)	1.864(4)
C(10)-C(4)	1.457(6)	C(9)-C(1)	1.431(5)	Si(23)-C(231)	1.870(5)
C(4)-C(5)	1.328(6)	C(1)-C(101)	1.496(6)	C(17)-C(18)	1.330(5)
C(4)-C(41)	1.497(6)	C(12)-C(13)	1.413(6)	C(17)-C(171)	1.507(5)
C(5)-C(6)	1.483(6)	C(12)-C(11)	1.410(6)	C(171)-C(173)	1.513(6)
C(6)-C(7)	1.514(5)	C(13)-C(20)	1.415(5)	C(171)-C(172)	1.528(6)
C(6)-Si(1)	1.968(4)	C(20)-C(19)	1.415(5)	C(18)-C(19)	1.462(5)
Si(1)-Si(11)	2.3424(15)	C(20)-C(14)	1.449(6)	C(19)-C(11)	1.433(6)
Si(1)-Si(13)	2.3485(15)	C(14)-C(15)	1.337(5)	C(11)-C(201)	1.503(6)
Si(1)-Si(12)	2.3507(15)	C(14)-C(141)	1.509(5)		

5.5.4 Bond angles for Mn(6-Hyp-Hgual)$_2$ (deg)

Bond angle	parameters	Bond angle	parameters	Bond angle	parameters
C(12)-Mn(1)-C(2)	135.70(17)	C(5)-C(4)-C(10)	122.7(4)	C(19)-C(20)-C(13)	107.8(4)
C(12)-Mn(1)-C(3)	111.88(17)	C(5)-C(4)-C(41)	121.2(4)	C(19)-C(20)-C(14)	126.1(3)
C(2)-Mn(1)-C(3)	39.48(18)	C(10)-C(4)-C(41)	116.1(4)	C(13)-C(20)-C(14)	126.0(4)
C(12)-Mn(1)-C(13)	39.57(17)	C(4)-C(5)-C(6)	129.7(4)	C(19)-C(20)-Mn(1)	71.1(2)
C(2)-Mn(1)-C(13)	112.57(16)	C(5)-C(6)-C(7)	115.9(3)	C(13)-C(20)-Mn(1)	68.8(2)
C(3)-Mn(1)-C(13)	117.16(15)	C(5)-C(6)-Si(1)	113.7(3)	C(14)-C(20)-Mn(1)	123.0(3)
C(12)-Mn(1)-C(11)	39.45(16)	C(7)-C(6)-Si(1)	114.3(3)	C(15)-C(14)-C(20)	123.7(4)
C(2)-Mn(1)-C(11)	173.45(17)	C(6)-Si(1)-Si(11)	102.90(12)	C(15)-C(14)-C(141)	119.8(4)
C(3)-Mn(1)-C(11)	134.57(18)	C(6)-Si(1)-Si(13)	114.32(13)	C(20)-C(14)-C(141)	116.5(3)
C(13)-Mn(1)-C(11)	66.40(17)	Si(11)-Si(1)-Si(13)	107.14(6)	C(14)-C(15)-C(16)	130.1(4)
C(12)-Mn(1)-C(1)	173.93(17)	C(6)-Si(1)-Si(12)	117.11(13)	C(15)-C(16)-C(17)	117.7(3)
C(2)-Mn(1)-C(1)	39.34(16)	Si(11)-Si(1)-Si(12)	107.37(5)	C(15)-C(16)-Si(2)	108.9(2)
C(3)-Mn(1)-C(1)	66.38(16)	Si(13)-Si(1)-Si(12)	107.29(6)	C(17)-C(16)-Si(2)	117.1(3)
C(13)-Mn(1)-C(1)	135.31(17)	C(113)-Si(11)-C(112)	107.2(2)	C(16)-Si(2)-Si(22)	117.89(12)
C(11)-Mn(1)-C(1)	145.88(16)	C(113)-Si(11)-C(111)	109.1(2)	C(16)-Si(2)-Si(21)	105.29(12)
C(12)-Mn(1)-C(10)	116.75(16)	C(112)-Si(11)-C(111)	107.1(2)	Si(22)-Si(2)-Si(21)	108.32(6)
C(2)-Mn(1)-C(10)	65.75(16)	C(113)-Si(11)-Si(1)	113.38(16)	C(16)-Si(2)-Si(23)	108.74(12)
C(3)-Mn(1)-C(10)	39.35(16)	C(112)-Si(11)-Si(1)	110.07(16)	Si(22)-Si(2)-Si(23)	110.11(6)
C(13)-Mn(1)-C(10)	146.92(15)	C(111)-Si(11)-Si(1)	109.81(15)	Si(21)-Si(2)-Si(23)	105.74(6)
C(11)-Mn(1)-C(10)	111.27(16)	C(121)-Si(12)-C(123)	109.0(2)	C(211)-Si(21)-C(213)	106.4(3)
C(1)-Mn(1)-C(10)	65.96(15)	C(121)-Si(12)-C(122)	106.9(2)	C(211)-Si(21)-C(212)	106.3(3)
C(12)-Mn(1)-C(20)	65.77(15)	C(123)-Si(12)-C(122)	105.9(2)	C(213)-Si(21)-C(212)	108.2(3)
C(2)-Mn(1)-C(20)	117.64(16)	C(121)-Si(12)-Si(1)	112.61(16)	C(211)-Si(21)-Si(2)	113.93(17)
C(3)-Mn(1)-C(20)	147.14(16)	C(123)-Si(12)-Si(1)	112.79(16)	C(213)-Si(21)-Si(2)	111.70(18)
C(13)-Mn(1)-C(20)	39.08(14)	C(122)-Si(12)-Si(1)	109.19(16)	C(212)-Si(21)-Si(2)	109.96(17)
C(11)-Mn(1)-C(20)	66.03(15)	C(131)-Si(13)-C(133)	109.0(2)	C(221)-Si(22)-C(223)	105.9(2)
C(1)-Mn(1)-C(20)	112.24(15)	C(131)-Si(13)-C(132)	105.6(2)	C(221)-Si(22)-C(222)	109.4(2)
C(10)-Mn(1)-C(20)	172.92(14)	C(133)-Si(13)-C(132)	107.1(2)	C(223)-Si(22)-C(222)	107.3(2)
C(12)-Mn(1)-C(19)	65.49(15)	C(131)-Si(13)-Si(1)	113.44(16)	C(221)-Si(22)-Si(2)	113.14(16)
C(2)-Mn(1)-C(19)	146.73(17)	C(133)-Si(13)-Si(1)	112.05(16)	C(223)-Si(22)-Si(2)	108.55(16)
C(3)-Mn(1)-C(19)	173.20(17)	C(132)-Si(13)-Si(1)	109.31(16)	C(222)-Si(22)-Si(2)	112.21(16)
C(13)-Mn(1)-C(19)	65.26(14)	C(8)-C(7)-C(71)	121.2(3)	C(233)-Si(23)-C(232)	104.7(2)
C(11)-Mn(1)-C(19)	39.43(15)	C(8)-C(7)-C(6)	124.6(3)	C(233)-Si(23)-C(231)	109.6(2)
C(1)-Mn(1)-C(19)	116.92(15)	C(71)-C(7)-C(6)	114.1(3)	C(232)-Si(23)-C(231)	106.8(2)
C(10)-Mn(1)-C(19)	135.27(15)	C(7)-C(71)-C(712)	110.0(4)	C(233)-Si(23)-Si(2)	113.07(16)
C(20)-Mn(1)-C(19)	38.59(14)	C(7)-C(71)-C(711)	114.9(4)	C(232)-Si(23)-Si(2)	112.87(16)
C(12)-Mn(1)-C(9)	146.08(16)	C(712)-C(71)-C(711)	110.2(4)	C(231)-Si(23)-Si(2)	109.47(15)
C(2)-Mn(1)-C(9)	65.63(15)	C(7)-C(8)-C(9)	125.9(4)	C(18)-C(17)-C(16)	125.6(3)
C(3)-Mn(1)-C(9)	65.87(14)	C(1)-C(9)-C(10)	107.5(3)	C(18)-C(17)-C(171)	119.8(3)
C(13)-Mn(1)-C(9)	173.45(16)	C(1)-C(9)-C(8)	124.5(3)	C(16)-C(17)-C(171)	114.5(3)
C(11)-Mn(1)-C(9)	116.15(15)	C(10)-C(9)-C(8)	127.9(4)	C(17)-C(171)-C(173)	115.6(3)
C(1)-Mn(1)-C(9)	39.33(15)	C(1)-C(9)-Mn(1)	68.6(2)	C(17)-C(171)-C(172)	110.4(3)
C(10)-Mn(1)-C(9)	38.99(14)	C(10)-C(9)-Mn(1)	70.0(2)	C(173)-C(171)-C(172)	109.7(3)
C(20)-Mn(1)-C(9)	135.36(14)	C(8)-C(9)-Mn(1)	124.0(2)	C(17)-C(18)-C(19)	126.6(3)
C(19)-Mn(1)-C(9)	112.45(14)	C(2)-C(1)-C(9)	107.7(4)	C(20)-C(19)-C(11)	108.2(3)

C(3)-C(2)-C(1)	109.1(4)	C(2)-C(1)-C(101)	126.9(4)	C(20)-C(19)-C(18)	128.6(4)
C(3)-C(2)-Mn(1)	70.5(2)	C(9)-C(1)-C(101)	125.4(4)	C(11)-C(19)-C(18)	123.2(3)
C(1)-C(2)-Mn(1)	71.1(2)	C(2)-C(1)-Mn(1)	69.5(2)	C(20)-C(19)-Mn(1)	70.3(2)
C(2)-C(3)-C(10)	108.0(4)	C(9)-C(1)-Mn(1)	72.1(2)	C(11)-C(19)-Mn(1)	68.4(2)
C(2)-C(3)-Mn(1)	70.0(2)	C(101)-C(1)-Mn(1)	125.2(3)	C(18)-C(19)-Mn(1)	126.0(2)
C(10)-C(3)-Mn(1)	72.1(2)	C(13)-C(12)-C(11)	108.7(4)	C(12)-C(11)-C(19)	107.2(4)
C(3)-C(10)-C(9)	107.8(4)	C(13)-C(12)-Mn(1)	70.6(2)	C(12)-C(11)-C(201)	127.8(4)
C(3)-C(10)-C(4)	126.0(4)	C(11)-C(12)-Mn(1)	70.9(2)	C(19)-C(11)-C(201)	125.0(4)
C(9)-C(10)-C(4)	126.2(4)	C(12)-C(13)-C(20)	108.2(4)	C(12)-C(11)-Mn(1)	69.7(2)
C(3)-C(10)-Mn(1)	68.5(2)	C(12)-C(13)-Mn(1)	69.8(2)	C(19)-C(11)-Mn(1)	72.2(2)
C(9)-C(10)-Mn(1)	71.0(2)	C(20)-C(13)-Mn(1)	72.2(2)	C(201)-C(11)-Mn(1)	125.1(3)
C(4)-C(10)-Mn(1)	123.7(3)				

5.5.5 Anisotropic displacement parameters ($A^2 \times 10^3$) for Mn(6-Hyp-Hgual)$_2$. The anisotropic displacement factor exponent takes the form:$-2\pi^2[h^2a^{*2}U11+ ... + 2hka^*b^*U12]$

atom	U11	U22	U33	U23	U13	U12
Mn(1)	34(1)	24(1)	18(1)	0(1)	0(1)	11(1)
C(2)	60(3)	24(2)	23(2)	1(2)	-3(2)	2(2)
C(3)	65(3)	30(2)	17(2)	-3(2)	-3(2)	28(2)
C(10)	39(2)	31(2)	19(2)	-3(2)	-1(2)	17(2)
C(4)	36(2)	49(3)	18(2)	-5(2)	2(2)	16(2)
C(41)	34(3)	99(4)	25(2)	-4(2)	-1(2)	28(3)
C(5)	31(2)	48(3)	22(2)	-5(2)	5(2)	2(2)
C(6)	34(2)	34(2)	16(2)	4(2)	5(2)	1(2)
Si(1)	25(1)	22(1)	14(1)	1(1)	3(1)	6(1)
Si(11)	29(1)	39(1)	19(1)	8(1)	2(1)	1(1)
C(111)	35(3)	70(3)	37(2)	10(2)	8(2)	2(2)
C(112)	61(3)	50(3)	52(3)	29(2)	6(3)	-1(3)
C(113)	61(3)	66(3)	20(2)	8(2)	-1(2)	-5(3)
Si(12)	43(1)	24(1)	27(1)	4(1)	4(1)	11(1)
C(121)	74(3)	33(2)	31(2)	8(2)	6(2)	-3(2)
C(122)	73(3)	35(2)	29(2)	-8(2)	5(2)	20(2)
C(123)	56(3)	39(3)	61(3)	11(2)	-9(3)	23(2)
Si(13)	25(1)	28(1)	27(1)	-1(1)	2(1)	3(1)
C(131)	36(3)	55(3)	46(3)	3(2)	18(2)	0(2)
C(132)	39(3)	52(3)	43(3)	-9(2)	-3(2)	-1(2)
C(133)	40(3)	51(3)	70(3)	18(3)	-5(2)	13(2)
C(7)	35(2)	23(2)	20(2)	-1(2)	0(2)	5(2)
C(71)	79(3)	29(2)	19(2)	6(2)	8(2)	16(2)
C(711)	76(4)	42(3)	39(3)	4(2)	5(2)	37(3)
C(712)	86(4)	25(2)	60(3)	5(2)	21(3)	2(3)
C(8)	34(2)	18(2)	19(2)	0(1)	-1(2)	5(2)
C(9)	27(2)	24(2)	18(2)	-4(1)	-4(2)	6(2)
C(1)	39(2)	23(2)	20(2)	0(2)	-3(2)	1(2)
C(101)	39(2)	43(3)	31(2)	13(2)	-1(2)	-8(2)
C(12)	34(2)	48(3)	21(2)	-5(2)	-4(2)	20(2)
C(13)	46(3)	34(2)	19(2)	0(2)	-3(2)	22(2)
C(20)	41(2)	23(2)	17(2)	0(2)	-2(2)	12(2)
C(14)	46(2)	21(2)	20(2)	3(2)	2(2)	3(2)
C(141)	58(3)	21(2)	42(2)	6(2)	10(2)	8(2)
C(15)	31(2)	32(2)	23(2)	8(2)	3(2)	4(2)
C(16)	26(2)	26(2)	18(2)	0(2)	0(2)	8(2)
Si(2)	25(1)	23(1)	14(1)	-1(1)	1(1)	7(1)
Si(21)	36(1)	37(1)	26(1)	12(1)	7(1)	7(1)
C(211)	71(4)	48(3)	68(3)	36(3)	23(3)	20(3)
C(212)	37(3)	73(4)	69(4)	27(3)	13(2)	4(3)
C(213)	102(5)	78(4)	25(2)	12(2)	16(3)	-2(4)
Si(22)	26(1)	32(1)	19(1)	-3(1)	-2(1)	6(1)
C(221)	36(3)	79(4)	36(2)	12(2)	5(2)	-5(3)
C(222)	38(3)	45(3)	62(3)	3(2)	-11(2)	19(2)
C(223)	50(3)	68(3)	36(3)	-17(2)	-15(2)	15(3)
Si(23)	43(1)	24(1)	26(1)	1(1)	3(1)	9(1)
C(231)	47(3)	40(3)	49(3)	10(2)	5(2)	20(2)

C(232)	74(4)	39(3)	31(2)	-5(2)	0(2)	15(2)
C(233)	63(3)	42(3)	40(3)	7(2)	2(2)	-4(2)
C(17)	33(2)	20(2)	19(2)	-2(1)	-4(2)	6(2)
C(171)	38(2)	31(2)	23(2)	4(2)	-3(2)	12(2)
C(172)	51(3)	49(3)	41(3)	13(2)	-13(2)	19(2)
C(173)	65(3)	38(2)	34(2)	17(2)	10(2)	27(2)
C(18)	35(2)	20(2)	16(2)	1(1)	2(2)	-1(2)
C(19)	33(2)	21(2)	16(2)	0(1)	-2(2)	3(2)
C(11)	35(2)	34(2)	22(2)	-5(2)	0(2)	5(2)
C(201)	36(2)	47(3)	39(2)	2(2)	10(2)	-1(2)

5.6 Crystallographic data for Fe(6-Hyp-Hgual)$_2$

5.6.1 Crystallographic data and structure refinement for Fe(6-Hyp-Hgual)$_2$

Empirical formula	$C_{48}H_{90}FeSi_8$
Formula weight (g/mol)	947.77
Temperature (K)	173(2)
Wavelength(Å)	0.71073
Crystal system, space group	triclinic, P(-1)
Unit cell dimensions (Å ,deg)	a=9.5990(10) α=102.891(8) b=16.524(2) β=91.357(8) c=18.5772(17) γ=96.984(9)
Volume (Å^3)	2847.0(5)
Z; calc. density (Mg/m^3)	2; 1.106
Absorption coefficient (mm^{-1})	0.462
F(000)	1032
Theta range for data collection (deg)	1.88 ~27.00
Limiting indices	$-5 \le h \le 5, -20 \le k \le 20, -23 \le l \le 23$
Reflections collected / unique	8059 / 7314[R(int)=0.0472]
Completeness to θ	27.00; 58.8%
Refinement method	full-matrix least-squares on F^2
Data / restraints / parameters	7314 / 0 / 514
(Goodness-of-fit on F^2)	1.009
Final R indices [I>2σ(I)]	R1=0.0505, wR2=0.1171
R indices (all data)	R1=0.0852, wR2=0.1338
Largest diff. peak and hole (e.Å^{-3})	1.289 and –0.292

5.6.2 Atomic coordinates (×10^4) and equivalent isotropic displacement parameters (Å^2×10^3) for Fe(6-Hyp-Hgual)$_2$, U(eq) is defined as one third of the trace of the orthogonalized Uij tensor.

atom	x/a	y/b	z/c	U(eq)	atom	x/a	y/b	z/c	U(eq)
Fe(1)	3733(1)	-3445(1)	204(1)	23(1)	C(12)	5518(6)	-3054(3)	889(2)	28(2)
Si(23)	785(2)	-1848(1)	3776(1)	31(1)	C(13)	4425(6)	-3465(3)	1249(2)	24(2)
Si(22)	1680(2)	221(1)	3240(1)	29(1)	C(20)	3247(6)	-3015(2)	1296(2)	22(2)
C(2)	2702(7)	-4588(2)	-307(2)	31(2)	C(14)	1925(6)	-3229(2)	1613(2)	25(2)
C(3)	4038(7)	-4471(2)	-588(2)	32(2)	C(141)	1564(6)	-4138(2)	1660(2)	34(2)
C(10)	4118(7)	-3751(3)	-912(2)	23(2)	C(15)	1035(6)	-2682(2)	1877(2)	26(2)
C(4)	5335(7)	-3417(3)	-1256(2)	27(2)	C(16)	1177(6)	-1745(2)	1959(2)	18(1)
C(41)	6751(7)	-3599(3)	-1019(2)	43(2)	Si(2)	2082(2)	-1203(1)	2938(1)	20(1)
C(5)	5223(6)	-2993(3)	-1788(2)	30(2)	Si(21)	4478(2)	-1309(1)	3135(1)	26(1)
C(6)	3937(6)	-2767(2)	-2127(2)	25(2)	C(211)	4805(7)	-2401(3)	3146(3)	45(2)
Si(1)	3097(2)	-3649(1)	-2983(1)	20(1)	C(212)	5110(7)	-634(3)	4066(2)	49(2)
Si(11)	643(2)	-3712(1)	-3172(1)	27(1)	C(213)	5614(6)	-916(3)	2450(2)	43(2)
C(111)	136(6)	-2775(3)	-3480(3)	45(2)	C(221)	2289(7)	758(3)	4219(2)	50(2)

C(112)	-339(6)	-3847(3)	-2344(2)	41(2)	C(222)	2658(7)	870(3)	2653(2)	46(2)
C(113)	-25(6)	-4648(3)	-3926(2)	45(2)	C(223)	-245(6)	286(3)	3150(3)	39(2)
Si(12)	4139(2)	-3236(1)	-4004(1)	28(1)	C(231)	-1139(7)	-1899(3)	3568(3)	51(2)
C(121)	3950(7)	-2109(3)	-3965(3)	51(2)	C(232)	1182(7)	-1246(3)	4757(2)	60(2)
C(122)	3337(6)	-3865(3)	-4917(2)	43(2)	C(233)	1140(7)	-2945(3)	3739(3)	53(2)
C(123)	6058(7)	-3326(3)	-3971(3)	43(2)	C(17)	1723(6)	-1401(2)	1311(2)	23(2)
Si(13)	3580(2)	-5028(1)	-3018(1)	29(1)	C(171)	887(5)	-722(2)	1145(2)	22(2)
C(131)	5455(6)	-5087(3)	-2794(3)	46(2)	C(172)	-539(6)	-1117(3)	758(2)	42(2)
C(132)	3204(6)	-5681(3)	-3985(2)	42(2)	C(173)	1671(6)	-156(2)	695(2)	35(2)
C(133)	2457(7)	-5541(3)	-2400(2)	43(2)	C(18)	2731(5)	-1663(2)	885(2)	20(2)
C(7)	2882(6)	-2398(2)	-1608(2)	24(2)	C(19)	3590(7)	-2314(2)	957(2)	19(2)
C(71)	2428(7)	-1591(2)	-1757(2)	34(2)	C(11)	4965(7)	-2355(2)	692(2)	27(2)
C(72)	981(7)	-1401(3)	-1497(3)	42(2)	C(201)	5766(6)	-1744(3)	303(2)	40(2)
C(73)	3553(7)	-852(3)	-1417(3)	56(2)	C(1)	1912(7)	-3947(2)	-427(2)	23(2)
C(8)	2382(5)	-2697(2)	-1037(2)	19(1)	C(101)	452(7)	-3828(3)	-214(2)	37(2)
C(9)	2800(6)	-3432(2)	-816(2)	18(2)					

5.6.3 Bond lengths [Å] for Fe(6-Hyp-Hgual)$_2$

bond	Bond lengths	bond	Bond lengths	bond	Bond lengths
Fe(1)-C(2)	2.037(4)	C(4)-C(5)	1.343(6)	C(1)-C(101)	1.489(7)
Fe(1)-C(3)	2.039(4)	C(4)-C(41)	1.503(7)	C(12)-C(13)	1.440(7)
Fe(1)-C(11)	2.041(4)	C(5)-C(6)	1.496(7)	C(12)-C(11)	1.442(6)
Fe(1)-C(13)	2.046(4)	C(6)-C(7)	1.503(6)	C(13)-C(20)	1.422(7)
Fe(1)-C(12)	2.057(5)	C(6)-Si(1)	1.980(4)	C(20)-C(19)	1.444(5)
Fe(1)-C(1)	2.058(6)	Si(1)-Si(12)	2.3591(17)	C(20)-C(14)	1.450(7)
Fe(1)-C(10)	2.074(4)	Si(1)-Si(11)	2.360(2)	C(14)-C(15)	1.341(6)
Fe(1)-C(20)	2.078(4)	Si(1)-Si(13)	2.3671(16)	C(14)-C(141)	1.522(5)
Fe(1)-C(9)	2.082(4)	Si(11)-C(112)	1.863(5)	C(15)-C(16)	1.510(5)
Fe(1)-C(19)	2.091(4)	Si(11)-C(113)	1.876(4)	C(16)-C(17)	1.521(5)
Si(23)-C(231)	1.865(6)	Si(11)-C(111)	1.879(5)	C(16)-Si(2)	1.968(4)
Si(23)-C(233)	1.872(5)	Si(12)-C(123)	1.867(7)	Si(2)-Si(21)	2.354(2)
Si(23)-C(232)	1.876(5)	Si(12)-C(122)	1.872(4)	Si(21)-C(213)	1.870(5)
Si(23)-Si(2)	2.3711(18)	Si(12)-C(121)	1.878(5)	Si(21)-C(211)	1.872(5)
Si(22)-C(223)	1.869(6)	Si(13)-C(131)	1.856(6)	Si(21)-C(212)	1.878(4)
Si(22)-C(221)	1.882(4)	Si(13)-C(133)	1.863(5)	C(17)-C(18)	1.317(6)
Si(22)-C(222)	1.883(5)	Si(13)-C(132)	1.881(4)	C(17)-C(171)	1.535(6)
Si(22)-Si(2)	2.3756(16)	C(7)-C(8)	1.342(5)	C(171)-C(172)	1.530(6)
C(2)-C(3)	1.404(7)	C(7)-C(71)	1.531(6)	C(171)-C(173)	1.531(6)
C(2)-C(1)	1.428(7)	C(71)-C(72)	1.526(7)	C(18)-C(19)	1.461(6)
C(3)-C(10)	1.443(6)	C(71)-C(73)	1.535(7)	C(19)-C(11)	1.424(7)
C(10)-C(9)	1.429(7)	C(8)-C(9)	1.462(5)	C(11)-C(201)	1.515(6)
C(10)-C(4)	1.455(7)	C(9)-C(1)	1.448(7)		

5.6.4 Bond angles for Fe(6-Hyp-Hgual)$_2$ (deg)

Bond angles	parameters	Bond angles	Parames	Bond angles	parames
C(2)-Fe(1)-C(3)	40.30(19)	C(3)-C(2)-C(1)	109.5(4)	C(2)-C(1)-C(9)	106.6(5)
C(2)-Fe(1)-C(11)	173.7(3)	C(3)-C(2)-Fe(1)	69.9(3)	C(2)-C(1)-C(101)	127.5(4)
C(3)-Fe(1)-C(11)	134.0(3)	C(1)-C(2)-Fe(1)	70.4(2)	C(9)-C(1)-C(101)	125.9(4)
C(2)-Fe(1)-C(13)	109.88(17)	C(2)-C(3)-C(10)	108.3(5)	C(2)-C(1)-Fe(1)	68.8(3)
C(3)-Fe(1)-C(13)	114.56(18)	C(2)-C(3)-Fe(1)	69.8(2)	C(9)-C(1)-Fe(1)	70.4(3)
C(11)-Fe(1)-C(13)	68.92(17)	C(10)-C(3)-Fe(1)	70.8(2)	C(101)-C(1)-Fe(1)	126.5(3)
C(2)-Fe(1)-C(12)	133.98(19)	C(9)-C(10)-C(3)	107.1(5)	C(13)-C(12)-C(11)	106.8(5)
C(3)-Fe(1)-C(12)	109.4(2)	C(9)-C(10)-C(4)	127.4(4)	C(13)-C(12)-Fe(1)	69.0(3)
C(11)-Fe(1)-C(12)	41.20(18)	C(3)-C(10)-C(4)	125.5(6)	C(11)-C(12)-Fe(1)	68.8(3)
C(13)-Fe(1)-C(12)	41.08(19)	C(9)-C(10)-Fe(1)	70.2(2)	C(20)-C(13)-C(12)	108.9(4)
C(2)-Fe(1)-C(1)	40.81(18)	C(3)-C(10)-Fe(1)	68.2(2)	C(20)-C(13)-Fe(1)	71.0(2)
C(3)-Fe(1)-C(1)	68.7(2)	C(4)-C(10)-Fe(1)	126.0(3)	C(12)-C(13)-Fe(1)	69.9(2)
C(11)-Fe(1)-C(1)	144.35(19)	C(5)-C(4)-C(10)	122.5(6)	C(13)-C(20)-C(19)	107.8(5)
C(13)-Fe(1)-C(1)	133.6(2)	C(5)-C(4)-C(41)	120.1(5)	C(13)-C(20)-C(14)	126.1(4)
C(12)-Fe(1)-C(1)	173.66(16)	C(10)-C(4)-C(41)	117.3(5)	C(19)-C(20)-C(14)	126.1(5)
C(2)-Fe(1)-C(10)	68.30(19)	C(4)-C(5)-C(6)	129.4(5)	C(13)-C(20)-Fe(1)	68.6(2)

C(3)-Fe(1)-C(10)	41.05(16)	C(5)-C(6)-C(7)	117.2(3)	C(19)-C(20)-Fe(1)	70.2(2)
C(11)-Fe(1)-C(10)	109.0(2)	C(5)-C(6)-Si(1)	112.6(3)	C(14)-C(20)-Fe(1)	125.8(3)
C(13)-Fe(1)-C(10)	145.6(2)	C(7)-C(6)-Si(1)	114.1(3)	C(15)-C(14)-C(20)	124.5(4)
C(12)-Fe(1)-C(10)	114.0(2)	C(6)-Si(1)-Si(12)	103.48(14)	C(15)-C(14)-C(141)	118.9(5)
C(1)-Fe(1)-C(10)	68.8(2)	C(6)-Si(1)-Si(11)	114.45(17)	C(20)-C(14)-C(141)	116.6(4)
C(2)-Fe(1)-C(20)	114.9(2)	Si(12)-Si(1)-Si(11)	107.14(7)	C(14)-C(15)-C(16)	130.2(5)
C(3)-Fe(1)-C(20)	145.16(16)	C(6)-Si(1)-Si(13)	116.54(14)	C(15)-C(16)-C(17)	117.5(3)
C(11)-Fe(1)-C(20)	68.4(2)	Si(12)-Si(1)-Si(13)	107.30(7)	C(15)-C(16)-Si(2)	108.4(2)
C(13)-Fe(1)-C(20)	40.33(18)	Si(11)-Si(1)-Si(13)	107.27(7)	C(17)-C(16)-Si(2)	116.4(3)
C(12)-Fe(1)-C(20)	68.5(2)	C(112)-Si(11)-C(113)	105.7(2)	C(16)-Si(2)-Si(21)	117.89(16)
C(1)-Fe(1)-C(20)	109.3(2)	C(112)-Si(11)-C(111)	109.3(3)	C(16)-Si(2)-Si(23)	104.70(14)
C(10)-Fe(1)-C(20)	173.15(18)	C(113)-Si(11)-C(111)	106.3(2)	Si(21)-Si(2)-Si(23)	108.38(7)
C(2)-Fe(1)-C(9)	68.07(16)	C(112)-Si(11)-Si(1)	113.13(19)	C(16)-Si(2)-Si(22)	109.04(13)
C(3)-Fe(1)-C(9)	68.19(18)	C(113)-Si(11)-Si(1)	109.5(2)	Si(21)-Si(2)-Si(22)	110.54(7)
C(11)-Fe(1)-C(9)	113.82(16)	C(111)-Si(11)-Si(1)	112.5(2)	Si(23)-Si(2)-Si(22)	105.44(7)
C(13)-Fe(1)-C(9)	173.5(2)	C(123)-Si(12)-C(122)	108.6(2)	C(213)-Si(21)-C(211)	109.1(3)
C(12)-Fe(1)-C(9)	144.7(2)	C(123)-Si(12)-C(121)	107.5(3)	C(213)-Si(21)-C(212)	106.1(2)
C(1)-Fe(1)-C(9)	40.96(18)	C(122)-Si(12)-C(121)	107.4(2)	C(211)-Si(21)-C(212)	106.9(2)
C(10)-Fe(1)-C(9)	40.21(18)	C(123)-Si(12)-Si(1)	109.91(16)	C(213)-Si(21)-Si(2)	113.06(19)
C(20)-Fe(1)-C(9)	134.2(2)	C(122)-Si(12)-Si(1)	113.38(17)	C(211)-Si(21)-Si(2)	112.7(2)
C(2)-Fe(1)-C(19)	145.6(3)	C(121)-Si(12)-Si(1)	109.86(18)	C(212)-Si(21)-Si(2)	108.6(2)
C(3)-Fe(1)-C(19)	173.5(2)	C(131)-Si(13)-C(133)	109.3(3)	C(18)-C(17)-C(16)	126.7(4)
C(11)-Fe(1)-C(19)	40.30(18)	C(131)-Si(13)-C(132)	105.2(3)	C(18)-C(17)-C(171)	120.7(3)
C(13)-Fe(1)-C(19)	68.06(16)	C(133)-Si(13)-C(132)	107.2(2)	C(16)-C(17)-C(171)	112.5(4)
C(12)-Fe(1)-C(19)	68.3(2)	C(131)-Si(13)-Si(1)	113.35(16)	C(172)-C(171)-C(173)	110.2(3)
C(1)-Fe(1)-C(19)	114.2(2)	C(133)-Si(13)-Si(1)	112.20(17)	C(172)-C(171)-C(17)	110.5(3)
C(10)-Fe(1)-C(19)	133.55(16)	C(132)-Si(13)-Si(1)	109.12(15)	C(173)-C(171)-C(17)	113.9(4)
C(20)-Fe(1)-C(19)	40.53(15)	C(8)-C(7)-C(6)	125.8(4)	C(17)-C(18)-C(19)	127.2(4)
C(9)-Fe(1)-C(19)	109.88(17)	C(8)-C(7)-C(71)	120.1(4)	C(11)-C(19)-C(20)	107.8(4)
C(231)-Si(23)-C(233)	106.8(3)	C(6)-C(7)-C(71)	114.1(4)	C(11)-C(19)-C(18)	124.0(4)
C(231)-Si(23)-C(232)	107.7(3)	C(72)-C(71)-C(7)	115.5(4)	C(20)-C(19)-C(18)	128.3(5)
C(233)-Si(23)-C(232)	106.8(2)	C(72)-C(71)-C(73)	110.4(4)	C(11)-C(19)-Fe(1)	68.0(2)
C(231)-Si(23)-Si(2)	110.24(17)	C(7)-C(71)-C(73)	109.2(5)	C(20)-C(19)-Fe(1)	69.3(2)
C(233)-Si(23)-Si(2)	113.50(19)	C(7)-C(8)-C(9)	125.0(4)	C(18)-C(19)-Fe(1)	128.2(3)
C(232)-Si(23)-Si(2)	111.48(18)	C(10)-C(9)-C(1)	108.5(4)	C(19)-C(11)-C(12)	108.7(4)
C(223)-Si(22)-C(221)	107.0(3)	C(10)-C(9)-C(8)	127.7(4)	C(19)-C(11)-C(201)	126.4(4)
C(223)-Si(22)-C(222)	109.7(2)	C(1)-C(9)-C(8)	123.8(5)	C(12)-C(11)-C(201)	124.8(6)
C(221)-Si(22)-C(222)	104.8(2)	C(10)-C(9)-Fe(1)	69.6(2)	C(19)-C(11)-Fe(1)	71.7(3)
C(223)-Si(22)-Si(2)	109.80(15)	C(1)-C(9)-Fe(1)	68.6(2)	C(12)-C(11)-Fe(1)	70.0(2)
C(221)-Si(22)-Si(2)	112.34(16)	C(8)-C(9)-Fe(1)	125.9(2)	C(201)-C(11)-Fe(1)	126.8(3)
C(222)-Si(22)-Si(2)	112.94(18)				

5.6.5 Anisotropic displacement parameters ($A^2 \times 10^3$) for Fe(6-Hyp-Hgual)$_2$. The anisotropic displacement factor exponent takes the form: $-2\pi^2 [h^2 a^{*2} U11 + ... + 2 h k a^* b^* U12]$

atom	U11	U22	U33	U23	U13	U12
Fe(1)	29(1)	21(1)	19(1)	2(1)	-3(1)	6(1)
Si(23)	32(2)	35(1)	28(1)	13(1)	6(1)	4(1)
Si(22)	39(2)	21(1)	26(1)	2(1)	1(1)	5(1)
C(2)	46(7)	21(2)	25(2)	2(2)	-3(3)	7(2)
C(3)	51(7)	27(2)	19(2)	-2(2)	-2(3)	24(3)
C(10)	18(7)	28(2)	22(2)	-1(2)	-2(2)	7(3)
C(4)	10(6)	45(2)	22(2)	-6(2)	3(3)	13(3)
C(41)	12(7)	85(4)	29(2)	-1(2)	2(3)	24(4)
C(5)	16(6)	44(2)	24(2)	-1(2)	7(2)	1(2)
C(6)	25(5)	29(2)	18(2)	2(2)	4(2)	2(2)
Si(1)	21(2)	22(1)	17(1)	4(1)	2(1)	3(1)
Si(11)	21(2)	27(1)	29(1)	3(1)	1(1)	-1(1)
C(111)	22(6)	48(3)	71(3)	22(2)	-13(3)	11(3)
C(112)	13(6)	56(3)	47(3)	4(2)	13(3)	-4(3)
C(113)	26(6)	53(3)	44(3)	-7(2)	2(3)	-7(3)
Si(12)	24(2)	38(1)	21(1)	10(1)	2(1)	-3(1)

C(121)	54(6)	46(3)	58(3)	31(2)	6(3)	-2(3)
C(122)	38(6)	66(3)	23(2)	9(2)	2(3)	-2(3)
C(123)	25(7)	67(3)	36(2)	11(2)	10(3)	2(3)
Si(13)	35(2)	23(1)	30(1)	5(1)	2(1)	5(1)
C(131)	32(7)	39(3)	66(3)	7(2)	-7(4)	15(3)
C(132)	53(6)	33(2)	35(2)	-6(2)	2(3)	16(3)
C(133)	64(6)	30(2)	35(2)	11(2)	10(3)	2(3)
C(7)	26(5)	20(2)	22(2)	2(1)	-6(2)	-1(2)
C(71)	57(7)	27(2)	21(2)	8(2)	8(3)	10(3)
C(72)	56(7)	36(2)	40(2)	11(2)	8(3)	23(3)
C(73)	90(7)	22(2)	52(3)	7(2)	18(3)	-1(3)
C(8)	15(5)	18(2)	21(2)	1(1)	0(2)	2(2)
C(9)	10(7)	23(2)	18(2)	-2(1)	-4(2)	4(2)
C(101)	40(7)	35(2)	34(2)	10(2)	2(3)	-8(3)
C(12)	11(6)	44(2)	25(2)	-1(2)	-5(2)	14(2)
C(13)	17(6)	36(2)	20(2)	2(2)	-2(2)	15(3)
C(20)	26(6)	24(2)	16(2)	2(1)	-2(2)	11(2)
C(14)	29(6)	21(2)	24(2)	5(2)	5(2)	3(2)
C(141)	45(6)	20(2)	40(2)	10(2)	10(3)	7(2)
C(15)	30(5)	24(2)	24(2)	8(2)	4(2)	-2(2)
C(16)	11(5)	22(2)	22(2)	3(1)	1(2)	6(2)
Si(2)	22(2)	22(1)	17(1)	3(1)	1(1)	3(1)
Si(21)	19(2)	32(1)	22(1)	1(1)	-2(1)	2(1)
C(211)	28(6)	49(3)	59(3)	11(2)	-10(3)	13(3)
C(212)	32(6)	69(3)	34(2)	-13(2)	-15(3)	12(3)
C(213)	14(6)	70(3)	41(3)	7(2)	4(3)	-2(3)
C(221)	74(7)	36(2)	33(2)	-7(2)	-9(3)	6(3)
C(222)	54(6)	34(2)	45(3)	7(2)	0(3)	-7(3)
C(223)	30(7)	36(2)	54(3)	12(2)	1(3)	17(3)
C(231)	22(7)	70(4)	70(4)	34(3)	12(4)	4(3)
C(232)	82(7)	71(3)	26(2)	16(2)	15(3)	-2(4)
C(233)	66(7)	45(3)	62(3)	36(2)	19(3)	15(3)
C(17)	31(5)	17(2)	17(2)	1(1)	-3(2)	-1(2)
C(171)	16(5)	27(2)	24(2)	7(2)	-1(2)	6(2)
C(172)	40(6)	45(3)	45(3)	17(2)	-15(3)	11(3)
C(173)	55(6)	28(2)	30(2)	14(2)	6(2)	20(2)
C(18)	22(5)	16(2)	18(2)	2(1)	-4(2)	-1(2)
C(19)	16(6)	22(2)	17(2)	-1(1)	-1(2)	2(2)
C(11)	24(7)	29(2)	24(2)	1(2)	-3(3)	3(2)
C(201)	39(6)	40(2)	35(2)	2(2)	4(3)	-4(3)
C(1)	19(7)	24(2)	23(2)	3(1)	-1(2)	1(2)

5.7 Crystallographic data for Fe(8-Hyp-Hgual)$_2$

5.7.1 Crystallographic data and structure refinement for Fe(8-Hyp-Hgual)$_2$

Empirical formula	$C_{48}H_{90}FeSi_8$
Formula weight (g/mol)	947.77
Temperature (K)	173(2)
Wavelength(Å)	0.71073
Crystal system, space group	triclinic, P1
Unit cell dimensions (Å,deg)	a=10.390(3) α=72.113(14) b=19.181(2) β=86.80(2) c=23.436(5) γ=76.305(19)
Volume (Å^3)	4317.7(17)
Z; calc. density (Mg/m^3)	2; 1.093Mg/m^3
Absorption coefficient (mm^{-1})	0.457 mm^{-1}
F(000)	1548
Theta range for data collection (deg)	2.08° ~25.00°
Limiting indices	$0 \le h \le 3, -21 \le k \le 21, -27 \le l \le 27$

Reflections collected / unique	6206 / 6206[R(int)=0.0000]
Completeness to θ	25.00; 34.9%
Refinement method	full-matrix least-squares on F^2
Data / restraints / parameters	6206 / 3 / 821
(Goodness-of-fit on F^2)	1.257
Final R indices [I>2σ(I)]	R1=0.0710, wR2=0.1728
R indices (all data)	R1=0.0864, wR2=0.1803
Largest diff. peak and hole ($e \cdot A^{-3}$)	1.464 and –0.414

5.7.2 Atomic coordinates ($\times 10^4$) and equivalent isotropic displacement parameters ($A^2 \times 10^3$) for Fe(8-Hyp-Hgual)$_2$. U(eq) is defined as one third of the trace of the orthogonalized Uij tensor.

atom	x/a	y/b	z/c	U(eq)	atom	x/a	y/b	z/c	U(eq)
Fe(2)	4341(6)	6331(1)	7127(1)	18(3)	C(71F)	-1880(50)	2854(12)	1771(10)	61(7)
Fe(1)	-1384(6)	-834(1)	8934(1)	20(3)	C(6A)	-1630(40)	1359(9)	8478(7)	28(5)
Si(1)	-283(13)	1066(2)	7077(2)	39(8)	C(11F)	2970(40)	2614(9)	1592(7)	43(5)
Si(11)	1940(14)	1052(3)	6770(2)	49(9)	C(73E)	6770(30)	7973(9)	7168(6)	32(4)
Si(12)	-1184(15)	500(3)	6474(2)	22(7)	C(233)	-2100(30)	-2566(9)	12200(7)	41(5)
Fe(3)	1849(6)	2920(1)	2812(1)	44(3)	C(7A)	-420(40)	1038(10)	8330(7)	33(5)
Si(2)	-3181(13)	-2430(2)	10779(2)	31(7)	C(9G)	2240(40)	3733(10)	3191(8)	38(5)
Si(13)	-1457(16)	2352(2)	6784(2)	33(8)	C(8A)	-140(30)	500(8)	7931(6)	23(4)
Si(21)	-2255(14)	-3737(2)	11052(2)	53(7)	C(532)	2500(30)	5248(9)	5160(7)	43(5)
Si(4)	5935(11)	7943(2)	5235(2)	36(6)	C(7G)	3470(40)	3014(8)	4164(6)	25(4)
Si(3)	3295(11)	4418(2)	8981(2)	11(7)	C(332)	970(40)	4321(11)	10136(8)	58(6)
Si(31)	4322(13)	4947(3)	9576(2)	26(7)	C(7F)	-1040(40)	2391(8)	2275(6)	29(4)
Si(6)	405(11)	1009(2)	2053(2)	32(6)	C(113)	2210(40)	1139(12)	5970(9)	74(8)
Si(32)	4415(15)	3124(2)	9250(2)	22(7)	C(72G)	5820(40)	2391(10)	3841(8)	56(6)
Si(5)	2800(13)	4580(3)	3934(2)	32(7)	C(411)	7960(40)	8080(10)	4018(8)	59(6)
Si(22)	-5455(14)	-2364(3)	11038(2)	30(8)	C(71A)	790(40)	1169(10)	8551(8)	43(5)
Si(43)	5876(16)	9223(3)	5033(2)	79(9)	C(11E)	2730(40)	7990(10)	6469(8)	51(6)
Si(33)	1109(13)	4467(2)	9299(2)	24(8)	C(3B)	-910(40)	-437(10)	9620(7)	26(4)
Si(23)	-2280(13)	-1907(2)	11412(2)	41(7)	C(10B)	-2150(40)	-701(9)	9727(6)	18(4)
Si(51)	4791(13)	4953(3)	3831(2)	28(7)	C(73D)	2160(40)	3758(11)	7244(8)	59(6)
Si(52)	1185(13)	5625(2)	3322(2)	59(7)	C(632)	-1030(40)	-493(12)	2374(9)	70(7)
Si(53)	2129(18)	4465(3)	4938(2)	53(9)	C(72A)	540(40)	1792(11)	8834(9)	61(7)
C(9D)	3970(40)	5584(7)	7958(6)	14(4)	C(11B)	290(40)	-2500(9)	9671(7)	40(5)
C(1E)	3610(40)	7231(9)	6418(7)	27(4)	C(4B)	-3470(50)	-268(9)	9788(7)	32(5)
C(9A)	-950(40)	-111(10)	8125(7)	31(6)	C(1G)	2160(40)	3948(8)	2585(7)	28(4)
Si(41)	7701(16)	7396(3)	4739(2)	124(9)	C(71D)	2000(40)	4386(9)	7526(7)	32(5)
Si(61)	2640(14)	328(3)	2035(2)	84(8)	C(72D)	1130(30)	5105(9)	7122(7)	43(5)
Si(42)	3937(14)	8000(3)	4709(2)	71(7)	C(611)	2620(30)	-692(9)	2148(7)	47(5)
Si(62)	-456(19)	1233(3)	1078(2)	132(11	C(213)	-540(40)	-3912(11)	11179(9)	52(6)
Si(63)	-757(16)	244(3)	2727(2)	113(9)	C(3G)	190(40)	3687(8)	2798(6)	23(4)
C(3D)	5770(40)	6146(9)	7767(7)	36(5)	C(5A)	-2870(40)	1292(10)	8313(8)	38(5)
C(2A)	-1490(40)	-1248(8)	8223(5)	15(4)	C(312)	4640(30)	4296(9)	10375(7)	42(5)
C(8D)	3160(30)	5003(7)	8113(5)	13(3)	C(511)	4620(40)	6009(12)	3629(10)	76(8)
C(41G)	-1140(40)	3336(11)	3991(8)	52(7)	C(412)	9350(40)	7174(13)	5141(11)	85(8)
C(9F)	1550(40)	2061(9)	2520(7)	32(5)	C(331)	370(40)	3716(10)	9164(8)	55(6)
C(1F)	2610(40)	2290(9)	2249(8)	32(5)	C(633)	320(40)	-275(10)	3455(8)	55(6)
C(5D)	5840(40)	4196(9)	7715(7)	25(4)	C(123)	-2880(50)	404(13)	6668(10)	60(8)
C(5B)	-4680(40)	-429(10)	9694(7)	37(5)	C(421)	4330(40)	8248(11)	3864(8)	62(6)
C(4D)	6340(50)	4772(10)	7793(8)	36(5)	C(221)	-6160(40)	-3050(11)	10813(9)	71(7)
C(121)	-1230(40)	1080(9)	5679(7)	44(5)	C(622)	-2470(60)	1450(20)	1088(17)	170(20)
C(9E)	4800(40)	6997(8)	6285(6)	16(4)	C(222)	-6660(40)	-1383(9)	10747(8)	54(6)
C(41A)	-4710(50)	763(11)	8116(9)	50(7)	C(313)	3370(30)	5906(9)	9584(7)	41(5)
C(6D)	4520(40)	4180(8)	7560(7)	23(4)	C(623)	160(40)	394(10)	795(9)	59(6)
C(2F)	3480(40)	2156(8)	2751(7)	35(4)	C(433)	7850(50)	9334(15)	5073(13)	103(12)
C(3E)	3940(40)	6013(9)	6423(6)	19(4)	C(612)	3450(40)	686(12)	1296(10)	84(8)
C(7E)	7130(40)	7242(8)	6401(7)	28(4)	C(512)	5960(40)	4531(10)	4542(8)	58(6)
C(6E)	7850(40)	6538(9)	6461(7)	41(5)	C(533)	330(50)	4513(12)	5027(9)	57(8)
C(122)	-70(40)	-442(11)	6496(9)	64(7)	C(2E)	2770(30)	6617(7)	6504(6)	26(4)
C(5F)	-500(40)	1695(10)	3428(9)	37(5)	C(10D)	5340(40)	5475(9)	7829(7)	25(5)
C(8B)	-2830(30)	-2032(8)	9901(6)	24(4)	C(8E)	5840(30)	7527(8)	6104(6)	20(4)

C(3F)	2970(40)	1850(8)	3280(7)	26(4)	C(73F)	-1540(30)	3640(9)	1451(7)	46(5)
C(5E)	7540(40)	5926(10)	6281(8)	39(6)	C(10A)	-2230(40)	-2(9)	8179(6)	20(5)
C(8F)	370(30)	2037(8)	2117(6)	28(4)	C(2G)	1000(40)	3979(7)	2323(7)	26(4)
C(71B)	-4520(40)	-2326(8)	9322(7)	28(4)	C(73B)	-5910(40)	-2062(12)	9054(10)	71(7)
C(3A)	-2690(40)	-719(8)	8263(6)	26(4)	C(72E)	8960(50)	7556(16)	6848(13)	102(11)
C(111)	2550(40)	1837(11)	6917(9)	60(7)	C(2D)	4590(40)	6699(11)	7814(8)	39(5)
C(6B)	-4920(30)	-1035(8)	9474(7)	35(5)	C(10F)	1700(40)	1820(8)	3099(7)	31(4)
C(71E)	7710(40)	7764(11)	6640(9)	46(6)	C(41D)	7680(40)	4735(12)	7881(10)	56(7)
C(41B)	-3500(30)	448(9)	9926(7)	41(5)	C(11G)	3330(40)	4234(10)	2221(8)	51(5)
C(7B)	-4120(30)	-1742(8)	9548(6)	24(4)	C(41F)	1090(30)	1077(9)	4158(7)	49(5)
C(211)	-2810(40)	-4294(10)	11771(7)	51(6)	C(223)	-5640(40)	-2659(10)	11879(7)	49(5)
C(131)	-980(40)	2895(10)	7260(8)	48(6)	C(422)	2460(40)	8756(14)	4833(11)	101(9)
C(9B)	-1830(40)	-1508(9)	9754(7)	24(4)	C(8G)	3110(30)	3692(8)	3652(7)	35(4)
C(11A)	1020(40)	-1239(8)	8098(6)	22(4)	C(11D)	2080(40)	6743(11)	7976(8)	48(6)
C(1A)	-410(40)	-876(8)	8152(6)	16(4)	C(423)	3640(40)	7100(11)	4867(9)	69(7)
C(431)	5350(30)	9810(9)	4276(7)	48(6)	C(6G)	2620(50)	2686(9)	4490(7)	31(4)
C(132)	-920(40)	2824(10)	5992(7)	50(6)	C(10E)	5060(40)	6258(10)	6302(7)	29(5)
C(2B)	30(40)	-1067(9)	9599(7)	43(5)	C(513)	5860(40)	4674(10)	3173(8)	53(6)
C(212)	-2450(30)	-4151(10)	10451(8)	53(6)	C(613)	3580(40)	274(12)	2640(9)	74(8)
C(321)	4050(30)	2628(9)	8744(7)	36(5)	C(6F)	-1350(40)	2218(9)	2855(7)	49(5)
C(322)	3920(30)	2659(9)	10018(7)	44(5)	C(1B)	-460(40)	-1719(9)	9660(7)	25(4)
C(432)	5060(30)	9603(9)	5603(7)	47(5)	C(4F)	640(40)	1524(9)	3569(8)	30(5)
C(333)	-10(30)	5412(10)	8922(8)	55(6)	C(4A)	-3240(50)	731(9)	8187(7)	31(5)
C(311)	5970(50)	5014(11)	9358(10)	50(7)	C(73G)	5320(40)	2048(12)	4932(9)	77(7)
C(631)	-2530(40)	704(12)	2868(9)	65(7)	C(72B)	-3560(40)	-2558(10)	8865(8)	47(5)
C(521)	880(30)	6441(9)	3634(7)	48(5)	C(413)	7330(40)	6535(11)	4601(9)	63(7)
C(323)	6190(50)	2955(13)	9257(10)	62(8)	C(73A)	1740(40)	464(10)	8965(8)	60(6)
C(112)	3040(40)	138(10)	7178(8)	52(6)	C(1D)	3520(40)	6355(9)	7929(7)	27(4)
C(522)	-420(40)	5342(12)	3306(9)	52(6)	C(41E)	6370(30)	5066(9)	6060(7)	43(5)
C(231)	-580(40)	-1734(11)	11162(9)	46(6)	C(7D)	3290(40)	4497(8)	7712(6)	18(4)
C(531)	3080(30)	3537(9)	5513(7)	43(5)	C(72F)	-3200(50)	3073(16)	1907(12)	101(10)
C(621)	30(40)	2026(10)	538(8)	58(6)	C(4E)	6390(40)	5788(8)	6220(7)	21(4)
C(133)	-3260(50)	2491(11)	6751(9)	43(6)	C(10G)	950(40)	3566(10)	3352(8)	38(5)
C(523)	1840(30)	5977(9)	2531(7)	44(5)	C(4G)	270(50)	3237(10)	3939(8)	37(6)
C(232)	-3490(30)	-975(9)	11426(7)	41(5)	C(5G)	1040(40)	2894(9)	4439(7)	32(5)
C(71G)	5020(40)	2651(9)	4315(7)	30(4)					

5.7.3 Bond lengths [Å] for Fe(8-Hyp-Hgual)$_2$

bonds	Bond lengths	bonds	Bond lengths	bonds	Bond lengths
Fe(2)-C(2D)	1.998(19)	Si(5)-C(8G)	1.962(15)	C(41A)-C(4A)	1.53(5)
Fe(2)-C(3E)	2.019(17)	Si(5)-Si(51)	2.322(16)	C(6D)-C(7D)	1.36(5)
Fe(2)-C(1E)	2.019(17)	Si(5)-Si(53)	2.374(9)	C(2F)-C(3F)	1.34(3)
Fe(2)-C(1D)	2.03(3)	Si(5)-Si(52)	2.408(10)	C(3E)-C(10E)	1.33(5)
Fe(2)-C(10D)	2.051(19)	Si(22)-C(221)	1.86(3)	C(3E)-C(2E)	1.52(4)
Fe(2)-C(3D)	2.06(3)	Si(22)-C(223)	1.888(18)	C(7E)-C(6E)	1.35(3)
Fe(2)-C(10E)	2.06(2)	Si(22)-C(222)	1.94(2)	C(7E)-C(8E)	1.45(4)
Fe(2)-C(9E)	2.094(19)	Si(43)-C(432)	1.79(2)	C(7E)-C(71E)	1.53(4)
Fe(2)-C(2E)	2.11(3)	Si(43)-C(431)	1.817(17)	C(6E)-C(5E)	1.47(3)
Fe(2)-C(9D)	2.112(19)	Si(43)-C(433)	2.13(5)	C(5F)-C(4F)	1.19(5)
Fe(1)-C(10B)	2.05(2)	Si(33)-C(333)	1.88(2)	C(5F)-C(6F)	1.57(3)
Fe(1)-C(10A)	2.055(18)	Si(33)-C(332)	1.897(19)	C(8B)-C(7B)	1.52(4)
Fe(1)-C(1A)	2.06(3)	Si(33)-C(331)	1.90(3)	C(8B)-C(9B)	1.56(4)
Fe(1)-C(3A)	2.06(3)	Si(23)-C(233)	1.882(16)	C(3F)-C(10F)	1.43(5)
Fe(1)-C(9B)	2.06(2)	Si(23)-C(231)	1.90(4)	C(5E)-C(4E)	1.31(5)
Fe(1)-C(2A)	2.072(14)	Si(23)-C(232)	1.94(2)	C(8F)-C(7F)	1.54(4)
Fe(1)-C(9A)	2.07(2)	Si(51)-C(511)	1.90(2)	C(71B)-C(73B)	1.51(5)
Fe(1)-C(2B)	2.08(3)	Si(51)-C(512)	1.96(3)	C(71B)-C(72B)	1.52(4)
Fe(1)-C(1B)	2.084(19)	Si(51)-C(513)	1.98(2)	C(71B)-C(7B)	1.52(3)
Fe(1)-C(3B)	2.10(2)	Si(52)-C(521)	1.878(16)	C(3A)-C(10A)	1.51(3)
Si(1)-C(8A)	1.957(14)	Si(52)-C(522)	1.88(4)	C(6B)-C(7B)	1.37(3)
Si(1)-Si(12)	2.372(11)	Si(52)-C(523)	1.91(2)	C(71E)-C(72E)	1.33(5)
Si(1)-Si(11)	2.377(15)	Si(53)-C(533)	1.85(4)	C(71E)-C(73E)	1.62(4)
Si(1)-Si(13)	2.381(8)	Si(53)-C(532)	1.86(2)	C(41B)-C(4B)	1.50(2)
Si(11)-C(113)	1.84(2)	Si(53)-C(531)	1.95(2)	C(9B)-C(1B)	1.41(5)

Si(11)-C(112)	1.86(2)	C(9D)-C(10D)	1.42(5)	C(9B)-C(10B)	1.49(2)
Si(11)-C(111)	1.89(2)	C(9D)-C(1D)	1.42(2)	C(11A)-C(1A)	1.50(5)
Si(12)-C(123)	1.83(5)	C(9D)-C(8D)	1.50(4)	C(2B)-C(3B)	1.37(4)
Si(12)-C(121)	1.849(17)	C(1E)-C(9E)	1.27(5)	C(2B)-C(1B)	1.42(3)
Si(12)-C(122)	1.89(2)	C(1E)-C(11E)	1.56(3)	C(71G)-C(72G)	1.49(3)
Fe(3)-C(1G)	1.98(2)	C(1E)-C(2E)	1.58(4)	C(71G)-C(73G)	1.54(2)
Fe(3)-C(3G)	1.98(3)	C(9A)-C(10A)	1.30(5)	C(71G)-C(7G)	1.61(5)
Fe(3)-C(2F)	1.99(3)	C(9A)-C(1A)	1.42(3)	C(5G)-C(4G)	1.35(4)
Fe(3)-C(2G)	2.012(16)	C(9A)-C(8A)	1.55(4)	C(5G)-C(6G)	1.60(5)
Fe(3)-C(10F)	2.05(2)	Si(41)-C(411)	1.84(2)	C(71F)-C(72F)	1.39(6)
Fe(3)-C(9F)	2.06(2)	Si(41)-C(412)	1.90(4)	C(71F)-C(7F)	1.43(3)
Fe(3)-C(1F)	2.059(19)	Si(41)-C(413)	1.90(2)	C(71F)-C(73F)	1.57(3)
Fe(3)-C(10G)	2.07(2)	Si(61)-C(613)	1.73(3)	C(6A)-C(7A)	1.34(5)
Fe(3)-C(3F)	2.10(2)	Si(61)-C(612)	1.89(3)	C(6A)-C(5A)	1.42(5)
Fe(3)-C(9G)	2.14(2)	Si(61)-C(611)	1.899(18)	C(7A)-C(71A)	1.49(5)
Si(2)-C(8B)	2.010(18)	Si(42)-C(423)	1.75(2)	C(7A)-C(8A)	1.56(2)
Si(2)-Si(21)	2.359(7)	Si(42)-C(422)	1.93(4)	C(9G)-C(1G)	1.35(2)
Si(2)-Si(23)	2.365(10)	Si(42)-C(421)	1.94(2)	C(9G)-C(8G)	1.42(3)
Si(2)-Si(22)	2.390(14)	Si(62)-C(621)	1.81(2)	C(9G)-C(10G)	1.45(5)
Si(13)-C(133)	1.83(4)	Si(62)-C(623)	1.89(2)	C(7G)-C(6G)	1.28(5)
Si(13)-C(131)	1.90(2)	Si(62)-C(622)	2.03(5)	C(7G)-C(8G)	1.46(2)
Si(13)-C(132)	1.92(2)	Si(63)-C(631)	1.90(4)	C(7F)-C(6F)	1.34(3)
Si(21)-C(213)	1.76(4)	Si(63)-C(632)	1.92(2)	C(71A)-C(72A)	1.50(2)
Si(21)-C(211)	1.84(2)	Si(63)-C(633)	1.95(2)	C(71A)-C(73A)	1.55(3)
Si(21)-C(212)	1.858(18)	C(3D)-C(10D)	1.42(3)	C(3B)-C(10B)	1.48(5)
Si(4)-C(8E)	1.953(15)	C(3D)-C(2D)	1.44(4)	C(10B)-C(4B)	1.45(5)
Si(4)-Si(41)	2.328(15)	C(2A)-C(3A)	1.43(4)	C(73D)-C(71D)	1.52(2)
Si(4)-Si(43)	2.340(7)	C(2A)-C(1A)	1.45(5)	C(11B)-C(1B)	1.51(3)
Si(4)-Si(42)	2.435(16)	C(8D)-C(7D)	1.524(18)	C(1G)-C(2G)	1.36(4)
Si(3)-C(8D)	1.993(13)	C(41G)-C(4G)	1.44(5)	C(1G)-C(11G)	1.56(5)
Si(3)-Si(33)	2.340(14)	C(9F)-C(10F)	1.30(2)	C(71D)-C(7D)	1.51(4)
Si(3)-Si(31)	2.378(10)	C(9F)-C(1F)	1.33(5)	C(71D)-C(72D)	1.52(3)
Si(3)-Si(32)	2.380(7)	C(9F)-C(8F)	1.61(4)	C(3G)-C(2G)	1.42(4)
Si(31)-C(311)	1.78(4)	C(1F)-C(2F)	1.45(3)	C(3G)-C(10G)	1.48(3)
Si(31)-C(313)	1.875(19)	C(1F)-C(11F)	1.54(3)	C(5A)-C(4A)	1.34(4)
Si(31)-C(312)	1.900(16)	C(5D)-C(4D)	1.39(4)	C(10A)-C(4A)	1.55(4)
Si(6)-C(8F)	2.016(16)	C(5D)-C(6D)	1.45(5)	C(2D)-C(1D)	1.40(5)
Si(6)-Si(63)	2.304(14)	C(5B)-C(4B)	1.41(5)	C(10F)-C(4F)	1.59(5)
Si(6)-Si(62)	2.376(10)	C(5B)-C(6B)	1.48(3)	C(41F)-C(4F)	1.42(2)
Si(6)-Si(61)	2.385(16)	C(4D)-C(41D)	1.40(5)	C(11D)-C(1D)	1.52(5)
Si(32)-C(323)	1.79(4)	C(4D)-C(10D)	1.52(4)	C(10E)-C(4E)	1.50(5)
Si(32)-C(321)	1.834(18)	C(9E)-C(10E)	1.37(2)	C(41E)-C(4E)	1.55(2)
Si(32)-C(322)	1.85(2)	C(9E)-C(8E)	1.60(4)	C(10G)-C(4G)	1.53(5)

5.7.4 Bond angles for Fe(8-Hyp-Hgual)$_2$ (deg)

Bond angles	parameter	Bond angles	parameter	Bond angles	parameter
C(2D)-Fe(2)-C(3E)	175.5(15)	C(211)-Si(21)-Si(2)	115.5(8)	C(8E)-C(7E)-C(71E)	119.0(19)
C(2D)-Fe(2)-C(1E)	108.4(7)	C(212)-Si(21)-Si(2)	112.6(7)	C(7E)-C(6E)-C(5E)	131(3)
C(3E)-Fe(2)-C(1E)	68.6(7)	C(8E)-Si(4)-Si(41)	118.9(9)	C(4F)-C(5F)-C(6F)	135(3)
C(2D)-Fe(2)-C(1D)	40.5(14)	C(8E)-Si(4)-Si(43)	106.7(5)	C(7B)-C(8B)-C(9B)	116.9(15)
C(3E)-Fe(2)-C(1D)	137.1(16)	Si(41)-Si(4)-Si(43)	109.6(5)	C(7B)-C(8B)-Si(2)	110(2)
C(1E)-Fe(2)-C(1D)	115.8(11)	C(8E)-Si(4)-Si(42)	113.0(11)	C(9B)-C(8B)-Si(2)	114.2(13)
C(2D)-Fe(2)-C(10D)	68.6(8)	Si(41)-Si(4)-Si(42)	106.0(4)	C(2F)-C(3F)-C(10F)	101(2)
C(3E)-Fe(2)-C(10D)	114.9(7)	Si(43)-Si(4)-Si(42)	101.3(5)	C(2F)-C(3F)-Fe(3)	66.7(12)
C(1E)-Fe(2)-C(10D)	171.3(17)	C(8D)-Si(3)-Si(33)	105.4(10)	C(10F)-C(3F)-Fe(3)	68.1(13)
C(1D)-Fe(2)-C(10D)	67.7(11)	C(8D)-Si(3)-Si(31)	113.5(7)	C(4E)-C(5E)-C(6E)	129(3)
C(2D)-Fe(2)-C(3D)	41.6(12)	Si(33)-Si(3)-Si(31)	107.5(4)	C(7F)-C(8F)-C(9F)	116.1(15)
C(3E)-Fe(2)-C(3D)	142.9(11)	C(8D)-Si(3)-Si(32)	117.7(5)	C(7F)-C(8F)-Si(6)	109(2)
C(1E)-Fe(2)-C(3D)	132.0(11)	Si(33)-Si(3)-Si(32)	107.0(5)	C(9F)-C(8F)-Si(6)	114.6(13)
C(1D)-Fe(2)-C(3D)	68.6(12)	Si(31)-Si(3)-Si(32)	105.2(4)	C(73B)-C(71B)-C(72B)	108.9(17)
C(10D)-Fe(2)-C(3D)	40.5(9)	C(311)-Si(31)-C(313)	107.4(13)	C(73B)-C(71B)-C(7B)	112.7(19)
C(2D)-Fe(2)-C(10E)	144.4(17)	C(311)-Si(31)-C(312)	100.4(15)	C(72B)-C(71B)-C(7B)	112(3)
C(3E)-Fe(2)-C(10E)	38.1(14)	C(313)-Si(31)-C(312)	109.7(8)	C(2A)-C(3A)-C(10A)	103(3)
C(1E)-Fe(2)-C(10E)	64.5(10)	C(311)-Si(31)-Si(3)	113.5(8)	C(2A)-C(3A)-Fe(1)	70.3(15)

C(1D)-Fe(2)-C(10E)	175.1(16)	C(313)-Si(31)-Si(3)	113.6(10)	C(10A)-C(3A)-Fe(1)	68.3(14)
C(10D)-Fe(2)-C(10E)	112.8(11)	C(312)-Si(31)-Si(3)	111.3(9)	C(7B)-C(6B)-C(5B)	128(3)
C(3D)-Fe(2)-C(10E)	115.2(15)	C(8F)-Si(6)-Si(63)	119.6(8)	C(72E)-C(71E)-C(7E)	121(2)
C(2D)-Fe(2)-C(9E)	115.1(11)	C(8F)-Si(6)-Si(62)	105.2(5)	C(72E)-C(71E)-C(73E)	107(2)
C(3E)-Fe(2)-C(9E)	64.7(10)	Si(63)-Si(6)-Si(62)	107.6(6)	C(7E)-C(71E)-C(73E)	109(3)
C(1E)-Fe(2)-C(9E)	35.9(13)	C(8F)-Si(6)-Si(61)	109.8(11)	C(6B)-C(7B)-C(8B)	123(2)
C(1D)-Fe(2)-C(9E)	144.4(7)	Si(63)-Si(6)-Si(61)	109.1(4)	C(6B)-C(7B)-C(71B)	123(3)
C(10D)-Fe(2)-C(9E)	137.1(15)	Si(62)-Si(6)-Si(61)	104.5(5)	C(8B)-C(7B)-C(71B)	113.7(17)
C(3D)-Fe(2)-C(9E)	111.9(13)	C(323)-Si(32)-C(321)	104.0(13)	C(1B)-C(9B)-C(10B)	107(3)
C(10E)-Fe(2)-C(9E)	38.4(7)	C(323)-Si(32)-C(322)	107.1(13)	C(1B)-C(9B)-C(8B)	126.8(17)
C(2D)-Fe(2)-C(2E)	132.4(12)	C(321)-Si(32)-C(322)	108.9(11)	C(10B)-C(9B)-C(8B)	126(3)
C(3E)-Fe(2)-C(2E)	43.1(10)	C(323)-Si(32)-Si(3)	114.6(10)	C(1B)-C(9B)-Fe(1)	71.0(15)
C(1E)-Fe(2)-C(2E)	45.0(11)	C(321)-Si(32)-Si(3)	113.9(8)	C(10B)-C(9B)-Fe(1)	68.3(11)
C(1D)-Fe(2)-C(2E)	107.2(14)	C(322)-Si(32)-Si(3)	108.0(8)	C(8B)-C(9B)-Fe(1)	128.9(14)
C(10D)-Fe(2)-C(2E)	143.0(11)	C(8G)-Si(5)-Si(51)	106.1(11)	C(9A)-C(1A)-C(2A)	108(3)
C(3D)-Fe(2)-C(2E)	173.9(8)	C(8G)-Si(5)-Si(53)	119.0(7)	C(9A)-C(1A)-C(11A)	127(3)
C(10E)-Fe(2)-C(2E)	69.3(12)	Si(51)-Si(5)-Si(53)	106.6(5)	C(2A)-C(1A)-C(11A)	125.2(14)
C(9E)-Fe(2)-C(2E)	68.7(11)	C(8G)-Si(5)-Si(52)	112.4(7)	C(9A)-C(1A)-Fe(1)	70.5(15)
C(2D)-Fe(2)-C(9D)	67.9(10)	Si(51)-Si(5)-Si(52)	106.6(4)	C(2A)-C(1A)-Fe(1)	69.9(15)
C(3E)-Fe(2)-C(9D)	112.5(9)	Si(53)-Si(5)-Si(52)	105.3(5)	C(11A)-C(1A)-Fe(1)	126.6(13)
C(1E)-Fe(2)-C(9D)	147.6(15)	C(221)-Si(22)-C(223)	102.8(11)	C(3B)-C(2B)-C(1B)	115(4)
C(1D)-Fe(2)-C(9D)	40.1(7)	C(221)-Si(22)-C(222)	107.6(13)	C(3B)-C(2B)-Fe(1)	71.9(17)
C(10D)-Fe(2)-C(9D)	39.9(12)	C(223)-Si(22)-C(222)	105.2(10)	C(1B)-C(2B)-Fe(1)	70.3(16)
C(3D)-Fe(2)-C(9D)	67.8(12)	C(221)-Si(22)-Si(2)	113.0(12)	C(72G)-C(71G)-C(73G)	111(2)
C(10E)-Fe(2)-C(9D)	137.3(7)	C(223)-Si(22)-Si(2)	110.6(12)	C(72G)-C(71G)-C(7G)	116(2)
C(9E)-Fe(2)-C(9D)	175.5(9)	C(222)-Si(22)-Si(2)	116.5(11)	C(73G)-C(71G)-C(7G)	114(3)
C(2E)-Fe(2)-C(9D)	112.1(12)	C(432)-Si(43)-C(431)	113.5(10)	C(4G)-C(5G)-C(6G)	128(3)
C(10B)-Fe(1)-C(10A)	114.9(10)	C(432)-Si(43)-C(433)	103.6(14)	C(72F)-C(71F)-C(7F)	115(3)
C(10B)-Fe(1)-C(1A)	171.2(15)	C(431)-Si(43)-C(433)	102.2(15)	C(72F)-C(71F)-C(73F)	101(2)
C(10A)-Fe(1)-C(1A)	65.5(11)	C(432)-Si(43)-Si(4)	112.8(8)	C(7F)-C(71F)-C(73F)	115(3)
C(10B)-Fe(1)-C(3A)	117.9(14)	C(431)-Si(43)-Si(4)	115.4(7)	C(7A)-C(6A)-C(5A)	128(2)
C(10A)-Fe(1)-C(3A)	43.2(9)	C(433)-Si(43)-Si(4)	107.9(9)	C(6A)-C(7A)-C(71A)	120.8(19)
C(1A)-Fe(1)-C(3A)	68.9(10)	C(333)-Si(33)-C(332)	106.5(10)	C(6A)-C(7A)-C(8A)	125(3)
C(10B)-Fe(1)-C(9B)	42.5(7)	C(333)-Si(33)-C(331)	108.0(13)	C(71A)-C(7A)-C(8A)	114(3)
C(10A)-Fe(1)-C(9B)	142.6(16)	C(332)-Si(33)-C(331)	105.0(11)	C(1G)-C(9G)-C(8G)	139(4)
C(1A)-Fe(1)-C(9B)	142.3(7)	C(333)-Si(33)-Si(3)	111.2(11)	C(1G)-C(9G)-C(10G)	102(3)
C(3A)-Fe(1)-C(9B)	112.6(13)	C(332)-Si(33)-Si(3)	111.7(13)	C(8G)-C(9G)-C(10G)	119(2)
C(10B)-Fe(1)-C(2A)	147.7(15)	C(331)-Si(33)-Si(3)	114.0(11)	C(1G)-C(9G)-Fe(3)	64.5(13)
C(10A)-Fe(1)-C(2A)	67.8(6)	C(233)-Si(23)-C(231)	107.8(13)	C(8G)-C(9G)-Fe(3)	133.6(13)
C(1A)-Fe(1)-C(2A)	41.1(12)	C(233)-Si(23)-C(232)	107.7(9)	C(10G)-C(9G)-Fe(3)	67.4(14)
C(3A)-Fe(1)-C(2A)	40.4(11)	C(231)-Si(23)-C(232)	110.4(12)	C(9A)-C(8A)-C(7A)	112(2)
C(9B)-Fe(1)-C(2A)	114.5(8)	C(233)-Si(23)-Si(2)	109.9(8)	C(9A)-C(8A)-Si(1)	114.7(15)
C(10B)-Fe(1)-C(9A)	134.8(7)	C(231)-Si(23)-Si(2)	112.1(7)	C(7A)-C(8A)-Si(1)	111.4(10)
C(10A)-Fe(1)-C(9A)	36.8(14)	C(232)-Si(23)-Si(2)	108.9(10)	C(6G)-C(7G)-C(8G)	124(3)
C(1A)-Fe(1)-C(9A)	40.3(8)	C(511)-Si(51)-C(512)	104.4(11)	C(6G)-C(7G)-C(71G)	118.5(18)
C(3A)-Fe(1)-C(9A)	68.6(13)	C(511)-Si(51)-C(513)	103.6(12)	C(8G)-C(7G)-C(71G)	118(3)
C(9B)-Fe(1)-C(9A)	177.3(7)	C(512)-Si(51)-C(513)	105.5(13)	C(6F)-C(7F)-C(71F)	128(3)
C(2A)-Fe(1)-C(9A)	68.1(8)	C(511)-Si(51)-Si(5)	114.8(13)	C(6F)-C(7F)-C(8F)	117(2)
C(10B)-Fe(1)-C(2B)	65.9(12)	C(512)-Si(51)-Si(5)	115.3(11)	C(71F)-C(7F)-C(8F)	115(2)
C(10A)-Fe(1)-C(2B)	141.3(11)	C(513)-Si(51)-Si(5)	112.0(10)	C(7A)-C(71A)-C(72A)	115(3)
C(1A)-Fe(1)-C(2B)	107.8(14)	C(521)-Si(52)-C(522)	108.8(15)	C(7A)-C(71A)-C(73A)	116(2)
C(3A)-Fe(1)-C(2B)	173.6(7)	C(521)-Si(52)-C(523)	106.0(9)	C(72A)-C(71A)-C(73A)	109.1(19)
C(9B)-Fe(1)-C(2B)	66.3(12)	C(522)-Si(52)-C(523)	111.3(11)	C(2B)-C(3B)-C(10B)	104(2)
C(2A)-Fe(1)-C(2B)	133.6(11)	C(521)-Si(52)-Si(5)	110.2(8)	C(2B)-C(3B)-Fe(1)	69.8(12)
C(9A)-Fe(1)-C(2B)	112.8(14)	C(522)-Si(52)-Si(5)	109.9(7)	C(10B)-C(3B)-Fe(1)	67.0(12)
C(10B)-Fe(1)-C(1B)	69.0(10)	C(523)-Si(52)-Si(5)	110.5(10)	C(4B)-C(10B)-C(3B)	127.7(17)
C(10A)-Fe(1)-C(1B)	176.0(10)	C(533)-Si(53)-C(532)	108.1(14)	C(4B)-C(10B)-C(9B)	124(3)
C(1A)-Fe(1)-C(1B)	110.7(11)	C(533)-Si(53)-C(531)	108.1(13)	C(3B)-C(10B)-C(9B)	108(3)
C(3A)-Fe(1)-C(1B)	135.1(9)	C(532)-Si(53)-C(531)	106.1(11)	C(4B)-C(10B)-Fe(1)	124.2(14)
C(9B)-Fe(1)-C(1B)	39.9(13)	C(533)-Si(53)-Si(5)	112.1(9)	C(3B)-C(10B)-Fe(1)	71.2(15)
C(2A)-Fe(1)-C(1B)	108.5(6)	C(532)-Si(53)-Si(5)	108.9(9)	C(9B)-C(10B)-Fe(1)	69.2(11)
C(9A)-Fe(1)-C(1B)	140.9(16)	C(531)-Si(53)-Si(5)	113.2(9)	C(5B)-C(4B)-C(10B)	126.9(19)
C(2B)-Fe(1)-C(1B)	40.0(9)	C(10D)-C(9D)-C(1D)	106(3)	C(5B)-C(4B)-C(41B)	118(3)
C(10B)-Fe(1)-C(3B)	41.8(13)	C(10D)-C(9D)-C(8D)	127.3(17)	C(10B)-C(4B)-C(41B)	114(3)
C(10A)-Fe(1)-C(3B)	114.5(7)	C(1D)-C(9D)-C(8D)	127(3)	C(9G)-C(1G)-C(2G)	118(4)
C(1A)-Fe(1)-C(3B)	129.5(15)	C(10D)-C(9D)-Fe(2)	67.8(13)	C(9G)-C(1G)-C(11G)	118(3)
C(3A)-Fe(1)-C(3B)	148.0(11)	C(1D)-C(9D)-Fe(2)	66.8(12)	C(2G)-C(1G)-C(11G)	122.9(16)
C(9B)-Fe(1)-C(3B)	70.3(10)	C(8D)-C(9D)-Fe(2)	131.3(12)	C(9G)-C(1G)-Fe(3)	77.4(15)
C(2A)-Fe(1)-C(3B)	169.6(16)	C(9E)-C(1E)-C(11E)	136(3)	C(2G)-C(1G)-Fe(3)	71.4(15)

C(9A)-Fe(1)-C(3B)	107.3(10)	C(9E)-C(1E)-C(2E)	111.9(18)	C(11G)-C(1G)-Fe(3)	127.7(17)
C(2B)-Fe(1)-C(3B)	38.3(10)	C(11E)-C(1E)-C(2E)	112(3)	C(7D)-C(71D)-C(73D)	114(3)
C(1B)-Fe(1)-C(3B)	68.8(7)	C(9E)-C(1E)-Fe(2)	75.3(13)	C(7D)-C(71D)-C(72D)	113(2)
C(8A)-Si(1)-Si(12)	114.2(8)	C(11E)-C(1E)-Fe(2)	124.3(12)	C(73D)-C(71D)-C(72D)	109.7(18)
C(8A)-Si(1)-Si(11)	104.7(11)	C(2E)-C(1E)-Fe(2)	70.4(9)	C(2G)-C(3G)-C(10G)	105(3)
Si(12)-Si(1)-Si(11)	106.5(5)	C(10A)-C(9A)-C(1A)	109(3)	C(2G)-C(3G)-Fe(3)	70.5(16)
C(8A)-Si(1)-Si(13)	118.6(6)	C(10A)-C(9A)-C(8A)	127(2)	C(10G)-C(3G)-Fe(3)	71.9(16)
Si(12)-Si(1)-Si(13)	105.5(5)	C(1A)-C(9A)-C(8A)	123(4)	C(4A)-C(5A)-C(6A)	132(3)
Si(11)-Si(1)-Si(13)	106.6(5)	C(10A)-C(9A)-Fe(1)	70.8(17)	C(3E)-C(2E)-C(1E)	95(3)
C(113)-Si(11)-C(112)	104.9(12)	C(1A)-C(9A)-Fe(1)	69.2(12)	C(3E)-C(2E)-Fe(2)	65.4(14)
C(113)-Si(11)-C(111)	106.7(13)	C(8A)-C(9A)-Fe(1)	135.5(15)	C(1E)-C(2E)-Fe(2)	64.6(13)
C(112)-Si(11)-C(111)	108.7(13)	C(411)-Si(41)-C(412)	102.1(16)	C(9D)-C(10D)-C(3D)	110(2)
C(113)-Si(11)-Si(1)	114.4(14)	C(411)-Si(41)-C(413)	109.9(9)	C(9D)-C(10D)-C(4D)	130(3)
C(112)-Si(11)-Si(1)	109.9(12)	C(412)-Si(41)-C(413)	112.5(13)	C(3D)-C(10D)-C(4D)	120(4)
C(111)-Si(11)-Si(1)	111.8(11)	C(411)-Si(41)-Si(4)	110.0(10)	C(9D)-C(10D)-Fe(2)	72.4(14)
C(123)-Si(12)-C(121)	106.9(14)	C(412)-Si(41)-Si(4)	112.9(9)	C(3D)-C(10D)-Fe(2)	70.2(11)
C(123)-Si(12)-C(122)	110.6(14)	C(413)-Si(41)-Si(4)	109.3(13)	C(4D)-C(10D)-Fe(2)	127.0(13)
C(121)-Si(12)-C(122)	105.1(10)	C(613)-Si(61)-C(612)	112.3(17)	C(7E)-C(8E)-C(9E)	117.5(15)
C(123)-Si(12)-Si(1)	113.6(8)	C(613)-Si(61)-C(611)	103.1(11)	C(7E)-C(8E)-Si(4)	113(2)
C(121)-Si(12)-Si(1)	109.6(9)	C(612)-Si(61)-C(611)	108.0(10)	C(9E)-C(8E)-Si(4)	111.4(13)
C(122)-Si(12)-Si(1)	110.6(11)	C(613)-Si(61)-Si(6)	112.8(11)	C(9A)-C(10A)-C(3A)	111(2)
C(1G)-Fe(3)-C(3G)	68.1(12)	C(612)-Si(61)-Si(6)	112.3(11)	C(9A)-C(10A)-C(4A)	128(3)
C(1G)-Fe(3)-C(2F)	112.1(15)	C(611)-Si(61)-Si(6)	107.6(12)	C(3A)-C(10A)-C(4A)	120(4)
C(3G)-Fe(3)-C(2F)	174.9(6)	C(423)-Si(42)-C(422)	114.9(19)	C(9A)-C(10A)-Fe(1)	72.5(14)
C(1G)-Fe(3)-C(2G)	39.9(12)	C(423)-Si(42)-C(421)	102.5(11)	C(3A)-C(10A)-Fe(1)	68.6(10)
C(3G)-Fe(3)-C(2G)	41.6(11)	C(422)-Si(42)-C(421)	109.1(12)	C(4A)-C(10A)-Fe(1)	124.4(12)
C(2F)-Fe(3)-C(2G)	135.4(11)	C(423)-Si(42)-Si(4)	110.4(12)	C(1G)-C(2G)-C(3G)	105.9(17)
C(1G)-Fe(3)-C(10F)	174.2(15)	C(422)-Si(42)-Si(4)	112.3(11)	C(1G)-C(2G)-Fe(3)	68.7(12)
C(3G)-Fe(3)-C(10F)	116.2(15)	C(421)-Si(42)-Si(4)	106.9(13)	C(3G)-C(2G)-Fe(3)	67.9(10)
C(2F)-Fe(3)-C(10F)	64.0(13)	C(621)-Si(62)-C(623)	106.9(12)	C(1D)-C(2D)-C(3D)	109(2)
C(2G)-Fe(3)-C(10F)	146.0(15)	C(621)-Si(62)-C(622)	108.4(17)	C(1D)-C(2D)-Fe(2)	70.9(14)
C(1G)-Fe(3)-C(9F)	146.7(7)	C(623)-Si(62)-C(622)	108.0(18)	C(3D)-C(2D)-Fe(2)	71.6(11)
C(3G)-Fe(3)-C(9F)	112.1(13)	C(621)-Si(62)-Si(6)	111.6(10)	C(9F)-C(10F)-C(3F)	111(3)
C(2F)-Fe(3)-C(9F)	64.7(13)	C(623)-Si(62)-Si(6)	111.5(9)	C(9F)-C(10F)-C(4F)	127(4)
C(2G)-Fe(3)-C(9F)	117.2(9)	C(622)-Si(62)-Si(6)	110.2(12)	C(3F)-C(10F)-C(4F)	122.1(18)
C(10F)-Fe(3)-C(9F)	36.8(7)	C(631)-Si(63)-C(632)	101.7(16)	C(9F)-C(10F)-Fe(3)	72.0(12)
C(1G)-Fe(3)-C(1F)	116.2(11)	C(631)-Si(63)-C(633)	113.8(12)	C(3F)-C(10F)-Fe(3)	71.7(15)
C(3G)-Fe(3)-C(1F)	133.2(10)	C(632)-Si(63)-C(633)	108.6(10)	C(4F)-C(10F)-Fe(3)	123.6(15)
C(2F)-Fe(3)-C(1F)	41.8(10)	C(631)-Si(63)-Si(6)	116.2(8)	C(9G)-C(8G)-C(7G)	121(2)
C(2G)-Fe(3)-C(1F)	109.6(7)	C(632)-Si(63)-Si(6)	107.4(10)	C(9G)-C(8G)-Si(5)	115.9(14)
C(10F)-Fe(3)-C(1F)	64.2(10)	C(633)-Si(63)-Si(6)	108.6(12)	C(7G)-C(8G)-Si(5)	109.1(10)
C(9F)-Fe(3)-C(1F)	37.8(13)	C(10D)-C(3D)-C(2D)	105(3)	C(7G)-C(6G)-C(5G)	130(2)
C(1G)-Fe(3)-C(10G)	64.9(12)	C(10D)-C(3D)-Fe(2)	69.3(15)	C(3E)-C(10E)-C(9E)	109(3)
C(3G)-Fe(3)-C(10G)	42.9(10)	C(2D)-C(3D)-Fe(2)	66.8(16)	C(3E)-C(10E)-C(4E)	125.1(19)
C(2F)-Fe(3)-C(10G)	142.1(11)	C(3A)-C(2A)-C(1A)	108.3(15)	C(9E)-C(10E)-C(4E)	126(4)
C(2G)-Fe(3)-C(10G)	68.5(7)	C(3A)-C(2A)-Fe(1)	69.3(10)	C(3E)-C(10E)-Fe(2)	69.1(15)
C(10F)-Fe(3)-C(10G)	115.1(12)	C(1A)-C(2A)-Fe(1)	69.0(11)	C(9E)-C(10E)-Fe(2)	72.0(12)
C(9F)-Fe(3)-C(10G)	139.3(17)	C(9D)-C(8D)-C(7D)	117(2)	C(4E)-C(10E)-Fe(2)	123.5(14)
C(1F)-Fe(3)-C(10G)	175.8(17)	C(9D)-C(8D)-Si(3)	112.3(13)	C(7F)-C(6F)-C(5F)	131(3)
C(1G)-Fe(3)-C(3F)	134.0(15)	C(7D)-C(8D)-Si(3)	112.2(9)	C(9B)-C(1B)-C(2B)	106(2)
C(3G)-Fe(3)-C(3F)	145.2(12)	C(10F)-C(9F)-C(1F)	112(4)	C(9B)-C(1B)-C(11B)	125(3)
C(2F)-Fe(3)-C(3F)	38.1(10)	C(10F)-C(9F)-C(8F)	129(3)	C(2B)-C(1B)-C(11B)	130(4)
C(2G)-Fe(3)-C(3F)	172.5(15)	C(1F)-C(9F)-C(8F)	119.0(17)	C(9B)-C(1B)-Fe(1)	69.1(13)
C(10F)-Fe(3)-C(3F)	40.2(13)	C(10F)-C(9F)-Fe(3)	71.2(12)	C(2B)-C(1B)-Fe(1)	69.7(11)
C(9F)-Fe(3)-C(3F)	65.6(10)	C(1F)-C(9F)-Fe(3)	71.1(14)	C(11B)-C(1B)-Fe(1)	128.7(11)
C(1F)-Fe(3)-C(3F)	67.9(7)	C(8F)-C(9F)-Fe(3)	130.1(15)	C(5F)-C(4F)-C(41F)	122(4)
C(10G)-Fe(3)-C(3F)	114.5(7)	C(9F)-C(1F)-C(2F)	102(2)	C(5F)-C(4F)-C(10F)	120(2)
C(1G)-Fe(3)-C(9G)	38.1(7)	C(9F)-C(1F)-C(11F)	134(3)	C(41F)-C(4F)-C(10F)	119(3)
C(3G)-Fe(3)-C(9G)	71.1(14)	C(2F)-C(1F)-C(11F)	124(3)	C(5A)-C(4A)-C(41A)	120(3)
C(2F)-Fe(3)-C(9G)	112.4(14)	C(9F)-C(1F)-Fe(3)	71.1(13)	C(5A)-C(4A)-C(10A)	122(4)
C(2G)-Fe(3)-C(9G)	68.2(8)	C(2F)-C(1F)-Fe(3)	66.6(11)	C(41A)-C(4A)-C(10A)	118(2)
C(10F)-Fe(3)-C(9G)	138.1(7)	C(11F)-C(1F)-Fe(3)	124.9(11)	C(2D)-C(1D)-C(9D)	109(3)
C(9F)-Fe(3)-C(9G)	174.6(7)	C(4D)-C(5D)-C(6D)	131(3)	C(2D)-C(1D)-C(11D)	126.1(17)
C(1F)-Fe(3)-C(9G)	142.9(17)	C(4B)-C(5B)-C(6B)	129(3)	C(9D)-C(1D)-C(11D)	124(3)
C(10G)-Fe(3)-C(9G)	40.4(14)	C(5D)-C(4D)-C(41D)	125(3)	C(2D)-C(1D)-Fe(2)	68.5(16)
C(3F)-Fe(3)-C(9G)	109.2(10)	C(5D)-C(4D)-C(10D)	117(4)	C(9D)-C(1D)-Fe(2)	73.1(13)
C(8B)-Si(2)-Si(21)	105.7(6)	C(41D)-C(4D)-C(10D)	118(2)	C(11D)-C(1D)-Fe(2)	121.7(15)
C(8B)-Si(2)-Si(23)	115.6(9)	C(1E)-C(9E)-C(10E)	111(3)	C(6D)-C(7D)-C(71D)	125.7(17)
Si(21)-Si(2)-Si(23)	109.1(4)	C(1E)-C(9E)-C(8E)	122.9(17)	C(6D)-C(7D)-C(8D)	119(3)

C(8B)-Si(2)-Si(22)	115.8(11)	C(10E)-C(9E)-C(8E)	126(3)	C(71D)-C(7D)-C(8D)	116(3)
Si(21)-Si(2)-Si(22)	103.0(5)	C(1E)-C(9E)-Fe(2)	68.8(14)	C(5E)-C(4E)-C(10E)	126(2)
Si(23)-Si(2)-Si(22)	106.8(4)	C(10E)-C(9E)-Fe(2)	69.6(12)	C(5E)-C(4E)-C(41E)	118(3)
C(133)-Si(13)-C(131)	110.4(13)	C(8E)-C(9E)-Fe(2)	130.4(13)	C(10E)-C(4E)-C(41E)	116(3)
C(133)-Si(13)-C(132)	106.9(13)	C(7D)-C(6D)-C(5D)	133.2(19)	C(9G)-C(10G)-C(3G)	109(2)
C(131)-Si(13)-C(132)	104.5(11)	C(3F)-C(2F)-C(1F)	113(3)	C(9G)-C(10G)-C(4G)	136(3)
C(133)-Si(13)-Si(1)	114.2(9)	C(3F)-C(2F)-Fe(3)	75.2(18)	C(3G)-C(10G)-C(4G)	115(4)
C(131)-Si(13)-Si(1)	112.4(9)	C(1F)-C(2F)-Fe(3)	71.5(16)	C(9G)-C(10G)-Fe(3)	72.3(16)
C(132)-Si(13)-Si(1)	107.8(8)	C(10E)-C(3E)-C(2E)	112.5(19)	C(3G)-C(10G)-Fe(3)	65.1(11)
C(213)-Si(21)-C(211)	102.2(13)	C(10E)-C(3E)-Fe(2)	72.8(14)	C(4G)-C(10G)-Fe(3)	122.5(13)
C(213)-Si(21)-C(212)	105.9(14)	C(2E)-C(3E)-Fe(2)	71.5(10)	C(5G)-C(4G)-C(41G)	119(3)
C(211)-Si(21)-C(212)	110.2(11)	C(6E)-C(7E)-C(8E)	122(2)	C(5G)-C(4G)-C(10G)	118(4)
C(213)-Si(21)-Si(2)	109.7(9)	C(6E)-C(7E)-C(71E)	119(3)	C(41G)-C(4G)-C(10G)	123(3)

5.7.5 Anisotropic displacement parameters ($A^2 \times 10^3$) for Fe(8-Hyp-Hgual)$_2$, The anisotropic displacement factor exponent takes the form: $-2\pi^2 [h^2 a^{*2} U11 + ... + 2 h k a^* b^* U12]$

atom	U11	U22	U33	U23	U13	U12
Fe(2)	17(8)	21(1)	17(1)	4(1)	1(2)	8(2)
Fe(1)	16(9)	22(1)	21(1)	7(1)	0(2)	5(2)
Si(1)	70(20)	19(2)	23(2)	8(2)	1(5)	2(4)
Si(11)	60(30)	32(3)	37(3)	3(2)	9(6)	9(5)
Si(12)	0(20)	35(3)	31(2)	13(2)	8(6)	1(5)
Fe(3)	74(9)	28(1)	25(1)	12(1)	5(2)	6(2)
Si(2)	50(20)	20(2)	19(2)	8(2)	7(5)	6(4)
Si(13)	30(20)	21(2)	41(3)	6(2)	16(6)	4(5)
Si(21)	90(20)	22(2)	32(2)	3(2)	7(6)	0(5)
Si(4)	63(19)	21(2)	23(2)	5(2)	6(5)	11(4)
Si(3)	0(20)	14(2)	17(2)	3(2)	9(5)	2(4)
Si(31)	30(20)	39(3)	18(2)	9(2)	1(5)	16(5)
Si(6)	36(19)	35(2)	28(2)	17(2)	6(5)	4(5)
Si(32)	0(20)	23(2)	34(2)	3(2)	5(5)	2(5)
Si(5)	30(20)	38(3)	24(2)	16(2)	11(5)	6(5)
Si(22)	20(30)	46(3)	32(2)	18(2)	5(6)	17(5)
Si(43)	160(30)	23(2)	32(3)	1(2)	27(6)	0(5)
Si(33)	0(20)	28(2)	39(3)	4(2)	12(6)	6(5)
Si(23)	70(20)	30(2)	23(2)	7(2)	14(5)	3(5)
Si(51)	0(20)	50(3)	36(2)	16(2)	1(5)	5(6)
Si(52)	120(20)	21(2)	33(2)	7(2)	1(5)	4(5)
Si(53)	110(30)	44(3)	26(2)	17(2)	20(6)	42(6)
Si(41)	260(30)	49(3)	45(3)	21(2)	3(7)	3(6)
Si(61)	170(20)	35(2)	48(3)	16(2)	1(6)	16(5)
Si(42)	110(20)	50(3)	46(3)	8(2)	14(6)	3(6)
Si(62)	340(30)	64(4)	20(2)	15(2)	16(6)	101(8)
Si(63)	250(30)	52(3)	36(3)	5(2)	6(6)	40(7)

5.8 Crystallographic data for Ni(6-HypHgual)$_2$

5.8.1 Crystallographic data and structure refinement for Ni(6-Hyp-Hgual)$_2$

Empirical formula	$C_{48}H_{90}NiSi_8$
Formula weight (g/mol)	950.62
Temperature (K)	173(2)
Wavelength(Å)	0,71073
Crystal system, space group	rhothorombic, Pbca

Unit cell dimensions (Å ,deg)	a=17.284(2) b=18.002(3) c=36.972(4)
Volume ($Å^3$)	11504(3)
Z; calc. density (Mg/m^3)	8; 1.098
Absorption coefficient (mm^{-1})	0.533
F(000)	4144
Theta range for data collection (deg)	1.97~24.00
Limiting indices	-5 ≤ h ≤ 19, -20 ≤ k ≤ 19, -11 ≤ l ≤4 2
Reflections collected / unique	10614 / 8953[R(int)=0.0583]
Completeness to θ	24.00; 99.1%
Refinement method	full-matrix least-squares on F^2
Data / restraints / parameters	8953 / 0 / 515
(Goodness-of-fit on F^2)	0.673
Final R indices [I>2σ(I)]	R1=0.0462, wR2=0.0691
R indices (all data)	R1=0.1452, wR2=0.0828
Largest diff. peak and hole ($e.Å^{-3}$)	0.000038(3) 0.285 and –0.265

5.8.2 Atomic coordinates (x 10^4) and equivalent isotropic displacement parameters (A^2 ×10^3) for Ni(6-Hyp-Hgual)$_2$. U(eq) is defined as one third of the trace of the orthogonalized Uij tensor.

atom	x/a	y/b	z/c	U(eq)	atom	x/a	y/b	z/c	U(eq)
Ni(1)	8495(1)	1076(1)	5271(1)	35(1)	C(8)	7086(3)	1216(3)	4687(1)	30(1)
Si(2)	7099(1)	1682(1)	6688(1)	28(1)	C(112)	6192(3)	-285(3)	3370(1)	54(2)
Si(21)	6072(1)	2242(1)	7009(1)	33(1)	C(1)	8223(3)	1987(3)	4908(1)	37(2)
Si(11)	6527(1)	696(1)	3316(1)	33(1)	C(171)	5978(3)	2406(3)	5875(1)	41(2)
Si(1)	7520(1)	918(1)	3741(1)	27(1)	C(72)	5413(3)	1207(3)	4620(1)	65(2)
Si(12)	7594(1)	2210(1)	3794(1)	36(1)	C(113)	6854(3)	811(3)	2836(1)	51(2)
Si(22)	6799(1)	412(1)	6634(1)	38(1)	C(2)	9029(4)	1869(4)	4938(1)	51(2)
Si(23)	8229(1)	1793(1)	7044(1)	38(1)	C(6)	7234(3)	335(3)	4166(1)	30(1)
Si(13)	8680(1)	473(1)	3484(1)	38(1)	C(4)	8443(3)	70(3)	4543(1)	34(1)
C(10)	8517(3)	815(3)	4681(1)	33(1)	C(73)	5687(3)	-144(3)	4543(1)	65(2)
C(71)	5899(3)	634(3)	4421(1)	41(2)	C(12)	8634(3)	179(3)	5636(1)	43(2)
C(101)	7812(3)	2678(3)	5021(1)	57(2)	C(41)	9029(3)	-495(3)	4662(1)	61(2)
C(9)	7906(3)	1342(3)	4746(1)	27(1)	C(222)	6415(3)	104(3)	7085(1)	59(2)
C(19)	7690(3)	1062(3)	5734(1)	24(1)	C(16)	7210(3)	2279(3)	6254(1)	31(1)
C(20)	8423(3)	1344(3)	5861(1)	32(1)	C(212)	5099(3)	1913(3)	6852(1)	52(2)
C(11)	7822(3)	328(3)	5595(1)	34(1)	C(141)	9376(3)	2389(3)	5954(1)	75(2)
C(211)	6103(3)	3278(2)	6940(1)	42(2)	C(173)	6110(3)	3190(3)	5737(1)	68(2)
C(15)	8030(3)	2483(3)	6162(1)	42(2)	C(131)	8601(3)	-536(3)	3362(2)	71(2)
C(7)	6763(3)	768(3)	4440(1)	26(1)	C(232)	9109(3)	1390(3)	6826(1)	68(2)
C(18)	6955(3)	1447(3)	5717(1)	23(1)	C(122)	7555(3)	2594(3)	3324(1)	50(2)
C(231)	8420(3)	2793(3)	7162(1)	69(2)	C(132)	9527(3)	595(3)	3784(1)	69(2)
C(221)	6024(3)	210(3)	6294(1)	49(2)	C(13)	8977(3)	797(3)	5791(1)	46(2)
C(17)	6732(3)	1994(3)	5934(1)	28(1)	C(3)	9211(3)	1164(4)	4802(1)	48(2)
C(5)	7874(3)	-126(3)	4323(1)	39(2)	C(123)	6766(3)	2611(3)	4045(1)	52(2)
C(121)	8510(3)	2538(3)	3999(1)	59(2)	C(233)	8100(3)	1258(3)	7476(1)	59(2)
C(14)	8565(3)	2080(3)	5997(1)	42(2)	C(223)	7663(3)	-170(3)	6531(1)	59(2)
C(111)	5674(3)	1318(3)	3376(1)	55(2)	C(133)	8915(3)	993(3)	3057(1)	48(2)
C(172)	5417(3)	2008(3)	5632(1)	59(2)	C(213)	6114(3)	2075(3)	7503(1)	53(2)
C(201)	7242(3)	-189(3)	5438(1)	47(2)					

5.8.3 Bond lengths [Å] for Ni(6-Hyp-Hgual)$_2$

Bonds	Bond lengths	bonds	Bond lengths	bonds	Bond lengths
Ni(1)-C(2)	2.099(5)	Si(1)-Si(13)	2.358(2)	C(19)-C(20)	1.443(6)
Ni(1)-C(3)	2.137(5)	Si(12)-C(121)	1.852(5)	C(19)-C(11)	1.435(6)
Ni(1)-C(12)	2.118(5)	Si(12)-C(123)	1.853(5)	C(20)-C(13)	1.398(6)
Ni(1)-C(11)	2.144(5)	Si(12)-C(122)	1.871(4)	C(20)-C(14)	1.439(7)

Ni(1)-C(1)	2.171(5)	Si(22)-C(223)	1.864(5)	C(11)-C(201)	1.487(6)
Ni(1)-C(13)	2.153(5)	Si(22)-C(222)	1.879(5)	C(11)-C(12)	1.437(7)
Ni(1)-C(19)	2.203(4)	Si(22)-C(221)	1.873(5)	C(15)-C(14)	1.325(7)
Ni(1)-C(10)	2.233(4)	Si(23)-C(232)	1.868(5)	C(15)-C(16)	1.503(6)
Ni(1)-C(9)	2.245(5)	Si(23)-C(233)	1.878(5)	C(7)-C(8)	1.342(6)
Ni(1)-C(20)	2.237(5)	Si(23)-C(231)	1.882(5)	C(7)-C(6)	1.515(6)
Si(2)-C(16)	1.940(5)	Si(13)-C(132)	1.850(5)	C(18)-C(17)	1.328(6)
Si(2)-Si(21)	2.361(2)	Si(13)-C(133)	1.880(4)	C(17)-C(171)	1.514(6)
Si(2)-Si(22)	2.351(2)	Si(13)-C(131)	1.875(5)	C(17)-C(16)	1.532(6)
Si(2)-Si(23)	2.364(2)	C(10)-C(3)	1.427(7)	C(5)-C(4)	1.324(6)
Si(21)-C(212)	1.875(5)	C(10)-C(9)	1.441(6)	C(5)-C(6)	1.499(6)
Si(21)-C(211)	1.882(5)	C(10)-C(4)	1.441(6)	C(14)-C(141)	1.516(7)
Si(21)-C(213)	1.855(4)	C(71)-C(73)	1.515(7)	C(172)-C(171)	1.504(6)
Si(11)-C(111)	1.864(5)	C(71)-C(7)	1.514(6)	C(1)-C(2)	1.414(7)
Si(11)-C(112)	1.869(5)	C(71)-C(72)	1.520(6)	C(171)-C(173)	1.519(6)
Si(11)-C(113)	1.875(4)	C(101)-C(1)	1.494(7)	C(2)-C(3)	1.402(7)
Si(11)-Si(1)	2.359(2)	C(9)-C(8)	1.452(6)	C(4)-C(41)	1.501(6)
Si(1)-C(6)	1.954(5)	C(9)-C(1)	1.416(6)	C(12)-C(13)	1.383(7)
Si(1)-Si(12)	2.338(2)	C(19)-C(18)	1.449(6)		

5.8.4 Bond angles for Ni(6-Hyp-Hgual)$_2$ (deg)

Bond angle	parameters	Bond angle	parameters	Bond angle	parameters
C(2)-Ni(1)-C(3)	38.65(19)	C(211)-Si(21)-Si(2)	109.51(17)	C(20)-C(19)-C(11)	107.5(5)
C(2)-Ni(1)-C(12)	147.4(2)	C(213)-Si(21)-Si(2)	113.35(18)	C(18)-C(19)-Ni(1)	121.0(3)
C(3)-Ni(1)-C(12)	120.5(2)	C(111)-Si(11)-C(112)	108.1(2)	C(20)-C(19)-Ni(1)	72.3(3)
C(2)-Ni(1)-C(11)	173.2(2)	C(111)-Si(11)-C(113)	106.5(2)	C(11)-C(19)-Ni(1)	68.5(3)
C(3)-Ni(1)-C(11)	144.4(2)	C(112)-Si(11)-C(113)	107.4(2)	C(13)-C(20)-C(14)	126.6(6)
C(12)-Ni(1)-C(11)	39.40(18)	C(111)-Si(11)-Si(1)	113.22(16)	C(13)-C(20)-C(19)	107.0(5)
C(2)-Ni(1)-C(1)	38.63(19)	C(112)-Si(11)-Si(1)	108.34(17)	C(14)-C(20)-C(19)	126.0(5)
C(3)-Ni(1)-C(1)	64.4(2)	C(113)-Si(11)-Si(1)	113.04(17)	C(13)-C(20)-Ni(1)	68.2(3)
C(12)-Ni(1)-C(1)	174.0(2)	C(6)-Si(1)-Si(12)	118.70(16)	C(14)-C(20)-Ni(1)	121.9(3)
C(11)-Ni(1)-C(1)	134.6(2)	C(6)-Si(1)-Si(13)	110.84(16)	C(19)-C(20)-Ni(1)	69.8(3)
C(2)-Ni(1)-C(13)	120.8(2)	Si(12)-Si(1)-Si(13)	108.98(8)	C(201)-C(11)-C(12)	125.6(5)
C(3)-Ni(1)-C(13)	121.2(2)	C(6)-Si(1)-Si(11)	105.11(15)	C(201)-C(11)-C(19)	127.5(5)
C(12)-Ni(1)-C(13)	37.79(18)	Si(12)-Si(1)-Si(11)	105.36(8)	C(12)-C(11)-C(19)	106.8(5)
C(11)-Ni(1)-C(13)	64.2(2)	Si(13)-Si(1)-Si(11)	107.06(7)	C(201)-C(11)-Ni(1)	122.8(3)
C(1)-Ni(1)-C(13)	144.3(2)	C(121)-Si(12)-C(123)	109.3(2)	C(12)-C(11)-Ni(1)	69.3(3)
C(2)-Ni(1)-C(19)	137.8(2)	C(121)-Si(12)-C(122)	107.0(2)	C(19)-C(11)-Ni(1)	73.0(3)
C(3)-Ni(1)-C(19)	174.9(2)	C(123)-Si(12)-C(122)	107.0(2)	C(14)-C(15)-C(16)	129.0(5)
C(12)-Ni(1)-C(19)	64.46(19)	C(121)-Si(12)-Si(1)	113.53(18)	C(8)-C(7)-C(6)	122.8(4)
C(11)-Ni(1)-C(19)	38.52(17)	C(123)-Si(12)-Si(1)	112.81(17)	C(8)-C(7)-C(71)	122.5(5)
C(1)-Ni(1)-C(19)	110.6(2)	C(122)-Si(12)-Si(1)	106.74(16)	C(6)-C(7)-C(71)	114.7(4)
C(13)-Ni(1)-C(19)	63.22(19)	C(223)-Si(22)-C(222)	107.4(2)	C(17)-C(18)-C(19)	125.7(5)
C(2)-Ni(1)-C(10)	64.06(19)	C(223)-Si(22)-C(221)	109.0(2)	C(18)-C(17)-C(171)	121.7(5)
C(3)-Ni(1)-C(10)	38.03(17)	C(222)-Si(22)-C(221)	106.5(2)	C(18)-C(17)-C(16)	124.0(5)
C(12)-Ni(1)-C(10)	117.4(2)	C(223)-Si(22)-Si(2)	112.83(18)	C(171)-C(17)-C(16)	114.3(4)
C(11)-Ni(1)-C(10)	115.0(2)	C(222)-Si(22)-Si(2)	106.91(17)	C(4)-C(5)-C(6)	129.7(5)
C(1)-Ni(1)-C(10)	63.8(2)	C(221)-Si(22)-Si(2)	113.78(17)	C(15)-C(14)-C(20)	123.1(6)
C(13)-Ni(1)-C(10)	144.7(2)	C(232)-Si(23)-C(233)	105.3(2)	C(15)-C(14)-C(141)	119.5(5)
C(19)-Ni(1)-C(10)	140.03(19)	C(232)-Si(23)-C(231)	109.2(3)	C(20)-C(14)-C(141)	117.4(5)
C(2)-Ni(1)-C(9)	63.06(19)	C(233)-Si(23)-C(231)	108.3(2)	C(7)-C(8)-C(9)	127.0(5)
C(3)-Ni(1)-C(9)	62.92(18)	C(232)-Si(23)-Si(2)	113.59(16)	C(9)-C(1)-C(2)	107.0(5)
C(12)-Ni(1)-C(9)	140.0(2)	C(233)-Si(23)-Si(2)	109.37(17)	C(9)-C(1)-C(101)	128.1(5)
C(11)-Ni(1)-C(9)	111.79(19)	C(231)-Si(23)-Si(2)	110.87(18)	C(2)-C(1)-C(101)	124.9(6)
C(1)-Ni(1)-C(9)	37.35(17)	C(132)-Si(13)-C(133)	105.8(2)	C(9)-C(1)-Ni(1)	74.2(3)
C(13)-Ni(1)-C(9)	175.7(2)	C(132)-Si(13)-C(131)	108.5(3)	C(2)-C(1)-Ni(1)	68.0(3)
C(19)-Ni(1)-C(9)	112.78(18)	C(133)-Si(13)-C(131)	107.2(2)	C(101)-C(1)-Ni(1)	124.0(3)
C(10)-Ni(1)-C(9)	37.53(16)	C(132)-Si(13)-Si(1)	113.08(17)	C(172)-C(171)-C(17)	114.0(4)
C(2)-Ni(1)-C(20)	116.7(2)	C(133)-Si(13)-Si(1)	110.63(17)	C(172)-C(171)-C(173)	109.8(5)
C(3)-Ni(1)-C(20)	143.9(2)	C(131)-Si(13)-Si(1)	111.36(18)	C(17)-C(171)-C(173)	112.0(5)
C(12)-Ni(1)-C(20)	63.22(19)	C(3)-C(10)-C(9)	105.9(5)	C(1)-C(2)-C(3)	109.1(5)
C(11)-Ni(1)-C(20)	63.94(19)	C(3)-C(10)-C(4)	126.6(6)	C(1)-C(2)-Ni(1)	73.4(3)
C(1)-Ni(1)-C(20)	115.4(2)	C(9)-C(10)-C(4)	127.4(5)	C(3)-C(2)-Ni(1)	72.1(3)
C(13)-Ni(1)-C(20)	37.06(17)	C(3)-C(10)-Ni(1)	67.3(3)	C(7)-C(6)-C(5)	114.9(4)

C(19)-Ni(1)-C(20)	37.92(16)	C(9)-C(10)-Ni(1)	71.7(3)	C(7)-C(6)-Si(1)	113.5(3)
C(10)-Ni(1)-C(20)	177.8(2)	C(4)-C(10)-Ni(1)	122.7(3)	C(5)-C(6)-Si(1)	115.0(3)
C(9)-Ni(1)-C(20)	140.6(2)	C(73)-C(71)-C(7)	111.9(5)	C(5)-C(4)-C(10)	122.1(5)
C(16)-Si(2)-Si(21)	104.65(16)	C(73)-C(71)-C(72)	110.5(4)	C(5)-C(4)-C(41)	120.2(5)
C(16)-Si(2)-Si(22)	119.42(15)	C(7)-C(71)-C(72)	114.5(5)	C(10)-C(4)-C(41)	117.8(5)
Si(21)-Si(2)-Si(22)	107.00(8)	C(10)-C(9)-C(8)	126.0(5)	C(13)-C(12)-C(11)	108.1(5)
C(16)-Si(2)-Si(23)	109.32(16)	C(10)-C(9)-C(1)	109.1(5)	C(13)-C(12)-Ni(1)	72.5(3)
Si(21)-Si(2)-Si(23)	107.74(7)	C(8)-C(9)-C(1)	124.7(5)	C(11)-C(12)-Ni(1)	71.3(3)
Si(22)-Si(2)-Si(23)	108.13(8)	C(10)-C(9)-Ni(1)	70.8(3)	C(15)-C(16)-C(17)	114.4(4)
C(212)-Si(21)-C(211)	107.2(2)	C(8)-C(9)-Ni(1)	122.6(3)	C(15)-C(16)-Si(2)	114.7(3)
C(212)-Si(21)-C(213)	106.8(2)	C(1)-C(9)-Ni(1)	68.5(3)	C(17)-C(16)-Si(2)	113.6(3)
C(211)-Si(21)-C(213)	107.1(2)	C(18)-C(19)-C(20)	128.0(5)	C(12)-C(13)-C(20)	110.5(5)
C(212)-Si(21)-Si(2)	112.55(16)	C(18)-C(19)-C(11)	124.4(5)	C(12)-C(13)-Ni(1)	69.7(3)
C(10)-C(3)-Ni(1)	74.7(3)	C(2)-C(3)-Ni(1)	69.2(3)	C(20)-C(13)-Ni(1)	74.7(3)
C(10)-C(3)-C(2)	108.8(5)				

5.8.5 Anisotropic displacement parameters ($A^2x\ 10^3$) for Ni(6-Hyp-Hgual)$_2$, The anisotropic displacement factor exponent takes the form: $-2\pi^2[\ h^2a^{*2}U11 + ... + 2\ h\ k\ a^*\ b^*\ U12\ ]$

atom	U11	U22	U33	U23	U13	U12
Fe(2)	17(8)	21(1)	17(1)	-4(1)	1(2)	-8(2)
Fe(1)	16(9)	22(1)	21(1)	-7(1)	0(2)	-5(2)
Si(1)	70(20)	19(2)	23(2)	-8(2)	-1(5)	-2(4)
Si(11)	60(30)	32(3)	37(3)	-3(2)	9(6)	9(5)
Si(12)	0(20)	35(3)	31(2)	-13(2)	-8(6)	-1(5)
Fe(3)	74(9)	28(1)	25(1)	-12(1)	-5(2)	6(2)
Si(2)	50(20)	20(2)	19(2)	-8(2)	7(5)	-6(4)
Si(13)	30(20)	21(2)	41(3)	-6(2)	16(6)	-4()
Si(21)	90(20)	22(2)	32(2)	-3(2)	-7(6)	0(5)
Si(4)	63(19)	21(2)	23(2)	-5(2)	6(5)	-11(4)
Si(3)	0(20)	14(2)	17(2)	-3(2)	9(5)	-2(4)
Si(31)	30(20)	39(3)	18(2)	-9(2)	-1(5)	-16(5)
Si(6)	36(19)	35(2)	28(2)	-17(2)	-6(5)	-4(5)
Si(32)	0(20)	23(2)	34(2)	-3(2)	5(5)	2(5)
Si(5)	30(20)	38(3)	24(2)	-16(2)	-11(5)	6(5)
Si(22)	20(30)	46(3)	32(2)	-18(2)	5(6)	-17(5)
Si(43)	160(30)	23(2)	32(3)	-1(2)	27(6)	0(5)
Si(33)	0(20)	28(2)	39(3)	-4(2)	12(6)	-6(5)
Si(23)	70(20)	30(2)	23(2)	-7(2)	-14(5)	-3(5)
Si(51)	0(20)	50(3)	36(2)	-16(2)	1(5)	-5(6)
Si(52)	120(20)	21(2)	33(2)	-7(2)	-1(5)	-4(5)
Si(53)	110(30)	44(3)	26(2)	-17(2)	20(6)	-42(6)
Si(41)	260(30)	49(3)	45(3)	-21(2)	3(7)	-3(6)
Si(61)	170(20)	35(2)	48(3)	-16(2)	1(6)	-16(5)
Si(42)	110(20)	50(3)	46(3)	-8(2)	-14(6)	-3(6)
Si(62)	340(30)	64(4)	20(2)	-15(2)	16(6)	-101(8)
Si(63)	250(30)	52(3)	36(3)	-5(2)	-6(6)	-40(7)

5.9 Crystallographic data for (3-Hyp-6-H$_2$gua)$_2$

5.9.1 Crystallographic data and structure refinement for (3-Hyp-6-H$_2$gua)$_2$

Empirical formula	$C_{24}H_{45}Si_4$
Formula weight (g/mol)	445.96
Temperature (K)	173(2)
Wavelength(Å)	0,71073
Crystal system, space group	monoclinic, C2/c
Unit cell dimensions (Å ,deg)	a=25.989(2) α=90
	b=19.2622(16) β=105.100(6)

	c=11.8707(12) γ=90
Volume (Å^3)	5737.4(9)
Z; calc. density (Mg/m^3)	8; 1.033
Absorption coefficient (mm^{-1})	0.215
F(000)	1960
Theta range for data collection (deg)	2.05 ~28.00
Limiting indices	-1≤h≤34, -1≤k≤25, -15≤l≤15
Reflections collected / unique	7700 / 6839[R(int)=0.0455]
Completeness to θ	28.00; 98.6%
Refinement method	full-matrix least-squares on F^2
Data / restraints / parameters	6839 / 0 / 284
(Goodness-of-fit on F^2)	1.002
Final R indices [I>2σ(I)]	R1=0.0603, wR2=0.1199
R indices (all data)	R1=0.1447, wR2=0.1533
Largest diff. peak and hole (e.Å^{-3})	0.284 and –0.251

5.9.2 Atomic coordinates (x 10^4) and equivalent isotropic displacement parameters (A^2 ×10^3) for (3-Hyp-6-H_2gua)$_2$. U(eq) is defined as one third of the trace of the orthogonalized Uij tensor

atom	x/a	y/b	z/c	U(eq)	atom	x/a	y/b	z/c	U(eq)
Si(1)	1505(1)	1854(1)	6490(1)	29(1)	C(133)	569(2)	3149(2)	6495(3)	53(1)
Si(11)	899(1)	926(1)	5878(1)	37(1)	C(71)	440(1)	4185(2)	1583(3)	38(1)
Si(12)	2275(1)	1388(1)	7784(1)	43(1)	C(123)	2841(1)	2020(2)	8173(4)	67(1)
Si(13)	1123(1)	2667(1)	7517(1)	39(1)	C(101)	1938(2)	4271(2)	5685(3)	51(1)
C(6)	297(1)	3099(2)	2831(2)	26(1)	C(113)	724(2)	532(2)	7166(3)	72(1)
C(5)	581(1)	2471(2)	2549(3)	28(1)	C(132)	840(2)	2206(2)	8614(4)	65(1)
C(4)	1040(1)	2229(2)	3239(2)	28(1)	C(73)	628(2)	3890(2)	567(3)	55(1)
C(10)	1338(1)	2615(2)	4251(2)	27(1)	C(72)	617(2)	4938(2)	1797(4)	63(1)
C(3)	1752(1)	2320(2)	5265(3)	29(1)	C(122)	2524(2)	641(3)	7080(4)	81(2)
C(2)	2035(1)	2952(2)	5829(3)	35(1)	C(131)	1617(2)	3315(2)	8348(4)	66(1)
C(9)	1365(1)	3335(2)	4306(3)	29(1)	C(112)	1187(2)	187(2)	5220(4)	78(1)
C(7)	624(1)	3724(2)	2647(3)	29(1)	C(121)	2134(2)	1085(3)	9166(3)	75(2)
C(1)	1801(1)	3528(2)	5310(3)	34(1)	C(111)	273(2)	1209(2)	4828(4)	61(1)
C(41)	1282(1)	1564(2)	2926(3)	38(1)	C(8)	1098(1)	3819(2)	3426(3)	32(1)

5.9.3 Bond lengths [Å] for (3-Hyp-6-H_2gua)$_2$

Bonds	Bond lengths	bonds	Bond lengths	bonds	Bond lengths
Si(1)-C(3)	1.954(3)	Si(13)-C(133)	1.870(4)	C(10)-C(3)	1.501(4)
Si(1)-Si(13)	2.3564(13)	Si(13)-C(131)	1.876(4)	C(3)-C(2)	1.489(4)
Si(1)-Si(12)	2.3601(13)	Si(13)-C(132)	1.878(4)	C(2)-C(1)	1.337(5)
Si(1)-Si(11)	2.3678(13)	C(6)-C(5)	1.500(4)	C(9)-C(8)	1.436(4)
Si(11)-C(111)	1.855(4)	C(6)-C(7)	1.523(4)	C(9)-C(1)	1.463(4)
Si(11)-C(113)	1.866(4)	C(6)-C(6)#1	1.538(5)	C(7)-C(8)	1.347(4)
Si(11)-C(112)	1.871(4)	C(5)-C(4)	1.342(4)	C(7)-C(71)	1.516(4)
Si(12)-C(122)	1.863(5)	C(4)-C(10)	1.453(4)	C(1)-C(101)	1.512(5)
Si(12)-C(121)	1.865(4)	C(4)-C(41)	1.515(4)	C(71)-C(72)	1.522(5)
Si(12)-C(123)	1.874(4)	C(10)-C(9)	1.389(4)	C(71)-C(73)	1.525(5)

5.9.4 Bond angles for (3-Hyp-6-H_2gua)$_2$ (deg)

Bond angles	parameter	Bond angles	parameter	Bond angles	parameter
C(3)-Si(1)-Si(13)	110.15(11)	C(123)-Si(12)-Si(1)	113.03(13)	C(2)-C(3)-C(10)	102.6(3)
C(3)-Si(1)-Si(12)	105.78(10)	C(133)-Si(13)-C(131)	108.5(2)	C(2)-C(3)-Si(1)	105.1(2)
Si(13)-Si(1)-Si(12)	108.44(5)	C(133)-Si(13)-C(132)	108.1(2)	C(10)-C(3)-Si(1)	117.7(2)
C(3)-Si(1)-Si(11)	116.04(10)	C(131)-Si(13)-C(132)	106.7(2)	C(1)-C(2)-C(3)	111.1(3)
Si(13)-Si(1)-Si(11)	108.94(5)	C(133)-Si(13)-Si(1)	110.56(13)	C(10)-C(9)-C(8)	127.2(3)

Si(12)-Si(1)-Si(11)	107.19(5)	C(131)-Si(13)-Si(1)	113.05(14)	C(10)-C(9)-C(1)	108.1(3)
C(111)-Si(11)-C(113)	108.2(2)	C(132)-Si(13)-Si(1)	109.77(14)	C(8)-C(9)-C(1)	123.5(3)
C(111)-Si(11)-C(112)	108.7(2)	C(5)-C(6)-C(7)	106.3(2)	C(8)-C(7)-C(71)	121.8(3)
C(113)-Si(11)-C(112)	104.0(2)	C(5)-C(6)-C(6)#1	111.8(2)	C(8)-C(7)-C(6)	117.0(3)
C(111)-Si(11)-Si(1)	112.40(13)	C(7)-C(6)-C(6)#1	116.7(2)	C(71)-C(7)-C(6)	121.0(3)
C(113)-Si(11)-Si(1)	109.85(14)	C(4)-C(5)-C(6)	123.6(3)	C(2)-C(1)-C(9)	109.1(3)
C(112)-Si(11)-Si(1)	113.35(16)	C(5)-C(4)-C(10)	121.7(3)	C(2)-C(1)-C(101)	127.3(3)
C(122)-Si(12)-C(121)	108.9(2)	C(5)-C(4)-C(41)	120.2(3)	C(9)-C(1)-C(101)	123.6(3)
C(122)-Si(12)-C(123)	105.6(2)	C(10)-C(4)-C(41)	118.0(3)	C(7)-C(8)-C(9)	126.4(3)
C(121)-Si(12)-C(123)	107.9(2)	C(9)-C(10)-C(4)	124.0(3)	C(7)-C(71)-C(72)	113.7(3)
C(122)-Si(12)-Si(1)	109.75(15)	C(9)-C(10)-C(3)	108.9(3)	C(7)-C(71)-C(73)	110.1(3)
C(121)-Si(12)-Si(1)	111.35(14)	C(4)-C(10)-C(3)	125.8(3)	C(72)-C(71)-C(73)	110.0(3)

5.9.5 Anisotropic displacement parameters ($A^2 \times 10^3$) for (3-Hyp-6-H_2gua)$_2$. The anisotropic displacement factor exponent takes the form: $-2\pi^2[h^2a^{*2}U11 + ... + 2hka^*b^*U12]$

atom	U11	U22	U33	U23	U13	U12
Si(1)	22(1)	35(1)	28(1)	-1(1)	4(1)	1(1)
Si(11)	38(1)	34(1)	36(1)	0(1)	4(1)	-5(1)
Si(12)	27(1)	60(1)	38(1)	17(1)	3(1)	4(1)
Si(13)	38(1)	42(1)	41(1)	-10(1)	16(1)	-2(1)
C(6)	23(2)	29(2)	25(2)	0(1)	1(1)	0(1)
C(5)	27(2)	28(2)	28(2)	-1(1)	4(1)	-5(1)
C(4)	25(2)	29(2)	29(2)	0(1)	7(1)	-1(1)
C(10)	20(1)	34(2)	27(2)	-1(1)	6(1)	-1(1)
C(3)	22(2)	37(2)	29(2)	1(1)	6(1)	3(1)
C(2)	24(2)	49(2)	29(2)	-3(2)	2(1)	-9(2)
C(9)	22(2)	34(2)	31(2)	-5(1)	8(1)	-4(1)
C(7)	28(2)	25(2)	36(2)	-3(1)	12(1)	2(1)
C(1)	29(2)	43(2)	31(2)	-4(2)	8(1)	-8(2)
C(41)	36(2)	37(2)	40(2)	-8(2)	5(2)	4(2)
C(8)	29(2)	26(2)	41(2)	-1(1)	10(1)	-3(1)
C(133)	49(2)	47(2)	67(3)	-4(2)	20(2)	13(2)
C(71)	30(2)	38(2)	44(2)	12(2)	6(2)	1(2)
C(123)	28(2)	87(3)	74(3)	25(3)	-6(2)	-3(2)
C(101)	54(2)	48(2)	45(2)	-13(2)	5(2)	-19(2)
C(113)	90(4)	70(3)	53(3)	6(2)	14(2)	-39(3)
C(132)	80(3)	61(3)	70(3)	-5(2)	51(3)	4(2)
C(73)	54(2)	75(3)	39(2)	20(2)	15(2)	15(2)
C(72)	67(3)	38(2)	77(3)	21(2)	6(2)	-1(2)
C(122)	66(3)	81(3)	93(4)	16(3)	14(3)	42(3)
C(131)	66(3)	80(3)	54(2)	-32(2)	17(2)	-18(3)
C(112)	92(4)	45(3)	97(4)	-18(3)	28(3)	-1(3)
C(121)	46(2)	126(4)	49(2)	34(3)	2(2)	-11(3)
C(111)	40(2)	62(3)	68(3)	9(2)	-9(2)	-17(2)

5.10 Crystallographic data for Ti(6-Hyp-Hgual)$_2$Cl$_2$

5.10.1 Crystallographic data and structure refinement for Ti(6-Hyp-Hgual)$_2$Cl$_2$

Empirical formula	$C_{48}H_{90}Cl_2Si_8Ti$
Formula weight (g/mol)	1010.71
Temperature (K)	173(2)
Wavelength(Å)	0.71073

Crystal system, space group	Triclinic,
Unit cell dimensions (Å ,deg)	a=9.2842(17) α=88.166(8) b=17..558(3) β=85.941(12) c=20.755(3) γ=78.459(11)
Volume ($Å^3$)	3306.1(10)
Z; calc. density (Mg/m^3)	3; 1.108
Absorption coefficient (mm^{-1})	0.387
F(000)	1192
Theta range for data collection (deg)	1.97 ~26.00
Limiting indices	$0 \le h \le 11, -21 \le k \le 21, -25 \le l \le 25$
Reflections collected / unique	13694 / 12863[R(int)=0.0346]
Completeness to θ	26.00; 98.9%
Refinement method	full-matrix least-squares on F^2
Data / restraints / parameters	12863 /143 / 660
(Goodness-of-fit on F^2)	0.845
Final R indices [I>2σ(I)]	R1=0.0455, wR2=0.1024
R indices (all data)	R1=0.0822, wR2=0.1095
Largest diff. peak and hole ($e.Å^{-3}$)	0.486 and –0.291

5.10.2 Atomic coordinates ($\times 10^4$) and equivalent isotropic displacement parameters ($A^2 \times 10^3$) for $Ti(6\text{-}Hyp\text{-}Hgual)_2Cl_2$. U(eq) is defined as one third of the trace of the orthogonalized Uij tensor.

atom	x/a	y/b	z/c	U(eq)	atom	x/a	y/b	z/c	U(eq)
Ti(1)	7593(1)	2416(1)	530(1)	24(1)	Cl(2)	7025(1)	3634(1)	1005(1)	32(1)
Cl(1)	10115(1)	2427(1)	387(1)	34(1)	C(10)	7974(3)	2262(2)	-662(1)	28(1)
Si(2)	6273(1)	1702(1)	3477(1)	25(1)	C(71)	10065(3)	4393(2)	-1332(2)	35(1)
Si(1)	8498(1)	3112(1)	-2460(1)	27(1)	C(101)	4939(4)	3954(2)	-164(2)	40(1)
Si(21)	8536(1)	1074(1)	3894(1)	34(1)	C(2)	5644(4)	2444(2)	-154(1)	34(1)
Si(11)	6942(1)	4339(1)	-2646(1)	32(1)	C(73)	9267(4)	5169(2)	-1030(2)	46(1)
Si(22)	4708(1)	2179(1)	4390(1)	35(1)	C(111)	5817(4)	4265(2)	-3356(2)	50(1)
Si(23)	5293(1)	725(1)	2991(1)	35(1)	C(141)	3715(3)	2880(2)	1525(2)	43(1)
Si(12)	10285(1)	2871(1)	-3341(1)	43(1)	C(41)	9955(4)	1038(2)	-802(2)	48(1)
Si(13)	6947(1)	2185(1)	-2486(1)	42(1)	C(72)	11617(4)	4156(2)	-1078(2)	53(1)
C(16)	6370(3)	2654(2)	2956(1)	25(1)	C(112)	8042(4)	5105(2)	-2871(2)	45(1)
C(11)	8652(4)	1342(2)	1281(1)	30(1)	C(211)	9169(4)	1680(2)	4507(2)	53(1)
C(6)	9725(3)	3069(2)	-1714(1)	27(1)	C(172)	7851(4)	4132(2)	2880(2)	43(1)
C(7)	9236(3)	3723(2)	-1230(1)	25(1)	C(232)	6752(4)	64(2)	2478(2)	54(1)
C(19)	7864(3)	1941(2)	1694(1)	23(1)	C(173)	10267(4)	3196(2)	2861(2)	44(1)
C(8)	8225(3)	3715(2)	-738(1)	25(1)	C(212)	8261(4)	143(2)	4332(2)	49(1)
C(18)	8527(3)	2389(2)	2125(1)	23(1)	C(231)	3699(4)	1084(2)	2479(2)	42(1)
C(17)	7894(3)	2732(1)	2669(1)	23(1)	C(113)	5644(4)	4684(2)	-1931(2)	47(1)
C(5)	10112(4)	2252(2)	-1437(1)	33(1)	C(223)	2753(4)	2475(2)	4146(2)	60(1)
C(1)	5981(3)	3188(2)	-275(1)	29(1)	C(133)	5141(4)	2509(2)	-2002(2)	60(1)
C(14)	5100(3)	2609(2)	1895(1)	29(1)	C(233)	4571(5)	130(2)	3668(2)	58(1)
C(9)	7437(3)	3082(2)	-573(1)	25(1)	C(222)	5278(4)	3065(2)	4700(2)	54(1)
C(15)	5144(3)	2843(2)	2501(1)	29(1)	C(131)	6519(5)	2093(2)	-3358(2)	65(1)
C(13)	6216(4)	1557(2)	1059(1)	31(1)	C(132)	7771(5)	1164(2)	-2213(2)	62(1)
C(20)	6330(3)	2066(2)	1563(1)	25(1)	C(221)	4741(5)	1463(2)	5088(2)	61(1)
C(4)	9401(4)	1888(2)	-983(1)	32(1)	C(213)	10043(4)	802(2)	3247(2)	62(1)
C(3)	6866(4)	1877(2)	-389(1)	32(1)	C(122)	11717(4)	3485(3)	-3282(2)	69(1)
C(12)	7626(4)	1118(2)	888(1)	35(1)	C(121)	9506(5)	3099(3)	-4152(2)	71(1)
C(171)	8617(3)	3283(2)	3023(1)	29(1)	C(123)	11245(6)	1823(2)	-3313(2)	110(2)
C(201)	10262(4)	967(2)	1316(2)	38(1)					

5.10.3 Bond lengths [Å] for Ti(6-Hyp-Hgual)$_2$Cl$_2$

bonds	Bond lengths	bonds	Bond lengths	bonds	Bond lengths
Ti(1)-Cl(2)	2.3304(9)	Si(11)-C(113)	1.879(3)	C(7)-C(8)	1.340(4)
Ti(1)-Cl(1)	2.3432(10)	Si(11)-C(111)	1.889(3)	C(7)-C(71)	1.532(4)
Ti(1)-C(3)	2.356(3)	Si(22)-C(223)	1.885(4)	C(19)-C(20)	1.440(4)
Ti(1)-C(13)	2.362(3)	Si(22)-C(221)	1.886(3)	C(19)-C(18)	1.455(4)
Ti(1)-C(12)	2.370(3)	Si(22)-C(222)	1.886(4)	C(8)-C(9)	1.467(4)
Ti(1)-C(2)	2.370(3)	Si(23)-C(231)	1.877(3)	C(18)-C(17)	1.337(4)
Ti(1)-C(20)	2.489(3)	Si(23)-C(232)	1.887(4)	C(17)-C(171)	1.518(4)
Ti(1)-C(10)	2.491(3)	Si(23)-C(233)	1.889(3)	C(5)-C(4)	1.331(4)
Ti(1)-C(11)	2.497(3)	Si(12)-C(121)	1.877(4)	C(1)-C(2)	1.414(4)
Ti(1)-C(1)	2.503(3)	Si(12)-C(123)	1.879(4)	C(1)-C(9)	1.426(4)
Ti(1)-C(9)	2.537(3)	Si(12)-C(122)	1.883(4)	C(1)-C(101)	1.506(4)
Ti(1)-C(19)	2.542(3)	Si(13)-C(133)	1.887(4)	C(14)-C(15)	1.343(4)
Si(2)-C(16)	1.975(3)	Si(13)-C(132)	1.888(4)	C(14)-C(20)	1.477(4)
Si(2)-Si(22)	2.3714(12)	Si(13)-C(131)	1.898(3)	C(14)-C(141)	1.530(4)
Si(2)-Si(21)	2.3773(12)	C(16)-C(15)	1.509(4)	C(9)-C(10)	1.441(4)
Si(2)-Si(23)	2.3781(11)	C(16)-C(17)	1.526(4)	C(13)-C(12)	1.407(4)
Si(1)-C(6)	1.978(3)	C(11)-C(12)	1.416(4)	C(13)-C(20)	1.422(4)
Si(1)-Si(12)	2.3700(13)	C(11)-C(19)	1.428(4)	C(4)-C(10)	1.478(4)
Si(1)-Si(11)	2.3793(12)	C(11)-C(201)	1.514(4)	C(4)-C(41)	1.522(4)
Si(1)-Si(13)	2.3827(12)	C(6)-C(5)	1.513(4)	C(3)-C(10)	1.417(4)
Si(21)-C(213)	1.870(4)	C(6)-C(7)	1.527(4)	C(3)-C(2)	1.420(4)
Si(21)-C(211)	1.881(3)	C(71)-C(73)	1.542(4)	C(171)-C(173)	1.522(4)
Si(21)-C(212)	1.897(3)	C(71)-C(72)	1.542(5)	C(171)-C(172)	1.546(4)
Si(11)-C(112)	1.874(3)				

5.10.4 Bond angles for Ti(6-Hyp-Hgual)$_2$Cl$_2$ (deg)

Bond angles	parameter	Bond angles	parameter	Bond angles	parameter
Cl(2)-Ti(1)-Cl(1)	93.51(3)	C(1)-Ti(1)-C(19)	147.38(10)	C(6)-C(7)-C(71)	114.0(2)
Cl(2)-Ti(1)-C(3)	134.89(8)	C(9)-Ti(1)-C(19)	171.02(8)	C(11)-C(19)-C(20)	108.0(2)
Cl(1)-Ti(1)-C(3)	108.73(8)	C(16)-Si(2)-Si(22)	103.00(9)	C(11)-C(19)-C(18)	125.3(3)
Cl(2)-Ti(1)-C(13)	110.87(8)	C(16)-Si(2)-Si(21)	114.93(9)	C(20)-C(19)-C(18)	126.5(2)
Cl(1)-Ti(1)-C(13)	133.88(8)	Si(22)-Si(2)-Si(21)	105.61(4)	C(11)-C(19)-Ti(1)	71.83(15)
C(3)-Ti(1)-C(13)	81.46(10)	C(16)-Si(2)-Si(23)	116.88(9)	C(20)-C(19)-Ti(1)	71.36(15)
Cl(2)-Ti(1)-C(12)	135.67(8)	Si(22)-Si(2)-Si(23)	108.93(5)	C(18)-C(19)-Ti(1)	118.34(17)
Cl(1)-Ti(1)-C(12)	101.59(9)	Si(21)-Si(2)-Si(23)	106.76(4)	C(7)-C(8)-C(9)	125.8(3)
C(3)-Ti(1)-C(12)	78.64(10)	C(6)-Si(1)-Si(12)	102.48(10)	C(17)-C(18)-C(19)	126.6(3)
C(13)-Ti(1)-C(12)	34.61(11)	C(6)-Si(1)-Si(11)	114.77(9)	C(18)-C(17)-C(171)	121.3(3)
Cl(2)-Ti(1)-C(2)	103.50(8)	Si(12)-Si(1)-Si(11)	108.02(4)	C(18)-C(17)-C(16)	123.9(2)
Cl(1)-Ti(1)-C(2)	136.02(8)	C(6)-Si(1)-Si(13)	117.77(9)	C(171)-C(17)-C(16)	114.6(2)
C(3)-Ti(1)-C(2)	34.97(11)	Si(12)-Si(1)-Si(13)	108.02(5)	C(4)-C(5)-C(6)	130.5(3)
C(13)-Ti(1)-C(2)	76.83(10)	Si(11)-Si(1)-Si(13)	105.31(5)	C(2)-C(1)-C(9)	107.8(3)
C(12)-Ti(1)-C(2)	93.97(11)	C(213)-Si(21)-C(211)	109.02(19)	C(2)-C(1)-C(101)	126.0(3)
Cl(2)-Ti(1)-C(20)	80.62(7)	C(213)-Si(21)-C(212)	107.40(17)	C(9)-C(1)-C(101)	126.0(3)
Cl(1)-Ti(1)-C(20)	124.45(7)	C(211)-Si(21)-C(212)	106.31(16)	C(2)-C(1)-Ti(1)	68.05(16)
C(3)-Ti(1)-C(20)	113.98(10)	C(213)-Si(21)-Si(2)	112.69(12)	C(9)-C(1)-Ti(1)	74.90(16)
C(13)-Ti(1)-C(20)	33.95(9)	C(211)-Si(21)-Si(2)	112.16(12)	C(101)-C(1)-Ti(1)	126.7(2)
C(12)-Ti(1)-C(20)	56.44(10)	C(212)-Si(21)-Si(2)	108.94(12)	C(15)-C(14)-C(20)	122.7(3)
C(2)-Ti(1)-C(20)	98.46(10)	C(112)-Si(11)-C(113)	108.33(16)	C(15)-C(14)-C(141)	120.2(3)
Cl(2)-Ti(1)-C(10)	122.12(7)	C(112)-Si(11)-C(111)	106.28(16)	C(20)-C(14)-C(141)	117.1(3)
Cl(1)-Ti(1)-C(10)	79.97(8)	C(113)-Si(11)-C(111)	108.45(16)	C(1)-C(9)-C(10)	108.1(2)
C(3)-Ti(1)-C(10)	33.86(9)	C(112)-Si(11)-Si(1)	111.38(11)	C(1)-C(9)-C(8)	124.5(3)
C(13)-Ti(1)-C(10)	114.41(10)	C(113)-Si(11)-Si(1)	113.12(11)	C(10)-C(9)-C(8)	127.4(3)
C(12)-Ti(1)-C(10)	101.58(10)	C(111)-Si(11)-Si(1)	109.00(12)	C(1)-C(9)-Ti(1)	72.24(15)
C(2)-Ti(1)-C(10)	56.56(10)	C(223)-Si(22)-C(221)	108.45(19)	C(10)-C(9)-Ti(1)	71.61(15)
C(20)-Ti(1)-C(10)	147.75(9)	C(223)-Si(22)-C(222)	108.06(18)	C(8)-C(9)-Ti(1)	120.84(18)
Cl(2)-Ti(1)-C(11)	113.71(7)	C(221)-Si(22)-C(222)	106.81(17)	C(14)-C(15)-C(16)	129.7(3)
Cl(1)-Ti(1)-C(11)	78.36(8)	C(223)-Si(22)-Si(2)	109.44(12)	C(12)-C(13)-C(20)	108.8(3)
C(3)-Ti(1)-C(11)	109.05(10)	C(221)-Si(22)-Si(2)	114.22(13)	C(12)-C(13)-Ti(1)	72.99(17)

C(13)-Ti(1)-C(11)	56.28(10)	C(222)-Si(22)-Si(2)	109.67(12)	C(20)-C(13)-Ti(1)	77.93(16)
C(12)-Ti(1)-C(11)	33.70(10)	C(231)-Si(23)-C(232)	107.49(16)	C(13)-C(20)-C(19)	106.9(3)
C(2)-Ti(1)-C(11)	127.46(10)	C(231)-Si(23)-C(233)	105.79(16)	C(13)-C(20)-C(14)	126.1(3)
C(20)-Ti(1)-C(11)	55.44(10)	C(232)-Si(23)-C(233)	108.80(17)	C(19)-C(20)-C(14)	126.9(2)
C(10)-Ti(1)-C(11)	120.73(9)	C(231)-Si(23)-Si(2)	115.83(11)	C(13)-C(20)-Ti(1)	68.12(16)
Cl(2)-Ti(1)-C(1)	78.70(7)	C(232)-Si(23)-Si(2)	111.57(12)	C(19)-C(20)-Ti(1)	75.39(16)
Cl(1)-Ti(1)-C(1)	116.46(7)	C(233)-Si(23)-Si(2)	107.05(12)	C(14)-C(20)-Ti(1)	122.34(18)
C(3)-Ti(1)-C(1)	56.36(10)	C(121)-Si(12)-C(123)	109.1(2)	C(5)-C(4)-C(10)	122.3(3)
C(13)-Ti(1)-C(1)	106.64(10)	C(121)-Si(12)-C(122)	106.56(19)	C(5)-C(4)-C(41)	121.6(3)
C(12)-Ti(1)-C(1)	127.52(10)	C(123)-Si(12)-C(122)	107.8(2)	C(10)-C(4)-C(41)	115.9(3)
C(2)-Ti(1)-C(1)	33.59(9)	C(121)-Si(12)-Si(1)	113.80(15)	C(10)-C(3)-C(2)	108.7(3)
C(20)-Ti(1)-C(1)	116.25(10)	C(123)-Si(12)-Si(1)	109.11(14)	C(10)-C(3)-Ti(1)	78.34(16)
C(10)-Ti(1)-C(1)	55.37(10)	C(122)-Si(12)-Si(1)	110.31(13)	C(2)-C(3)-Ti(1)	73.08(16)
C(11)-Ti(1)-C(1)	161.01(10)	C(133)-Si(13)-C(132)	108.09(18)	C(13)-C(12)-C(11)	108.7(3)
Cl(2)-Ti(1)-C(9)	89.12(7)	C(133)-Si(13)-C(131)	107.65(19)	C(13)-C(12)-Ti(1)	72.40(16)
Cl(1)-Ti(1)-C(9)	84.97(7)	C(132)-Si(13)-C(131)	105.14(17)	C(11)-C(12)-Ti(1)	78.10(16)
C(3)-Ti(1)-C(9)	55.85(9)	C(133)-Si(13)-Si(1)	111.72(12)	C(17)-C(171)-C(173)	114.5(2)
C(13)-Ti(1)-C(9)	131.82(10)	C(132)-Si(13)-Si(1)	115.90(14)	C(17)-C(171)-C(172)	109.5(2)
C(12)-Ti(1)-C(9)	133.20(9)	C(131)-Si(13)-Si(1)	107.85(12)	C(173)-C(171)-C(172)	109.1(3)
C(2)-Ti(1)-C(9)	55.61(10)	C(15)-C(16)-C(17)	115.6(2)	C(3)-C(10)-C(9)	107.0(3)
C(20)-Ti(1)-C(9)	149.11(10)	C(15)-C(16)-Si(2)	112.01(18)	C(3)-C(10)-C(4)	126.2(3)
C(10)-Ti(1)-C(9)	33.28(9)	C(17)-C(16)-Si(2)	116.11(19)	C(9)-C(10)-C(4)	126.8(3)
C(11)-Ti(1)-C(9)	152.25(10)	C(12)-C(11)-C(19)	107.6(3)	C(3)-C(10)-Ti(1)	67.81(15)
C(1)-Ti(1)-C(9)	32.86(9)	C(12)-C(11)-C(201)	127.1(3)	C(9)-C(10)-Ti(1)	75.11(15)
Cl(2)-Ti(1)-C(19)	82.97(6)	C(19)-C(11)-C(201)	125.0(3)	C(4)-C(10)-Ti(1)	122.66(19)
Cl(1)-Ti(1)-C(19)	91.25(7)	C(12)-C(11)-Ti(1)	68.20(16)	C(7)-C(71)-C(73)	115.0(3)
C(3)-Ti(1)-C(19)	133.13(9)	C(19)-C(11)-Ti(1)	75.26(16)	C(7)-C(71)-C(72)	110.1(3)
C(13)-Ti(1)-C(19)	55.78(9)	C(201)-C(11)-Ti(1)	126.8(2)	C(73)-C(71)-C(72)	109.7(3)
C(12)-Ti(1)-C(19)	55.57(9)	C(5)-C(6)-C(7)	116.7(2)	C(1)-C(2)-C(3)	108.4(3)
C(2)-Ti(1)-C(19)	130.50(10)	C(5)-C(6)-Si(1)	111.28(19)	C(1)-C(2)-Ti(1)	78.36(17)
C(20)-Ti(1)-C(19)	33.25(9)	C(7)-C(6)-Si(1)	115.61(19)	C(3)-C(2)-Ti(1)	71.95(17)
C(10)-Ti(1)-C(19)	153.60(9)	C(8)-C(7)-C(6)	124.5(2)		
C(11)-Ti(1)-C(19)	32.90(9)	C(8)-C(7)-C(71)	121.4(2)		

5.10.5 Anisotropic displacement parameters ($A^2 \times 10^3$) for Ti(6-Hyp-Hgual)$_2$Cl$_2$. The anisotropic displacement factor exponent akes the form: $-2\pi^2 [h^2 a^{*2} U11 + ... + 2 h k a^* b^* U12]$

atom	U11	U22	U33	U23	U13	U12
Ti(1)	30(1)	21(1)	22(1)	-1(1)	-4(1)	-8(1)
Cl(1)	31(1)	42(1)	31(1)	0(1)	-4(1)	-10(1)
Si(2)	27(1)	24(1)	23(1)	3(1)	-4(1)	-7(1)
Si(1)	36(1)	22(1)	21(1)	-1(1)	-2(1)	-5(1)
Si(21)	31(1)	33(1)	37(1)	5(1)	-9(1)	-4(1)
Si(11)	35(1)	29(1)	29(1)	0(1)	-3(1)	-1(1)
Si(22)	36(1)	43(1)	26(1)	4(1)	3(1)	-6(1)
Si(23)	47(1)	28(1)	34(1)	7(1)	-12(1)	-16(1)
Si(12)	60(1)	32(1)	28(1)	-1(1)	11(1)	4(1)
Si(13)	65(1)	36(1)	33(1)	4(1)	-17(1)	-25(1)
C(16)	31(2)	20(1)	24(1)	-1(1)	-1(1)	-5(1)
C(11)	46(2)	20(1)	24(2)	1(1)	-5(1)	-4(1)
C(6)	28(2)	32(2)	23(1)	-3(1)	-2(1)	-7(1)
C(7)	27(2)	24(2)	26(2)	-1(1)	-9(1)	-5(1)
C(19)	24(2)	20(1)	24(1)	2(1)	-2(1)	-4(1)
C(8)	33(2)	19(1)	23(1)	-2(1)	-6(1)	-4(1)
C(18)	21(2)	22(1)	24(1)	5(1)	-5(1)	-1(1)
C(17)	27(2)	17(1)	25(2)	4(1)	-4(1)	-2(1)
C(5)	35(2)	35(2)	26(2)	-9(1)	-5(1)	5(1)
C(1)	26(2)	37(2)	23(2)	4(1)	-6(1)	-6(1)
C(14)	22(2)	32(2)	33(2)	12(1)	-5(1)	-7(1)
C(9)	29(2)	24(1)	21(1)	0(1)	-4(1)	-4(1)
C(15)	25(2)	27(2)	32(2)	10(1)	2(1)	0(1)
C(13)	42(2)	31(2)	27(2)	6(1)	-11(1)	-18(2)

C(20)	29(2)	23(1)	25(2)	8(1)	-8(1)	-10(1)
C(4)	40(2)	24(2)	28(2)	-3(1)	-10(1)	4(1)
C(3)	48(2)	29(2)	25(2)	0(1)	-11(2)	-18(2)
C(12)	61(2)	20(2)	26(2)	1(1)	-7(2)	-14(2)
C(171)	34(2)	26(2)	27(2)	-1(1)	-5(1)	-7(1)
C(201)	45(2)	28(2)	34(2)	-3(1)	-3(2)	11(2)
Cl(2)	45(1)	21(1)	29(1)	-2(1)	-1(1)	-7(1)
C(10)	41(2)	24(2)	20(1)	-2(1)	-9(1)	-6(1)
C(71)	36(2)	42(2)	29(2)	1(1)	-3(1)	-16(2)
C(101)	33(2)	44(2)	37(2)	10(2)	0(2)	5(2)
C(2)	35(2)	48(2)	25(2)	7(1)	-10(1)	-20(2)
C(73)	56(2)	33(2)	55(2)	-1(2)	-6(2)	-23(2)
C(111)	52(2)	52(2)	43(2)	2(2)	-16(2)	0(2)
C(141)	28(2)	54(2)	42(2)	16(2)	-6(2)	-3(2)
C(41)	67(3)	29(2)	40(2)	-5(2)	-9(2)	9(2)
C(72)	37(2)	61(2)	66(2)	-7(2)	-8(2)	-20(2)
C(112)	53(2)	27(2)	53(2)	5(2)	-3(2)	-4(2)
C(211)	43(2)	55(2)	65(2)	4(2)	-29(2)	-12(2)
C(172)	51(2)	22(2)	58(2)	-5(2)	-11(2)	-8(2)
C(232)	78(3)	30(2)	54(2)	-4(2)	-13(2)	-6(2)
C(173)	35(2)	37(2)	63(2)	-11(2)	-17(2)	-10(2)
C(212)	53(2)	37(2)	57(2)	14(2)	-22(2)	-4(2)
C(231)	45(2)	45(2)	41(2)	6(2)	-12(2)	-24(2)
C(113)	40(2)	56(2)	38(2)	-2(2)	2(2)	8(2)
C(223)	36(2)	79(3)	60(2)	-3(2)	7(2)	-1(2)
C(133)	54(3)	75(3)	59(2)	14(2)	-15(2)	-33(2)
C(233)	79(3)	52(2)	54(2)	22(2)	-22(2)	-39(2)
C(222)	64(3)	53(2)	43(2)	-15(2)	4(2)	-7(2)
C(131)	111(4)	56(2)	41(2)	4(2)	-29(2)	-42(3)
C(132)	107(4)	36(2)	54(2)	6(2)	-24(2)	-33(2)
C(221)	82(3)	68(3)	32(2)	10(2)	11(2)	-15(2)
C(213)	43(2)	62(3)	67(3)	15(2)	-1(2)	17(2)
C(122)	49(3)	96(3)	60(3)	4(2)	11(2)	-14(2)
C(121)	104(4)	87(3)	24(2)	-9(2)	10(2)	-31(3)
C(123)	151(5)	49(3)	94(4)	14(2)	68(4)	38(3)

5.11 Crystallographic data for Zr(6-Hyp-Hgual)$_2$Cl$_2$

5.11.1 Crystallographic data and structure refinement for Zr(6-Hyp-Hgual)$_2$Cl$_2$

Empirical formula	$C_{48}H_{90}Cl_2Si_8Zr$
Formula weight (g/mol)	1054.05
Temperature (K)	173(2)
Wavelength(Å)	0.71073
Crystal system, space group	Triclinic, P(-1)
Unit cell dimensions (Å ,deg)	a=9.2207(18) α=88.04(3) b=17..480(4) β=85.83(3) c=20.729(4) γ=78.83(3)
Volume (Å^3)	3268.4(11)
Z; calc. density (Mg/m^3)	2; 1.165
Absorption coefficient (mm^{-1})	0.428
F(000)	1228
Theta range for data collection (deg)	1.53 ~26.00
Limiting indices	$-11 \le h \le 11, -21 \le k \le 21, -25 \le l \le 25$
Reflections collected / unique	13717 / 12871[R(int)=0.0338]
Completeness to θ	26.00; 100.0%
Refinement method	full-matrix least-squares on F^2
Data / restraints / parameters	12871 / 86 / 684
(Goodness-of-fit on F^2)	1.048
Final R indices [I>2σ(I)]	R1=0.0511, wR2=0.1145
R indices (all data)	R1=0.0803, wR2=0.1318
Largest diff. peak and hole (e.Å^{-3})	0.546 and –0.460

5.11.2 Atomic coordinates ($\times 10^4$) and equivalent isotropic displacement parameters ($A^2 \times 10^3$) for $Zr(6\text{-Hyp-Hgual})_2Cl_2$. U(eq) is defined as one third of the trace of the orthogonalized Uij tensor.

atom	x/a	y/b	z/c	U(eq)	atom	x/a	y/b	z/c	U(eq)
Zr(1)	2629(1)	2444(1)	533(1)	26(1)	Cl(11)	5264(1)	2430(1)	378(1)	39(1)
Cl(12)	2001(1)	3715(1)	1012(1)	36(1)	C(12)	606(4)	2433(2)	-193(2)	40(1)
C(2)	2608(5)	1087(2)	927(2)	37(1)	C(13)	1836(5)	1876(2)	-423(2)	38(1)
C(3)	1193(5)	1534(2)	1098(2)	36(1)	C(20)	2927(4)	2277(2)	-695(2)	30(1)
C(10)	1323(4)	2045(2)	1593(2)	28(1)	C(14)	4367(4)	1911(2)	-1011(2)	38(1)
C(4)	112(4)	2602(2)	1913(2)	32(1)	C(141)	4944(6)	1064(2)	-823(2)	54(1)
C(41)	-1252(4)	2874(3)	1542(2)	48(1)	C(15)	5091(4)	2274(2)	-1461(2)	37(1)
C(5)	152(4)	2848(2)	2515(2)	32(1)	C(16)	4677(4)	3091(2)	-1741(2)	31(1)
C(6)	1378(4)	2653(2)	2971(2)	29(1)	Si(2)	3438(1)	3110(1)	-2479(1)	29(1)
Si(1)	1243(1)	1702(1)	3489(1)	26(1)	Si(21)	1878(1)	2186(1)	-2492(1)	43(1)
Si(11)	223(1)	733(1)	3018(1)	36(1)	C(211)	77(5)	2508(3)	-2010(2)	59(1)
C(111)	-528(6)	155(3)	3703(2)	60(1)	C(212)	1458(7)	2090(3)	-3360(2)	67(2)
C(112)	-1372(5)	1095(3)	2509(2)	44(1)	C(213)	2715(7)	1171(3)	-2215(2)	61(1)
C(113)	1661(6)	51(2)	2518(2)	54(1)	Si(22)	1900(1)	4332(1)	-2670(1)	34(1)
Si(12)	-310(1)	2193(1)	4394(1)	37(1)	C(221)	770(5)	4259(3)	-3377(2)	53(1)
C(121)	-304(6)	1488(3)	5097(2)	62(1)	C(222)	595(5)	4682(3)	-1962(2)	52(1)
C(122)	283(6)	3076(3)	4693(2)	59(1)	C(223)	3010(5)	5097(2)	-2894(2)	50(1)
C(123)	-2259(5)	2496(3)	4153(3)	63(1)	Si(23)	5223(2)	2859(1)	-3357(1)	45(1)
Si(13)	3490(1)	1065(1)	3902(1)	36(1)	C(231)	6153(9)	1808(3)	-3334(4)	119(3)
C(131)	4980(5)	771(3)	3247(3)	64(1)	C(232)	4437(7)	3090(3)	-4160(2)	70(2)
C(132)	4150(5)	1680(3)	4495(3)	60(1)	C(233)	6662(6)	3466(4)	-3305(3)	75(2)
C(133)	3193(5)	150(2)	4354(2)	52(1)	C(17)	4192(4)	3738(2)	-1261(2)	30(1)
C(7)	2899(4)	2724(2)	2683(2)	25(1)	C(171)	5008(4)	4412(2)	-1355(2)	38(1)
C(71)	3638(4)	3280(2)	3028(2)	30(1)	C(172)	4237(5)	5176(2)	-1052(2)	50(1)
C(72)	5280(5)	3190(3)	2859(2)	48(1)	C(173)	6566(5)	4160(3)	-1100(3)	59(1)
C(73)	2874(5)	4126(2)	2888(2)	45(1)	C(18)	3151(4)	3730(2)	-776(2)	27(1)
C(8)	3550(4)	2367(2)	2146(2)	26(1)	C(19)	2377(4)	3093(2)	-611(2)	28(1)
C(9)	2861(4)	1920(2)	1722(2)	26(1)	C(11)	919(4)	3183(2)	-309(2)	32(1)
C(1)	3643(4)	1312(2)	1315(2)	32(1)	C(201)	-122(4)	3943(3)	-193(2)	44(1)
C(101)	5238(5)	943(2)	1337(2)	43(1)					

5.11.3 Bond lengths [Å] for $Zr(6\text{-Hyp-Hgual})_2Cl_2$

Bonds	Bond lengths	Bonds	Bond lengths	Bonds	Bond lengths
Zr(1)-Cl(12)	2.4134(11)	Si(1)-Si(13)	2.3592(15)	C(15)-C(16)	1.511(5)
Zr(1)-Cl(11)	2.4230(11)	Si(11)-C(112)	1.871(4)	C(16)-C(17)	1.512(5)
Zr(1)-C(13)	2.465(4)	Si(11)-C(113)	1.878(5)	C(16)-Si(2)	1.970(4)
Zr(1)-C(3)	2.474(4)	Si(11)-C(111)	1.882(4)	Si(2)-Si(23)	2.3566(16)
Zr(1)-C(12)	2.483(4)	Si(12)-C(123)	1.871(5)	Si(2)-Si(22)	2.3619(16)
Zr(1)-C(2)	2.486(4)	Si(12)-C(122)	1.873(5)	Si(2)-Si(21)	2.3636(16)
Zr(1)-C(20)	2.561(3)	Si(12)-C(121)	1.876(4)	Si(21)-C(211)	1.873(5)
Zr(1)-C(10)	2.570(3)	Si(13)-C(132)	1.869(5)	Si(21)-C(213)	1.881(5)
Zr(1)-C(11)	2.580(4)	Si(13)-C(131)	1.869(5)	Si(21)-C(212)	1.887(4)
Zr(1)-C(1)	2.589(3)	Si(13)-C(133)	1.881(4)	Si(22)-C(223)	1.864(4)
Zr(1)-C(19)	2.599(3)	C(7)-C(8)	1.340(5)	Si(22)-C(222)	1.869(4)
Zr(1)-C(9)	2.609(3)	C(7)-C(71)	1.515(5)	Si(22)-C(221)	1.880(4)
C(2)-C(1)	1.410(5)	C(71)-C(72)	1.508(5)	Si(23)-C(233)	1.864(6)
C(2)-C(3)	1.412(6)	C(71)-C(73)	1.536(5)	Si(23)-C(232)	1.864(5)
C(3)-C(10)	1.410(5)	C(8)-C(9)	1.450(5)	Si(23)-C(231)	1.870(5)
C(10)-C(9)	1.435(5)	C(9)-C(1)	1.429(5)	C(17)-C(18)	1.340(5)
C(10)-C(4)	1.467(5)	C(1)-C(101)	1.490(5)	C(17)-C(171)	1.515(5)
C(4)-C(5)	1.338(5)	C(12)-C(11)	1.404(5)	C(171)-C(172)	1.520(6)
C(4)-C(41)	1.512(5)	C(12)-C(13)	1.410(6)	C(171)-C(173)	1.545(6)

C(5)-C(6)	1.508(5)	C(13)-C(20)	1.409(5)	C(18)-C(19)	1.454(5)
C(6)-C(7)	1.509(5)	C(20)-C(19)	1.430(5)	C(19)-C(11)	1.423(5)
C(6)-Si(1)	1.968(3)	C(20)-C(14)	1.475(5)	C(11)-C(201)	1.496(5)
Si(1)-Si(12)	2.3567(16)	C(14)-C(15)	1.325(6)		
Si(1)-Si(11)	2.3591(15)	C(14)-C(141)	1.519(5)		

5.11.4 Bond angles for Zr(6-Hyp-Hgual)$_2$Cl$_2$ (deg)

Bond angles	**parameter**	**Bond angles**	**parameter**	**Bond angles**	**parameter**
Cl(12)-Zr(1)-Cl(11)	95.61(5)	C(11)-Zr(1)-C(9)	146.85(11)	C(101)-C(1)-Zr(1)	124.4(3)
Cl(12)-Zr(1)-C(13)	133.65(10)	C(1)-Zr(1)-C(9)	31.91(10)	C(11)-C(12)-C(13)	109.0(3)
Cl(11)-Zr(1)-C(13)	108.54(11)	C(19)-Zr(1)-C(9)	174.79(11)	C(11)-C(12)-Zr(1)	77.7(2)
Cl(12)-Zr(1)-C(3)	110.64(10)	C(1)-C(2)-C(3)	108.6(3)	C(13)-C(12)-Zr(1)	72.8(2)
Cl(11)-Zr(1)-C(3)	132.37(10)	C(1)-C(2)-Zr(1)	77.9(2)	C(20)-C(13)-C(12)	108.1(3)
C(13)-Zr(1)-C(3)	81.50(12)	C(3)-C(2)-Zr(1)	73.0(2)	C(20)-C(13)-Zr(1)	77.5(2)
Cl(12)-Zr(1)-C(12)	103.92(11)	C(10)-C(3)-C(2)	108.8(3)	C(12)-C(13)-Zr(1)	74.2(2)
Cl(11)-Zr(1)-C(12)	135.18(10)	C(10)-C(3)-Zr(1)	77.5(2)	C(13)-C(20)-C(19)	107.6(3)
C(13)-Zr(1)-C(12)	33.10(14)	C(2)-C(3)-Zr(1)	73.9(2)	C(13)-C(20)-C(14)	125.5(3)
C(3)-Zr(1)-C(12)	77.00(13)	C(3)-C(10)-C(9)	107.2(3)	C(19)-C(20)-C(14)	126.9(3)
Cl(12)-Zr(1)-C(2)	135.02(9)	C(3)-C(10)-C(4)	126.2(3)	C(13)-C(20)-Zr(1)	70.0(2)
Cl(11)-Zr(1)-C(2)	101.44(11)	C(9)-C(10)-C(4)	126.6(3)	C(19)-C(20)-Zr(1)	75.40(19)
C(13)-Zr(1)-C(2)	78.89(12)	C(3)-C(10)-Zr(1)	70.1(2)	C(14)-C(20)-Zr(1)	120.4(2)
C(3)-Zr(1)-C(2)	33.09(13)	C(9)-C(10)-Zr(1)	75.43(19)	C(15)-C(14)-C(20)	122.7(3)
C(12)-Zr(1)-C(2)	92.59(13)	C(4)-C(10)-Zr(1)	119.7(2)	C(15)-C(14)-C(141)	121.0(4)
Cl(12)-Zr(1)-C(20)	121.84(8)	C(5)-C(4)-C(10)	123.0(3)	C(20)-C(14)-C(141)	116.2(4)
Cl(11)-Zr(1)-C(20)	81.63(9)	C(5)-C(4)-C(41)	120.0(3)	C(14)-C(15)-C(16)	129.4(3)
C(13)-Zr(1)-C(20)	32.48(12)	C(10)-C(4)-C(41)	116.9(3)	C(15)-C(16)-C(17)	116.5(3)
C(3)-Zr(1)-C(20)	113.21(12)	C(4)-C(5)-C(6)	129.0(3)	C(15)-C(16)-Si(2)	111.0(3)
C(12)-Zr(1)-C(20)	53.76(13)	C(5)-C(6)-C(7)	115.3(3)	C(17)-C(16)-Si(2)	116.2(2)
C(2)-Zr(1)-C(20)	101.78(12)	C(5)-C(6)-Si(1)	111.7(2)	C(16)-Si(2)-Si(23)	102.27(12)
Cl(12)-Zr(1)-C(10)	82.08(9)	C(7)-C(6)-Si(1)	116.4(2)	C(16)-Si(2)-Si(22)	114.01(12)
Cl(11)-Zr(1)-C(10)	124.35(8)	C(6)-Si(1)-Si(12)	102.47(11)	Si(23)-Si(2)-Si(22)	108.19(6)
C(13)-Zr(1)-C(10)	112.50(12)	C(6)-Si(1)-Si(11)	117.72(11)	C(16)-Si(2)-Si(21)	118.54(12)
C(3)-Zr(1)-C(10)	32.39(11)	Si(12)-Si(1)-Si(11)	108.76(6)	Si(23)-Si(2)-Si(21)	107.90(6)
C(12)-Zr(1)-C(10)	98.34(12)	C(6)-Si(1)-Si(13)	114.65(12)	Si(22)-Si(2)-Si(21)	105.43(6)
C(2)-Zr(1)-C(10)	53.96(12)	Si(12)-Si(1)-Si(13)	105.84(6)	C(211)-Si(21)-C(213)	108.4(2)
C(20)-Zr(1)-C(10)	144.92(11)	Si(11)-Si(1)-Si(13)	106.62(6)	C(211)-Si(21)-C(212)	107.9(3)
Cl(12)-Zr(1)-C(11)	79.87(9)	C(112)-Si(11)-C(113)	107.8(2)	C(213)-Si(21)-C(212)	105.3(2)
Cl(11)-Zr(1)-C(11)	118.38(9)	C(112)-Si(11)-C(111)	105.6(2)	C(211)-Si(21)-Si(2)	111.99(17)
C(13)-Zr(1)-C(11)	53.94(13)	C(113)-Si(11)-C(111)	108.5(2)	C(213)-Si(21)-Si(2)	115.31(18)
C(3)-Zr(1)-C(11)	105.25(12)	C(112)-Si(11)-Si(1)	115.87(14)	C(212)-Si(21)-Si(2)	107.40(17)
C(12)-Zr(1)-C(11)	32.13(12)	C(113)-Si(11)-Si(1)	111.75(16)	C(223)-Si(22)-C(222)	108.0(2)
C(2)-Zr(1)-C(11)	124.73(13)	C(111)-Si(11)-Si(1)	106.91(16)	C(223)-Si(22)-C(221)	106.4(2)
C(20)-Zr(1)-C(11)	53.25(12)	C(123)-Si(12)-C(122)	107.8(2)	C(222)-Si(22)-C(221)	108.0(2)
C(10)-Zr(1)-C(11)	115.84(11)	C(123)-Si(12)-C(121)	108.3(2)	C(223)-Si(22)-Si(2)	111.49(15)
Cl(12)-Zr(1)-C(1)	115.10(8)	C(122)-Si(12)-C(121)	106.9(2)	C(222)-Si(22)-Si(2)	113.35(15)
Cl(11)-Zr(1)-C(1)	79.42(9)	C(123)-Si(12)-Si(1)	109.47(17)	C(221)-Si(22)-Si(2)	109.30(16)
C(13)-Zr(1)-C(1)	108.00(12)	C(122)-Si(12)-Si(1)	109.79(16)	C(233)-Si(23)-C(232)	106.4(3)
C(3)-Zr(1)-C(1)	53.76(13)	C(121)-Si(12)-Si(1)	114.36(17)	C(233)-Si(23)-C(231)	108.3(4)
C(12)-Zr(1)-C(1)	124.64(13)	C(132)-Si(13)-C(131)	109.5(3)	C(232)-Si(23)-C(231)	108.8(3)
C(2)-Zr(1)-C(1)	32.18(12)	C(132)-Si(13)-C(133)	106.4(2)	C(233)-Si(23)-Si(2)	110.17(18)
C(20)-Zr(1)-C(1)	121.17(11)	C(131)-Si(13)-C(133)	107.3(2)	C(232)-Si(23)-Si(2)	113.41(19)
C(10)-Zr(1)-C(1)	53.34(11)	C(132)-Si(13)-Si(1)	111.61(16)	C(231)-Si(23)-Si(2)	109.6(2)
C(11)-Zr(1)-C(1)	156.71(12)	C(131)-Si(13)-Si(1)	112.30(16)	C(18)-C(17)-C(16)	124.2(3)
Cl(12)-Zr(1)-C(19)	89.89(8)	C(133)-Si(13)-Si(1)	109.40(15)	C(18)-C(17)-C(171)	121.1(3)
Cl(11)-Zr(1)-C(19)	87.48(9)	C(8)-C(7)-C(6)	124.4(3)	C(16)-C(17)-C(171)	114.7(3)
C(13)-Zr(1)-C(19)	53.70(12)	C(8)-C(7)-C(71)	120.8(3)	C(17)-C(171)-C(172)	116.0(3)
C(3)-Zr(1)-C(19)	129.73(12)	C(6)-C(7)-C(71)	114.7(3)	C(17)-C(171)-C(173)	108.8(3)
C(12)-Zr(1)-C(19)	53.24(12)	C(72)-C(71)-C(7)	114.2(3)	C(172)-C(171)-C(173)	109.7(4)
C(2)-Zr(1)-C(19)	131.79(12)	C(72)-C(71)-C(73)	109.5(3)	C(17)-C(18)-C(19)	125.9(3)
C(20)-Zr(1)-C(19)	32.16(11)	C(7)-C(71)-C(73)	109.8(3)	C(11)-C(19)-C(20)	107.8(3)
C(10)-Zr(1)-C(19)	147.67(11)	C(7)-C(8)-C(9)	125.6(3)	C(11)-C(19)-C(18)	124.7(3)
C(11)-Zr(1)-C(19)	31.88(11)	C(1)-C(9)-C(10)	107.9(3)	C(20)-C(19)-C(18)	127.4(3)
C(1)-Zr(1)-C(19)	152.59(11)	C(1)-C(9)-C(8)	124.8(3)	C(11)-C(19)-Zr(1)	73.32(19)

Cl(12)-Zr(1)-C(9)	84.96(8)	C(10)-C(9)-C(8)	127.1(3)	C(20)-C(19)-Zr(1)	72.45(19)
Cl(11)-Zr(1)-C(9)	92.20(8)	C(1)-C(9)-Zr(1)	73.25(19)	C(18)-C(19)-Zr(1)	118.4(2)
C(13)-Zr(1)-C(9)	131.11(11)	C(10)-C(9)-Zr(1)	72.41(19)	C(12)-C(11)-C(19)	107.5(3)
C(3)-Zr(1)-C(9)	53.47(11)	C(8)-C(9)-Zr(1)	116.2(2)	C(12)-C(11)-C(201)	126.7(3)
C(12)-Zr(1)-C(9)	128.95(12)	C(2)-C(1)-C(9)	107.5(3)	C(19)-C(11)-C(201)	125.6(3)
C(2)-Zr(1)-C(9)	53.35(11)	C(2)-C(1)-C(101)	126.6(3)	C(12)-C(11)-Zr(1)	70.1(2)
C(20)-Zr(1)-C(9)	152.84(11)	C(9)-C(1)-C(101)	125.7(3)	C(19)-C(11)-Zr(1)	74.81(19)
C(10)-Zr(1)-C(9)	32.16(11)	C(2)-C(1)-Zr(1)	69.9(2)	C(201)-C(11)-Zr(1)	124.5(3)
		C(9)-C(1)-Zr(1)	74.83(19)		

5.11.5 Anisotropic displacement parameters ($A^2 \times 10^3$) for $Zr(6\text{-Hyp-Hgual})_2Cl_2$. The anisotropic displacement factor exponent takes the form: $-2\pi^2 [h^2 a^{*2} U11 + ... + 2 h k a^* b^* U12]$

atom	U11	U22	U33	U23	U13	U12
Zr(1)	28(1)	24(1)	26(1)	-1(1)	-2(1)	-8(1)
Cl(11)	30(1)	50(1)	38(1)	-1(1)	-2(1)	-10(1)
Cl(12)	48(1)	26(1)	35(1)	-3(1)	2(1)	-8(1)
C(2)	59(3)	25(2)	31(2)	-1(1)	-3(2)	-15(2)
C(3)	46(2)	33(2)	35(2)	4(2)	-7(2)	-20(2)
C(10)	28(2)	30(2)	29(2)	8(1)	-3(1)	-10(1)
C(4)	21(2)	37(2)	38(2)	12(2)	0(1)	-6(1)
C(41)	27(2)	68(3)	45(2)	22(2)	-5(2)	-2(2)
C(5)	21(2)	31(2)	39(2)	9(2)	5(1)	2(1)
C(6)	30(2)	23(2)	32(2)	-4(1)	3(1)	-4(1)
Si(1)	24(1)	27(1)	26(1)	2(1)	-1(1)	-4(1)
Si(11)	44(1)	30(1)	38(1)	6(1)	-10(1)	-13(1)
C(111)	80(4)	56(3)	54(3)	21(2)	-22(3)	-36(3)
C(112)	41(2)	48(2)	48(2)	7(2)	-11(2)	-20(2)
C(113)	72(3)	30(2)	57(3)	-7(2)	-13(2)	2(2)
Si(12)	32(1)	45(1)	30(1)	2(1)	5(1)	-4(1)
C(121)	69(3)	76(3)	37(2)	12(2)	11(2)	-13(3)
C(122)	64(3)	54(3)	55(3)	-17(2)	7(2)	-6(2)
C(123)	35(2)	84(4)	63(3)	-3(3)	5(2)	2(2)
Si(13)	27(1)	37(1)	43(1)	6(1)	-6(1)	-2(1)
C(131)	36(2)	74(3)	69(3)	15(3)	5(2)	18(2)
C(132)	52(3)	52(3)	79(3)	8(2)	-30(3)	-11(2)
C(133)	58(3)	41(2)	55(3)	16(2)	-16(2)	-5(2)
C(7)	24(2)	21(2)	29(2)	2(1)	-2(1)	-1(1)
C(71)	33(2)	28(2)	31(2)	0(1)	-5(2)	-8(2)
C(72)	37(2)	45(2)	67(3)	-13(2)	-13(2)	-15(2)
C(73)	51(3)	28(2)	56(3)	-3(2)	-7(2)	-6(2)
C(8)	20(2)	26(2)	31(2)	2(1)	-2(1)	-3(1)
C(9)	28(2)	20(2)	28(2)	0(1)	1(1)	-2(1)
C(1)	41(2)	22(2)	31(2)	0(1)	-1(2)	-2(2)
C(101)	45(2)	36(2)	39(2)	-4(2)	0(2)	13(2)
C(12)	33(2)	57(3)	35(2)	6(2)	-11(2)	-21(2)
C(13)	53(2)	34(2)	33(2)	-1(2)	-13(2)	-20(2)
C(20)	39(2)	29(2)	23(2)	-3(1)	-8(1)	-5(2)
C(14)	43(2)	33(2)	33(2)	-10(2)	-7(2)	6(2)
C(141)	78(3)	31(2)	46(2)	-2(2)	-13(2)	9(2)
C(15)	36(2)	39(2)	31(2)	-9(2)	-2(2)	7(2)
C(16)	25(2)	38(2)	28(2)	-2(1)	1(1)	-2(2)
Si(2)	34(1)	25(1)	25(1)	-2(1)	1(1)	-2(1)
Si(21)	60(1)	38(1)	36(1)	3(1)	-12(1)	-21(1)
C(211)	53(3)	75(3)	55(3)	8(2)	-12(2)	-27(3)
C(212)	110(5)	59(3)	44(3)	2(2)	-27(3)	-40(3)
C(213)	94(4)	41(2)	55(3)	4(2)	-14(3)	-27(3)
Si(22)	32(1)	32(1)	34(1)	-2(1)	0(1)	1(1)
C(221)	52(3)	56(3)	48(2)	1(2)	-14(2)	-1(2)
C(222)	41(2)	59(3)	47(2)	-3(2)	4(2)	10(2)
C(223)	56(3)	29(2)	60(3)	5(2)	0(2)	-3(2)
Si(23)	58(1)	35(1)	32(1)	0(1)	16(1)	8(1)
C(231)	156(7)	53(3)	109(5)	13(3)	73(5)	47(4)

C(232)	101(4)	82(4)	29(2)	-4(2)	8(2)	-25(3)
C(233)	47(3)	115(5)	58(3)	6(3)	18(2)	-14(3)
C(17)	28(2)	33(2)	26(2)	-1(1)	-4(1)	-1(2)
C(171)	38(2)	42(2)	37(2)	-1(2)	-1(2)	-16(2)
C(172)	62(3)	33(2)	60(3)	-1(2)	-3(2)	-20(2)
C(173)	41(3)	67(3)	73(3)	-4(3)	-5(2)	-23(2)
C(18)	28(2)	24(2)	28(2)	-5(1)	-3(1)	-2(1)
C(19)	29(2)	33(2)	21(2)	-1(1)	-2(1)	-4(1)
C(11)	24(2)	42(2)	30(2)	3(2)	-1(1)	-5(2)
C(201)	31(2)	55(3)	39(2)	9(2)	3(2)	5(2)

5.12 Crystallographic data for Hf(6-Hyp-Hgual)$_2$Cl$_2$

5.12.1 Crystallographic data and structure refinement for Hf(6-Hyp-Hgual)$_2$Cl$_2$

Empirical formula	$C_{48}H_{90}Cl_2Si_8Hf$
Formula weight (g/mol)	1141.32
Temperature (K)	173(2)
Wavelength(Å)	0.71073
Crystal system, space group	Triclinic, P(-1)
Unit cell dimensions (Å ,deg)	a=9.208(3) α=88.771(12) b=17..480(3) β=85.612(19) c=20.605(4) γ=79.03(3)
Volume (Å^3)	3246.4(13)
Z; calc. density (Mg/m^3)	2; 1.247
Absorption coefficient (mm^{-1})	1.868
F(000)	1276
Theta range for data collection (deg)	2.26 ~25.00
Limiting indices	$0 \le h \le 10$, $-20 \le k \le 20$, $-24 \le l \le 24$
Reflections collected / unique	11053 / 10350[R(int)=0.0513]
Completeness to θ	25.00; 90.70%
Refinement method	full-matrix least-squares on F^2
Data / restraints / parameters	10350 / 0 / 612
(Goodness-of-fit on F^2)	0.945
Final R indices [I>2σ(I)]	R1=0.0519, wR2=0.1186
R indices (all data)	R1=0.0821, wR2=0.1276
Largest diff. peak and hole (e.Å^{-3})	1.928 and –1.472

5.12.2 Atomic coordinates (×10^4) and equivalent isotropic displacement parameters (A^2 × 10^3) for Hf(6-Hyp-Hgual)$_2$Cl$_2$. U(eq) is defined as one third of the trace of the orthogonalized Uij tensor.

atom	x/a	y/b	z/c	U(eq)	atom	x/a	y/b	z/c	U(eq)
Hf(1)	2655(1)	2445(1)	520(1)	36(1)	Cl(11)	5257(2)	2471(1)	396(1)	51(1)
Cl(12)	1992(2)	3707(1)	1004(1)	49(1)	C(12)	697(9)	2396(5)	-209(4)	50(2)
C(2)	2644(11)	1091(4)	902(4)	54(2)	C(13)	1907(10)	1875(5)	-448(3)	48(2)
C(3)	1245(9)	1534(4)	1080(3)	40(2)	C(20)	2997(10)	2304(4)	-713(3)	49(2)
C(10)	1352(8)	2063(4)	1579(4)	39(2)	C(14)	4472(10)	1943(4)	-1023(4)	50(2)
C(4)	153(8)	2601(4)	1901(4)	44(2)	C(141)	5125(12)	1118(4)	-847(4)	76(3)
C(41)	-1185(9)	2877(5)	1544(4)	64(2)	C(15)	5154(9)	2330(5)	-1480(4)	53(2)
C(5)	205(8)	2844(4)	2513(4)	46(2)	C(16)	4672(9)	3128(4)	-1749(4)	46(2)
C(6)	1410(8)	2650(4)	2965(4)	38(2)	Si(2)	3393(2)	3114(1)	-2476(1)	39(1)
Si(1)	1303(2)	1688(1)	3478(1)	37(1)	Si(21)	1875(3)	2162(1)	-2478(1)	49(1)
Si(11)	279(2)	721(1)	2993(1)	43(1)	C(211)	38(10)	2468(5)	-1980(5)	69(3)
C(111)	-452(11)	133(5)	3667(4)	66(3)	C(212)	1435(12)	2050(5)	-3343(4)	74(3)
C(112)	-1328(9)	1093(4)	2505(4)	53(2)	C(213)	2761(12)	1174(5)	-2197(4)	76(3)
C(113)	1649(10)	55(4)	2455(4)	61(2)	Si(22)	1857(2)	4311(1)	-2675(1)	44(1)
Si(12)	-283(3)	2182(1)	4394(1)	53(1)	C(221)	778(11)	4213(5)	-3375(4)	73(3)

C(121)	-273(13)	1472(6)	5093(5)	85(3)	C(222)	549(9)	4646(5)	-1970(4)	63(2)
C(122)	341(12)	3078(5)	4705(5)	84(3)	C(223)	2921(10)	5088(4)	-2909(5)	64(2)
C(123)	-2232(10)	2484(6)	4164(5)	86(3)	Si(23)	5199(3)	2848(1)	-3368(1)	61(1)
Si(13)	3521(2)	1054(1)	3893(1)	50(1)	C(231)	6134(17)	1806(6)	-3356(7)	159(8)
C(131)	5023(10)	756(5)	3227(5)	83(3)	C(232)	4371(13)	3074(7)	-4179(5)	94(4)
C(132)	4223(11)	1663(6)	4491(5)	78(3)	C(233)	6606(11)	3471(7)	-3319(5)	92(4)
C(133)	3225(11)	169(5)	4336(5)	77(3)	C(17)	4183(7)	3776(4)	-1259(3)	33(2)
C(7)	2946(7)	2733(3)	2675(3)	30(2)	C(171)	4972(8)	4457(4)	-1352(4)	46(2)
C(71)	3667(8)	3287(4)	3036(4)	39(2)	C(172)	4156(9)	5219(4)	-1024(4)	53(2)
C(72)	5328(8)	3201(4)	2856(5)	58(2)	C(173)	6529(9)	4245(5)	-1118(5)	68(3)
C(73)	2918(10)	4124(4)	2917(4)	58(2)	C(18)	3152(8)	3761(4)	-773(3)	35(2)
C(8)	3577(8)	2383(4)	2147(4)	39(2)	C(19)	2396(8)	3093(4)	-610(3)	38(2)
C(9)	2889(8)	1927(4)	1704(4)	38(2)	C(11)	943(9)	3157(4)	-312(4)	47(2)
C(1)	3668(9)	1324(4)	1300(4)	44(2)	C(201)	-144(9)	3905(5)	-203(4)	62(2)
C(101)	5283(9)	938(5)	1320(4)	61(2)					

5.12.3 Bond lengths [Å] for $Hf(6\text{-}Hyp\text{-}Hgual)_2Cl_2$

Bond	Bond lengths	Bond	Bond lengths	Bond	Bond lengths
Hf(1)-Cl(12)	2.3922(19)	Si(1)-Si(12)	2.368(3)	C(15)-C(16)	1.490(10)
Hf(1)-Cl(11)	2.399(2)	Si(11)-C(112)	1.859(8)	C(16)-C(17)	1.515(9)
Hf(1)-C(12)	2.448(8)	Si(11)-C(113)	1.860(9)	C(16)-Si(2)	1.978(8)
Hf(1)-C(13)	2.449(6)	Si(11)-C(111)	1.870(8)	Si(2)-Si(22)	2.339(3)
Hf(1)-C(3)	2.456(6)	Si(12)-C(123)	1.867(9)	Si(2)-Si(21)	2.369(3)
Hf(1)-C(2)	2.479(7)	Si(12)-C(121)	1.879(10)	Si(2)-Si(23)	2.373(3)
Hf(1)-C(20)	2.548(7)	Si(12)-C(122)	1.908(9)	Si(21)-C(213)	1.863(9)
Hf(1)-C(10)	2.548(7)	Si(13)-C(133)	1.833(9)	Si(21)-C(212)	1.880(9)
Hf(1)-C(11)	2.559(8)	Si(13)-C(132)	1.873(9)	Si(21)-C(211)	1.901(9)
Hf(1)-C(19)	2.574(7)	Si(13)-C(131)	1.880(10)	Si(22)-C(221)	1.841(9)
Hf(1)-C(1)	2.587(7)	C(7)-C(8)	1.301(9)	Si(22)-C(222)	1.845(9)
Hf(1)-C(9)	2.594(7)	C(7)-C(71)	1.512(8)	Si(22)-C(223)	1.856(8)
C(2)-C(3)	1.398(11)	C(71)-C(73)	1.517(10)	Si(23)-C(233)	1.854(10)
C(2)-C(1)	1.417(11)	C(71)-C(72)	1.525(10)	Si(23)-C(231)	1.861(10)
C(3)-C(10)	1.420(10)	C(8)-C(9)	1.477(9)	Si(23)-C(232)	1.893(11)
C(10)-C(9)	1.432(10)	C(9)-C(1)	1.406(10)	C(17)-C(18)	1.329(9)
C(10)-C(4)	1.436(10)	C(1)-C(101)	1.514(11)	C(17)-C(171)	1.509(8)
C(4)-C(5)	1.346(11)	C(12)-C(13)	1.364(11)	C(171)-C(173)	1.523(11)
C(4)-C(41)	1.480(11)	C(12)-C(11)	1.401(10)	C(171)-C(172)	1.542(10)
C(5)-C(6)	1.489(10)	C(13)-C(20)	1.432(10)	C(18)-C(19)	1.490(9)
C(6)-C(7)	1.525(9)	C(20)-C(19)	1.400(11)	C(19)-C(11)	1.413(10)
C(6)-Si(1)	1.981(7)	C(20)-C(14)	1.486(12)	C(11)-C(201)	1.497(11)
Si(1)-Si(13)	2.345(3)	C(14)-C(15)	1.335(11)		
Si(1)-Si(11)	2.360(3)	C(14)-C(141)	1.501(11)		

5.12.4 Bond angles for $Hf(6\text{-}Hyp\text{-}Hgual)_2Cl_2$

Bond angles	parameter	Bond angles	parameter	Bond angles	parameter
Cl(12)-Hf(1)-Cl(11)	94.33(7)	C(19)-Hf(1)-C(9)	174.4(2)	C(13)-C(12)-C(11)	109.8(7)
Cl(12)-Hf(1)-C(12)	104.6(2)	C(1)-Hf(1)-C(9)	31.5(2)	C(13)-C(12)-Hf(1)	73.9(4)
Cl(11)-Hf(1)-C(12)	136.2(2)	C(3)-C(2)-C(1)	107.6(7)	C(11)-C(12)-Hf(1)	78.2(4)
Cl(12)-Hf(1)-C(13)	133.2(2)	C(3)-C(2)-Hf(1)	72.6(4)	C(12)-C(13)-C(20)	108.1(7)
Cl(11)-Hf(1)-C(13)	109.9(2)	C(1)-C(2)-Hf(1)	78.0(4)	C(12)-C(13)-Hf(1)	73.8(4)
C(12)-Hf(1)-C(13)	32.4(3)	C(2)-C(3)-C(10)	110.0(6)	C(20)-C(13)-Hf(1)	77.2(4)
Cl(12)-Hf(1)-C(3)	110.56(19)	C(2)-C(3)-Hf(1)	74.5(4)	C(19)-C(20)-C(13)	106.6(8)
Cl(11)-Hf(1)-C(3)	132.32(19)	C(10)-C(3)-Hf(1)	77.1(4)	C(19)-C(20)-C(14)	128.9(7)
C(12)-Hf(1)-C(3)	77.0(2)	C(3)-C(10)-C(9)	105.4(7)	C(13)-C(20)-C(14)	124.4(7)
C(13)-Hf(1)-C(3)	82.2(2)	C(3)-C(10)-C(4)	126.7(7)	C(19)-C(20)-Hf(1)	75.2(4)
Cl(12)-Hf(1)-C(2)	135.2(2)	C(9)-C(10)-C(4)	127.8(7)	C(13)-C(20)-Hf(1)	69.6(4)
Cl(11)-Hf(1)-C(2)	102.1(2)	C(3)-C(10)-Hf(1)	70.0(4)	C(14)-C(20)-Hf(1)	119.4(5)
C(12)-Hf(1)-C(2)	91.7(3)	C(9)-C(10)-Hf(1)	75.6(4)	C(15)-C(14)-C(20)	120.3(7)
C(13)-Hf(1)-C(2)	79.1(3)	C(4)-C(10)-Hf(1)	120.5(5)	C(15)-C(14)-C(141)	120.8(8)

C(3)-Hf(1)-C(2)	32.9(3)	C(5)-C(4)-C(10)	122.2(7)	C(20)-C(14)-C(141)	118.8(8)
Cl(12)-Hf(1)-C(20)	120.48(18)	C(5)-C(4)-C(41)	119.8(8)	C(14)-C(15)-C(16)	129.5(8)
Cl(11)-Hf(1)-C(20)	82.4(2)	C(10)-C(4)-C(41)	118.0(7)	C(15)-C(16)-C(17)	116.5(7)
C(12)-Hf(1)-C(20)	53.9(3)	C(4)-C(5)-C(6)	129.7(7)	C(15)-C(16)-Si(2)	111.1(5)
C(13)-Hf(1)-C(20)	33.2(2)	C(5)-C(6)-C(7)	115.0(6)	C(17)-C(16)-Si(2)	116.6(5)
C(3)-Hf(1)-C(20)	114.7(2)	C(5)-C(6)-Si(1)	112.7(4)	C(16)-Si(2)-Si(22)	114.2(2)
C(2)-Hf(1)-C(20)	102.9(2)	C(7)-C(6)-Si(1)	116.0(5)	C(16)-Si(2)-Si(21)	119.2(2)
Cl(12)-Hf(1)-C(10)	81.45(17)	C(6)-Si(1)-Si(13)	116.0(2)	Si(22)-Si(2)-Si(21)	106.27(12)
Cl(11)-Hf(1)-C(10)	123.19(17)	C(6)-Si(1)-Si(11)	117.2(2)	C(16)-Si(2)-Si(23)	100.9(2)
C(12)-Hf(1)-C(10)	98.8(2)	Si(13)-Si(1)-Si(11)	106.69(11)	Si(22)-Si(2)-Si(23)	108.00(11)
C(13)-Hf(1)-C(10)	113.6(2)	C(6)-Si(1)-Si(12)	101.8(2)	Si(21)-Si(2)-Si(23)	107.44(11)
C(3)-Hf(1)-C(10)	32.9(2)	Si(13)-Si(1)-Si(12)	105.82(12)	C(213)-Si(21)-C(212)	106.4(4)
C(2)-Hf(1)-C(10)	54.7(3)	Si(11)-Si(1)-Si(12)	108.40(11)	C(213)-Si(21)-C(211)	108.3(4)
C(20)-Hf(1)-C(10)	146.8(2)	C(112)-Si(11)-C(113)	106.6(4)	C(212)-Si(21)-C(211)	107.2(5)
Cl(12)-Hf(1)-C(11)	79.66(18)	C(112)-Si(11)-C(111)	105.4(4)	C(213)-Si(21)-Si(2)	114.7(3)
Cl(11)-Hf(1)-C(11)	119.49(18)	C(113)-Si(11)-C(111)	108.6(4)	C(212)-Si(21)-Si(2)	107.4(3)
C(12)-Hf(1)-C(11)	32.4(2)	C(112)-Si(11)-Si(1)	115.2(3)	C(211)-Si(21)-Si(2)	112.4(3)
C(13)-Hf(1)-C(11)	53.7(3)	C(113)-Si(11)-Si(1)	113.4(3)	C(221)-Si(22)-C(222)	108.4(4)
C(3)-Hf(1)-C(11)	105.0(2)	C(111)-Si(11)-Si(1)	107.3(3)	C(221)-Si(22)-C(223)	105.5(4)
C(2)-Hf(1)-C(11)	124.1(2)	C(123)-Si(12)-C(121)	108.3(5)	C(222)-Si(22)-C(223)	108.7(4)
C(20)-Hf(1)-C(11)	53.2(3)	C(123)-Si(12)-C(122)	108.0(5)	C(221)-Si(22)-Si(2)	109.2(3)
C(10)-Hf(1)-C(11)	115.3(2)	C(121)-Si(12)-C(122)	107.0(5)	C(222)-Si(22)-Si(2)	112.3(3)
Cl(12)-Hf(1)-C(19)	89.08(17)	C(123)-Si(12)-Si(1)	110.5(3)	C(223)-Si(22)-Si(2)	112.6(3)
Cl(11)-Hf(1)-C(19)	88.56(16)	C(121)-Si(12)-Si(1)	113.8(3)	C(233)-Si(23)-C(231)	109.1(7)
C(12)-Hf(1)-C(19)	53.4(2)	C(122)-Si(12)-Si(1)	109.0(3)	C(233)-Si(23)-C(232)	106.5(5)
C(13)-Hf(1)-C(19)	53.7(2)	C(133)-Si(13)-C(132)	106.0(5)	C(231)-Si(23)-C(232)	108.8(6)
C(3)-Hf(1)-C(19)	130.1(2)	C(133)-Si(13)-C(131)	107.7(4)	C(233)-Si(23)-Si(2)	109.7(3)
C(2)-Hf(1)-C(19)	132.1(2)	C(132)-Si(13)-C(131)	108.5(5)	C(231)-Si(23)-Si(2)	110.3(4)
C(20)-Hf(1)-C(19)	31.7(2)	C(133)-Si(13)-Si(1)	110.0(3)	C(232)-Si(23)-Si(2)	112.3(4)
C(10)-Hf(1)-C(19)	147.3(2)	C(132)-Si(13)-Si(1)	112.7(3)	C(18)-C(17)-C(171)	121.1(6)
C(11)-Hf(1)-C(19)	32.0(2)	C(131)-Si(13)-Si(1)	111.7(3)	C(18)-C(17)-C(16)	123.9(6)
Cl(12)-Hf(1)-C(1)	115.23(17)	C(8)-C(7)-C(71)	122.0(6)	C(171)-C(17)-C(16)	115.0(6)
Cl(11)-Hf(1)-C(1)	79.39(18)	C(8)-C(7)-C(6)	123.6(6)	C(17)-C(171)-C(173)	110.4(6)
C(12)-Hf(1)-C(1)	124.0(2)	C(71)-C(7)-C(6)	114.4(6)	C(17)-C(171)-C(172)	115.0(6)
C(13)-Hf(1)-C(1)	108.4(3)	C(7)-C(71)-C(73)	110.5(6)	C(173)-C(171)-C(172)	109.3(6)
C(3)-Hf(1)-C(1)	53.5(2)	C(7)-C(71)-C(72)	113.4(6)	C(17)-C(18)-C(19)	125.2(6)
C(2)-Hf(1)-C(1)	32.4(2)	C(73)-C(71)-C(72)	109.2(6)	C(20)-C(19)-C(11)	108.7(7)
C(20)-Hf(1)-C(1)	122.2(3)	C(7)-C(8)-C(9)	126.4(6)	C(20)-C(19)-C(18)	126.3(7)
C(10)-Hf(1)-C(1)	53.5(2)	C(1)-C(9)-C(10)	109.1(6)	C(11)-C(19)-C(18)	125.0(6)
C(11)-Hf(1)-C(1)	156.2(2)	C(1)-C(9)-C(8)	124.8(7)	C(20)-C(19)-Hf(1)	73.1(4)
C(19)-Hf(1)-C(1)	153.4(2)	C(10)-C(9)-C(8)	125.9(6)	C(11)-C(19)-Hf(1)	73.4(4)
Cl(12)-Hf(1)-C(9)	85.40(15)	C(1)-C(9)-Hf(1)	74.0(4)	C(18)-C(19)-Hf(1)	118.9(4)
Cl(11)-Hf(1)-C(9)	90.98(17)	C(10)-C(9)-Hf(1)	72.1(4)	C(12)-C(11)-C(19)	106.7(7)
C(12)-Hf(1)-C(9)	129.1(2)	C(8)-C(9)-Hf(1)	116.7(4)	C(12)-C(11)-C(201)	127.9(7)
C(13)-Hf(1)-C(9)	131.5(2)	C(9)-C(1)-C(2)	107.8(7)	C(19)-C(11)-C(201)	125.1(7)
C(3)-Hf(1)-C(9)	53.3(2)	C(9)-C(1)-C(101)	126.8(7)	C(12)-C(11)-Hf(1)	69.4(5)
C(2)-Hf(1)-C(9)	53.4(2)	C(2)-C(1)-C(101)	125.2(7)	C(19)-C(11)-Hf(1)	74.6(4)
C(20)-Hf(1)-C(9)	153.6(2)	C(9)-C(1)-Hf(1)	74.5(4)	C(201)-C(11)-Hf(1)	126.0(5)
C(10)-Hf(1)-C(9)	32.3(2)	C(2)-C(1)-Hf(1)	69.6(4)		
C(11)-Hf(1)-C(9)	146.7(2)	C(101)-C(1)-Hf(1)	125.2(5)		

5.12.5 Anisotropic displacement parameters ($A^2 \times 10^3$) for Hf(6-Hyp-Hgual)$_2$Cl$_2$. The anisotropic displacement factor exponent takes the form: $-2\pi^2[h^2a^{*2}U11 + ... + 2hka^*b^*U12]$

atom	U11	U22	U33	U23	U13	U12
Hf(1)	36(1)	36(1)	36(1)	0(1)	-3(1)	-10(1)
Cl(11)	37(1)	59(1)	57(1)	-5(1)	-4(1)	-8(1)
Cl(12)	51(1)	37(1)	55(1)	-3(1)	5(1)	-3(1)
C(2)	86(7)	36(4)	43(4)	5(3)	-16(5)	-15(5)
C(3)	52(5)	35(4)	41(4)	10(3)	-26(4)	-21(4)
C(10)	30(4)	44(4)	39(4)	8(3)	5(3)	-1(3)
C(4)	35(4)	45(4)	50(5)	9(4)	-2(4)	-4(4)
C(41)	44(5)	86(6)	61(6)	28(5)	-15(5)	-5(5)
C(5)	30(4)	37(4)	65(6)	6(4)	-6(4)	9(3)

C(6)	31(4)	35(4)	44(4)	-3(3)	5(3)	1(3)
Si(1)	41(1)	37(1)	34(1)	5(1)	-4(1)	-7(1)
Si(11)	50(1)	34(1)	46(1)	6(1)	-12(1)	-9(1)
C(111)	82(7)	53(5)	72(6)	17(4)	-22(5)	-27(5)
C(112)	46(5)	55(5)	61(5)	10(4)	-13(4)	-11(4)
C(113)	75(7)	37(4)	66(6)	-2(4)	-11(5)	1(4)
Si(12)	46(1)	63(1)	42(1)	1(1)	2(1)	3(1)
C(121)	97(9)	95(7)	54(6)	-1(5)	15(6)	-6(7)
C(122)	103(9)	78(7)	66(7)	-20(5)	4(6)	-4(6)
C(123)	39(6)	128(9)	81(7)	-17(6)	7(5)	7(6)
Si(13)	31(1)	52(1)	64(2)	-2(1)	-9(1)	4(1)
C(131)	50(6)	77(7)	107(9)	17(6)	-5(6)	25(5)
C(132)	69(7)	87(7)	86(7)	14(6)	-40(6)	-21(6)
C(133)	70(7)	80(6)	75(7)	6(5)	-31(6)	5(5)
C(7)	18(3)	24(3)	44(4)	-5(3)	-1(3)	5(3)
C(71)	37(4)	31(4)	47(4)	-6(3)	-8(4)	-4(3)
C(72)	38(5)	46(5)	90(7)	-4(4)	-20(5)	-7(4)
C(73)	63(6)	36(4)	77(6)	-13(4)	-19(5)	-3(4)
C(8)	25(4)	37(4)	53(5)	1(3)	-6(4)	-1(3)
C(9)	35(4)	31(4)	42(4)	4(3)	1(4)	6(3)
C(1)	42(5)	34(4)	50(5)	0(3)	2(4)	7(3)
C(101)	56(6)	52(5)	58(5)	-9(4)	1(5)	34(4)
C(12)	43(5)	71(5)	41(4)	6(4)	-5(4)	-24(5)
C(13)	60(6)	61(5)	28(4)	-9(4)	-4(4)	-27(5)
C(20)	67(6)	55(5)	24(4)	-3(3)	-6(4)	-11(4)
C(14)	58(6)	38(4)	50(5)	-13(4)	-5(4)	1(4)
C(141)	110(9)	44(5)	59(6)	-10(4)	-11(6)	26(5)
C(15)	45(5)	54(5)	52(5)	-3(4)	7(4)	10(4)
C(16)	38(5)	41(4)	56(5)	-8(4)	10(4)	-4(4)
Si(2)	45(1)	33(1)	36(1)	-6(1)	0(1)	-4(1)
Si(21)	67(2)	41(1)	42(1)	0(1)	-12(1)	-16(1)
C(211)	60(6)	81(6)	70(6)	10(5)	-2(5)	-24(5)
C(212)	110(9)	66(6)	57(6)	-1(4)	-28(6)	-35(6)
C(213)	121(9)	53(5)	59(6)	4(4)	-14(6)	-27(6)
Si(22)	39(1)	40(1)	49(1)	-5(1)	-1(1)	6(1)
C(221)	103(8)	45(5)	63(6)	-7(4)	-11(6)	8(5)
C(222)	42(5)	71(6)	65(6)	-1(5)	5(5)	12(4)
C(223)	61(6)	46(5)	79(6)	6(4)	1(5)	-2(4)
Si(23)	70(2)	47(1)	52(1)	-2(1)	20(1)	13(1)
C(231)	202(16)	71(7)	141(12)	28(7)	121(12)	81(9)
C(232)	113(10)	123(9)	51(6)	-17(6)	15(6)	-38(8)
C(233)	52(6)	156(11)	66(7)	3(7)	19(6)	-23(7)
C(17)	24(4)	33(3)	38(4)	-1(3)	4(3)	1(3)
C(171)	42(5)	47(4)	48(5)	-5(3)	1(4)	-11(4)
C(172)	53(5)	38(4)	67(6)	-8(4)	3(4)	-6(4)
C(173)	53(6)	70(6)	86(7)	-19(5)	-6(5)	-24(5)
C(18)	35(4)	32(3)	36(4)	0(3)	-6(3)	2(3)
C(19)	24(4)	50(4)	35(4)	5(3)	-2(3)	6(3)
C(11)	42(5)	56(5)	43(4)	-2(4)	3(4)	-8(4)
C(201)	34(5)	87(6)	53(5)	5(5)	17(4)	8(5)
C(01)	65(7)	78(7)	103(9)	-19(6)	-9(7)	-31(6)
C(02)	66(8)	82(7)	98(9)	-42(7)	24(7)	-40(7)
C(03)	63(8)	77(8)	140(12)	-40(8)	1(9)	-33(6)
C(011)	240(30)	90(11)	90(12)	-1(9)	25(15)	28(14)
C(012)	220(20)	109(13)	80(11)	-2(9)	14(14)	36(16)
C(013)	350(40)	121(15)	124(16)	38(12)	-60(20)	-10(20)

6 List of Abbreviations

Binap	binaphthylcyclopentadien
^{n}Bu	neo-butyl
^{t}Bu	tertiary-butyl
COSY	correlated spectroscopy
Cp	cyclopentadienyl
Cp*	pentamethylcyclopentadienyl
DEPT	distortionless enhancement by polarisation transfer
DME	1,2-dimethoxyethane
Et	ethyl
Fig.	figure
GooF	goodness-of-fit
Hyp	hypersilyl, -tris(trimethylsilyl)silyl
iPr	iso-propyl
Me	methyl
MeLi	methyllithium
Ph	phenyl
py	pyridinyl
TMEDA	tetramethylethelenediamine
RT	room temperature
THF	tetrahydrofuran

7 Numbering List of the new Complexes

Abbreviation (numbering)		Compounds	Formula
Li(6-Hyp-Hgual)	(**1**)	Lithium[6-tris(trimethylsilyl)silyl-1,6-dihydro-guaiazulene-1-id]	$LiC_{24}H_{45}Si_4$
K(6-Hyp-Hgual)	(**2**)	Potassium[6-tris(trimethylsilyl)silyl-1,6-dihydro-guaiazulene-1-id]	$KC_{24}H_{45}Si_4$
$(thf)_4K$(6-Hyp-Hgual)	(**2a**)	Tetrakis(tetrahydrofuran)-potassium[6-tris(trimethylsilyl)silyl-1,6-dihydro-guaiazulene-1-id]	$KC_{40}H_{77}Si_4O_4$
K(8-Hyp-Hgual)	(**3**)	Potassium[8-tris(trimethylsilyl)silyl-1,8-dihydro-guaiazulene-1-id]	$KC_{24}H_{45}Si_4$
$(thf)_4K$(8-Hyp-Hgual)	(**3a**)	Tetrakis(tetrahydrofuran)-potassium[8-tris(trimethylsilyl)silyl-1,8-dihydro-guaiazulene-1-id]	$KC_{40}H_{77}Si_4O_4$
Cs(6-Hyp-Hgual)	(**4**)	Cesium[6-tris(trimethylsilyl)silyl-1,6-dihydro-guaiazulene-1-id]	$CsC_{24}H_{45}Si_4$
Mn(6-Hyp-Hgual)$_2$	(**5**)	Manganese(II)-bis[6-tris(trimethylsilyl)silyl-1,6-dihydro-guaiazulene-1-id]	$MnC_{48}H_{90}Si_8$
Fe(6-Hyp-Hgual)$_2$	(**6**)	Iron(II)-bis[6-tris(trimethylsilyl)silyl-1,6-dihydro-guaiazulene-1-id])]	$FeC_{48}H_{90}Si_8$
Fe(8-Hyp-Hgual)$_2$	(**7**)	Iron(II)-bis[8-tris(trimethylsilyl)silyl-1,8-dihydro-guaiazulene-1-id])]	$FeC_{48}H_{90}Si_8$
Ni(6-Hyp-Hgual)$_2$	(**8**)	Nickel(II)-bis[6-tris(trimethylsilyl)silyl-1,6-dihydro-guaiazulene-1-id]	$NiC_{48}H_{90}Si_8$
(3-Hyp-6-Hgua)$_2$	(**9**)	Bis[3-tris(trimethylsilyl)silyl-3,6-dihydro-6-guaiazulenyle]	$C_{48}H_{90}Si_8$
Ti(6-Hyp-Hgual)$_2Cl_2$	(**10**)	Titanium(IV)-bis[6-tris(trimethylsilyl)silyl-1,6-dihydro-guaiazulene-1-id]-dichloride	$TiC_{48}H_{90}Si_8Cl_2$
Zr(6-Hyp-Hgual)$_2Cl_2$	(**11**)	Zirconium(IV)-bis[6-tris(trimethylsilyl)silyl-1,6-dihydro-guaiazulene-1-id]-dichloride	$ZrC_{48}H_{90}Si_8Cl_2$
Hf(6-Hyp-Hgual)$_2Cl_2$	(**12**)	Hafnium(IV)-bis[6-tris(trimethylsilyl)silyl-1,6-dihydro-guaiazulene-1-id]-dichloride	$HfC_{48}H_{90}Si_8Cl_2$
ZrCp*(6-Hyp-Hgual)$Cl_2\cdot$KCl	(**13**)	Zirconium(IV)-pentamethylcyclopentadienyl-[6-tris(trimethylsilyl)silyl-1,6-dihydro-guaiazulene-1-id]-dichloride·KCl	$ZrC_{34}H_{60}Si_4Cl_2\cdot KCl$
2,6-bis(Hyp)-H_2gua	(**14**)	2,6-bis[tris(trimethylsilyl)silyl]-2,6-dihydro-guaiazulene	$C_{33}H_{72}Si_8$
Li[(2,6-bis(Hyp)-Hgual)]	(**15**)	Lithium{2,6-bis[tris(trimethylsilyl)silyl]-2,6-dihydro-guaiazulene-2-id}	$LiC_{33}H_{71}Si_8$

8 Literature

[1] P. D. Lickiss; C. M. Smith, *Coordination Chemistry Reviews* **1995**, 145, 75-124

[2] M. E. Jung; B. Hoffmann; B. Rausch; J. -M. Contreras; *Org. Lett, (Communication;* **2003**, *5*(17), 3159-3161

[3] M. C. Pirrung; L. Fallon; J. Zhu; Y. R. Lee; Photochemically Removable Silyl Protecting Groups. *J. Am. Chem. Soc.* **2001**, *123*(16), 3638-3643

[4] K. W. Klinkhammer; W. Schwarz, *Angew. Chem*. **1995**, 107, 1449

[5] W. Köstler; G. Linti, in: Organosilicon Chemistry III (Hrsg.: N. Auner, J. Weis), Wiley-VCH, Weinheim, **1998**, p. 182-188

[6] N. Wiberg, *Coord. Chem. Rev*. **1997**, 163, 217-252

[7] S. P. Mallela; F. Schwan; R. A.Geanangel. *Inorg. Chem*. **1996**, 35, 745

[8] N. Wiberg, made at the Xth International Symposium on Organosilicon Chemistry in Posnan, Poland, **1993**

[9] Y. Apeloig; M. Yuzefovich; M. Bendikov; D. Bravo-Zhivotovskii; K. W. Klinkhammer. *Organometallics* **1997**, 16, 1265-1269

[10] A. G. Brook; S. Nyburg; F. Abdesaken; G. Gutekunst; R. K. M. K. Kallary; Y. C. Poon; *J. Am. Chem. Soc.* **1982**, *104*, 5668

[11] (a) G. R. Newkome; E. He; C. N. Moorefield, *Chem. Rev*. **1999**, 99, 1689-1746; (b)R. van Heerbeek, P. C. J. Kamer; P. W. N. M. van Leeuwen; and J. N. H. Reek, *Chemical Reviews* **2002**, 102, 3717–3756; (c) L. Resconi; L. Cavallo; A. Fait; F. Piemontesi; *Chem. Rev.* **2000**; *100*(4); 1253-1346; (d) C.-O. Turrin; J. Chiffre; D. de Montauzon; G. Balavoine; E. Manoury; A.-M. Caminade; J.-P. Majoral; *Organometallics* **2002**; *21*(9); 1891-1897

[12] G. E. Osterom; R. J. van Haaren; J. N. H. Reek; P. C. J. Kamer; P. W. N. M. van Leeuwen. *Chem. Commun.* **1999**, 1119

[13] G. Linti, H. Urban, in: Organosilicon Chemistry III (Hrsg.: N. Auner, J. Weis), Wiley-VCH, Weinheim, **1998**, p. 189-194

[14] J. Arnold; T. D. Tilley; L. Arnold; A. L. Rheingold and J. Steven, *Inorg.Chem*. **1987**, 26, 2106-2109

[15] D. Wittenberg, M. V. George and H. Gilman, *J. Am. Chem. Soc*. **1959**, 81, 4812

[16] H. Gilman; C. L. Smith, *J. Organometall. Chem*., **1966**, 6, 665

[17] H. Gilman; C. L. Smith, *J. Organomet. Chem*. **1967**, 8, 245.

[18] (a) H. Gilman; C. L. Smith, *J. Am. Chem. Soc*., **1964**, 86, 1454.
(b) H. Gilman; C. L. Smith, *J. Organomet. Chem*., **1968**, 14, 91-101

[19] G. Becker; H.-M. Hartmann; A. Munch; H. Riffel, *Z. Anorg. Allg. Chem*. **1993**, 619, 1777

[20] G. Gutekunst; G. Adrian; G. Brook, *J. Organomet. Chem*. **1982**, 225, 1-3

[21] A. Heine; R. Herbst-Irmer; G. M. Sheldrick; D. Stalke, *Inorg.Chem*., **1993**, 32, 2694-2698

[22] K. W. Klinkhammer, *Habilitation*, **1998**, Universität Stuttgart

[23] R. E. Wochele, *Dissertation*, Universität Stuttgart, **2001**

[24] K. W. Klinkhammer, *Chem. Eur. J*. **1997**, 3, 1418

[25]C. Marschner, *Eur. J. Inorg. Chem*. **1998**, 221-226

[26] K. W. Klinkhammer; J. Klett; Y. Xiong; S. L. Yao, *Eur. J. Inorg. Chem.* **2003**, 18, 3417-3424

[27] M. Kehrwald; W. Kostler; A. Rodig; G. Linti; T. Blank; N. Wiberg, *Organometallics* **2001**; *20*(5); 860-867

[28] M. L. Sierra; V. Srini; J. De Mel and J. P. Oliver, *Organometallics* **1989**, 8, 2312

[29] C. Krempner and H. Oehme, *J. Organomet. Chem*. **1994**, 464, C7

[30] A. M. Arif; A. H. Cowley; T. M. Elkins and R. A. Jones, *J. Chem. Soc., Chem. Commun*. **1986**, 1776

[31] F. H. Elsner; H.-G. Woo and T. D. Tilley, *J. Am. Chem. Soc*. **1988**, 110, 313

[32] S. P. Mallela and R. A. Geanangel, *Inorg. Chem*. **1990**, 29, 3525

[33] S. P. Mallela and R. A. Geanangel, *Inorg. Chem*. **1994**, 33, 1115

[34] S. P. Mallela and R. A. Geanangel, *Inorg. Chem*. **1991**, 30, 1480

[35] A. Heine and D. Stalke, *Angew. Chem., Int. Edn. Engl*. **1994,** 33, 113

[36] M. Haase and U. Klingebiel, *Z. Anorg. All. Chem*. **1985**, 524, 106

[37] S. P. Mallela and R. A. Geanangel, *Inorg. Chem*. **1993**, 32, 602

[38] W. P. Freemann, T. D. Tilley, A. L. Rheingold and R. L. Ostrander, *Angew. Chem., Int. Edn. Engl*., **1993**, 32, 1744

[39] S. P. Mallela and R. A. Geanangel, *Inorg. Chim. Acta*. **1992**, 202, 211

[40] M. J. Sanganee; P. G. Steel; D. K. Whelligan; *J. Org. Chem.;* **2003**, *68*(8), 3337-3339

[41] H. Gilaman and R. L. Harrel, *J. Organomet. Chem*. **1967**, 9, 67

[42] M. E. Lee; M. A. North and P. Gaspar, *Phosphorous Sulfur Silicon*, **1991**, 56, 203

[43] A. G. Brook; R. K. M. R. Kallury and Y. C. Poon, *Organometallics*, **1982**, 1, 987

[44] W. C. Still, *J.Org. Chem*., **1976**,41, 3063

[45] D. J. Ager and I. Fleming, *J. .Chem. Soc. Chem. Commun*., **1978**, 177

[46] P. M. Bishop; J. R. Pearson and J. K. Sutherland, *J. Chem. Soc., Chem. Commun.,* **1983**, 123

[47] S. Sato; I. Matsuda and Y. Izumi, *J. Organomet. Chem*., **1988**, 344, 71

[48] M. Koreeda and S. Koo, *Tetrahedron Lett.,* **1990**, 31, 831

[49] D. J., Ager and I. Fleming, *J. Chem. Soc., Chem. Commun*., **1978**, 177

[50] G. Wickham; H.A. Olszowy and W. Kitching, *J. Org.Chem*., **1982**, 47, 3788

[51] W. Engel; I. Fleming and R. H. Smithers, *J. Chem. Soc., Perkin Tans*. **1986**, 1, 1637

[52] W. Oppolzer; R. J.Mills; W. Pachinger and T. Stevenson, *Helv. Chim. Acta*, **1986**, 69, 1542

[53] W. Tuckmantel; K. Oshima and H. Nozak, *Chem. Ber,***1986**, 119, 1581

[54] P. F. Hudrlik; A. M. Hudrlik; T. Yimenu; M. A. Waugh and G. Nagendrappa, *Tetrahedron* **1988**, 44, 3791

[55] R. D. Brown, *Trans. Faraday Soc*. **1948**, 44, 984

[56] M. Mayot; G. Berthier; B.Pullman; *J.Chim. physique Physico-Chim. Biol*. **1953**, 50, 170

[57] Self consistent field methode: A.Julg, *J. Chim.Phys*. **1955**, 52, 377

[58] Hueckel molecular orbital methode: A. Pullman & G. Berthier, *C. r.* **1949**, 229, 761

[59] Ab initio methode (G70; STO 3G): G. Ott. *Dissertation*, p. 52, Tuebingen **1980**

[60] Houben Weyl, *Methoden der Organischen Chemie*, vierte Auflage, V/2c, page 249-302

[61] P. Brügger, P. Uebelhart, R. W. Kanz, R. Sigrist, and H. -J. Hansen, *Helvetica Chimica Acta* **1998**, 81, 2201-2217

[62] S. Takekuma; K. Sasaki; M. Nakatsuji; M. Sasaki; T. Minematsu; and H. Takekuma, *Bulletin of the Chemical Society of Japan* **2004**, 77(2), 379-380

[63]K. Kollmar, *J. Am. Chem. Soc*. **1979**, 101, 4832

[64] R. C. Haddon; K. Raghavachari, *J. Am. Chem.Soc.* **1982**, 104, 3516

[65] U. Behrens, *Angew. Chem*. **1987**, 99, 134

[66] R. Burton and G. Wilkinson, *Chem. Ind*. (London) **1958**, 1205

[67] R. Burton; M. L. H. Green; E.W.Abel; and G.Wilkinson, *Chem., Ind*. (London) **1958**, 1592.

[68] R. Burton; L. Pratt; and G. Wilkinson; *J. Chem. Soc*. **1960**, 4290

[69] R. Burton; L.Pratt und G. Wilkinson; *J. chem. Soc*. **1963**, 3290

[70] M. R. Churchill, Chem. Commun., **1966**, 450; *Inorg. Chem*. **1967**, 6, 190

[71] F. A. Cotton; B. E. Hanson; J. R. Kolb; P. Lahuerta; G. G. Stanley; B. R. Stults; A. J. White, *J. Am. Chem. Soc.* **1977**, *99*, 3673

[72] M. R. Churchill and P. H. Bird, *Chem. Commun*. **1967**, 746

[73] J. S. McKechnie and I. C. Paul, *Chem. Commun*. **1967**,747

[74] M. R. Churchill; P. H. Bird, *Inorg. Chem*. **1968**, 7, 1545

[75] P. H. Bird and M.R.Churchill, *Chem. Commun*. **1968**, 145

[76] M. R. Churchill; R. A. Lashewycz; F. J. Rotella, *Inorg. Chem*. **1977**, 16, 265

[77] M. R. Churchill; and P. H. Bird, *Inorg. Chem*. **1968**, 7, 1793

[78] M. R. Churchill and P. H. Bird, *J. Am. Chem. Soc*. **1968**, 90, 3241

[79] R. B. King, *J. Am. Chem. Soc.* **1966**, 88, 2075

[80] H.-F. Klein; B. Hammerschmitt and G. Lull, *Inorg. Chim. Acta*, **1994**, 218, 143-149

[81] M. R. Churchill, *Progr. Inorg. Chem*. **1970**, 11, 71

[82] E. O. Fischer; J. Müller, *J. organometal. chem*., **1964**, 1, 464-470

[83] R. M. Churchill and J. Wormald, C*hem. Commun*. **1968**, 1033-1034; *Inorg.Chem*. **1969**, 8(4) 716

[84] P. Burger; H.-U. Hund; K. Evertz and H.-H. Brintzinger, *J. Organomet. Chem*. **1989,** 378, 153-161

[85] P.-J. Sinnerma; P. J. Shapiro; B. Hoehn; B. Twamley, *J. Organomet. Chem*. **2003**, *676*, 73-79

[86] K. Hafner and H. Weldes, *Annalen der Chemie* **1957**, 606, 90

[87] R. N. McDonald; H. E. Petty; N. Lee Wolfe; and J. V. Paukstels, *J. Org. Chem*. **1974**, 39(13), 1877-1887

[88] G. R. Knox and P. L. Pauson, *J. Chem. Soc*. **1961**, 4610

[89] Alt, H. G.; Koppl, A.; *Chem. Rev.;* **(Review); 2000**; *100*(4); 1205-1222.

[90] R.M.Waymouth, *Science* **1995**, 267, 217

[91] J. A. Ewen, *J. Am. Chem. Soc*., **1988**, 110, 6325

[92] C. Elschenbroich / A. Salzer, Organometallchemie B. E. Teubner Stuttgart **1998**, p. 58

[93] K. W. Klinkhammer, Yun Xiong, unpublished results

[94] U. Baumeister, K. Schenzel, R. Zink, K. Hassler, *J. Organomet. Chem*. **1997**, 543, 117-124

[95] K. W. Klinkhammer, W. Schwarz, *Z. Allg. Anorg. Chem*.**1993**, 619, 1777

[96] M. L. Sierra; V. S. J. de Mel, J. P. Oliver, *Organometallics* **1989**, 8, 2312

[97] R. Leichinger, *Dissertation*, Universität Stuttgart **1995**

[98] R. H. Cox, *J Mag. Res*., **1974**, 14, 317

[99] C. Elschenbroich, *Organometallchemie*, 4. Auflage, B. G. Teubner **2003**, p. 45

[100] R. E. Dinnebier; U. Behrens; and F. Olbrich*, *Organometallics* **1997**, 16, 3855-3858

[101] R. E. Dinnebier; M. Schneider; S. van Smaalen; F. Olbrich; U. Behrens. *Acta Crystallogr., Sect. B.* **1999**, 55, 35

[102] R. E. Dinnebier; S. Neander and U. Behrens, F. Olbrich, *Organometallics* **1999**, 18, 2915-2918

[103] C. Üffing; R. Köppe, and Hansgeorg Schnöckel, *Organometallics* **1998**, 17, 3512-3515

[104] W. Nie; C.-T. Qian; Y.-F Chen; and J. Sun, *Organometallics* **2001**, 20, 5780-5783

[105] W. J. Evans; T. J. Boyle; and J. W. Ziller, *Organometallics* **1992**, 11, 3903-3907

[106] D. Malaba; L. Chen; C. A. Tessier; W. J. Youngs, *J. Organometallics* **1992**, 11, 1007-1009

[107] Y. Apelogig; M. Yuzefovich; M. Bendikov; and D. Bravo-Zhivotovskii, K. W. Klinkhammer, *Organometallics* **1997**, 16, 1265-1269.

[108] T. Gross and H. Oehme, *Organometallics* **1999**, 18 (10), 1815 -1817

[109] J. Lorberth; S.-H. Shin; S. Wocadlo; W. Massa, *Angew. Chem*. **1989**, 101, 793-794; *Angew. Chem*. Int. Ed. Engl. **1989**, 28, 735-736

[110] R. E. Dinnebier; U. Behrens; F. Olbrich. *Organometallics* **1997**, 16, 3855-3858

[111] W. P. Schaeffer; D. Cotter; J. E. Bercaw. *Acta Crystallogr*. **1993**. C49, 1489-1492

[112] P. Jutzi; W. Lefers; B. Hampel; S. Pohl; W. Saak, *Angew. Chem*. **1987**, 99, 563-564; *Angew. Chem*., Int. ed. Engl. **1987**, 26, 583-584

[113] V. Jordan; U. Behrens; F. Olbrich; E. Weiss, *J. Organomet. Chem*. **1996**, 517, 81-88

[114] G. Rabe; H. W. Roesky; D. Stalk; F. Pauer; G. Sheldrick; *J. Organomet.Chem*. **1991**, 403, 11-19

[115] P. Lutzi and N. Burfold. *Chem. Rev*. **1999**, 99, 969-990

[116] C. Krüger; F. Lutz; M. Nolte; G. Erker; M. Aulbach, *J. Organomet. Chem.* **1993**, 79, 4652

[117] G. Erker; M. Aulbach; M. Knickmeier; D. Wonbermühle; C. Krüger; S. Werner, *J. Am.Chem. Soc*. **1993**, 115, 4590

[118] W. D. Luck; A. Streitwieser, Jr. *J. Am. Chem. Soc*. **1981**, 103, 3241

[119] J. Okuda; E. Herdtweck, *J.Organomet. Chem*. **1989**, 373, 99

[120] D. Vos; A. Salmon; H. -G. Stammler; B. Neumann; and P. Jutzi, *Organometallics* **2000**, 19, 3874-3878

[121] D. P. Freyberg; J. L. Robbins; K. N. Raymond; and J. C. Smart, *J. Am. Chem. Soc*. **1979**, 101, 892-897

[122] L. Hedberg and K. Hedberg, *J. Chem. Phys*. **1970**, 53, 1228

[123] A. Haaland, *Inorg. Nucl. Chem. Lett*. **1979**, 15, 267

[124] A. Almenningen; A. Haaland; and S. Samdal, *J.Organomet.Chem*. **1978**, 149, 219

[125] Koch, T.; Blaurock, S.; Somoza, F. B., Jr.; Voigt, A.; Kirmse, R.; Hey-Hawkins, E.; *Organometallics;* **2000**; *19*(13); 2556-2563.

[126] O´hare, D. Murphy; V. Diamond; G. M. Arnold; P. Mountford. *Organometallics* **1994**, 13, 4689

[127] T. Repo; M. Kinga; L. Mutikainen, Y.-C. Su; M. Leskelä and M. Polamo, *Acta Chemica Scadinavica* **1996**, 50, 1116-1120

[128] W. A. Herrmann; R. A. Nwander; H. Riepl; W. Scherer; and C. R. Whitaker, *Organometallics* **1993**, 12, 4342-4349

[129] Shannon, R. D. (1976) `Revised effective ionic radii in halides and chalcogenides', *Acta Cryst.* **A32**, 751. This includes further oxidation states and coordination numbers

[130] B. J. Grimmond; J. Y. Corey; and N. P. Rath, *Organometallics* **1999**, 18, 404-412

[131] A. Clearfield; D. K. Warner; C. H. Saldarriaga-Molina; and R. Ropal; and I. Bernal, *Can. J. Chem*. **1975**, 53, 1622-1629

[132] S. L. Colletti and R. L. Halterman, *Organometallics* **1991**, 10, 3438-3448

[133] N. E. Grimmer; N. J. Coville; C. B. de Koning; J. M. Smith; L. M. Cook, *J. Organomet. Chem*. **2000**, 61, 112-127

[134] O. W. Lofthus; C. Slebodnick, and P. A. Deck, *Organometallics* **1999**, 18, 3702-3708

[135] P. Jutzi; E. Schlüter; S. Pohl; W. Saak, *Chem. Ber*. **1985**, 118, 1959-1967

[136] P. Jutzi; W. Leffers; S. Pohl; W. Saak, *Chem. Ber*. **1989**, 122, 1449-1456

[137] M. F. Lappert; A. Singh; L. Engelhardt; A. H. White, *J. Organomet. Chem*. **1984**, 262, 271-278

[138] A. Hammel; W. Schwarz; J. Weidlein, *J. Acta. Crystallogr*. **1990**, C46, 2337-2339

[139] (a) G. M. Sheldrick, Programm SHELX-86, Göttingen **1986**; (b) G. M. Sheldrick, Programm SHELXL-93, Göttingen **1997**

[140] Herrmann/Brauer, *Synthetic Methods of Organometallic and Inorganic Chemistry*, Ed. by W. A. Herrmann, Vol. 2, N. Auner, U. Klingbiel, Groups 1, 2, 13 and 14. pp. 186-193